



Kent Academic Repository

Georgiou, Leoni (2018) *Locomotor signals in the trabecular structure of the femur in extant and extinct hominoids*. Doctor of Philosophy (PhD) thesis, University of Kent,.

Downloaded from

<https://kar.kent.ac.uk/74095/> The University of Kent's Academic Repository KAR

The version of record is available from

This document version

UNSPECIFIED

DOI for this version

Licence for this version

UNSPECIFIED

Additional information

Versions of research works

Versions of Record

If this version is the version of record, it is the same as the published version available on the publisher's web site. Cite as the published version.

Author Accepted Manuscripts

If this document is identified as the Author Accepted Manuscript it is the version after peer review but before type setting, copy editing or publisher branding. Cite as Surname, Initial. (Year) 'Title of article'. To be published in *Title of Journal*, Volume and issue numbers [peer-reviewed accepted version]. Available at: DOI or URL (Accessed: date).

Enquiries

If you have questions about this document contact ResearchSupport@kent.ac.uk. Please include the URL of the record in KAR. If you believe that your, or a third party's rights have been compromised through this document please see our [Take Down policy](https://www.kent.ac.uk/guides/kar-the-kent-academic-repository#policies) (available from <https://www.kent.ac.uk/guides/kar-the-kent-academic-repository#policies>).

Locomotor signals in the trabecular structure of the femur in extant and extinct hominoids

by

Leoni Georgiou
School of Anthropology and Conservation
University of Kent

A Dissertation Presented in Fulfilment of the Requirements for
the Degree of Doctor of Philosophy
December 2018
Word Count: 39,932

Abstract

The evolution of bipedalism has been the focus of paleoanthropological research, as it is one of the defining traits of hominins. Adaptations for this form of locomotion are found throughout the hominin fossil record, however definitive traits of obligate bipedal locomotion are only found in the genus *Homo*. The degree of arboreality, as well as the biomechanics of bipedal gait in earlier hominins are still debated and it is unclear how this trait evolved into the form seen in modern humans. Identifying the links between the locomotion and morphology of extant taxa is integral in reconstructing the locomotion of extinct taxa and for this purpose the great apes are good analogues to extinct hominins. Inferences of behaviour in extinct taxa are usually made based on external morphological traits. With novel, non-destructive methods however studies have been able to analyse the internal trabecular structure in fossils. Trabecular bone remodels throughout life in response to mechanical loading and even though non-mechanical factors affect trabecular structure, research has shown that the resulting patterns can be informative about joint postures used during locomotion. Understanding how this structure varies in extant apes with different locomotor repertoires will help reconstruct the past behaviour of hominins. In this doctoral dissertation I analysed, for the first time holistically, the trabecular patterns of the femur in extant ape taxa, to identify links with locomotor behaviour and eventually reconstruct the locomotion of extinct hominins from Sterkfontein, South Africa.

I analysed, with a whole-epiphysis method, the trabecular patterns throughout the femoral head of African apes, orangutans and modern humans and identified a functional signal in the trabecular patterns, which can be linked to habitual behaviours. African apes and orangutans showed two regions of high bone volume across the femoral head, consistent with the predicted regions of peak loading during vertical climbing and terrestrial quadrupedalism, while modern humans showed one region of high bone volume, consistent with the predicted region of peak loading during bipedalism. Furthermore, overall trabecular

architecture generally followed predictions, distinguishing humans from other apes through their greater strut alignment and lower overall bone volume.

Additionally, using the same whole-epiphysis approach, I analysed the trabecular patterns of the distal femoral epiphysis in extant great apes. Results suggested that the distal femur holds a less clear functional signal than the femoral head. Chimpanzees and orangutans showed high bone volume in the posterosuperior region of the condyles, consistent with the use of highly flexed knee postures during vertical climbing. This was not found in gorillas or modern humans. Humans were distinguished from other apes by their greater strut alignment, reflective of the more stereotypical loading of the condyles during bipedal locomotion but did not show the lower bone volume found in prior human studies. Furthermore, the human trabecular pattern was not as distinct as initially predicted based on their different locomotor mode to the other apes.

Finally, using geometric morphometrics and a whole-epiphysis approach, I analysed statistically the patterns of subchondral trabecular bone in the femoral head and distal epiphysis of extant apes and extinct hominins from Sterkfontein, South Africa. Results showed that two specimens confidently attributed to *A. africanus* (StW 522, TM 1513) had a modern human-like trabecular pattern, suggesting that this taxon had a biomechanically similar bipedal gait to modern humans and did not frequently climb. Conversely, a geologically younger specimen (StW 311), attributed either to early *Homo* or *Paranthropus robustus*, had a trabecular pattern more similar to non-human apes, suggesting that they engaged in both bipedalism and vertical climbing.

Together, the findings of this dissertation provide a better understanding of the links between trabecular structure of the femur and locomotor behaviour in extant apes, as well as illustrate the importance of analysing trabecular structure within entire epiphyses. Additionally, results here provide insight into the evolution of locomotion in the hominin lineage and the diversity of bipedal gaits among Plio-Pleistocene, South African hominins.

Acknowledgments

First and foremost, I would like to express my gratitude to my PhD supervisors Matthew Skinner and Tracy Kivell who have made this project possible. I am grateful to both for the inspiring discussions, thoughtful feedback and encouragement throughout the last three years. Most importantly, I am very thankful to Matthew Skinner for encouraging me to apply for this PhD and for his support and guidance through the many difficulties of this dissertation. Both have taught me a great deal and for that I am truly grateful.

I am thankful to the School of Anthropology and Conservation and the University of Kent for granting me a 50th Anniversary Scholarship, as this supported my research. Further funding from the School of Anthropology and Conservation allowed me to attend international conferences and present my research. I am also thankful that my research was supported by Tracy Kivell's European Research Council Starting Grant #336301.

My research was made possible by the CT data provided by my supervisors, as well as the skeletal material gathered from several museum and collections in the UK as well Germany. For access to the material I would like to thank Anneke Van Heteren (Zoologische Staatssammlung München), Inbal Livne (Powell-Cotton Museum), Christophe Boesch and Jean-Jacques Hublin (Max Planck Institute for Evolutionary Anthropology), and Brigit Grosskopf (Georg-August University of Göttingen). Also, I am thankful to Zewdi Tsegai for facilitating access to material. For CT scanning of the specimens I would like to thank David Plotzki (Max Planck Institute for Evolutionary Anthropology) and Keturah Smithson (University of Cambridge). Additionally, I am grateful for having great collaborators, Dieter Pahr and Laura Buck, who have greatly influenced this research.

In the last three years, many people have contributed to stimulating conversations which I am very grateful for. Christopher Dunmore, Klara Komza, Tom

Davies, Ameline Bardo, Kim Deckers and Alastair Key. I am very thankful for the support and inspiration, as my colleagues and more importantly as my friends. Additional thanks go to my PhD colleagues and friends who made my life in Canterbury particularly enjoyable, Ana Curto and Adriana Lowe.

I would like to thank my parents, Kyriaki and Nikos, as well as my sister Stephania, for their immense support during my PhD. While physically being at the other side of Europe, they were next to me in each step of the way. Also, Victoria and Andreas I am truly grateful for your inspiration, support and encouragement. I would not have been here if it wasn't for you.

Finally, I would like to acknowledge the huge support I have had from Lawrence Sampson. Your patience, love and positive demeanour have helped me overcome the difficulties of this PhD and have made the whole process a lot more enjoyable.

Table of contents

Abstract	2
Acknowledgments	4
Contents	6
Figures	9
Tables	12
1 General Introduction	13
1.1. <i>Primate locomotion</i>	14
1.2. <i>Anatomy and kinematics of the ape hindlimb</i>	17
1.3. <i>The evolution of bipedalism in hominins</i>	21
1.4. <i>Trabecular bone and bone functional adaptation</i>	24
1.5. <i>Trabecular bone and cortical bone</i>	28
1.6. <i>Functional signals in the trabecular structure of extant taxa</i>	30
1.7. <i>Functional signals in the trabecular structure of fossil hominids</i>	33
1.8. <i>The whole-epiphysis approach to trabecular bone analysis</i>	35
1.9. <i>Trabecular bone and body mass</i>	36
1.10. <i>Trabecular bone ontogeny</i>	38
1.11. <i>New methods in trabecular analysis: Geometric morphometrics</i>	41
1.12. <i>Summary</i>	43
2 Materials and Methods	44
2.1. <i>Sample and Scanning</i>	45
2.2. <i>Segmentation</i>	47
2.3. <i>Trabecular architecture analysis</i>	48
2.4. <i>Geometric morphometrics</i>	51
2.5. <i>Statistical analysis</i>	56
3 Trabecular architecture of the great ape and human femoral head	57
<i>Abstract</i>	58
3.1. <i>Introduction</i>	59
3.1.1. <i>Locomotion, hip morphology and predicted joint posture</i>	62
3.2. <i>Materials and Methods</i>	67

3.2.1. Study sample.....	67
3.2.2. Trabecular architecture analysis.....	69
3.2.3. Statistical analysis.....	70
3.3. Results.....	70
3.3.1. BV/TV distribution in the femoral head.....	70
3.3.2. Quantitative analysis of trabecular parameters in the femoral head	73
3.4. Discussion.....	77
3.4.1. Distribution of BV/TV within the femoral head.....	77
3.4.2. Quantitative analysis of trabecular structure	80
3.5. Conclusion.....	84
Supplementary material.....	85
4 Trabecular bone patterning in the hominoid distal femur.....	107
Abstract.....	108
4.1. Introduction.....	109
4.1.1. Locomotion, morphology and predicted knee posture/loading.....	112
4.1.2. Hypotheses.....	115
4.2. Materials and Methods.....	117
4.2.1. Sample and scanning.....	117
4.2.2. Trabecular architecture analysis.....	119
4.2.3. Statistical analysis.....	121
4.3. Results.....	122
4.3.1. Quantitative and qualitative analysis of trabecular parameters.....	122
4.3.2. Trabecular architecture and between-species regional relationships.....	135
4.4. Discussion.....	138
4.4.1. Within-species trabecular patterns.....	138
4.4.2. Between-species trabecular differences.....	142
4.5. Conclusion.....	146
Supplementary material.....	147

5 Locomotor diversity in South African fossil hominins during the Early Pleistocene	174
<i>Abstract</i>	175
5.1. <i>Introduction</i>	176
5.2. <i>Materials and Methods</i>	181
5.2.1. <i>Sample, segmentation and trabecular architecture analysis</i>	181
5.2.2. <i>Landmarking and BV/TV values extraction</i>	182
5.2.3. <i>Statistical analysis</i>	184
5.3. <i>Results</i>	184
5.3.1. <i>Behavioural signals in the femur of non-human apes</i>	184
5.3.2. <i>Behavioural signals in obligate bipedal taxa</i>	187
5.3.3. <i>Trabecular distribution patterns and locomotion of hominins at Sterkfontein</i>	189
5.4. <i>Discussion</i>	193
<i>Supplementary material</i>	197
6 General Discussion, Conclusion, Limitations and Future Directions	205
6.1. <i>General Discussion</i>	206
6.1.1. <i>Does the femoral trabecular architecture of extant non-human apes hold locomotor signals?</i>	208
6.1.2. <i>Is Homo sapiens femoral trabecular pattern unique?</i>	211
6.1.3. <i>Can the trabecular patterns of the femur be used to infer locomotion in extinct hominins?</i>	213
6.1.4. <i>How do the trabecular patterns of the extinct hominins compare to those of the extant taxa?</i>	214
6.2. <i>Conclusion</i>	217
6.3. <i>Limitations and future directions</i>	218
References	220
Appendix	255

Figures

Figure 2.1. Example of RCA segmentation of a <i>Gorilla</i> distal femur.....	47
Figure 2.2. Example of processing steps prior to meshing.....	49
Figure 2.3. Distribution maps.....	51
Figure 2.4. Repeatability test for fixed landmarks used in the proximal and distal femur.....	54
Figure 2.5. Template of landmarks used for the proximal and distal femur.....	55
Figure 3.1. Comparison of hip posture during different habitual locomotor activities in great apes and humans.....	64
Figure 3.2. <i>Pan</i> BV/TV distribution in the femoral head.....	71
Figure 3.3. <i>Gorilla</i> BV/TV distribution in the femoral head.....	71
Figure 3.4. <i>Pongo</i> BVTV distribution in the femoral head.....	72
Figure 3.5. <i>Homo</i> BV/TV distribution in the femoral head.....	73
Figure 3.6. Bivariate plot of mean bone volume fraction (BV/TV) and mean degree of anisotropy (DA) for each individual and species in the sample.....	76
Figure 3.7. A histogram of mean BV/TV and DA value distributions in the studied taxa.....	77

Figure 4.1. Comparison of knee posture during different habitual locomotor activities in great apes and humans.....	112
Figure 4.2. Processing steps of a <i>Gorilla</i> specimen, showing a parasagittal view through the lateral condyle.....	119
Figure 4.3. Partitioning of the lateral condyle into sub-regions in a <i>Pan</i> specimen.....	121
Figure 4.4. <i>Pan</i> BV/TV distribution.....	124
Figure 4.5. <i>Gorilla</i> BV/TV distribution.....	125
Figure 4.6. <i>Pongo</i> BV/TV distribution.....	126
Figure 4.7. <i>Homo</i> BV/TV distribution.....	128
Figure 4.8. Bone volume fraction (BV/TV) and degree of anisotropy (DA) results for each region and taxon.....	130
Figure 4.9. Trabecular number (Tb.N), separation (Tb.Sp) and thickness (Tb.Th) results for each region and taxon.....	132
Figure 4.10. Results of principal components analysis of three trabecular variables (Tb.N, Tb.Sp. and DA) in all analysed regions.....	134
Figure 4.11. Inferior index for BV/TV and DA.....	135
Figure 4.12. Posterior index for BV/TV and DA.....	137

Figure 5.1. Non-human great ape hip flexion angles during terrestrial quadrupedalism and vertical climbing, and BV/TV distribution in the femoral head.....	186
Figure 5.2. Human hip flexion angles during bipedal locomotion and BV/TV distribution in the femoral head of <i>Homo</i>	188
Figure 5.3. PCA of the relative BV/TV distribution in the femoral head.....	190
Figure 5.4. PCA of the relative BV/TV distribution in the distal femur.....	191
Figure 5.5. BV/TV distribution in the subchondral layer of the femoral head and within the femoral head in the fossil taxa.....	193

Tables

Table 2.1. Femoral head landmark description.....	52
Table 2.2. Distal femur landmark description.....	53
Table 3.1. Study sample taxonomic composition, re-sampled voxel size range, sex, and microCT scanning parameters.....	68
Table 3.2. Trabecular architecture results.....	74
Table 3.3. Results of pairwise comparisons between taxa.....	75
Table 4.1. Taxonomic composition of the study sample, voxel size range (after resampling), sex distribution and microCT scanning parameters.....	118
Table 4.2. Trabecular architecture results by condyle and region.....	123
Table 4.3. Indices results for lateral and medial condyle.....	136
Table 5.1. Intertaxon pairwise permutational MANOVA tests of the first three principal components.....	184
Table 5.2. Permutational Hotelling's T2 results.....	189

Chapter 1

General Introduction

The aim of my dissertation was twofold. My first aim was to identify potential links between the trabecular bone architecture of the femur in extant hominids and their locomotor behaviour, while my second aim was to infer the locomotor behaviour of extinct hominins based on their femoral trabecular patterns. Below I review differences in great ape locomotion and hindlimb morphology and our current understanding of the evolution of hominin bipedalism. Following this, I review trabecular bone functional adaptation, comparative studies of trabecular bone variation across primates, and recent methodological developments in the analysis of trabecular structure.

1.1. Primate locomotion

Great apes include modern humans as well as the taxa most closely related to them. Extant apes have been studied to understand the evolution of bipedalism in hominins. They use several locomotor types at different frequencies depending on their habitat and their hindlimb shows numerous adaptations linked to their behaviour. These include variation in the shape of the pelvis and of the proximal femur, as well as variation in the knee and soft tissue anatomy of the hindlimb.

Chimpanzees are primarily terrestrial knuckle-walkers but a considerable proportion of their time is spent engaging in other terrestrial as well as arboreal activities, such as vertical climbing, suspension, bipedalism and leaping (e.g. Hunt, 1992; Doran, 1993a,b,1997; Isler, 2005). The small moment arms about the joints and the long muscle fascicles in the hindlimb allow them to acquire various joint positions during locomotion while moving their joints over large ranges (Payne, 2001; Payne et al. 2006 a,b). During development, *Pan* locomotion changes from mostly forelimb dominated behaviours, such as clinging and armhanging, to assisted bipedalism with frequent hindlimb use and eventually quadrupedalism (Doran, 1992). During adulthood, there are several differences in arboreal locomotor behaviours between the sexes, with female chimpanzees generally being more

arboreal and using more quadrupedalism above branches than males (Doran, 1993b). During knuckle-walking and vertical climbing the majority of their weight is bared by their hindlimbs, which are responsible for propulsion (Demes et al. 1994; Hannah et al. 2017). Of great interest has been the bipedal locomotion of *Pan*, even though this form of locomotion is rather facultative. During bipedalism these apes have an erect trunk, like modern humans, but maintain bent hips and knees in order to balance (Tuttle, 1969; Ankel-Simons, 2007; D'Aout et al. 2004) and compared to humans they take shorter steps with a higher frequency (Pontzer et al. 2014).

Similar to chimpanzees, gorillas knuckle-walk when terrestrial. Furthermore, they are frequently arboreal. Different *Gorilla* species vary in locomotor behaviours depending on their habitats which range from forests in high altitudes to lowland rainforests (Doran and McNeilage, 1998). Western lowland gorillas (*Gorilla gorilla gorilla*) for example are more arboreal than mountain gorillas (*Gorilla beringei beringei*) and spend more time feeding as well as travelling between food sources (Tutin and Fernandez, 1985; Kuroda, 1992; Remis, 1994; Doran, 1996,1997). Gorillas exhibit strong sexual dimorphism and this is reflected in the frequency of arboreality, with females engaging in more suspensory locomotion especially in seasons of fruit deficiency (Remis, 1999). Furthermore, age seems to have an effect on the preferred locomotor mode and locomotor changes occur faster in *Gorilla* than in *Pan* (Doran, 1997). At younger ages gorillas swing with a higher frequency, a behaviour which does not occur very often in older and especially larger individuals (Doran, 1997). The increase in size with age also influences the way they climb, with larger individuals climbing closer to the trunk of a tree or on bigger branches (Remis, 1995; Remis, 1999; Isler, 2005).

Orangutans are the most arboreal of the great apes but when locomoting on the ground they typically fist-walk (Tuttle, 1969 and references therein). They differ from the African apes in their use of torso-pronograde suspensory locomotion, but they also employ a more diverse array of positional behaviours while navigating intricate canopies (Cant, 1987; Isler and Thorpe, 2003; Thorpe and Crompton, 2006; Thorpe et al. 2009). Occasionally orangutans engage in bipedal locomotion; mainly

while walking on tree branches (Thorpe and Crompton, 2006). Locomotor differences are found between different *Pongo* species as well as between individuals of the same species (Thorpe and Crompton, 2005; Thorpe and Crompton, 2006) and environmental variables have a strong influence on the frequency of use of their different gaits (Manduell et al. 2012). For example, *Pongo abelii* individuals in Sumatra use less suspensory locomotion and more pronograde locomotion compared to their Bornean counterparts of *Pongo pygmaeus*. Additionally, Sumatran orangutans descend less frequently to the ground because of the presence of the Sumatran tiger (Sugardjito and van Hooff, 1986). Unlike gorillas and chimpanzees, sex and age do not have a great influence on the locomotor preferences of orangutans (Thorpe and Crompton, 2005; Manduell et al. 2012).

Humans are the only obligate bipedal apes. Their form of bipedalism is unique in that the hips and the knees remain mostly extended through the gait cycle (Alexander, 1991; 2004). The gait cycle includes the stance and swing phases with several sub-events (Kharb et al. 2011). The beginning of a cycle is marked by initial contact of one foot with the ground. This is followed by toe-off and swing of the opposing foot, while the grounded foot progresses to heel rise. Finally, the opposite foot makes contact with the ground and the cycle is repeated for the newly grounded foot. The trajectory of the centre of mass resembles an inverted pendulum and travels from the lowest point at heel-strike to the highest at mid-stance ensuring balance (Cavagna et al. 1976; Lee and Farley, 1998). Six important lower limb actions occur during the gait cycle: pelvic rotation, pelvic tilt, stance knee flexion, heel rise, ankle plantarflexion and hip adduction (Saunders et al. 1953; McMahon, 1984; Della Croce et al. 2001). During infancy humans crawl or locomote with some support, while unaided bipedalism typically occurs around the age of 1 year and is associated with changes in locomotor control (Forssberg, 1985). Adult humans also engage in running, a behaviour that is mechanically different to walking (e.g. Mann and Hagy, 1980; Ounpuu, 1990,1994; van den Bogert et al. 1999; Giarmatzis et al. 2015).

Even though general locomotor categories are oversimplifications of actual behaviour there are several differences in the locomotion of great apes and these

are expected to be reflected in the skeleton. Varying positioning of the hindlimbs while navigating through the various habitats of these primates results in differing loads on their joints and the expectation is that trabecular organization, specifically in the hip and knee joints, will reveal a functional signal that can be linked to their locomotor repertoires. Variation across populations, subspecies and sexes, mainly in the frequency of positional behaviours, should be taken into account when conducting inter-specific comparisons. Furthermore, the kinematics of hindlimb joints and the soft tissue anatomy need to be understood before attempting to reconstruct behaviour as these define the resulting forces on the skeleton.

1.2. Anatomy and kinematics of the ape hindlimb

The femur is central to two main joints of the hindlimb involved in locomotion, the hip and the knee. The hip is a complex joint formed by the innominate and the proximal femur. The innominate, or pelvic girdle, consists of three separate bones: the ilium the ischium and the pubis which fuse during development. In humans, the ilium is short and broad and extends from the posterior to the anterior of the body. Conversely, in non-human apes it is long and flat and is located at the posterior of the body (Aiello and Dean, 2002). The acetabulum, a concave surface formed where the three pelvic bones meet, is where the femoral head articulates with the pelvis. Its shape defines the mobility of the hip. In *Pan* and *Pongo*, the acetabulum is relatively shallow (Jenkins, 1972; Zihlman et al. 2011), while in *Homo* it is relatively deep. The acetabulum of *Gorilla* is the deepest of the apes (Schultz, 1969). These bony adaptations potentially allow extensive mobility in *Pan* and *Pongo* and restrict movement in *Homo* and *Gorilla*.

The morphology of the proximal femur also contributes to the biomechanics of the hip. In *Homo* the head is relatively large, the neck long and the greater trochanter lengthened mediolaterally (Lovejoy, 1975; Jungers, 1988; Harmon, 2007). The long femoral neck compensates for the mechanical disadvantage brought about

by the shape of the ilium and the remoteness of the hip joints to the muscles. The human femur is at a valgus angle resulting in adduction of their hips during the stance phase (O'Neil et al. 2015). These traits produce three lines of major stress across the proximal femur during locomotion, which is reflected in the trabecular organisation (Ryan and Krovitz, 2006; Skuban et al. 2009). Furthermore, the distribution of cortical bone in the femoral neck is unique in humans. They show a gradient with reduced bone in the superior compared to the inferior region of the neck (Lovejoy, 1988; Lovejoy et al. 2002), as opposed to apes that have equal amounts of cortical bone across the two regions (Lovejoy, 1988; Rafferty, 1998). This is consistent with the differing loading patterns during locomotion. In *Pongo*, the morphology of the proximal femur is in some ways similar to that of *Homo*, sharing the large head and long neck, but lacks a subchondral insertion of a ligamentum teres (Ruff, 2002; Harmon, 2007). In *Gorilla* the femoral head is relatively small and is located inferiorly to the greater trochanter, while the neck is short and the greater trochanter is superiorinferiorly lengthened. *Pan* shares all the traits of *Gorilla* except that the trochanteric fossa is deeper (Harmon, 2007).

Movement in the knee is generally more restricted than in the hip. The knee is comprised of the distal femur and the proximal tibia. The shape of the distal femoral epiphysis varies between apes. In humans the condyles are equal in size and the epiphysis is square when viewed from below (Tardieu, 1981). Furthermore, the condyles are elliptical in shape, increasing the radius of curvature (Heiple and Lovejoy 1971; Tardieu, 1981). In African apes and *Pongo* the epiphysis is more mediolaterally than anteroposteriorly expanded. Additionally, the condyles are more circular, and the medial condyle is generally larger than the lateral (Tardieu, 1981). In the non-human apes these traits allow greater rotation of the knee during locomotion. In humans the knee only rotates slightly during the last phase of stance (Tardieu, 1981) and traits assist with extension of the knee.

Apes also differ in foot kinematics (Griffin et al. 2010a). When walking bipedally, humans place the heel on the ground and subsequently weight is transferred from the lateral part of the foot to the medial (Elftman and Manter, 1935;

Napier, 1967; Inman et al. 1981). The transverse and longitudinal arches result in partial contact of the foot with the ground. African apes can also place their heel on the ground with some variation (Gebo, 1992), however the lack of foot arches means the base of the foot is in full contact with the substrate. When walking above small branches, chimpanzees keep their heel elevated but on larger substrates may place their heel on the substrate at the end of the swing phase. When walking terrestrially, they are always plantigrade. Gorillas are also plantigrade and place their heel on the ground but show less flexibility than chimpanzees in heel elevation (Gebo, 1992). Orangutans show the greatest variation in foot positioning, and in contrast to the African apes when arboreal they mostly move with an elevated heel (Gebo, 1992). Additionally, orangutans can use their feet for grasping.

In addition to bony anatomy, soft tissue anatomy affects the ability of joints to move within a certain range. Furthermore, soft tissue helps distribute stress over a wider area, as shown in the pelvis of humans during single leg stance (Phillips et al. 2007). In studies of locomotion, muscle anatomy has contributed a lot to our understanding of primate behaviour. Even though great apes do not differ significantly in muscle architecture (Myatt et al. 2011), some subtle differences can be detected which are attributed to the different demands for stability and mobility in their habitats. The main features that define a muscle's contribution to movement are the muscle fascicle length and the moment arm length. A greater muscle fascicle length relative to moment arm length allows wider movement about a joint (Alexander et al. 1981; Alexander, 1993; Payne et al. 2006b). The variation of these muscle traits in primates shows that non-human apes can move their joints across a wider range than humans (Payne et al. 2006a, b). Furthermore, individuals that are specialised for specific types of locomotion are expected to recruit less muscle activity, resulting in reduced stress on the skeleton (Basmajian, 1965; Cartmill et al. 1987; Hunt, 1991a; Thorpe and Crompton, 2006).

In chimpanzees, the anterior gluteal muscles attach to the ilium, which is lengthier than that of humans, and are used during quadrupedal locomotion to extend the hip, whereas in humans they have a different function: to abduct the hip.

These abductor muscles are unique in their structure and action and may help in reducing tensile stress during single leg stance (Lovejoy, 2005b). Chimpanzees lack this apparatus. The gluteus maximus differs in size between human and chimpanzees. In humans, it is the largest muscle and its origin is found posteriorly on the pelvis, while its attachment is posteriorly and laterally on the proximal femur (Lovejoy, 1988). It is the main extensor of the hip. In chimpanzees and other apes, it is much smaller and does not contribute as much to hip extension (Stern and Susman, 1981; Lieberman et al. 2006). Furthermore, in humans hip musculature assists with the balance of the trunk on top of the hindlimbs (Bergmann et al. 1997; Bergmann et al. 2001; Phillips et al. 2007). Gorillas have large knee extensors and the musculature of the hindlimb is mainly concentrated proximally serving to stabilize the hip joint (Zihlman et al. 2011). Orangutans on the other hand have large knee flexors (Zihlman et al. 2011) and a less restricted hip joint, as the muscles are distributed differently to those of gorillas. Furthermore, orangutans have a distinct gluteus minimus configuration where the muscle is separated into two: the gluteus minimus proper and the gluteus scansorius (Sigmon, 1974). Their musculature contributes to their extremely flexible hindlimbs that can assume the most diverse positions of the apes.

Stress induced on the skeleton from locomotion and muscular activity should affect the underlying trabecular bone. Specifically, joint positioning during the most frequent and demanding locomotor activities is expected to be reflected in the trabecular bone distribution of major joints. Therefore, apes will have relatively discrete organizational patterns especially within the hip and knee that when studied can reveal behavioural signals. The aim of this study is to identify these patterns in the proximal and distal femur of extant hominids and their links to locomotion with the ultimate goal to infer locomotion in extinct hominins.

1.3. The evolution of bipedalism in hominins

Bipedalism has long been considered one of the defining traits of the hominin lineage (e.g. Darwin, 1871). Traditionally it was thought that this type of locomotion evolved in a savannah or more open environment (Dart, 1925; Wheeler, 1992; Potts, 1998) however it is now widely accepted that it likely evolved in a forested environment (e.g. Clarke and Tobias, 1995; WoldeGabriel et al. 2001; Sénut, 2006; White et al. 2009). Of course, bipedalism could have evolved multiple times in the hominin lineage and many theories have been proposed to explain its adaptive significance (e.g. Etkin, 1954; Dart, 1959; Rose, 1976; Wheeler, 1984; Jablonski and Chaplin, 1993; Hunt, 1996; Kirschmann, 1999; Thorpe et al. 2007; Wall-Scheffler et al. 2007; Watson et al. 2008). Some suggest that it increased survival and/or reproduction by freeing the hands for other activities (Etkin, 1954; Hewes, 1961; Washburn, 1967; Kirschmann, 1999), some of which could have increased feeding efficiency (Eiseley, 1953; Bartholomew and Birdsell, 1953; Jolly, 1970; Lovejoy, 1981). Others suggest it could have evolved to scan the environment (Dart, 1959; Rose, 1976) or as a form of display (Jablonski and Chaplin, 1993). Furthermore, the biomechanical differences between early hominin and modern human bipedalism have been the subject of debate (Stern and Susman, 1983; Susman et al. 1984; Ward, 2002; Carey and Crompton, 2005; Lovejoy and McCollum, 2010; Raichlen et al. 2010). Evidence from the fossil record as well as behavioural observations from extant apes have contributed to the study of the evolution of this trait.

The ability to extend the hindlimb can be traced back to at least 6 million years ago in the hominin lineage, close to the panin-hominin split (Arnason et al. 1998; Pickford and Senut, 2001a; Eizirik et al. 2004; Crompton et al. 2008; Moorjani et al. 2016). *Orrorin tugenensis*, an early hominin, displays a mosaic of femoral traits that suggest it could have walked bipedally but may also have engaged in arboreal behaviours (Pickford and Senut, 2001b; Senut et al. 2001; Senut, 2003; Crompton et al. 2008; Richmond and Jungers, 2008). Furthermore, fossils of other early hominins, such as *Ardipithecus ramidus*, can provide information about the evolution of

bipedalism. Adaptations for upright bipedalism are found in the pelvis, femur and spine of *Ar. ramidus*, and specializations for other locomotor types are absent (Lovejoy et al. 2009a,b). Its pelvis differs to that of chimpanzees with a clearly modified upper ilium but it lacks adaptations of later hominins, indicating that this portion of the pelvis was potentially the first to be modified during the transition to a more bipedal gait. Additional adaptations for bipedalism are found in later hominins, including broadening of the sacrum, lordosis of the spine and modification of the abductor apparatus for the prevention of pelvic tilt (Lovejoy and McCollum, 2010). However, uncertainty about the function of these morphological traits has sustained the debate over the form and extent of bipedalism in later hominins, specifically those belonging to the *Australopithecus* genus. These species are widely recognized as bipedal hominins but the degree of their arboreality has been questioned. Several of their skeletal features that could be suggestive of arboreality are regarded as evolutionary retentions by some (e.g. Berge, 1994), while for others they are indicative of the commitment to an arboreal environment (e.g. Senut, 1981). Furthermore, the biomechanics of australopith bipedal locomotion has been debated (Stern and Susman, 1983; White and Suwa, 1987; Ward, 2002; Lovejoy et al. 2002; Carey and Crompton, 2005; Raichlen et al. 2010). Some researchers propose that they were efficient, upright bipedal walkers that used extended hindlimbs like modern humans (Carey and Crompton, 2005; Lovejoy and McCollum, 2010; Raichlen et al. 2010), while others suggest that they used a bent-hip, bent-knee locomotion when bipedal, similar to chimpanzees (Stern and Susman, 1983; Susman et al. 1984). This debate mainly stemmed from the fact that some traits of the *A. afarensis* pelvis were considered indicative of biomechanical similarities with bipedal chimpanzees (Stern and Susman, 1983). Recent studies though support that this taxon did not rely on a bent-hip, bent-knee gait (Crompton et al. 1998; Sellers et al. 2004; Pontzer et al. 2009).

Several biomechanically different bipedal gaits may have coexisted during the Plio-Pleistocene (Haile-Selassie et al. 2012; DeSilva et al. 2013). *Australopithecus afarensis* (3.7-3 Ma) and *A. africanus* (3-2.4 Ma) show combinations of primitive and derived traits in the shoulder (Berger, 1994), the pelvis (Stern and Susman, 1983;

Lovejoy, 2005a), the femur (Lovejoy and Heiple, 1970; Tardieu, 1981; Lovejoy, 2007; Harmon, 2009a) and the foot (Clarke and Tobias, 1995; Ward et al. 2011), that suggest they were habitual bipeds which engaged in varying degrees of arboreal locomotion. The proportions of their limbs (Richmond et al. 2002; Green et al. 2007) and relative size of their hindlimb joints (Jungers, 1988) are intermediate between extant apes and modern humans, indicating that their gait was, to an extent, functionally different to that of modern humans. Similarly, the more recent *Australopithecus sediba* (1.977 Ma) shows a combination of hindlimb traits indicating both arboreal locomotion and habitual bipedalism (Berger et al. 2010; Kibii et al. 2011; Zipfel et al. 2011), however its lower limb anatomy, and specifically that of the foot, suggests that *A. sediba* had a distinct form of bipedal locomotion (DeSilva et al. 2013). Its contemporaneous taxon *Paranthropus robustus* (2-1.5 Ma) shows adaptations for bipedal locomotion in the pelvis and femur (Napier, 1964; Robinson, 1972), though the morphology of its pelvis is less human-like than that of *A. africanus*, perhaps indicating a less efficient form of bipedal locomotion in this taxon (Napier, 1964). Together, these findings indicate that more than one form of bipedalism probably existed during the Plio-Pleistocene and research up to now has not clarified how the bipedalism of modern humans emerged after that time. More definitive traits of *H. sapiens*-like obligate bipedalism are found in *H. erectus* (Day, 1971; Ruff, 2008, 2009; Hatala et al. 2016), however the form of bipedal locomotion of earlier *Homo* taxa is debated (Susman and Stern, 1982; Berillon, 1999; Wood and Collard, 1999; Bramble and Lieberman, 2004; Harcourt-Smith and Aiello, 2004). Study of species such as *Homo naledi* (Berger et al. 2015), which has highly derived foot morphology but retains ape-like curved hand phalanges, indicate that interpretations of behaviour based on the external morphology of isolated postcranial elements can be problematic. However, additional information could be gleaned by studying traits that change through development. Specifically, trabecular analysis can provide evidence for past behaviours in hominins as this tissue changes throughout an individual's lifetime.

1.4. Trabecular bone and bone functional adaptation

Trabecular (or cancellous) bone is the porous tissue found in the epiphyses of long bones as well as short and irregular bones such as the metacarpals, the sternum, the pelvis and the vertebrae (Keaveny et al. 2001). It is composed of groups of lamellar bone (Choi and Goldstein, 1992) and is very similar in composition to cortical bone. This tissue's main function is to absorb the load applied on joints and transfer it to the diaphyseal cortical bone (Currey, 2002) and to provide essential stiffening of the bone while retaining its lightness (Parr et al. 2013). Its structure changes through deposition of bone by osteoblasts and resorption by osteoclasts (Dempster, 1992; Ott, 1996). Bone is created and replaced constantly to repair damage and its turnover rate is controlled by genes (Kelly et al. 1991; Garnero et al. 1996). This tissue also functions as a mineral reserve and is important in maintaining homeostasis (Rodan, 1998).

The mechanical properties of trabecular bone have been studied extensively and they vary across anatomical site, between sexes and different pathological states (Goldstein, 1987; Keaveny et al. 2001; Yeni et al 2011). The amount of trabecular bone tissue as well as the degree of trabecular strut alignment determine a bone's mechanical strength (Goulet et al. 1994; Maquer et al. 2015) and are expressed through two variables: Bone volume fraction (BV/TV) and degree of anisotropy (DA). BV/TV is the ratio of bone to total volume within a specific region, while DA is the level of trabecular strut alignment. Fully isotropic structures have struts that point in all directions, while fully anisotropic structures have struts that point in one main direction. Additionally, the number of trabeculae (Tb.N.) and their thickness (Tb.Th), as well as the separation of the trabecular struts (Tb.Sp) are important parameters which help describe the mechanical properties of trabecular bone and are measured in trabecular studies (Kleerekoper et al. 1985; Goldstein et al. 1993; McCalden, McGeough and Court-Brown, 1997). The efficiency of this tissue is related to the direction of load and differs when a bone is under compression, tension or shear

forces (Keaveny et al. 1994; Ford and Keaveny, 1996; Kopperdahl and Keaveny, 1998; Keaveny et al. 2001).

Wolff (1892) was one of the first to propose that trabecular bone reflects loads incurred on the skeleton during an individual's life. This concept is known as "Wolff's law", or, more accurately, "bone functional adaptation", and it suggests that the orientation of trabecular struts within a joint adjusts in response to applied forces by aligning to the direction of primary load (e.g. Pontzer et al. 2006; Barak et al. 2011). The apparent density of cancellous bone and its links to bone strength was initially assessed using scanning electron microscopy (Keaveny and Hayes, 1993). Studies then focused on producing simple analytical models to understand the properties of trabeculae, and more specifically the mechanisms of deformation and failure (Gibson, 1985; Rajan, 1985). With improved computational models, the focus shifted to trabecular bone's mechanical properties, investigating dependence of strength, modulus and apparent density on anatomical locations, ages and the directions of loading (Keaveny and Hayes, 1993), as well as comparing pathological to healthy bone (e.g. Hipp et al. 1992). Research then focused on specific regions of interest (2D) or volumes of interest (3D) at different sites of the skeleton. Finite element models (FEM) were integral to these studies, as they realistically represent the in vivo structure (Fyhrie and Hamid, 1993; Hollister et al. 1994; Van Rietbergen et al. 1995). The new methods were used to measure loading and elastic properties of trabecular bone (Feldkamp et al. 1989; Hollister et al. 1994; Van Rietbergen et al. 1995, 1996; Ulrich et al. 1997). More recently clinical studies focused on understanding how trabecular morphology is affected by age-related diseases, such as osteoporosis (e.g. Chen et al. 2010; Nikodem, 2012), as well as implications for bone fracture susceptibility (e.g. Ciarelli et al. 2000; Sran et al. 2007; Hordon et al. 2000).

Recent research has focused on testing bone functional adaptation via experimental methods in various taxa and sites of the skeleton using three-dimensional, non-destructive methods. Pontzer and colleagues (2006) studied the sensitivity of trabecular strut orientation to altered load direction in the distal femur

of guinea fowl. Compared to a control group, they found that trabecular struts responded to changes in load orientation from exercise on inclined treadmills (Pontzer et al. 2006). Age, activity level and phylogeny were controlled for, thus these changes were correlated to the mechanical stimulus. Similar results were found in the distal tibia of sheep. Comparison of two groups of sheep that exercised daily on treadmills with different inclinations revealed that the trabecular struts of the distal tibia in the group on the more inclined treadmill shifted in response to changes in the tibial angle (Barak et al. 2011). Furthermore, compared to a sedentary group, exercised groups had relatively higher BV/TV, Tb.Th and Tb.N, lower Tb.Sp and more plate-like trabeculae, suggesting that both changes in the direction as well as in the magnitude/frequency of load can stimulate remodelling. Furthermore, Volpato and colleagues (2008) demonstrated that bipedally-trained and untrained Japanese macaques show significantly different DA patterns across the ilium and proximal femur. Differences in the DA of the trained macaque were consistent with the transition to bipedalism, but the bipedal pattern was different to that of humans reflecting the different shape and size of the pelvis, as well as the genetic differences between the taxa (Ruff et al. 2006; Ryan and Ketcham, 2005). Tb.Th and BV/TV distribution patterns did not differ between macaques, reflecting similar habitual activities in the two groups. Mazurier and colleagues (2010) further showed that a bipedal-trained macaque exhibited a thicker cortico-trabecular complex (CTC) underlying the tibial plateau, especially in the medial condyle, reflecting loads associated with bipedalism. The CTC was defined as the most dense bone beneath the articular surface, which includes both the cortical shell and the adjacent trabeculae. The links between trabecular distribution and locomotor loads have been further explored using computer simulation. Boyle and Kim (2001) subjected an initially isotropic model of the proximal femur to the predominant forces from walking and climbing stairs, while a space optimisation algorithm assigned material to areas of greatest loading. The struts aligned to the direction of the principal load and the resultant pattern resembled that of the human proximal femur reflecting, this tissues' importance in responding to the mechanical loading of locomotion. Together, these experimental studies offer strong support for bone functional adaptation and reveal that a wealth of information can be gained from trabecular

analysis.

Some studies, however, have produced contradictory results. For example, Carlson and colleagues (2008) failed to find differences in the DA of the distal femoral metaphysis across three groups of mice with different assigned locomotor modes. The first group was restricted to moving in a linear direction, the second was restricted to moving in a turning tube and the third was allowed to move freely with no limitations in direction. Their results indicated that the groups did not differ significantly in the orientation of their trabeculae despite the differences in the predominant moving direction, which resulted in their suggestion that the trabecular bone of the knee may not be an appropriate subject when attempting to reconstruct locomotor modes. Furthermore, Wallace and colleagues (2014) found that cortical bone growth is not closely connected to local strain magnitude in the tibia of sheep. Even though they found that exercise induced bone formation, the regions of greatest bone deposition did not coincide with regions of presumed highest loading. These studies highlight the complexity of studying functional signals with trabecular bone, especially since it is not completely clear how remodelling is triggered. Some suggest that low frequency, high intensity loads stimulate remodelling, while others suggest that high frequency, low intensity loads are most important (Whalen et al. 1988; Rubin et al. 1990; Rubin et al. 2001; Judex et al. 2003; Scherf et al. 2013). Furthermore, a range of activities which fall between the extremes may affect the final structure. Along with these, factors such as age, sex, diet, genetics and hormones (Simkin et al. 1987; Martinon-Torres, 2003) contribute to the variation. Research has shown that bone mineral density and bone turnover rate are largely hereditary (e.g. Dequeker et al. 1987; Kelly et al. 1991; Harris et al. 1998) and that different genes regulate the response of bone at different sites of the skeleton (Judex et al. 2002, 2009). Furthermore, some difference in trabecular architecture between taxa are systemic and could be attributed to factors other than mechanical stimulus. For example, analysis in epiphyses throughout the skeleton revealed systemic patterns in the BV/TV of *Pan* and *Homo*, but not DA, indicating that some parameters can be less informative about functional history than others in certain cases (Tsegai et al.

2018a). Therefore, interpretations of trabecular structure should be made with caution.

Despite the complexities and contradictions in previous studies, overall trabecular analysis has found support for bone functional adaptation. Trabecular struts align parallel to the trajectories of major load (e.g. Pontzer et al. 2006; Volpato et al. 2008) and bone mass increases in regions of highest loading (e.g. Mazurier et al. 2010). This can occur through increased thickness and/or number of trabeculae (Barak et al. 2011). Since trabecular patterns show links to load, the structure of this tissue reflects mechanical stimuli. However, trabecular bone functions within a wider framework which includes the adjacent cortical structure.

1.5. Trabecular bone and cortical bone

Trabecular bone does not function in isolation, as it interacts with the surrounding cortical shell. Both tissues react to load and can be informative about the mechanical loading history of a bone. In cortical bone studies, diaphyseal cross-sectional shape and robusticity have been shown to reflect loading (e.g. Ruff, 1987; Jones et al. 1977; van der Meulen et al. 1993; Ruff et al. 1994, 2006; Shaw and Stock, 2009a), as well as mobility patterns (Shaw and Stock, 2009b, 2013) and can differentiate between taxa/individuals with different locomotor repertoires (e.g. Burr et al. 1989; Marchi, 2005; Ruff, 2009).

Correlations between cortical traits and locomotion have been found in great apes. Carlson (2005) found that African apes with increased arboreal locomotion have more circular femoral cross-sections than those that engage in less climbing, which perhaps reflects more variable loading of the femoral diaphysis during arboreal locomotion compared to terrestrial locomotion. Furthermore, Ruff (2002) found that variation in relative forelimb to the hindlimb strength, as indicated by cortical cross-sectional properties, reflects frequency of climbing in apes. More

suspensory taxa, such as orangutans, show relatively stronger forelimb shafts than hindlimb shafts than more terrestrial or leaping taxa. Additionally, African apes show variation in their proportional strengths consistent with differences in the frequency of their climbing. Chimpanzees show relatively higher ratios of forelimb to hindlimb strength than gorillas, while lowland gorillas show higher ratios than mountain gorillas (Ruff, 2002). Variation in between limb robustness is also found in humans that engage in different habitual behaviours. Highly mobile, terrestrial foragers show stronger lower limb bones, while humans that incorporate a great proportion of marine mobility in their repertoire show stronger upper limb bones (Stock and Pfeiffer, 2001). Furthermore, between humans and non-human apes, cortical cross-sectional traits show differences that reflect loading. In the femoral neck, for example, the distribution of cortical bone differs between ape taxa. Humans show a thin superior cortex that thickens distally, perhaps resulting from tension along the superior cortex and compression along the inferior cortex of the neck during bipedal gait, while African apes show a more evenly distributed thick cortex perhaps resulting from larger axially compressive loads (Lovejoy, 1988; Ohman et al. 1997; Rafferty, 1998). Furthermore, cortical bone distribution in the distal tibia and talus of *Pan* and *Homo* reflects variation in dorsiflexion at the talocrural joint and levels of mobility at the talonavicular joint (Tsegai et al. 2017). Together, these studies suggest that both cortical and trabecular bone may hold functional signals and it is important to study both tissues.

Cross-sectional properties have been used to infer past behaviour (Ruff and Hayes, 1983; Brock and Ruff, 1988; Ruff et al. 1993; Trinkaus et al. 1994; Nikita et al. 2011; Stock and Macintosh, 2016), however, inferences of behaviour based solely on cortical cross-sectional shape should be made with caution, as studies have indicated that cortical bone is not always preferentially reinforced in regions of highest load (e.g. Demes et al. 1998; Wallace et al. 2014) and other factors such as climate (e.g. Pearson, 2000) may affect diaphyseal robusticity. Understanding the relationship between cortical and trabecular bone is also important in anthropological studies. Shaw and Ryan (2012) examined the correlation between trabecular bone distribution and cross-sectional, mid-diaphyseal cortical bone in the humerus and

femur of primates. They found a correlation between the architecture of the two tissues in the humerus, suggesting that the trabecular and cortical bone of this bone respond to overall loading in a similar manner. However, they did not find a correlation in the architecture of the two in the femur implying that the relationship of the two tissues varies across skeletal sites and is perhaps complex. The sensitivity of trabecular bone to mechanical loading may be affected by the response of cortical bone. Since diaphyseal cortical bone for example responds to changes in loading direction (Carlson and Judex, 2007), the response of epiphyseal trabecular bone may in such cases be reduced. This highlights the dependency of the two tissues.

Although the value of studying cortical structure in combination with trabecular bone is recognised, analysis of cortical bone properties was not within the scope of this doctoral dissertation. The emphasis of my dissertation was functional signals in the trabecular bone of the femur in extant apes, as trabecular bone remodels at a faster rate than cortical bone and it can yield information about how an individual loaded its limbs throughout life (Eriksen, 1986; Currey, 2002; Eriksen, 2010), therefore it can be more informative than cortical bone about joint positioning in extinct hominins. It can reflect the actual joint loading in individuals rather than implied joint positioning based on external morphology, which may be inaccurate in instances of phylogenetic lag, rendering it remarkably valuable in studies of functional morphology and locomotion.

1.6. Functional signals in the trabecular structure of extant taxa

Trabecular structure has been studied across several skeletal sites in mammals (e.g. Thomason, 1985a,b; Dumont et al. 2013; Chirchir et al. 2016; Amson et al. 2017; Mielke et al. 2018) and more specifically primates (e.g. MacLatchy and Muller, 2002; Ryan and Ketcham, 2002; Ducher et al. 2004; Maga et al. 2006; Lazenby et al. 2011a; Schilling et al. 2013; Matarazzo, 2015) to understand the relationship between this tissues' morphology and individual behaviour. Two-dimensional studies

provided a first overview of trabecular architecture (e.g. Rafferty and Ruff, 1994), however they lacked valuable information about the three-dimensional structure of trabecular bone. Studies analysing a volume of interest within epiphyses have provided more informative insight into trabecular architecture and a considerable amount of that research focused on the proximal femur of primates. MacLatchy and Muller (2002) compared the femoral head and neck structure of two strepsirrhines, *Perodicticus potto* [potto] and *Galago senegalensis* [bushbaby] and found differences linked to variation in loading. The two taxa, despite not showing differences in femoral head BV/TV, showed differences in trabecular orientation with *G. senegalensis* having more anisotropic trabeculae reflecting the more stereotypical loading of their femur. This link was also apparent in the femoral neck trabecular structure, where *G. senegalensis* had anisotropic trabeculae, but also significantly lower bone density than *P. potto*. Similar results were found for leaping versus non-leaping primates (Ryan and Ketcham, 2002), as well as for primates that are specialised for one mode of locomotion versus non-specialised primates (Scherf, 2008). In both studies, taxa in which the femur experiences more stereotypical loading (i.e. leaping and specialised primates) showed more anisotropic proximal femoral trabecular structure.

Modern humans were also shown to have highly anisotropic femoral head structure, compared to African apes and *Pongo*, reflecting their more specialised locomotion (Ryan and Shaw, 2012, 2015; Ryan et al. 2018). Additionally, primary strut orientation is similar between human populations, as well as between *Pan* and *Gorilla* (Ryan et al. 2018), which reflects the similar loading patterns in these groups during bipedal and knuckle-walking locomotion respectively. Studies have also shown that the BV/TV of the proximal (e.g. Ryan and Shaw, 2015) and distal (e.g. Chang et al. 2008) femur reflects activity level in humans. The femoral head of highly active human hunter-gatherers shows higher BV/TV than that of more sedentary agriculturalists (Ryan and Shaw, 2015; Saers et al. 2016; Ryan et al. 2018). Additional studies have revealed locomotor signals in other joints of the ape hindlimb. Mazurier and colleagues (2010) showed that humans have a thicker cortico-trabecular complex in the medial condyle of the proximal tibia than *Pan*, which is consistent

with the location of maximum force during adduction of the knee in bipedal locomotion (Mazurier et al. 2010). Furthermore, Maga and colleagues (2006) showed that the calcaneal trabecular structure differs in modern humans to African apes and *Pongo*, by having higher DA, lower BV/TV and a unique pattern of trabecular orientation. Additionally, Griffin and colleagues (2010b) showed that the first and second metatarsals of humans differ from those of other great apes in having higher DA in the dorsal aspect of the metatarsal head, which reflects propulsion with the forefoot during bipedal locomotion.

However, the predicted functional signals within trabecular structure are not always clear. Schilling and colleagues (2013) studied the trabecular structure of the lunate, the scaphoid, and the capitate in apes, baboons and spider monkeys. They analysed VOIs from the three bones and found that BV/TV did not reflect their locomotor modes. Furthermore, Scherf and colleagues (2013) did not find a link between the trabecular structure of the humerus and respective locomotion in *Pongo pygmaeus*, *Pan troglodytes* and *Homo sapiens*. Some studies of the trabecular bone of hindlimb joints also failed to find locomotor links. Fajardo and colleagues (2007) evaluated femoral neck trabecular structure in New World monkeys, Old World monkeys and apes and found no significant differences between taxa assigned to different locomotor groups despite presumed differences in their loading patterns. Furthermore, they found no significant differences in superior/inferior distributions of trabecular bone, though they noted that quadrupeds appear to have higher BV/TV inferiorly and that suspensory taxa have more even BV/TV distributions. Similarly, studies of the trabecular distribution in the humeral and femoral heads of Old-world monkeys, chimpanzees and howler monkeys (Ryan and Walker, 2010), as well as the femoral head of anthropoids (Shaw and Ryan, 2012) failed to find a functional signal in the trabecular distribution. Furthermore, calcaneal trabecular architecture was found to be similar between humans and chimpanzees despite their variation in Achilles tendon length (Kuo et al. 2013), which appears to contradict previous research in potoroos showing that the complete disuse of the Achilles tendon has a great effect on calcaneal trabecular architecture (Biewener et al. 1996).

Generally, studies in extant taxa have demonstrated that trabecular structure shows links to behaviour and more precisely that the trabecular bone of the major primate hindlimb joints holds locomotor signals. Taxa that are specialised for one mode of locomotion have more aligned trabeculae compared to taxa with more variable locomotion (e.g. MacLatchy and Muller, 2002; Scherf, 2008) and trabecular organisation in key joints reflects loading from locomotor behaviours (e.g. Mazurier et al. 2010; Ryan et al. 2018). Therefore, determining the links between trabecular bone structure and locomotion may be useful to studies of the locomotion of extinct hominins.

1.7. Functional signals in the trabecular structure of fossil hominids

Trabecular studies have provided insight into the behaviour of extinct hominins. Using two-dimensional radiographs, Rook and colleagues (1999) compared the iliac trabecular structure of *Oreopithecus* to that of *Homo*, *Pan*, *Hylobates* and *Papio* and concluded that this hominin shares traits with *Homo* linked to bipedality. Similarly, by analysing iliac trabecular patterns, Macchiarelli and colleagues (1999) found that *A. africanus* and *P. robustus* have a unique trabecular pattern which may have developed as a result of both arboreal climbing and bipedalism. Pelvic trabecular organisation has also revealed that humans and chimpanzees have different patterns of strut orientation above the acetabulum which reflect their hip biomechanics and that Neanderthals have a pattern which resembles that of humans (Martinon-Torres, 2003). Femoral trabecular patterns have also been used to infer locomotion in fossil hominoids. Scherf (2008) studied the proximal femoral structure in Old World monkeys, New World monkeys and apes, they compared the trabecular patterns found to those of two Miocene apes, *Paidopithecus rhenanus* and *Pliopithecus vindobonensis*. Their results revealed that the structure in these Miocene apes was not the same as any of the studied taxa and that they were generalists that occasionally engaged in high impact activities. More recently, Ryan and colleagues (2018) found human-like femoral head trabecular

structure in *Australopithecus africanus* and *Paranthropus robustus*. Although individuals of the extinct taxa had significantly higher BV/TV than modern humans (apart from one highly active human group), they overlapped in DA values with the modern human groups and almost all showed human-like primary strut orientation. Similar results were found for the distal tibia (Barak et al. 2013a) and talus (DeSilva and Devlin, 2012). Barak and colleagues (2013a) showed that humans use an extended ankle during locomotion while chimpanzees use a more flexed ankle, and this is reflected in the different trabecular strut orientation of the distal tibia in the two taxa. Comparison with *Australopithecus africanus* specimens from Sterkfontein revealed that the trabecular strut orientation in these hominins is similar to that of humans, suggesting the use of an extended ankle. However, other parameters fall mostly between the human and chimpanzee ranges. Similarly, DeSilva and Devlin (2012) found that trabecular patterns in the talus of *A. africanus* are generally more similar to humans than African apes, *Pongo* and *Papio*, though similarities across taxa suggest that this may not solely be a result of mechanical loading.

Analysis of the *A. africanus* and *P. robustus* trabecular structure has produced mixed results. The trabecular structure of the femur (Ryan et al. 2018) and the tibia (Barak et al 2013a) suggests that these taxa are similar to modern humans, specifically in DA values and strut orientation. These results have been interpreted as showing that these hominins were obligate bipeds and potentially had a biomechanically similar gait to modern humans. However, the trabecular patterns of the ilium (Macchiarelli et al. 1999) and the talus (DeSilva and Devlin, 2012) suggest that *A. africanus* and *P. robustus* also share some trabecular traits with African apes and *Pongo*. This perhaps indicates that these taxa were not specialised, obligate bipeds but also engaged in some arboreal behaviours. Therefore, these studies have produced inconsistent results that complicate inferences of behaviour in these extinct hominins.

The majority of trabecular research, in both extant and extinct taxa, has focused on isolated regions within the epiphyses. Therefore, the lack of a strong functional signal in some studies may be an artefact of analysing a subvolume which

excludes much of the diversity in the trabecular structure. The size and placement of a VOI has been shown to have a significant effect on results (Fajardo and Müller, 2001; Maga et al. 2006; Lazenby et al. 2011b; Kivell et al. 2011). For example, analysis of the primate capitate and third metacarpal revealed that the VOI location, and to a lesser extent the size of the VOI, affects findings relating to trabecular connectivity, DA and the principal orientation of trabeculae (Kivell et al. 2011). The assumption of bone continuity (Harrigan et al. 1988; Hoffer et al. 2000) could also be violated. These factors should be taken into consideration when interpreting results from studies that focus on just one small VOI of a given bone, though the influence of size and location of the VOI may not be as great when the shape of the structure is spherical (Maga et al. 2006; Marangalou et al. 2014). Alternatively, trabecular structure can be analysed within entire epiphyses.

1.8. The whole-epiphysis approach to trabecular bone analysis

More recently research has focused on analysing entire epiphyses with a new 3D method called medtool (see Gross et al. 2014 for description). Medtool (www.dr-pahr.at) quantifies trabecular structure throughout an epiphysis and visualises the 3D distribution of BV/TV and DA in the form of a colour map in which values are represented by a selected colour range. The resulting colour maps depict the distribution of parameters across the epiphysis allowing for better interpretation of joint loading.

This holistic approach has been used to investigate trabecular architecture variation in the third metacarpal of knuckle-walking (*Pan*, *Gorilla*) and suspensory apes (*Pongo*, *Hylobates*, *Symphalangus*) in comparison to humans, that mainly use their hands for manipulation (Tsegai et al. 2013). Results showed that BV/TV distribution in the third metacarpal head coincides with the predicted regions of highest stress based on differences in hand posture during habitual activities. Furthermore, DA is high in knuckle-walking taxa, low in suspensory brachiators and

variable in humans. This is consistent with predictions based on loading of the hand in more stereotypical postures during knuckle walking, compared to climbing and manipulative behaviours. The same approach was used to investigate functional signals in the trabecular structure of metacarpals and infer hand use of *Australopithecus africanus* (Skinner et al. 2015). The authors showed that trabecular bone distribution matches predictions of peak loading during predominant hand postures in humans and non-human apes and concluded that *A. africanus* may have loaded their hands in a more human-like way. Additionally, holistic investigations using medtool revealed locomotor-related patterns in the talus and distal tibia of *Pan* and *Homo* (Tsegai et al. 2017) and detected bilateral asymmetry in the thumb of these taxa (Stephens et al. 2016). These studies demonstrate that analysing the whole epiphysis provides additional information about trabecular structure, such as the 3D and subarticular distribution of parameters, as well as evidence about potential joint posture which could be missed when analysing isolated volumes within the centre of an epiphysis. However, this method is limited in that it lacks statistical comparisons (up to this point), something that was possible with the traditional VOI studies.

The trabecular architecture of hindlimb joints has been studied extensively using VOIs (see above), though never using a whole-epiphysis approach. The aim of this doctoral dissertation is to identify locomotor-related trabecular patterns in the femur of hominids by analysing the femoral head and distal femur holistically, with the ultimate aim of inferring the locomotor behaviour of South African extinct hominins.

1.9. Trabecular bone and body mass

One factor affecting trabecular structure is body mass. Doube and colleagues (2011) investigated allometric relationships in the trabecular structure of the femoral head in a wide range of mammals and birds, ranging from 3 to 3400 kg. They

concluded that BV/TV and DA do not scale to body mass in mammals but other parameters, such as Tb.Th and Tb.Sp, scale with positive allometry suggesting that larger mammals have relatively thicker trabeculae and that their trabeculae are relatively more widely spaced. However, the slopes for Tb.Th and Tb.Sp indicate a negative allometric relationship for these parameters, suggesting that their relationship with body mass is the opposite to what the authors reported and therefore that larger mammals have relatively thinner trabeculae and that their trabeculae are relatively less widely spaced. Furthermore, they showed that larger mammals have relatively few trabeculae which is reflected in the negative allometric relationship of connectivity (Conn.D) with body mass. Ryan and Shaw (2013) evaluated the allometric relationships of trabecular parameters within the humeral and femoral heads in a sample of primates. They performed both conventional and phylogenetic regressions and found that DA does not scale to body size. However, they found a weak, positive allometric relationship between BV/TV and body size. Furthermore, in contrast to what Doube and colleagues (2011) reported, they found that Tb.N, Tb.Th and Tb.Sp scale with negative allometry suggesting that large primates have relatively few, thin trabeculae, that are closer to each other compared to small animals. These results were largely in accordance to allometric relationships found previously in primate vertebrae (Cotter et al. 2009). Barak and colleagues (2013b) conducted a meta-analysis of existing data on trabecular allometry in mice, rats and humans. They did not find an allometric relationship between BV/TV or DA with body mass, but found a negative allometric relationship for Tb.N, Tb.Th and Tb.Sp, similar to what was found by Ryan and Shaw (2013). They also investigated the correlation of Tb.Th and Tb.N with BV/TV and found that the relationships differ between rodents and humans. Similarly, Barak and colleagues (2011) found that in rodents, higher BV/TV was achieved through increasing the number of trabeculae whereas in humans it was achieved through increasing their thickness, suggesting that BV/TV is increased through different mechanisms depending on the size of the animal. These studies found a negative correlation between body mass and Tb.N but a positive correlation with Tb.Th and Tb.Sp, indicating that larger animals have absolutely fewer, thicker and more widely spaced trabecular.

Overall, these studies suggest that Tb.N, Tb.Th and Tb.Sp can be significantly affected by body mass and therefore this should be taken into account when interpreting the trabecular structure, especially in comparative studies in which the sample varies substantially either intra- and/or interspecifically in body mass.

1.10. Trabecular bone ontogeny

Trabecular architecture changes while an individual is growing, and many studies have focused on how trabecular parameters change through early development. Both modelling and remodelling of bone in response to strain vary with age (Bertram and Swartz, 1991; Ruff et al. 1994; Lieberman et al. 2003), with changes in bone structure being more obvious during childhood. Studies have suggested that ontogenetic loading defines the adult structure (Pearson and Lieberman, 2004; Pettersson et al. 2010), however research showing the effects of adult mechanical loading on bone modelling suggests that adult loading patterns are also important for the final pattern (Ruff et al. 2006 and references therein). Therefore, both childhood as well as adult mechanical loading are likely represented, to varying extents, in the adult bone form. The ontogeny of trabecular bone is well documented in some regions of the human skeleton (e.g. Ding et al. 2005; Ryan and Krovitz, 2006; Raichlen et al. 2015; Milovanovic et al. 2017), but far less so in other apes (e.g. Zeininger, 2013; Tsegai et al. 2018b).

The human pelvis and associated soft tissues start emerging *in utero* from one mesenchymal mass that originates from the lateral mesoderm (Chevallier, 1977; Lee and Ebersson, 2006; Pomikal and Streicher, 2010). The hindlimb starts developing at 3 weeks and is pivotal in the development of the pelvis, as normal morphogenesis of the acetabulum depends on the interactions with the femoral head (Harrison, 1961; Lee and Ebersson, 2006) and is controlled by muscular loading of the hip (Hall, 1972; Pitsillides, 2006). The trabecular structure of the proximal femur derives from two growth plates; the capital epiphyseal plate of the femoral head and the apophyseal

plate of the greater trochanter (Taussig et al. 1976; Serrat et al. 2007). The separate compartments eventually fuse to form one continuous trabecular structure. In the distal femur, the diaphysis of humans is elongated by preferential deposition of bone on the medial compartment of the distal portion during development, leading to the human valgus angle (Tardieu and Preuschoft, 1995 and references therein). Additionally, in humans the sacrum becomes more curved, the pelvic girdle becomes more stable and lumbar lordosis starts appearing (Le Damany, 1905; Abitbol, 1987a,b; Tardieu, 2000; Tardieu et al. 2013). These skeletal changes are linked to the development of a bipedal gait and the associated loads are expected to be reflected in the trabecular architecture.

Analysis of ontogenetic trabecular patterns in the human hindlimb has shown that the patterns show links to different locomotor phases during development. Ryan and Krovitc (2006) used a sample of bones from humans that ranged in age from a foetus to 8-10 years old to show that trabecular patterns reflect locomotion-related loading at each developmental stage. Their results revealed an initial decrease in BV/TV, Tb.N and DA from 6 to 12 months postnatally and a slight increase between the ages of 2 and 3, associated with a shift to unaided walking. These are consistent with findings from the femoral neck (Milovanovic et al. 2017). Furthermore, Raichlen and colleagues (2015) used a sample of tibiae from children aged 1 to 8 years and kinematic data from an age-matched population to show that trabecular orientation in the distal tibial metaphysis reflects locomotion at different ages. Specifically, they showed an association between changes in tibial angle variation and DA. Older individuals had higher and less variable DA, which may be linked to greater stability as gait matures (Sutherland et al. 1980; Adolph, 2003). Eventually patterns converge towards a bipedal adult pattern, though trabecular architecture continues to change, to a lesser extent, until later ages. For example, bone volume fraction in the femoral neck declines with age in both sexes, but the effect is more intense in women (Slemenda et al. 1996). Furthermore, trabecular number in the proximal tibia decreases with age and this loss appears to vary between sexes (Ding et al. 2005) but always leads to decreased mechanical integrity of the tibia.

Variation in trabecular structure during growth is less well-documented in non-human apes. Zeininger (2013) analysed the trabecular structure within VOIs of the talus, calcaneus and first metatarsal in African apes and found that trabecular parameters do not vary significantly with age. Though she generally did not find differences in DA between the age groups of the taxa, results showed that the orientation of trabeculae in the talus changes as age increases in the African apes, perhaps reflecting changes in joint positioning during development. Interestingly, chimpanzees presented more differences in trabecular structure across age groups than gorillas, perhaps reflecting the different rates of their locomotor development (Doran, 1997). More recently, Tsegai and colleagues (2018b) investigated trabecular ontogenetic variation in the chimpanzee humerus, femur and tibia and found that BV/TV as well as Tb.Th increase with age in all the studied skeletal elements. Together with a higher ratio of femoral to humeral BV/TV at later ages, this reflects increased loading of these elements during chimpanzee development, perhaps associated with the increasing use of knuckle-walking. DA in the humerus and tibia also reflects the transition to increased terrestrial knuckle-walking at the age of 5 years (Sarringhaus et al. 2014), as at this age DA starts increasing. Furthermore, BV/TV distribution changes through growth in all three elements and patterns reflect changing loading conditions within each of the joints.

Despite evidence for a link between trabecular bone structure and changes in locomotion during ontogeny, some propose that there is a basic genetic blueprint which dictates how trabecular bone is distributed. Cunningham and Black (2009a,b,c) reported that trabecular, as well as cortical bone, in the ilia of prenatal and neonatal humans are distributed in a similar manner to adults. They propose that since the hindlimb is not bearing any weight at this point of the development (Walker, 1991) this pattern should be interpreted based on other parameters, such as genetic factors and involuntary limb movement while *in utero*. They further suggest that remodelling of the tissue is superimposed on the pre-existing pattern when load is applied. However, the studies presented here show a strong link between trabecular morphology and loads associated with developing locomotor skills at different ages. Since locomotor maturity can affect trabecular structure, the age of a specimen is an

important variable in studies aiming to determine locomotion from trabecular patterns.

1.11. New methods in trabecular analysis: Geometric morphometrics

Recently, geometric morphometrics have been incorporated into trabecular bone analyses to better quantify and compare potential variation in bone structure across different taxa (Sylvester and Terhune, 2017). Traditionally, geometric morphometrics (GM) have been used to examine external, rather than internal, morphological variation in skeletal elements. In GM, overall form (size and shape) or isolated shape (with variation in size removed) is compared using homologous landmarks on specimens which define the structure (Bookstein, 1991; Dryden and Mardia, 1998; Mitteroecker and Gunz, 2009). Three types of landmarks are used: Type I landmarks which are clearly identifiable, biologically homologous points on the structure (e.g. the intersection of tissues), Type II landmarks which are points defined based on the geometry (e.g. the tip of a curve) and Type III landmarks which are points that are defined relative to other points of the structure (e.g. one end of the longest dimension) (Bookstein, 1991). After landmarks are defined on all specimens, they are centred, scaled and rotated to minimize Euclidean distances between homologous landmarks; a method known as Procrustes analysis (Rohlf and Slice, 1990; Bookstein, 1996; Dryden and Mardia, 1998). This landmark-based analysis can be extended to surfaces that lack identifiable landmarks by using semilandmarks (Bookstein, 1997; Gunz et al. 2005). Semilandmarks are allowed to move following certain optimization criteria (Mitteroecker and Gunz, 2009) and do not represent anatomical traits. Three different types of semi-landmarks have been described (Weber and Bookstein, 2011; Cooke and Terhune, 2015): Type IV which are semilandmarks on curves, Type V which are semi-landmarks on surfaces and Type VI which are constructed semilandmarks. In trabecular analysis geometric

morphometrics can be used to identify homologous landmarks across specimens so that trabecular structure can be compared across three-dimensional surfaces.

Sylvester and Terhune (2017) used GM to assess trabecular variation across the articular surfaces of the talus and distal femur in apes. Semilandmarks were used to locate appropriate homologous locations across the surfaces of these bones where VOIs were placed to sample trabecular bone. Trabecular parameters were extracted at each location and compared between samples. Results revealed that trabecular parameters are not evenly distributed across articular surfaces and that the 3D distribution of parameters may be more important than looking at mean values. Similar methodology was applied to study BV/TV and DA distributions in the metacarpals of apes (Dunmore et al. in press) and revealed locomotor-linked patterns in the trabecular bone. What these studies add to trabecular analysis is the ability to statistically compare the distribution of trabecular parameters over large surfaces. In prior studies, variation in trabecular parameters within a structure was evaluated with the use of multiple VOIs (e.g. Ryan and Ketcham, 2002; Barak et al. 2013a; Barak et al. 2017). However, using VOIs misses the fine detail that landmark-based analyses can provide, as analysis is confined to these selected locations. Results from these studies highlight the importance of the distribution of trabecular parameters in understanding variation of joint position during locomotion, and therefore the need to incorporate three-dimensional statistical analysis into trabecular studies. In this doctoral dissertation, geometric morphometrics and the whole-epiphysis approach are combined to analyse trabecular patterns beneath the subchondral layer of the femoral epiphyses and better understand locomotor signals in the femur of hominoids.

1.12. Summary

The evolution of bipedalism, from its initial appearance to the modern form, has received great attention over the last decades. Many have tried to investigate how this trait evolved however the debate persists. Trabecular bone analysis can be of great value in this research. This tissue's overall structure increases the bones' integrity while maintaining a light structure and is correlated to joint loads. Given that individuals with different locomotor repertoires position their limbs in various ways and apply different loads on their limbs we expect that they will have distinct trabecular networks. Therefore, analysing these patterns in extant apes can help understand relationships with behaviour and eventually understand extinct hominin locomotion.

Expanding on prior research which focused on small subvolumes, I analyse the whole trabecular structure within the femoral head and the distal femoral epiphysis of great apes and humans to identify locomotor signals. Furthermore, I extend this methodology to the analysis of extinct hominin trabecular patterns in an attempt to understand their modes of locomotion.

Chapter 2

Materials and Methods

2.1. Sample and Scanning

Individuals from four ape genera were selected to investigate variation in the trabecular bone of the femur in extant hominids. The *Pan* sample was comprised of two subspecies. *Pan troglodytes verus* individuals came from the Tai forest collection of the Max Planck Institute for Evolutionary Anthropology. *Pan troglodytes troglodytes* individuals came from a collection of the Smithsonian National Museum of Natural History. Four of the *P.t.troglodytes* individuals were from Gabon and one was from Cameroon. The *Gorilla* individuals were selected from the Primate collection of the Powell-Cotton museum. All were western lowland gorillas (*Gorilla gorilla gorilla*); one individual was from the Democratic Republic of the Congo and thirteen individuals were from Cameroon. The *Pongo* individuals came from the Mammal collection of the Zoologische Staatssammlung München. The *Pongo* sample consisted of one *Pongo abelii* individual, one unspecified and five *Pongo pygmaeus* individuals. All specimens were adult and showed no signs of pathologies. The non-human apes were wildshot, except two orangutans which came from zoos. The captive orangutans were only included in the analysis when they showed no significant differences to the wild individuals.

The *Homo sapiens* individuals were from two 19th-20th century cemeteries in Germany. One was located at the village of Inden and the other in Gottingen. These individuals were selected as they were considered representative of modern human populations which (presumably) do not frequently engage in significant levels of high impact activities, such as running, since my aim was to identify a bipedal walking signal in humans. However, as there were no life history data for these individuals this assumption was approached with caution. Additional specimens, for which the life history information was available, were scanned from the skeletal collection curated by the Skeletal Biology Research Centre at the University of Kent. Inspection of the resulting scans however revealed non-bone inclusions which could not be separated from the trabecular structure during segmentation and therefore the

scans could not be used. Further human specimens were excluded from analysis due to permission issues.

Three fossil specimens were included in this dissertation to help identify locomotor signals in the femur of Plio-Pleistocene South African hominins. Two were proximal femora (StW 311 and StW 522) that came from the Sterkfontein caves in South Africa and are curated at the University of Witwatersrand, South Africa. Both preserve a complete femoral head but incomplete proximal femoral epiphyses. StW 522 preserves the femoral neck and part of the proximal diaphysis, while StW 311 only has a partial femoral neck. Originally, these were both assigned to *Australopithecus africanus* based on the remains and the age of the stratigraphic layer they were found in, however after a review of the Sterkfontein stratigraphy (Kuman and Clarke, 2000) StW 311 was given a younger age. The additional specimen was a distal femur from Sterkfontein (TM 1513) curated at the Ditsong museum, South Africa. This was also assigned to *A. africanus*. TM 1513 is nearly complete, only missing part of the lateral portion of the articulation for the patella. Furthermore, to examine variation in the trabecular patterns of the femoral head in extinct obligate bipeds, a fossil *Homo sapiens* (OHALO II H2) curated at the University of Tel Aviv, and two Neanderthal specimens (Krapina 213 and Krapina 214) curated at the Croatian Museum of Natural History were included in the analysis. These specimens preserve complete proximal epiphyses. Additional fossil specimens (D322 15, D322 16, SK 82, SK 97, SK 3121 and SKW 19) were scanned and processed, however were excluded from analyses as either they did not preserve enough of the trabecular structure or they presented issues during segmentation.

Micro-computed tomographic scans of the extant sample were obtained using a Nikon XT 225 ST microCT scanner in the Cambridge Biotomography Centre (*Gorilla*) and a BIR ACTIS 225/300 industrial microCT scanner in the Department of Human Evolution at the MPI (*Pan, Pongo, Homo* and fossils). Both epiphyses were scanned separately to achieve the highest possible resolution and resolutions ranged from 0.030 to 0.085 μm . Scans were reconstructed from 1080 projections into 16-bit TIFF image stacks of isotropic voxel sizes. The scans were reoriented into approximal

anatomical position in AVIZO 6.3[®] (Visualization Sciences Group, SAS) and cropped to reduce dataset size. Large scans were down-sampled before further processing.

2.2. Segmentation

In preparation for analysis in medtool 4.1 the extant sample scans and the Neanderthals were converted from 16-bit unsigned short datasets into 8-bit datasets using the Ray Casting Algorithm (Scherf and Tilgner, 2009) (Figure 2.1). This algorithm separates bone from air by tracking the edges of the trabeculae and cortical bone. It requires the definition of three values: a lower and upper threshold of the greyscale range of bone, as well as an edge strength value which represents the difference between grey values in neighbouring bone voxels. The three parameters are selected independently for each individual and tested prior to final segmentation. The product of the segmentation is a binary dataset where everything that is not bone has a value of 0, while bone has a value of 1.

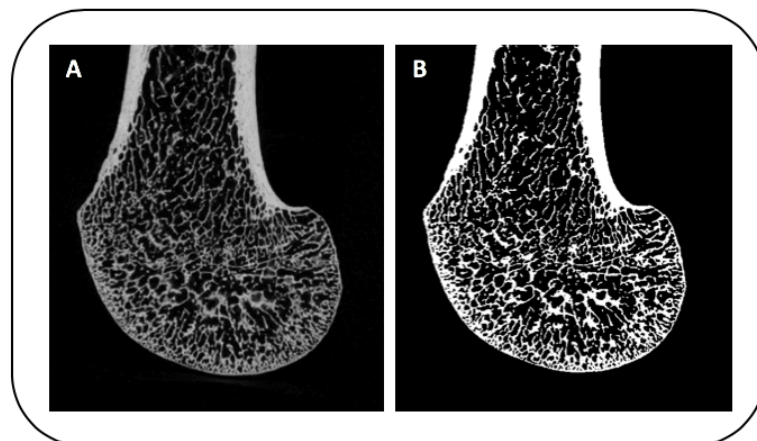


Figure 2.1. Example of RCA segmentation of a Gorilla distal femur. (A) Original greyscale dataset. (B) Resulting segmented dataset.

The remaining fossils were segmented using the MIA-clustering method (Dunmore et al. 2018). This method requires the definition of a grid-size and a set

number of classes. Voxels are assigned to the different classes on a probability basis. Initially, this is done with a global segmentation within each sub-volume, or grid, and then a local fuzzy c-means segmentation. Voxels in overlapping cubes are assigned to the class with the highest membership probability. In this dissertation grid-size was selected by measuring the thickness of the thickest trabeculae in a cross-section of the fossils and selecting a slightly higher value. Three classes were used for the *A. africanus* fossils and two for the *H. sapiens* to distinguish inclusions from bone and air. Finally, a labels-field was used in AVIZO 6.3® (Visualization Sciences Group, SAS) to isolate the cortical and trabecular structure and obtain the segmented binary file.

2.3. Trabecular architecture analysis

Following segmentation, the binary datasets were processed in medtool 4.1 (www.dr-pahr.at). A clean filter was initially applied to remove voxels defined as bone which are not attached to the main structure. This was used to eliminate “noise” voxels which were incorrectly classified as bone. Subsequently, a close operation was performed to seal holes along the outer cortical bone. In this operation a sphere of predefined size was used to identify small inconsistencies in the outer shell and then classify them as bone. The size of the sphere was selected based on the mean thickness of trabeculae.

Morphological filters were then used to define the area of the whole structure. Seven rays, one in each direction of a unit cube and three across the diagonals, were used to detect the edges of the cortical shell. These identified the first voxels in each direction that were marked as “bone”, or had a value of 1, and the last voxels on the opposite end to identify the area of the structure. All outer voxels that were met and marked as bone more, or equal, to 5 out of 7 times were considered as edge voxels. A closing operation with a spherical kernel then “closed” all voxels between those of the external shell, by assigning them a value of 1. This resulted in a dataset where the area of the bone (including the cortical shell,

trabecular bone and the inner air) had a value of 1 and everything surrounding the cortical shell had a value of 0. Next, the area deep to the cortical shell was defined. Voxels of the outer shell were identified and the first empty voxels deep to those were used to mark the beginning of the trabecular area. In the resulting dataset all voxels of the outer shell and air were given a value of 0, and the inner voxels a value of 1 (Figure 2.2A). In this step, both an opening and a closing operation were performed to ensure accurate isolation of the inner area.

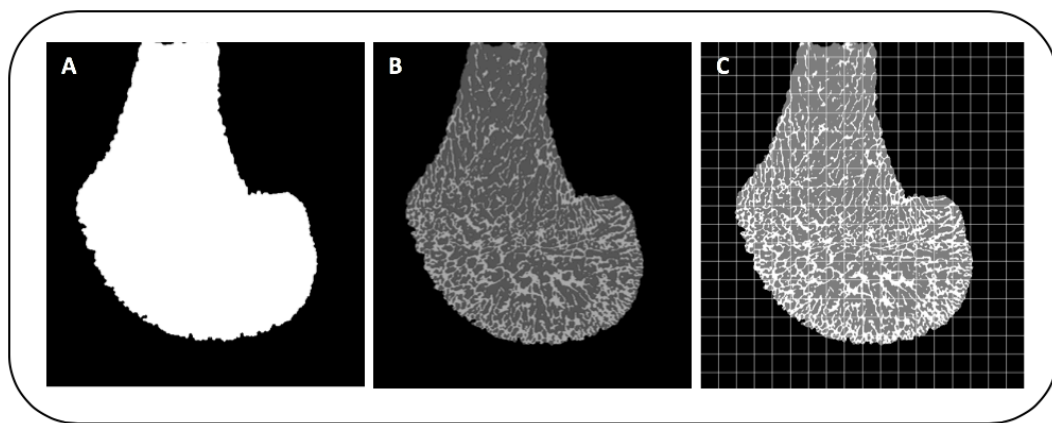


Figure 2.2. Example of processing steps prior to meshing. (A) Definition of inner trabecular area. (B) Trichromatic dataset with defined outer air (0), inner air (1) and trabecular bone (2). (C) Background grid used to measure BV/TV and DA.

During the definition of the different areas, separation of trabecular from cortical bone was sometimes problematic, specifically in c-shaped regions of the bone. This was overcome by applying a corrective filter within a manually defined bounding box. The filter runs an iterative algorithm within the selected volume and re-assigns voxels to bone or air. This step was added when inspection of the initial separation of areas revealed errors.

Next, the defined trabecular area, was subtracted from the whole bone area to separate the area occupied by the cortical shell. This was then subtracted from the segmented dataset to isolate the trabecular structure for subsequent analysis. Pixel-based trabecular thickness was calculated from the trabecular structure dataset using the BoneJ plugin in ImageJ. BoneJ calculates the mean thickness of the

trabeculae by fitting maximal spheres in all the points of the structure. Local thickness is equal to the diameter of the largest sphere fitting within the structure and that contains each point. The weighted average is then calculated. This was used to validate the size of the sphere used in each specimen in the initial close filter. When this calculated sphere size differed to the initial sphere size used, the previous steps (from the close filter to the subtraction of the cortical shell) were repeated.

The inner area and trabecular structure datasets were then combined to create a trichromatic mask (Figure 2.2B). In this, the outer air had a value of 0, the air between trabeculae had a value of 1 and trabecular bone had a value of 2. Before trabecular analysis, the isolated inner structure was used to create a 3D mesh. The resolution of the inner area dataset was coarsened by a factor of 4 and a cleaning filter, followed by a closing operation, was applied. Tetrahedral finite elements with a size of 0.6 mm were fitted to the resulting dataset, creating the model of the inner area and smoothing of the mesh was achieved through optimization filters. Tetrahedral elements were preferred over hexahedral elements as they have been previously used in similar trabecular analysis (e.g. Tsegai et al. 2013; Skinner et al. 2016) and research has shown that finite element models built with tetrahedral elements produce better results in trabecular analysis than hexahedral element models (Ulrich et al. 1998).

Finally, the trichromatic dataset was divided into rectangular cells with 3.5mm width (Figure 2.2C) and a spherical sampling sphere of 7.5 mm was used to calculate local BV/TV and DA at each node of the grid. The size of the sphere was chosen to ensure a meaningful measurement of trabeculae. BV/TV was calculated as the ratio of bone voxels to air voxels within each sphere and DA was calculated with the Mean Intercept Length method and as $DA=1-(\text{smallest eigenvalue}/\text{largest eigenvalue})$. The calculated values were then interpolated onto the centre of the different tetrahedral elements. This resulted in the visualisation of the 3D distribution of these values, where BV/TV and DA values were represented by a colour scale (Figure 2.3). Additionally, in the proximal femur a Paraview function was used to threshold BV/TV values and visualise internal concentrations.

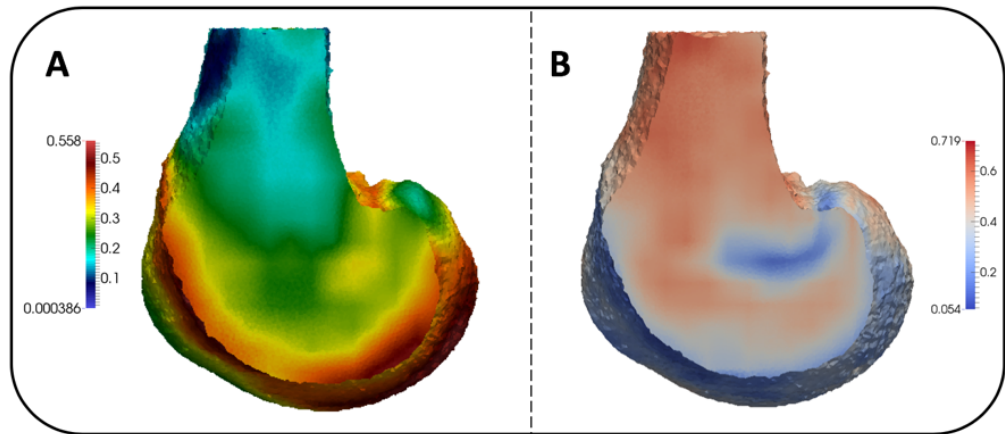


Figure 2.3. Distribution maps. (A) BV/TV distribution map. (B) DA distribution map.

Medtool 4.1 was further used to obtain mean values for trabecular parameters within regions of the epiphyses. Trabecular separation (Tb.Sp) and trabecular thickness (Tb.Th) were calculated based on the Hildebrand and Ruesegger (1997) method, which is similar to what is described in the BoneJ plugin. Trabecular number (Tb.N) was calculated as $Tb.N=1/(Tb.Th+Tb.Sp)$.

2.4. Geometric morphometrics

Interspecific differences in BV/TV distributions beneath the subchondral layer were examined statistically using geometric morphometrics in combination with the approach described above. Homologous landmarks were selected on the femoral head and the distal femoral articular surface of the four studied taxa (described in Tables 2.1 and 2.2). BV/TV values at each landmark were used for further statistical analysis.

Table 2.1. Femoral head landmark description.

Landmark	Description	Type
1	Medial point on head-neck border at neck midline	III
2	Lateral point on head-neck border at neck midline	III
3	Posterior point on head-neck border at neck midline	III
4	Anterior point on head-neck border at neck midline	III
5	Superior point at midpoint of the head	III
6-12	Curve between fixed landmarks 1 and 3	IV
13-19	Curve between fixed landmarks 3 and 2	IV
20-26	Curve between fixed landmarks 2 and 4	IV
27-33	Curve between fixed landmarks 4 and 1	IV
34-41	Semilandmarks between fixed landmarks 1 and 5	Semilandmarks
42-49	Semilandmarks between fixed landmarks 5 and 2	Semilandmarks
50-57	Semilandmarks between fixed landmarks 3 and 5	Semilandmarks
58-65	Semilandmarks between fixed landmarks 5 and 4	Semilandmarks
66-109	Semilandmarks across the inferior-posterior quarter	Semilandmarks
110-153	Semilandmarks across the superior-posterior quarter	Semilandmarks
154-197	Semilandmarks across the superior-anterior quarter	Semilandmarks
198-241	Semilandmarks across the inferior-anterior quarter	Semilandmarks

Table 2.2. Distal femur landmark description.

Landmark	Description	Type
1	Point where superior border meets medial edge of patellar groove	III
2	Point where medial border of patellar groove meets medial border of medial condyle	II
3	Medialmost point of superior border of medial condyle	III
4	Lateralmost point of superior border of medial condyle	III
5	Deepest point of intercondylar notch	II
6	Medialmost point of superior border of lateral condyle	III
7	Lateralmost point of superior border of lateral condyle	III
8	Point where lateral border of patellar groove meets lateral border of lateral condyle	II
9	Point where superior border meets lateral edge of patellar groove	III
10-14	Curve between fixed landmarks 1 and 2	IV
15-23	Curve between fixed landmarks 2 and 3	IV
24-26	Curve between fixed landmarks 3 and 4	IV
27-34	Curve between fixed landmarks 4 and 5	IV
35-41	Curve between fixed landmarks 5 and 6	IV
42-43	Curve between fixed landmarks 6 and 7	IV
44-49	Curve between fixed landmarks 7 and 8	IV
50-52	Curve between fixed landmarks 9 and 1	IV
53-120	Semilandmarks across the patellofemoral articulation	Semilandmarks
121-169	Semilandmarks across the lateral condyle	Semilandmarks
170-253	Semilandmarks across the medial condyle	Semilandmarks

Prior to landmarking, the surface tetrahedra of each model were extracted and Poisson surface reconstruction was used in MeshLab to smooth the surface. The fixed homologous landmarks were first identified for both epiphyses and a repeatability test was used to evaluate their reliability. For this, the fixed landmarks were selected on three individuals of the same taxon at ten different occasions and their PCA coordinates were visualised using R v3.4.1 (R Core Team, 2017) (Figure 2.4). Since the difference between each set of repeated landmarks was smaller than the difference between individuals these landmarks were deemed appropriate.

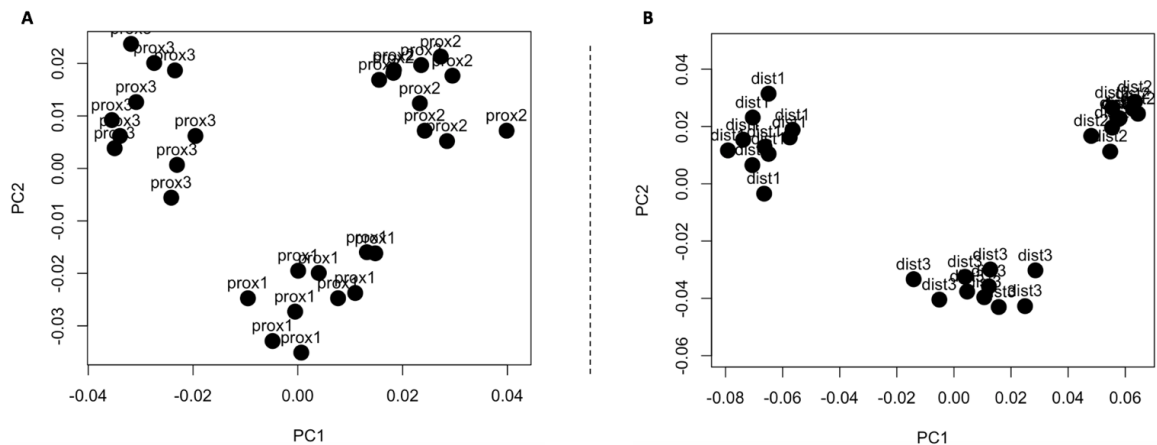


Figure 2.4. Repeatability test for fixed landmarks used in the proximal and distal femur.

(A) Repetitions of fixed landmarks on the femoral head of three *Gorilla gorilla* specimens; prox1 is specimen M95, prox2 is specimen M96 and prox3 is specimen M798. PC1 explains 53% of the variance and PC2 explains 35% of the variance. (B) Repetitions of fixed landmarks on the distal femur of three *Pan troglodytes* versus specimens; dist1 is specimen MPITC 11778, dist2 is specimen MPITC 11800 and dist3 is specimen MPITC 13434. PC1 explains 68% of the variance and PC2 explains 18% of the variance.

The landmark template used for both epiphyses are shown in Figure 2.5. In the proximal femur, five fixed landmarks were selected; one in each direction of the head-neck boundary and one on the surface of the femoral head at the midpoint of the four corner landmarks. Four curves were then defined along the boundary of the articulation between the corner landmarks. In the distal femur, nine fixed landmarks were selected on the boundary of the articular surface following Gould (2014). Eight curves were defined between these fixed landmarks. The curve extending along the later border of the articulation for the patella was excluded as it is missing in TM1513.

Equally-spaced semilandmarks were then defined across the articular surface for each epiphysis (Figure 2.5). In the proximal femur two hundred and eight semilandmarks were defined, while in the distal femur two hundred and one semilandmarks were defined. Both the fixed landmarks and the curve landmarks were placed on all individuals using Checkpoint (Stratovan Corporation), while the

surface semilandmarks were placed on one specimen and then projected on the remaining specimens using the Morpho package in R v3.4.1 (R Core Team, 2017) for each epiphysis. Semilandmarks were then relaxed onto the surface of the specimens reducing bending energy. Subsequently, the curve as well as surface semilandmarks were allowed to slide in 3D while minimising Procrustes distance.

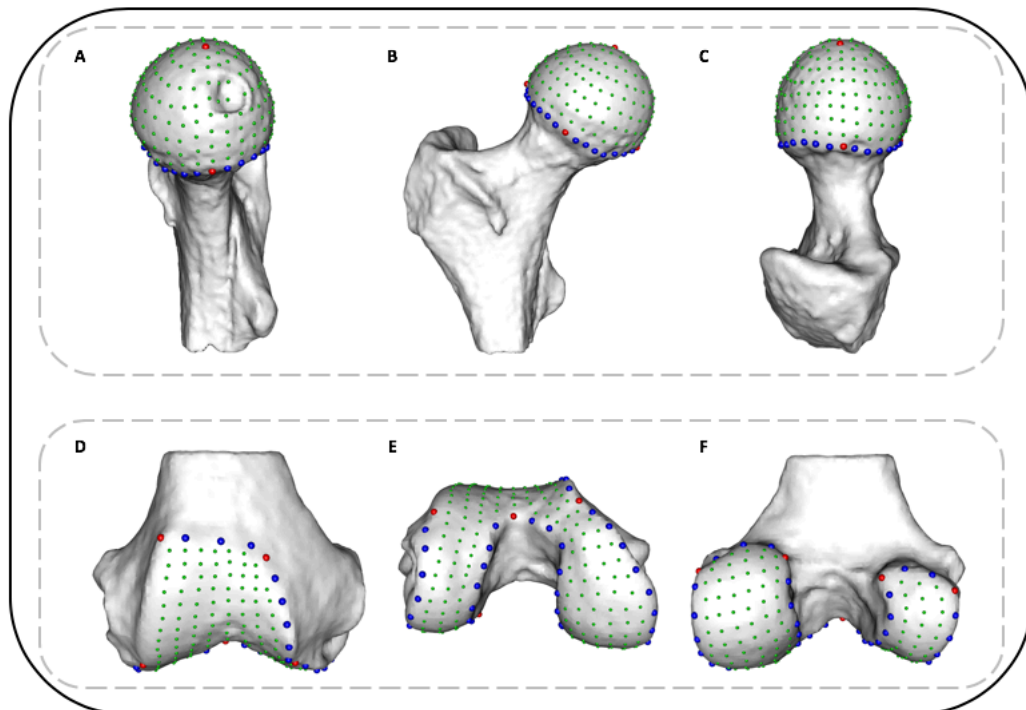


Figure 2.5. Template of landmarks used for the proximal and distal femur. Fixed landmarks are displayed in red, curve landmarks are displayed in blue and patch landmarks are displayed in green. (A) Lateral (B) anterior and (C) superior views of the proximal femur. (D) Anterior, (E) inferior and (F) posterior views of the distal femur.

The resulting landmarks of each individual were matched to the closest neighbouring tetrahedron of their distribution map using nearest neighbour interpolation. This utilises the coordinates of each landmark to find the surface tetrahedron of the individual's BV/TV distribution map with the closest centroid coordinates. Since the centroid holds the BV/TV value of the tetrahedron this value can be extracted to the landmark. Here BV/TV values were extracted for all the landmarks of the individuals and average distribution maps were constructed to

visualise taxon-specific patterns of trabecular bone distribution, as well as compare patterns interspecifically.

2.5. Statistical analysis

All statistical analyses were performed using R v3.4.1 (R Core Team, 2017). The Kruskal-Wallis test was used to test for interspecific differences in trabecular parameters and the Wilcoxon rank sum test was used for post-hoc pairwise comparisons. Furthermore, principal components (PC) analyses were used to further evaluate interspecific differences.

Additionally, to test for interspecific differences in the landmark-based distribution I performed a PCA and a pairwise permutational MANOVA test. The first three principal components, which explain more than 50% of the variation in the PCA, were used in the latter as the initial number of variables (i.e. BV/TV values at each landmark) exceeded the number of individuals. Finally, permutational Hotelling's T^2 tests with Bonferroni corrections were carried out to evaluate whether the distributions of the fossils could belong to the extant taxa samples. The permutational Hotelling's T^2 tests could not be performed for *Pan troglodytes troglodytes* or *Pongo* due to their small sample sizes.

Chapter 3

Trabecular architecture of the great ape and human femoral head

Abstract

Studies of femoral trabecular structure have shown that the orientation and volume of bone is associated with variation in loading and could be informative about individual joint positioning during locomotion. In this study I analyse for the first time trabecular bone patterns throughout the femoral head using a whole-epiphysis approach to investigate how potential trabecular variation in humans and great apes relates to differences in locomotor modes. Trabecular architecture was analysed using microCT scans of *Pan troglodytes* (n=20), *Gorilla gorilla* (n=14), *Pongo* sp. (n=5) and *Homo sapiens* (n=12) in medtool 4.1. My results revealed differences in bone volume fraction (BV/TV) distribution patterns, as well as overall trabecular parameters of the femoral head between great apes and humans. *Pan* and *Gorilla* showed two regions of high BV/TV in the femoral head, consistent with hip posture and loading during two discrete locomotor modes; knuckle-walking and climbing. Most *Pongo* specimens also displayed two regions of high BV/TV, but these regions were less discrete and there was more variability across the sample. In contrast, *Homo* showed only one main region of high BV/TV in the femoral head and had the lowest BV/TV, as well as the most anisotropic trabeculae. The *Homo* trabecular structure is consistent with stereotypical loading with a more extended hip compared with great apes, which is characteristic of modern human bipedalism. My results suggest that holistic evaluations of femoral head trabecular architecture can reveal previously undetected patterns linked to locomotor behaviour in extant apes and can provide further insight into hip joint loading in fossil hominins and other primates.

3.1. Introduction

The morphology of the proximal femur has played a key role in the reconstruction of locomotion in extant and extinct primates (e.g. McHenry and Corruccini, 1978; Burr et al. 1982; Ruff et al. 1991; Ruff and Runestad, 1992; Ruff, 1995; Harmon, 2007; Harmon, 2009b; Ruff and Higgins, 2013) and particularly in understanding the form of bipedalism used by australopiths (Stern and Susman, 1983; Susman et al. 1984; Crompton, et al. 1998; Carey and Crompton, 2005; Harmon, 2009a; Lovejoy and McCollum, 2010; Raichlen et al. 2010; DeSilva et al. 2013). External morphology provides considerable evidence of functional links between morphology and locomotion. However, due to possible phylogenetic lag, which results in traits that are no longer functionally significant being present, inferences about behaviour based on external traits alone have been questioned (e.g. Ward, 2002). Variation in internal trabecular bone structure across different regions of the skeleton can provide additional evidence to help reconstruct joint postures and to infer potential differences in locomotor behaviour in extant and extinct primates (e.g. Thomason 1985a,b; Ryan and Ketcham, 2002; Volpato et al. 2008; Ryan and Shaw, 2012; Tsegai et al. 2013; Skinner et al. 2015; Stephens et al. 2016). Indeed, the ability of trabecular bone to reflect mechanical loading was first noted in the human proximal femur (Ward, 1838; Wolff, 1892, 1986). It is not yet fully understood how mechanical or non-mechanical factors trigger and ultimately affect the organisation of trabeculae. For example, a range of activities, including high strain/low frequency loading and low strain/high frequency loading have been shown to elicit trabecular reorganisation (Rubin et al. 1990; Rubin et al. 2001; Judex et al. 2003; Wallace et al. 2014). Furthermore, differences in body mass (Scherf, 2008; Cotter et al. 2009; Doube et al. 2011; Fajardo et al. 2013; Ryan and Shaw, 2013), hormones (e.g. Gunness-Hey and Hock, 1984; Miyakoshi, 2004; Walsh, 2015), and genetic or systemic factors (Havill et al. 2010; Tsegai et al. 2018a) have been shown to influence aspects of trabecular structure as well. However, computational (e.g. Huiskes et al. 2000; Keaveny et al. 2001) and experimental studies have

demonstrated that modelling of trabeculae is correlated with applied loads, and trabecular strut reorganisation can be instigated by changes in the direction, magnitude and/or frequency of load (Biewener et al. 1996; Mittra et al. 2005; Pontzer et al. 2006; Polk et al, 2008; Barak et al. 2011). Furthermore, trabecular bone volume fraction (BV/TV) and trabecular strut alignment (degree of anisotropy, or DA) explain up to 98% of bone stiffness (i.e. Young's modulus of elasticity) (Stauber et al. 2006; Maquer et al. 2015; Odgaard et al. 1997). Thus, variation in the distribution of BV/TV and DA can provide insight into joint loading and, in turn, locomotor behaviours in primates.

Several studies have revealed that variation in the trabecular architecture of the primate hip and proximal femur is associated with differences in locomotion (e.g. Rafferty and Ruff, 1994; MacLatchy and Muller, 2002; Volpato et al. 2008; Ryan and Shaw, 2012; Saers et al. 2016). For example, Volpato and colleagues (2008) demonstrated that the orientation of trabecular struts in the ilium and femoral neck is associated with joint positioning in the hip of bipedally-trained Japanese macaques and reflects alterations in the direction of load. Comparable changes in trabecular structure that reflect differences in joint orientation were also found in the distal femora of guinea fowls (Pontzer et al. 2006) and distal tibiae of sheep (Barak et al. 2011). Furthermore, Scherf (2008) found that trabecular structure within the femoral head, neck and both trochanters of climbing primates (e.g. *Alouatta seniculus*) had more isotropic architecture, while specialised primates (e.g. *Homo sapiens*) in which the femur experienced more stereotypical loading had more anisotropic structure. Similar results were found in leaping primates, which in comparison to non-leaping primate species, had more anisotropic trabeculae in the inferior aspect of the femoral head (Ryan and Ketcham, 2002), and a different principal strut orientation (Ryan and Ketcham, 2005).

More recently, Ryan and Shaw (2012) investigated the trabecular patterns of the femoral head in several anthropoid taxa and found that different suites of trabecular variables could distinguish among taxa and locomotor groups. In particular, modern humans were distinct in having relatively few, highly anisotropic

trabeculae that are thin and plate-like, *Pan* had relatively numerous, thick and isotropic trabeculae, while *Pongo* had relatively few and isotropic trabeculae. Additional studies investigating different human samples have also shown that femoral head trabecular structure reflects variation in mobility levels, with more sedentary agriculturalists having relatively low BV/TV compared with more active foragers (Ryan and Shaw, 2015; Saers et al. 2016; Ryan et al. 2018). Interestingly, more active human foragers have relatively high BV/TV that falls within the range of most extant hominoids apart from *Pan* (Ryan et al. 2018). Despite this overlap in BV/TV between some human samples and other hominoids, humans have consistently been shown to have the most anisotropic femoral head structure compared to other great apes (Ryan and Shaw, 2015; Ryan et al. 2018). Furthermore, the human trabecular pattern has been shown to develop during ontogeny when independent bipedalism develops and the gait matures (Ryan and Krovitz, 2006; Reissis and Abel, 2012; Milovanovic et al. 2017). Altogether, these studies suggest that the trabecular bone of the femoral head holds a strong functional signal of locomotor loading in primates.

Conversely, other studies have failed to detect a strong locomotor signal in the femoral head (Ryan and Walker, 2010; Shaw and Ryan, 2012), femoral neck (Fajardo et al. 2007) and distal femur (Carlson et al. 2008). Carlson and colleagues (2008) did not detect differences in the DA of the distal femoral metaphysis between mice with turning locomotion and mice with non-turning locomotion. Similarly, Ryan and Walker (2010) did not find any significant differences in the DA and BV/TV patterns of the femoral head in a broad sample of platyrrhines and catarrhines. Furthermore, Shaw and Ryan (2012), who examined the subarticular trabecular and mid-diaphyseal cortical patterns in the femur and humerus of a sample of primates, concluded that only the mid-diaphyseal cortical bone contains a clear functional signal linked to the differential use of the two limbs between different locomotor groups.

The discrepancy in the findings of previous studies may, in part, be an artefact of the volume-of-interest (VOI) method that was used. A VOI quantifies only a

subsample of trabecular structure within a given region and results can vary depending on its size and position (Fajardo and Müller, 2001; Kivell et al. 2011). Additionally, challenges arise when extracting homologous VOIs in taxa that vary in external morphology. Prior research has demonstrated that additional functional insight can be gained from investigating the trabecular architecture within an epiphysis as a whole (Tsegai et al. 2013; Skinner et al. 2015; Stephens et al. 2016; Sylvester and Terhune, 2017; Tsegai et al. 2017). Here I apply a whole-epiphysis approach to study the trabecular structure throughout the femoral head of chimpanzees (*Pan troglodytes*), lowland gorillas (*Gorilla gorilla*), orangutans (*Pongo* sp.) and humans (*Homo sapiens*), which vary in locomotor behaviours and are relevant to the reconstruction of locomotion in fossil hominins.

3.1.1. Locomotion, hip morphology and predicted joint posture

Habitual locomotor activities and associated hip joint angles vary between great apes and humans (Figure 3.1). Chimpanzees are predominantly terrestrial/arboreal quadrupedal knuckle-walkers, but also engage frequently in arboreal climbing and, less so, bipedalism (Hunt, 1991b; Doran, 1992, 1993a). In all these locomotor modes, the hindlimb plays key role in propulsion and experiences higher vertical force than the forelimb (Demes et al. 1994; Hannah et al. 2017). During terrestrial quadrupedalism in chimpanzees, the mean hip angle at foot touchdown is 65° and at toe-off it is 98.2° (Finestone et al. 2018). Kinematics during chimpanzee vertical climbing have, to my knowledge, only been studied in one individual and show that the flexion-extension range at the hip increases substantially compared with terrestrial quadrupedalism, with hip angles ranging from ~25° to ~105° (Nakano et al. 2006). A more comprehensive study of bonobos (n=4 adults), which share similar hindlimb anatomy with chimpanzees (e.g. Payne et al. 2006; Myatt et al. 2011), yielded hip angles ranging from 55° to 135° during vertical climbing (Isler, 2005).

Lowland gorillas are also predominantly quadrupedal knuckle-walkers (Remis, 1995; Crompton et al. 2010). They often engage in arboreal climbing and bipedalism, but less frequently than chimpanzees (Remis, 1995; Crompton et al. 2010). During terrestrial quadrupedalism in gorillas, hip angles range from 77° at foot touchdown to 120.6° at toe-off (Finestone et al. 2018). During vertical climbing, hip angle range is similar to that of bonobos, ranging from approximately 45° to 135° (Isler, 2005). *Gorilla* climbing frequency and technique varies with sex and body size, with the range of hip flexion-extension being reduced in larger males compared to smaller females (Remis, 1995; Remis, 1999; Isler, 2005). However, gorillas show less intraspecific variation in climbing techniques than bonobos (Isler, 2005).

Orangutans employ a complex set of locomotor behaviours, which are mostly torso orthograde, including vertical climbing, bridging, suspension from various limbs, and terrestrial quadrupedalism (Cant, 1987; Isler and Thorpe, 2003; Thorpe and Crompton, 2006; Thorpe et al. 2009). Their hips are more mobile than those of other apes, which allows them to use their hindlimbs in more varied ways (Morbeck and Zihlman, 1988; Tuttle and Cortright, 1988; Isler, 2005). During terrestrial locomotion, the orangutan hip angle is 68.3° at touchdown and 107.3° at toe-off (Finestone et al. 2018). During vertical climbing, orangutans are able to lift their feet further above their hips than African apes, such that their flexion-extension angle ranges from around 30° to 135° (Isler, 2005).

Adult humans walk exclusively terrestrially on two legs, extending both their hips and knees (Alexander, 1994). During the gait cycle, hip extension reaches 160° at touchdown and 175° at toe-off (Abbass and Abdulrahman, 2014). Humans also engage in running, which alters the joint angle of the hip and the resulting load on the femoral head (Ounpuu, 1990; Ounpuu, 1994; van den Bogert et al. 1999; Giarmatzis et al. 2015). Increase in speed is linked to more flexed hip joints and a generally increased range of motion at the hip (Mann and Hagy, 1980; Novacheck, 1998). At touchdown during running the hip is flexed at 30-40°, while also being externally rotated, and at push off it is extended and internally rotated (Slocum and

James, 1968). Furthermore, during running (3.5m/s), loads have been shown to increase to greater than double that of walking (1.5 m/s) (van den Bogert et al.1999).

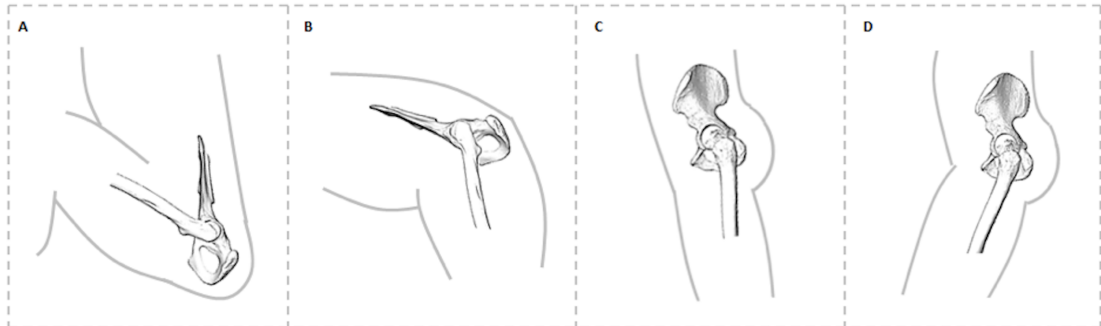


Figure 3.1. Comparison of hip posture during different habitual locomotor activities in great apes (A-B) and humans (C-D). (A) Great ape hip posture in maximum hip flexion (~55-60 degrees) during climbing (Isler, 2005). (B) Great ape hip posture at toe-off (~110 degrees) during terrestrial knuckle-walking (Finestone et al. 2018). (C) Human hip posture at toe-off (~175 degrees). (D) Human hip posture at heel-strike (~160 degrees).

Great apes and humans vary in the external morphology of the hip joint. Chimpanzees and gorillas have a relatively small femoral head, a short femoral neck as well as a superoinferiorly expanded greater trochanter compared to orangutans (McHenry and Corruccini, 1978; Harmon, 2007). Chimpanzees have a “laterally facing acetabulum” (Jenkins, 1972), however comparative quantitative data of acetabulum anteversion do not exist for apes and humans (Hogervorst et al. 2009 and references therein). Furthermore, in gorillas the acetabulum is relatively deep, compared to other apes (Schultz, 1969), perhaps reducing capacity for mobility at the hip. In orangutans the greater trochanter is less superoinferiorly expanded than in the African apes and is positioned inferiorly to the femoral head, which may enhance rotational capacity at the hip joint (Aiello and Dean, 2002; Harmon 2007). Orangutans also have a relatively large head, long neck, and a greater trochanter that is less superoinferiorly expanded than that of African apes and which is positioned inferiorly relative to the femoral head (Aiello and Dean, 2002; Harmon, 2007). These features of the orangutan proximal femur, plus the absence of a subchondral ligamentum teres insertion at the centre of the femoral head (Crelin, 1988; Ward, 1991; Ruff,

2002; Harmon, 2007), enhance rotational capacity and allow greater mobility at the hip joint compared to other hominoids.

Humans have a long femoral neck and a valgus angle at the knee, which compensate for the mechanical disadvantage of increased bi-acetabular distance (Lovejoy, 1975; McHenry and Corruccini, 1978; Rafferty, 1998; Lovejoy et al. 2002; Harmon, 2007) and result in adduction of the hips during the stance phase (O'Neill et al. 2015). The greater trochanter is less superoinferiorly expanded compared to other apes (Harmon, 2007). Furthermore, the human acetabulum is relatively deep and the femoral head is relatively large (Schultz, 1969; Jungers, 1988). This hip morphology is thought to help dissipate the increased load that occurs when supporting body mass over two, rather than four, limbs. Biomechanical studies have revealed that the peak contact force on the human hip during walking is directed posteriorly, laterally and inferiorly (Pedersen et al. 1997) and is located at the posterior aspect (Paul, 1976; English and Kilvington, 1979). Furthermore, pressure on the acetabulum is mainly located posteriorly during different activities, such as standing up or sitting down (Yoshida et al. 2006). Lack of congruence between the femoral head and the acetabulum, combined with an anterior-facing acetabulum result in the anterior region of the femoral head not being fully covered by the acetabulum during bipedal locomotion (Hogervorst et al. 2009; Bonneau et al. 2014). Thus, the anterior region of the femoral head and acetabulum play a smaller role in load transmission compared to other regions of the hip joint.

Examining the potential links between internal femoral bone structure and extant ape locomotion will greatly facilitate attempts to reconstruct the locomotion of extinct hominins (e.g. Skinner et al. 2015). Here I provide this comparative context by analysing the trabecular architecture throughout the entire femoral head in extant great apes and humans that vary in their locomotor behaviours. I quantify BV/TV, DA, trabecular number (Tb.N), trabecular separation (Tb.Sp) and trabecular thickness (Tb.Th) throughout the femoral head. Based on the locomotor and biomechanical studies reviewed above, I make the following predictions regarding species variation in femoral head trabecular structure:

1. BV/TV distribution in the femoral head

The distribution of BV/TV throughout the femoral head will reflect joint positioning and loading during habitual locomotion. In *Pan* I expect high BV/TV to extend from the posterior and superior aspect of the femoral head to the anterior region, reflecting hip angles and loading during knuckle-walking locomotion and vertical climbing (Finestone et al. 2018; Isler 2005). I predict that *Gorilla* will show a similar pattern of BV/TV distribution, although the region of high BV/TV is expected to extend over a smaller area of the femoral head compared with that of *Pan*, reflecting a reduced range of motion (Hammond, 2014) and different flexion/extension angles at the *Gorilla* hip during knuckle-walking and climbing (Finestone et al. 2018; Isler 2005). I predict that *Pongo* will show the most variable BV/TV distribution pattern, reflecting loading of the femoral head at different hip joint angles, with high BV/TV spanning the whole of the superior area of the femoral head. Finally, I expect a more restricted region of high BV/TV in *Homo* that will be concentrated superiorly and posteriorly on the femoral head, reflecting the stereotypical loading pattern of bipedal locomotion.

2. Mean trabecular parameters in the femoral head

I hypothesise that relative interspecific differences in mean BV/TV values will be consistent with those of previous trabecular studies on the femur (e.g. Georgiou et al. 2018; Ryan et al. 2018; Tsegai et al. 2018a) and other postcranial elements (e.g. Maga et al. 2006; Cotter et al. 2009; Scherf et al. 2013; Tsegai et al. 2013; Tsegai et al. 2017), such that *Pan* will have the highest BV/TV, *Homo* will have the lowest, and *Gorilla* and *Pongo* will be intermediate between these two taxa. Furthermore, mean DA of the entire femoral head will reflect the range of motion of the hip joint during habitual locomotion. *Pan* and *Gorilla* will display intermediate DA values, showing less anisotropic femoral heads than *Homo*, because they engage in both terrestrial and arboreal behaviours that employ an increased range of motion at the hip. *Pongo* will be the most isotropic, reflecting their highly mobile hip joint and diverse positioning of the proximal femur during their varied quadrumanous locomotor

behaviours. *Homo* will be the most anisotropic, consistent with more stereotypical loading of the hip joint during bipedal locomotion.

In addition to BV/TV and DA, I quantify mean Tb.N, Tb.Sp and Tb.Th within the femoral head to better understand potential variation in the trabecular architecture across my sample and for comparison with previous studies (e.g. Ryan and Shaw, 2012; Ryan and Shaw, 2015; Ryan et al. 2018). In primates these parameters scale negatively allometrically with body size (Barak et al. 2013b; Ryan and Shaw, 2013) meaning results may be affected by body mass. BV/TV and DA are expected to better reflect functional adaptations, as DA does not to scale with body mass and BV/TV either shows no relationship (Doubé et al. 2011; Barak et al. 2013b) or a weak positively allometric relationship (Ryan and Shaw, 2013) with body mass.

3.2. Materials and Methods

3.2.1. Study sample

Microcomputed tomographic scans were used to analyse trabecular morphology in the femoral head of great apes and humans. Details of the study sample are provided in Table 3.1. The *P. troglodytes* sample (n=20) is comprised of two subspecies; *Pan troglodytes verus* (n=15) from the Tai Forest collection curated at the Max Planck Institute for Evolutionary Anthropology in Leipzig, Germany, and *Pan troglodytes troglodytes* (n=5) curated at the Smithsonian National Museum of Natural History in Washington, D.C., USA. The *Gorilla gorilla gorilla* sample (n=14) is from the Powell-Cotton Museum, UK, of which 13 individuals are from Cameroon and one is from the Democratic Republic of the Congo. The *Pongo* sample (n=5 and all female) is from the Zoologische Staatssammlung München, Germany. Four of the individuals are *P. pygmaeus*, while one is *P. abelii*. The *H. sapiens* sample (n=12) is curated at the Georg-August-Universität Göttingen, Germany. Ten of the individuals come from a Catholic cemetery in Göttingen, which was used between 1851 and

1889, and two come from a cemetery in the village of Inden that was used between 1877 and 1924. All specimens were adult based on complete epiphyseal fusion throughout the skeleton and none showed obvious signs of pathology.

Table 3.1. Study sample taxonomic composition, voxel size range, sex, and microCT scanning parameters.

Taxon	Locomotor mode	N	Sex	Voxel size (mm)	Scanning
<i>Pan troglodytes</i>	Arboreal/ knuckle-walker	20	13 female, 6 male, 1 unknown	0.04-0.05	kV:120-130, μ A: 80-100, 0.25 or 0.5mm brass
<i>Gorilla gorilla gorilla</i>	Terrestrial knuckle-walker	14	7 female, 7 male	0.05-0.08	kV:130-170, μ A: 110-160, 0.1-0.5mm copper
<i>Pongo sp.</i>	Arboreal/ torso-orthograde suspension	5	5 female	0.04-0.045	kV:140, μ A: 140, 0.5mm brass
<i>Homo sapiens</i>	Bipedal	12	3 female, 8 male, 1 unknown	0.06-0.07	kV:130-140, μ A: 100-140, 0.5mm brass

The *Pan*, *Pongo* and *Homo* samples were scanned at the Department of Human Evolution in the Max Planck Institute for Evolutionary Anthropology, Leipzig, Germany using a BIR ACTIS 225/300 industrial microCT scanner. The *Gorilla* sample was scanned at the Cambridge Biotomography Centre in the Department of Zoology at the University of Cambridge, Cambridge, UK using a Nikon XT 225 ST microCT scanner. All specimens were scanned at the highest possible resolution based on the size of the bone, ranging from 0.029-0.082 mm, and were reconstructed into 16-bit TIFF stacks with isometric voxel sizes. Reconstructed datasets were re-oriented to the same anatomical position and cropped in AVIZO 6.3[®] (Visualization Sciences Group, SAS). All specimens, except six gorillas, were re-sampled due to computational limitations of medtool 4.1(www.dr-pahr.at) and resultant resolutions

are given in Table 3.1. Bone was segmented from air using the Ray Casting Algorithm (Scherf and Tilgner, 2009).

3.2.2. Trabecular architecture analysis

Patterns of trabecular bone distribution throughout the whole femoral head were analysed in medtool 4.1 (www.dr-pahr.at), following the protocol described by Gross and colleagues (2014). A series of morphological filters were applied to identify and remove the cortical shell, thus isolating the trabecular structure. The resulting isolated trabecular structure was used to calculate trabecular thickness using the BoneJ plug-in (version 1.4.1, Doube et al. 2010) for ImageJ (Schneider et al. 2012) to validate the parameters used in the morphological filters for the separation of the cortical shell (see Gross et al. 2014). The trabecular area and trabecular structure were used to create a trinary mask defining the outer air, inner air and trabecular bone. A 3D rectangular background grid with a size of 3.5mm was superimposed on the trinary mask and a sphere with a diameter of 7.5mm was used to measure BV/TV at each node in medtool 4.1. BV/TV was calculated as the ratio of bone to total volume in the sampling spheres. The isolated trabecular structure and a mesh size of 0.6mm were used to create 3D tetrahedral meshes of all individuals, using CGAL 4.4 (CGAL, Computational Geometry, <http://www.cgal.org>) and BV/TV values were then interpolated on the tetrahedral elements of each mesh. Distribution maps of BV/TV were visualised using Paraview v4.0.1 (Ahrens et al. 2005). The femoral head for each specimen was manually isolated in AVIZO 6.3[®] by positioning the mediolateral axis facing superoinferiorly and cropping at the head-neck junction to ensure homology across specimens. Trabecular parameters (BV/TV, DA, Tb.N, Tb.Sp, Tb.Th) for the femoral head were calculated using an in-house script in medtool 4.1. Mean BV/TV, DA, Tb.Sp and Tb.Th were quantified within the entire epiphysis and Tb.N was calculated from the means of Tb.Sp and Tb.Th. DA was calculated as $DA = 1 - [\text{smallest eigenvalue} / \text{largest eigenvalue}]$, as they were calculated using the mean-intercept-length method (Whitehouse, 1974; Odgaard, 1997). Tb.Sp and Tb.Th were calculated

based on the Hildebrand and Ruesegger (1997) method; Tb.N was then calculated as $Tb.N=1/(Tb.Th+Tb.Sp)$.

3.2.3. Statistical analysis

Statistical analysis was performed in R v3.4.1 (R Core Team, 2017). The Kruskal-Wallis test was used to evaluate interspecies differences in mean trabecular parameters (BV/TV, DA, Tb.N, Tb.Sp, Tb.Th) of the femoral head and a Wilcoxon rank sum test with Bonferroni correction was used for post-hoc pairwise comparisons.

3.3. Results

3.3.1. BV/TV distribution in the femoral head

In *Pan*, BV/TV distribution maps of the femoral head reveal concentrations of high BV/TV in the superior aspect of the femoral head (Figure 3.2; Supplementary material for the whole sample). In most *Pan* individuals (n=12) there are two distinct concentrations, one located more posteriorly and one located more anteriorly, whereas in some individuals one concentration spans the whole of the superior region of the articulation. While the posterior concentration is always present in *Pan*, the location, extent and isolation of the anterior concentration varies between individuals.

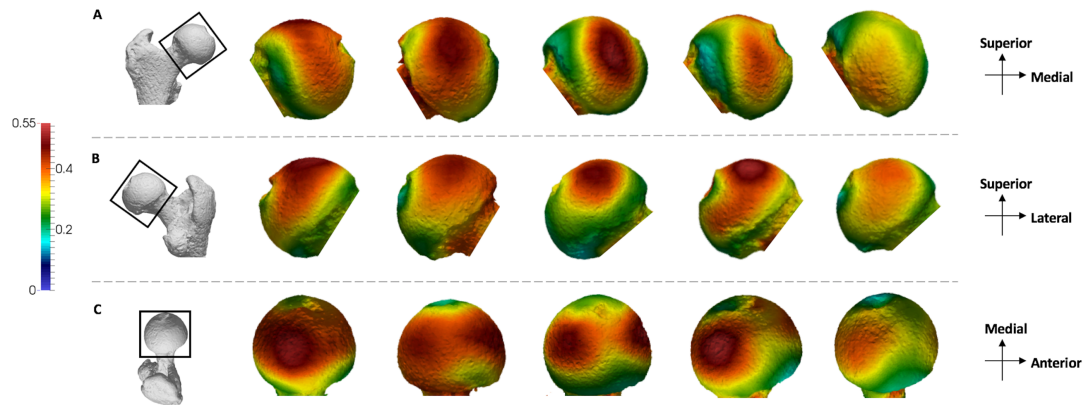


Figure 3.2. *Pan* BV/TV distribution in the femoral head. Five *Pan* specimens showing variation in the BV/TV distribution across the sample in (A) anterior, (B) posterior and (C) superior views. BV/TV is scaled to 0- 0.55. All specimens are from the right side. Specimens from left to right (F-female, M-male): MPITC 14996 (F), USNM 220063 (F), USNM 176228 (M), MPITC 11781 (M), MPITC 11786 (F).

The pattern of BV/TV distribution in *Gorilla* is similar to that found in *Pan* (Figure 3.3). Two concentrations of high BV/TV are seen in the superior aspect, one located anteriorly, and one located posteriorly. Unlike in *Pan* however, these concentrations are distinct from each other in all but three *Gorilla* individuals, in which a region of high BV/TV spans across the superior region of the femoral head. There is no apparent difference in the size of the two regions of high BV/TV.

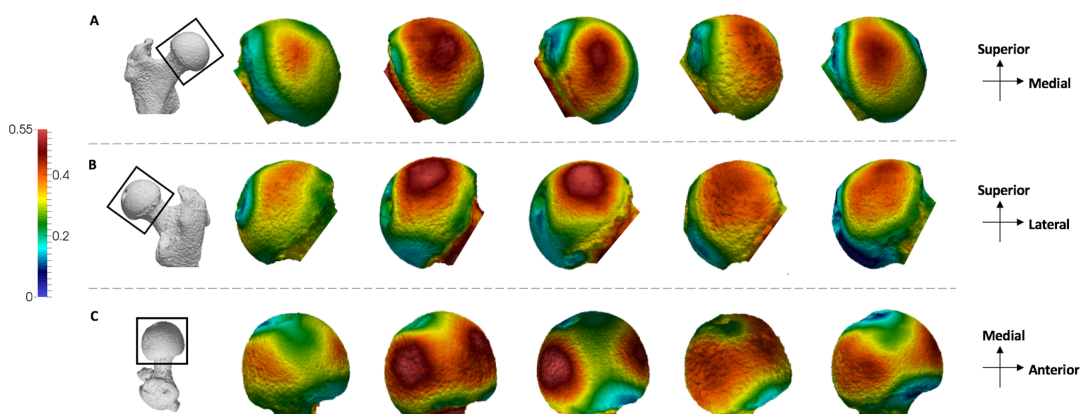


Figure 3.3. *Gorilla* BV/TV distribution in the femoral head. Five *Gorilla* specimens showing variation in the BV/TV distribution across the sample in (A) anterior, (B) posterior and (C) superior views. BV/TV is scaled to 0-0.55. All specimens are from the right side. Specimens from left to right (F-female, M-male): M96 (F), M264 (M), M372 (M), M856 (F), FC123 (M).

Pongo shows a slightly different BV/TV pattern compared to *Pan* and *Gorilla* (Figure 3.4). The *P. pygmaeus* individuals show the two concentrations of high BV/TV, one in the anterior and one in the posterior, similar to what is found in the African apes, however intermediate values persist over the superior portion of the femoral head. The extent of this concentration differs between *P. pygmaeus* individuals: in two individuals it is restricted more in the superior aspect of the head, whereas in the other two it is enlarged and covers the majority of the femoral head, from the anterior to the posterior. When the two concentrations are more well-defined, the posterior concentration is generally more mediolaterally expanded than the anterior concentration. The *P. abelii* individual shows lower BV/TV than the other specimens and does not show two distinct concentrations.

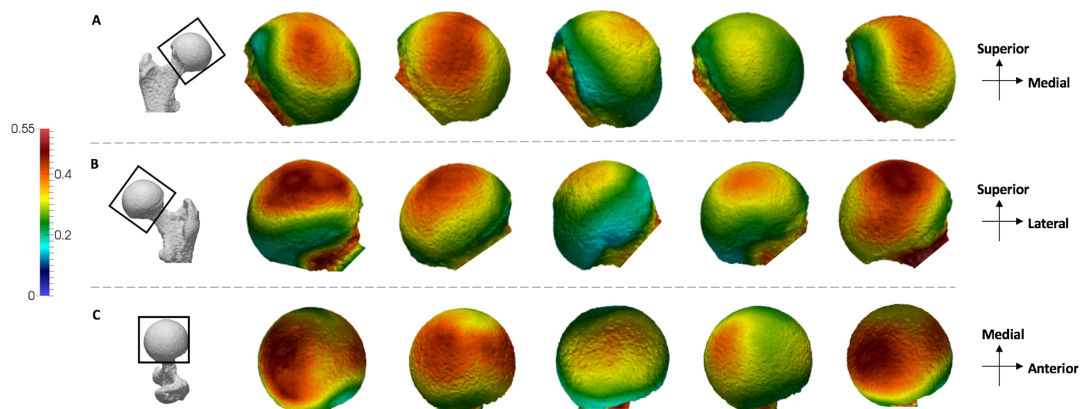


Figure 3.4. *Pongo* BVTV distribution in the femoral head. Five *Pongo* specimens showing variation in the BV/TV distribution across the sample in (A) anterior, (B) posterior and (C) superior views. BV/TV is scaled to 0- 0.55. All specimens are from the right side. Specimens from left to right (All female): ZSM 1909 0801, 1907 0660, 1973 0270, 1907 0483, 1907 0633b.

Homo shows a different pattern to the great apes (Figure 3.5). All individuals show one region of high BV/TV located in the posterior and superior aspect of the femoral head. Intermediate values of BV/TV expand across the whole of the superior aspect of the head of *Homo*, but with no apparent second concentration of high BV/TV in the anterior region as found in great apes. *Homo* individuals also display intermediate BV/TV on the inferior aspect of the head. This expansion of intermediate BV/TV values along the inferior is not seen in the other apes.

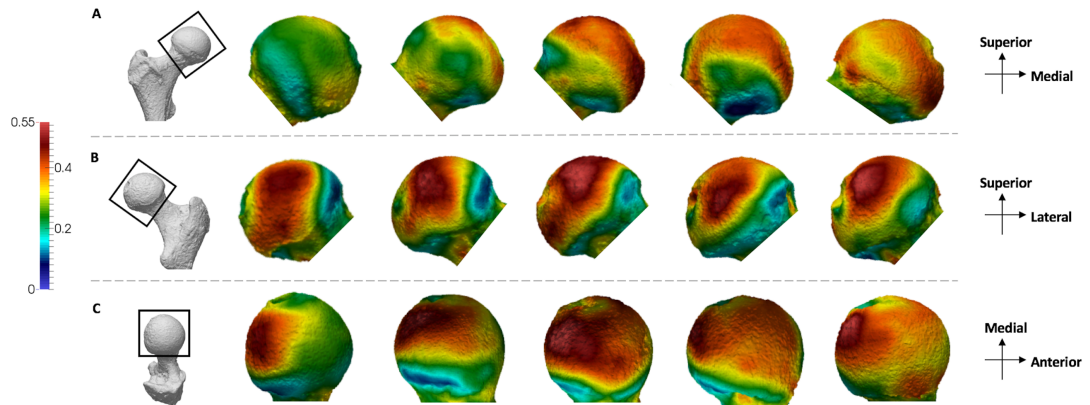


Figure 3.5. *Homo* BV/TV distribution in the femoral head. Five *Homo* specimens showing variation in the BV/TV distribution across the sample in (A) anterior, (B) posterior and (C) superior views. BV/TV is scaled to 0-0.55. All specimens are from the right side. Specimens from left to right (F-female, M-male): CAMPUS 36 (F), CAMPUS 93 (M), CAMPUS 74 (F), CAMPUS 417 (sex unknown), CAMPUS 81 (M).

3.3.2. Quantitative analysis of trabecular parameters in the femoral head

Quantitative analysis of the mean trabecular parameters over the femoral head revealed several differences across taxa. Results for each parameter in the different taxa are presented in Table 3.2 and statistical results of species pairwise comparisons, after Bonferroni corrections, are presented in Table 3.3.

Table 3.2. Trabecular architecture results. Mean, standard deviation and coefficient of variation for five trabecular parameters quantified throughout the femoral head.

Taxon	<i>Pan</i>	CV	<i>Gorilla</i>	CV	<i>Pongo</i>	CV	<i>Homo</i>	CV
BV/TV	0.39 (0.03)	8.6	0.35 (0.05)	14.8	0.33 (0.04)	13.4	0.30 (0.05)	16.0
DA	0.15 (0.03)	21.6	0.18 (0.04)	21.8	0.15 (0.02)	14.7	0.23 (0.04)	17.9
Tb.N (1/mm)	1.19 (0.11)	9.4	0.83 (0.09)	10.7	0.92 (0.04)	4.4	0.87 (0.1)	11.4
Tb.Sp (mm)	0.56 (0.06)	10.0	0.81 (0.08)	9.8	0.78 (0.07)	8.4	0.84 (0.14)	16.6
Tb.Th (mm)	0.29 (0.03)	11.8	0.40 (0.08)	19.1	0.31 (0.03)	10.9	0.32 (0.03)	9.9

Pan shows significantly higher BV/TV in the femoral head than *Pongo* ($p=0.05$) and *Homo* ($p<0.001$), and although its mean BV/TV value was higher than that of *Gorilla*, this difference was not statistically significant (Tables 3.2 and 3.3). *Homo* has the lowest mean BV/TV compared with all the great apes but is only significantly different from *Pan*. *Homo* has significantly higher DA in the femoral head than all other apes (*Pan* $p<0.001$; *Gorilla* $p<0.05$; *Pongo* $p<0.01$), while *Pan*, *Pongo* and, less so, *Gorilla* are more isotropic and not significantly different from each other. With regards to the architectural parameters, *Pan* shows the most distinct trabecular structure with significantly higher Tb.N than all other apes (*Gorilla* $p<0.001$; *Homo* $p<0.001$; *Pongo* $p<0.01$) and significantly lower Tb.Sp (all $p<0.001$) and lower Tb.Th than *Gorilla* ($p<0.001$) and *Homo* ($p<0.05$).

Table 3.3. Results of pairwise comparisons between taxa. Bonferroni-corrected p-values of each pairwise comparison for all trabecular parameters. Significant results are indicated by grey shading.

	<i>Pan-Gorilla</i>	<i>Pan - Pongo</i>	<i>Pan - Homo</i>	<i>Gorilla - Pongo</i>	<i>Gorilla - Homo</i>	<i>Pongo - Homo</i>
BV/TV	0.14	<0.05	<0.001	1	0.14	1
DA	0.24	1	<0.001	1	<0.05	<0.01
Tb.N	<0.001	<0.01	<0.001	0.33	1	1
Tb.Sp	<0.001	<0.001	<0.001	1	1	1
Tb.Th	<0.001	1	<0.05	0.09	0.05	1

Differences in mean BV/TV and DA across taxa were further evaluated using a bivariate plot (Figure 3.6) and a line histogram of the distribution of values in each taxon (Figure 3.7). The data depicted in these figures are mean values for each individual across the entire femoral head. In the bivariate plot *Pan* shows a combination of high BV/TV and low DA, in contrast to humans that show the opposite pattern. *Gorilla* overlaps with both of these taxa but shows higher BV/TV than humans. *Pongo* individuals overlap with the African apes, with lower DA values than humans, but with BV/TV values that overlap with all other taxa.

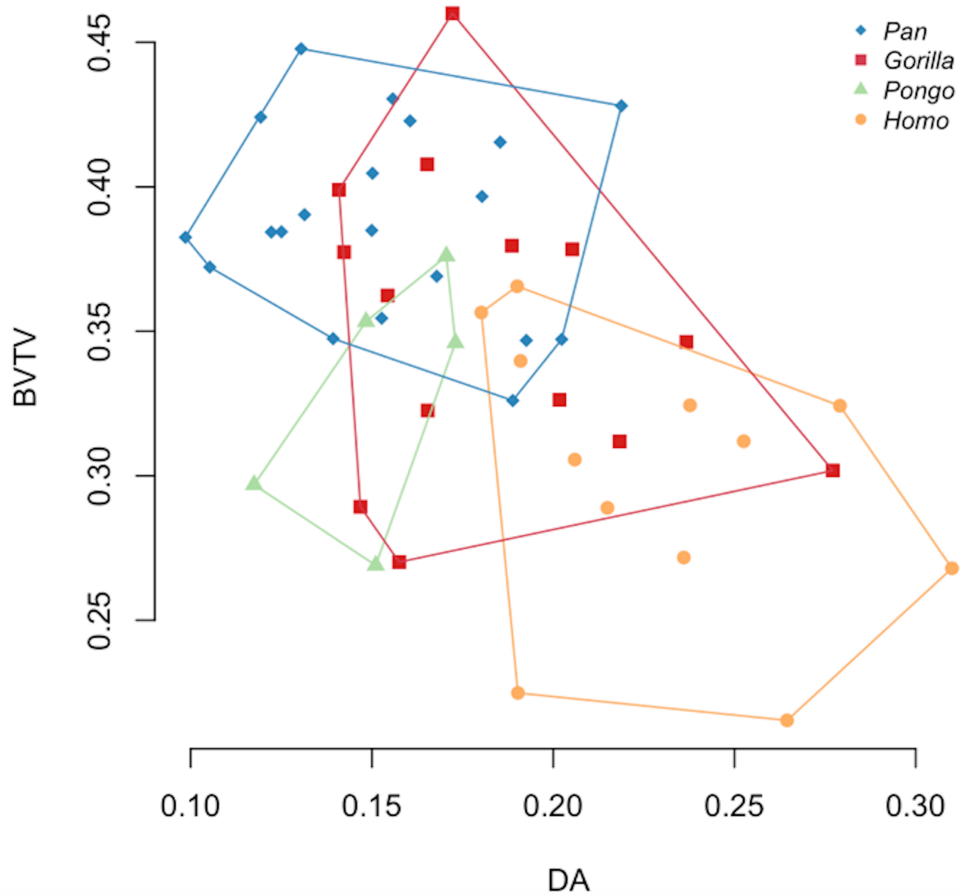


Figure 3.6. Bivariate plot of mean bone volume fraction (BV/TV) and mean degree of anisotropy (DA) for each individual and species in the sample.

These differences are reflected in the distribution of BV/TV and DA values in the taxa (Figure 3.7). *Pan* shows the highest mean BV/TV and most individuals close to the mean (0.39), whereas *Gorilla* shows a lower mean value but most individuals between 0.3 and 0.4. *Pongo* shows a similar mean to *Gorilla*, however the distribution of values more greatly resembles that of *Pan*. *Homo* shows the lowest BV/TV values distributed over a wider area. The DA plot shows that *Pan*, *Gorilla* and *Pongo* present similarly low mean DA values, but *Pongo* differs in distribution with more individuals around the mean. *Homo* shows a different distribution with the highest mean DA but a wider distribution of values in the sample.

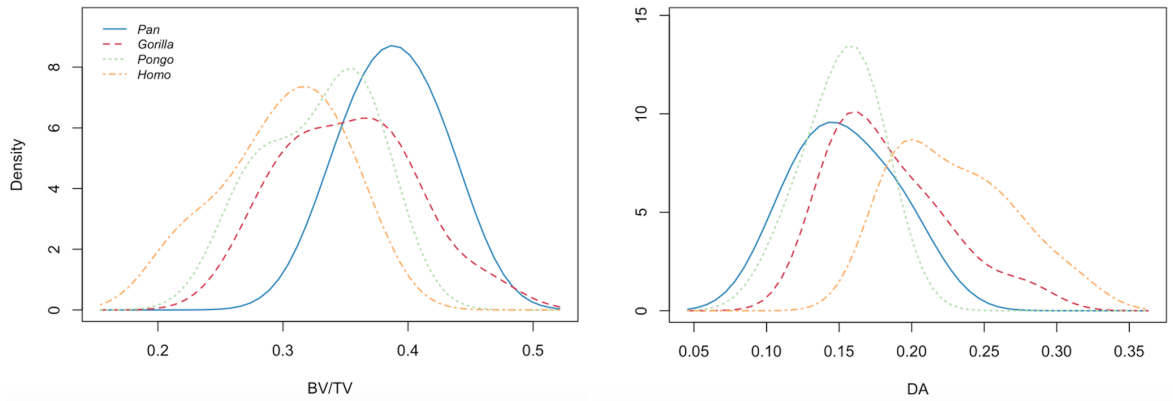


Figure 3.7. A histogram of mean BV/TV and DA value distributions in the studied taxa.

3.4. Discussion

My study investigated the variation in trabecular patterns of the femoral head in great apes and humans. Qualitative and quantitative results supported my hypotheses that trabecular bone would reflect differences in locomotor patterns, but not necessarily in the way I predicted. *Pan* and *Gorilla* displayed trabecular structures consistent with their terrestrial as well as arboreal quadrupedal locomotion, while *Homo* showed a distinct trabecular pattern indicative of stereotypical loading during bipedal locomotion. However, the African apes showed a BV/TV distribution pattern that was different to what was expected, and their trabecular structure did not differ significantly from *Pongo*.

3.4.1. Distribution of BV/TV within the femoral head

I predicted that African apes would display a region of high BV/TV extending from the posterosuperior to the anterior region of the femoral head, reflecting the flexed hip postures and loading incurred during knuckle-walking and vertical climbing. However, instead of a continuous band of high BV/TV across the femoral head, *Pan* displayed two main regions of high BV/TV, indicating two regions of high loading; one in the posterosuperior aspect of the femoral head and one located more

anteriorly. The majority of Tai chimpanzee (75% of the *Pan* sample) locomotion is terrestrial quadrupedalism (Doran, 1993a). Ground reaction forces remain high throughout the stance phase during terrestrial knuckle-walking (Barak et al. 2013a) and the hip remains flexed (Finestone et al. 2018), both of which are consistent with high loading of the posterosuperior region of the femoral head and the high BV/TV concentration that was found in this region. While Tai chimpanzees engage less frequently in vertical climbing (Doran, 1993a), it is possible that this results in similarly high loading of the femoral head, as it involves high propulsive forces from the hindlimbs (Hanna et al. 2017). During climbing, the hip can be flexed to a maximum of 25° to 55° (Isler, 2005; Nakano et al. 2006), which would result in the anterior aspect of the head contacting the lunate surface of the acetabulum. This is consistent with the second region of high BV/TV found in the anterior portion of the femoral head in *Pan*. The anterior concentration was more variable between individuals, but this could not be explained by subspecies differences within the sample. Thus, the more variable anterior BV/TV pattern may reflect interindividual variability in vertical climbing frequency (Doran, 1993b) or hip range of motion during climbing (Isler, 2005; Nakano et al. 2006).

Gorilla displayed a similar pattern to *Pan*, with two regions of high BV/TV within the femoral head. The two regions, one in the posterior and one in the anterior aspect of the head, are, as in *Pan*, consistent with hip posture and loading during terrestrial quadrupedalism and vertical climbing, as these modes of locomotion comprise the majority of *Gorilla* locomotion (Doran, 1997; Crompton et al. 2010; Remis, 1995). However, unlike *Pan*, these regions were better defined and more discrete in most *Gorilla* individuals (11 out of 14 individuals). This more discrete pattern is perhaps due to their greater body mass. Greater mass is related to restricted range of motion in joints (Hammond, 2014), which could result in less variability in joint positioning during locomotion and may explain the more well-defined concentrations in *Gorilla*. The two concentrations appeared closer to each other in *Gorilla* than in *Pan*, which is also consistent with the reduced range of motion at the hip joint of *Gorilla* (Isler, 2005; Hammond, 2014). Significant sex and body size related differences in joint mobility are prominent in *Gorilla*, with females showing a

larger range of motion than males and flexion-extension ranges varying between the sexes by up to or even more than 30° (Isler, 2005; Hammond, 2014). These differences were not detected in the BV/TV distribution maps and *Gorilla* does not seem to be more variable than *Pan*. However, this could not be tested statistically in the current study.

I predicted that the BV/TV distribution pattern of the *Pongo* femoral head would differ from that of African apes and humans because of their more varied quadrumanous locomotor behaviours (Thorpe and Crompton, 2005; Thorpe and Crompton, 2006), more mobile hip joints (Crelin, 1988; Ward, 1991), and increased range of motion at the hip during vertical climbing compared to African apes (Isler, 2005). Four of the five *Pongo* individuals in my sample showed the same two regions of high BV/TV found in African apes, however these were not as distinct and, instead, there was a continuous concentration of BV/TV spanning the superior aspect of the femoral head. This is perhaps unsurprising since *Pongo* uses a variety of hip postures while navigating their arboreal environment (Thorpe and Crompton, 2005; Thorpe and Crompton, 2006; Payne et al. 2006; Thorpe et al. 2009), which potentially results in higher loading across the whole superior surface of the femoral head. *Pongo* also vertically climbs less frequently than African apes (Thorpe and Crompton, 2006), which may be reflected by the less defined anterior concentration of high BV/TV in *Pongo* compared with *Pan* and, especially, with *Gorilla*. Although my sample of *Pongo* is small (n=5) and all individuals were female, there was greater variation in the BV/TV distributions along the anterior and posterior aspects of the femoral head than was found in African apes. The one *P. abelii* specimen in my sample differed from the *P. pygmaeus* individuals in having only one superior concentration of high BV/TV. Although locomotor differences have been documented between *P. pygmaeus* and *P. abelii* (Sugardjito and van Hooff, 1986; Cant, 1987), a larger sample of both species is needed to determine if this variation in the trabecular pattern is characteristic of each species.

Homo showed a distinct trabecular pattern that is consistent with my predictions and similar to previous results showing the density distribution of

trabeculae adjacent to cortical bone (Treece and Gee, 2014). All *Homo* individuals displayed one main region of high BV/TV, located posteriorly and superiorly on the femoral head. This concentration was positioned more medially than the posterior concentration seen in great apes and closer to the fovea capitis, which is consistent with loading of the femur at a valgus angle. Intermediate BV/TV values continued along the superior aspect of the femoral head in *Homo*. This is consistent with loading that occurs throughout the gait cycle over the articulating surface but suggests that peak loading is occurring at the posterosuperior region, which is in contact with the acetabulum during walking (Bonneau et al. 2012; Bonneau et al. 2014). Of course, humans also engage in other activities that involve more flexed hip joint postures, such as running, jumping, or climbing stairs, all of which impose high loads on the lower limb (van den Bogert et al. 1999; Giarmatzis et al. 2015) and could result in some trabecular reorganisation, explaining the extended area of intermediate BV/TV values I found across the femoral head. Unfortunately, it is not yet known exactly how the peak load is distributed over the femoral head during these activities. However, all individuals lack the anterior concentration found in apes, further supporting the interpretation that high BV/TV in the anterior region could be linked to arboreal behaviours or more specifically vertical climbing.

3.4.2. Quantitative analysis of trabecular structure

Quantitative analysis of the femoral head trabecular structure only partially supported my hypotheses. As expected, *Homo* displayed the lowest mean BV/TV in my sample but was only significantly different from that of *Pan*. My results confirm previous studies showing that modern humans, particularly those that are less active, have relatively lower BV/TV across the skeleton compared with highly mobile modern humans and other primates (Chirchir et al. 2015; Ryan and Shaw, 2015; Saers et al. 2016; Chirchir et al. 2017). Furthermore, *Homo* showed significantly higher DA than great apes, which is consistent with the more stereotypical loading of the hip joint during bipedal locomotion and in accordance with previous results from the proximal (Ryan and Shaw, 2015; Ryan et al. 2018) as well as the distal femur

(Georgiou et al. 2018). *Homo* has narrower acetabulae than other great apes, with expanded cranial lunate surfaces, as well as shortened dorsal surfaces, which result in a distinctively-shaped dorso-cranially expanded lunate surface that may restrict movement in the parasagittal plane (San Millán et al. 2015). Furthermore, in *Homo* the iliofemoral ligament limits extension and external rotation (Myers et al. 2011), the ischiofemoral ligament limits internal rotation and the pubofemoral ligament limits abduction (Wagner et al. 2012), all of which result in a more restrictive and stereotypical motion and loading of the femoral head that is reflected in the trabecular structure.

As predicted, mean BV/TV was highest in *Pan*, which is consistent with previous studies showing relatively high BV/TV in the African ape femur (Ryan and Shaw, 2015; Georgiou et al. 2018; Ryan et al. 2018; Tsegai et al. 2018a) and other postcranial elements (e.g. Cotter et al. 2009; Scherf et al. 2013; Tsegai et al. 2017). BV/TV in *Pan* did not differ significantly from *Gorilla*, reflecting their generally similar locomotor repertoire. Overall, the quantitative analysis highlighted *Pan* as being distinct from the other taxa. *Pan* not only showed the highest BV/TV values, but also differed significantly from all taxa in Tb.N and Tb.Sp, showing consistently higher Tb.N and lower Tb.Sp, again resembling previous findings (Ryan and Shaw, 2015). Furthermore, *Pan* showed significantly lower Tb.Th than *Gorilla* and *Homo*. Additionally, mean DA was lowest in *Pan*, as well as *Pongo*, but only differed significantly from *Homo*. Less data is available on the femoral ligaments of non-human apes however *Pan* and *Pongo* seem to have less restrictive ligaments than *Homo* (Sonntag, 1923; 1924).

The trabecular structure of *Gorilla* and *Pongo* was not as distinct. *Gorilla* mean BV/TV did not differ significantly from any other taxon, and they only differed significantly in Tb.N, Tb.Sp and Tb.Th from *Pan*, as well as in DA from *Homo*. *Gorilla* has less variable positioning of their lower limbs during locomotion, compared to other non-human apes, as was shown in vertical climbing (Isler, 2005), however this is not displayed as clearly in their DA values as was initially predicted. The lack of significant differences in BV/TV and DA with *Pan* can perhaps be explained by the

similar shape of their hip joints (San Millán et al. 2015) and overall similarities in locomotion (Doran, 1997). None of great apes differed significantly in DA, despite clear differences in locomotor behaviours and hip morphology. *Pongo* has a cranio-ventrally expanded lunate surface and a smaller acetabular fossa than other apes. They also show the largest articular surfaces and relatively shallow acetabulae (Schultz, 1969), which may be responsible for the increased mobility of the femoral head. Furthermore, *Pongo* has a greater capacity for abduction and external rotation than non-suspensory taxa (Hammond, 2014). Thus, *Pongo* was expected to display significantly lower DA values than all other taxa, which was not the case, but this result may also reflect my small sample size for this taxon.

My results showed that *Pan* has relatively numerous, thinner and compactly organised trabeculae, while *Gorilla* and *Homo* have relatively few, thicker and more separated trabeculae. *Pongo* has relatively few, thinner and more separated trabeculae. These results are largely in accordance with previous analyses of femoral head trabeculae (Ryan and Shaw, 2012; 2015) which showed that humans have relatively less numerous, thin and highly anisotropic trabeculae compared to other anthropoids, *Pan* have relatively high numbers of thick, isotropic trabeculae and *Pongo* have relatively few, isotropic trabeculae. *Gorilla* showed the thickest trabeculae (Table 2), in support of previous studies suggesting that larger taxa have absolutely thicker trabeculae (Barak et al. 2013b; Ryan and Shaw, 2013; Tsegai et al. 2013). However, the difference was not found to be significant, possibly due to the small sample sizes in my study. Allometric relationships were not tested in my study because my sample sizes were not large enough to test this intraspecifically, however previous research has shown that these trabecular parameters can vary predictably with body size interspecifically (Cotter et al. 2009; Doube et al. 2011; Barak et al. 2013b; Ryan and Shaw, 2013). Across a large sample of mammals, Tb.Th and Tb.Sp were shown to increase with size (Doube et al. 2011). In primates, Tb.N, Tb.Th and Tb.Sp present negatively allometric relationships with body mass (Barak et al. 2013b; Ryan and Shaw, 2013), resulting in fewer, thinner and less separated trabeculae in larger taxa. These studies suggest that absolute trabecular parameters, and specifically Tb.N, Tb.Sp and Tb.Th, do not necessarily directly reflect locomotor

modes as they could reflect body-size related or systemic differences between taxa. Nevertheless, since my sample includes apes that are relatively similar in body size compared to the more diverse samples of previous studies (Doube et al. 2011; Barak et al. 2013b; Ryan and Shaw, 2013), I would expect that allometry does not have a significant effect on the variation observed here.

The absence of a clear functional signal in the mean trabecular parameters may be due to methodological limitations of the whole-epiphysis approach. The mean value of any given trabecular parameter can obscure or homogenise any potential distinct variation in specific regions of the femoral head, as demonstrated by the BV/TV distribution maps and previous studies (Sylvester and Terhune, 2017). This is where the traditional VOI approach, in which the trabecular architecture of specific regions of an epiphysis can be quantified and compared, is potentially more functionally informative (e.g. Ryan and Shaw, 2012; 2015; Ryan et al. 2018). Additionally, the lack of a strong functional signal in these parameters could be due to non-mechanical factors affecting trabecular structure. Trabecular bone also functions as a reserve of minerals and is important in maintaining homeostasis, hence its structure will, to some extent, be affected by this (Rodan, 1998; Clarke, 2008). Genes control for the rate of remodelling and bone mineral density, as well as the response to mechanical strain in different skeletal sites (Smith et al. 1973; Dequeker et al. 1987; Kelly et al. 1991; Garnero et al. 1996; Hauser et al. 1997; Judex et al. 2002; Judex et al. 2004). These factors, along with the fact that trabecular bone remodels in response to a range of magnitudes and frequencies of load (Whalen et al. 1988; Rubin et al. 1990; Rubin et al. 2001; Judex et al. 2003; Scherf et al. 2013), complicate interpretations. Age, hormones, sex and other factors (e.g. Simkin et al. 1987; Pearson and Lieberman, 2004; Suuriniemi et al. 2004; Kivell, 2016; Wallace et al. 2017; Tsegai et al. 2018a) influence trabecular bone modelling, thus these factors should not be ignored. Nonetheless, future research will aim to use techniques that will allow statistical comparisons of the trabecular distribution patterns in the femoral head of apes, rather than mean parameters, for more accurate interpretation of locomotor patterns in extinct hominins.

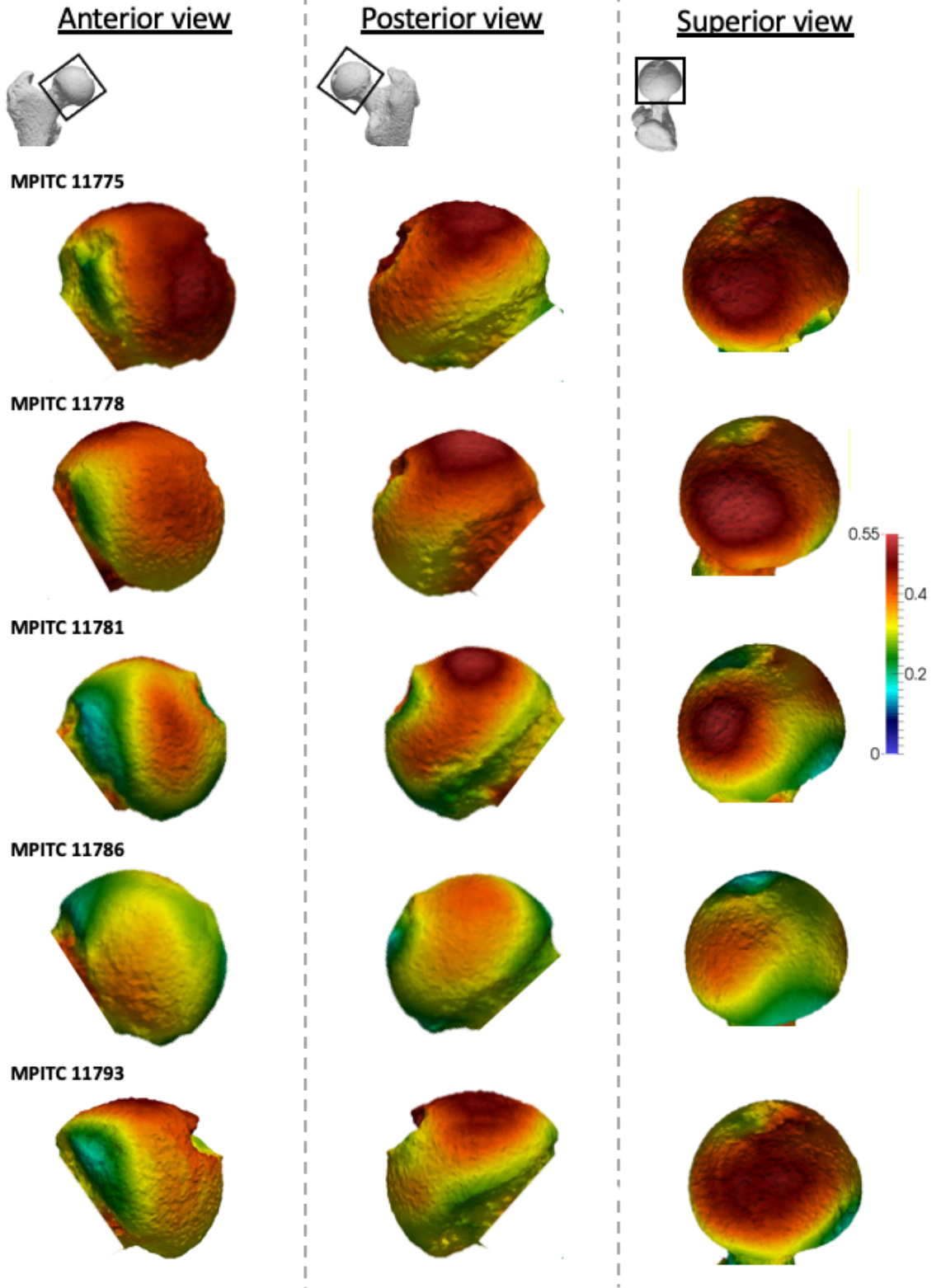
3.5. Conclusion

This study showed that the trabecular architecture of the femoral head in great apes and humans reflects habitual hip postures during locomotion. *Pan* and *Gorilla* showed similar BV/TV distribution patterns, with generally two distinct high BV/TV regions that are consistent with hip postures during knuckle-walking and vertical climbing. *Pongo* showed a BV/TV distribution pattern that is characteristic of their highly mobile hips and complex locomotion, however they do not differ as significantly as predicted from African apes. Finally, *Homo* showed a distinct pattern of BV/TV distribution, with one posterosuperior region of high BV/TV, the lowest overall BV/TV values and highest DA values, which is consistent with stereotypical loading during locomotion. Despite mean trabecular parameters not demonstrating locomotor differences as clearly as predicted, they largely match results from previous VOI studies (Ryan and Shaw, 2015; Ryan et al. 2018). My research reveals that there are distinct patterns of BV/TV distribution that generally distinguish the locomotor groups and provide a valuable comparative sample for future research on the evolution of gait in hominins.

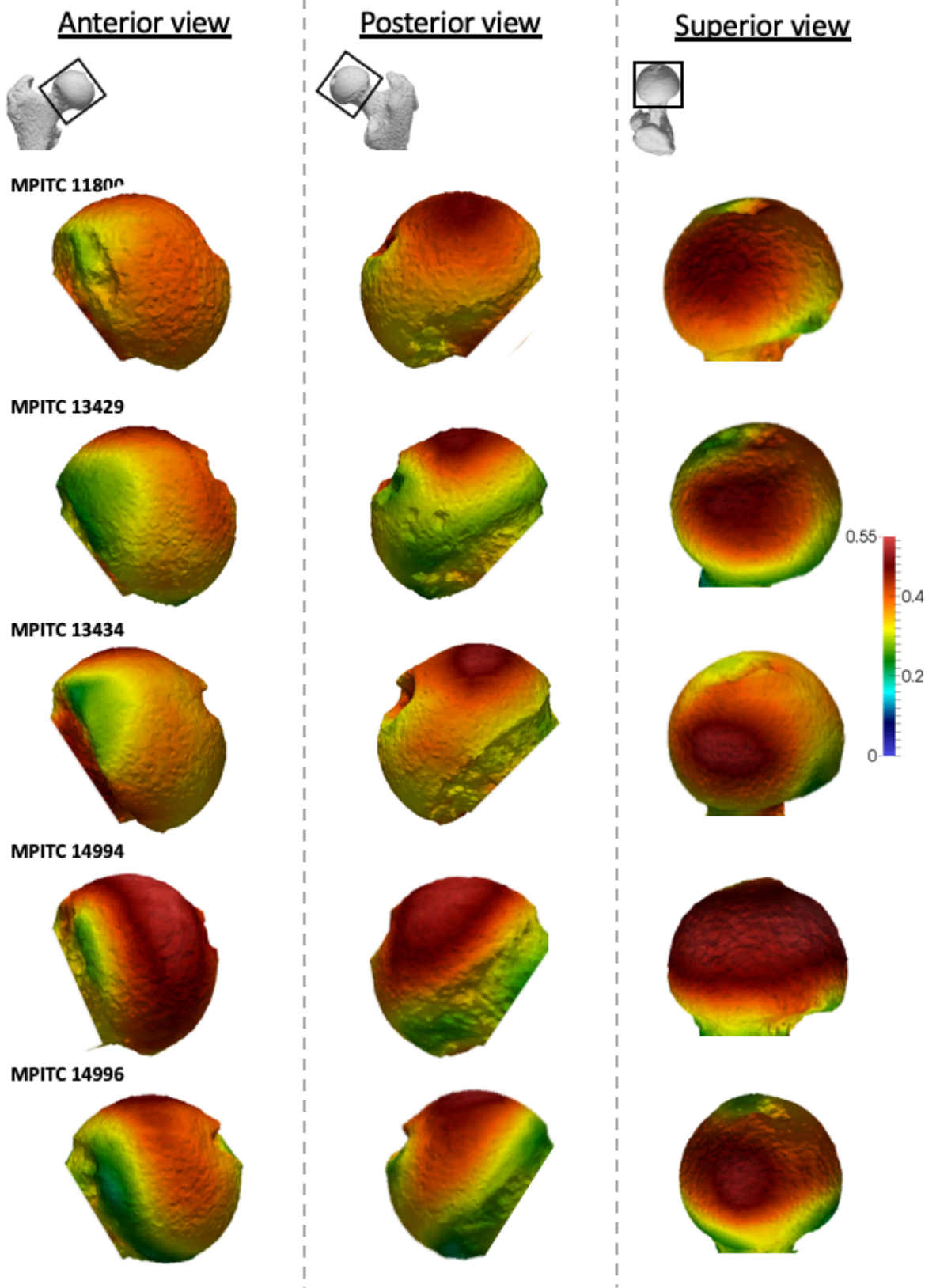
Supplementary material

Specimens scaled from 0-55%

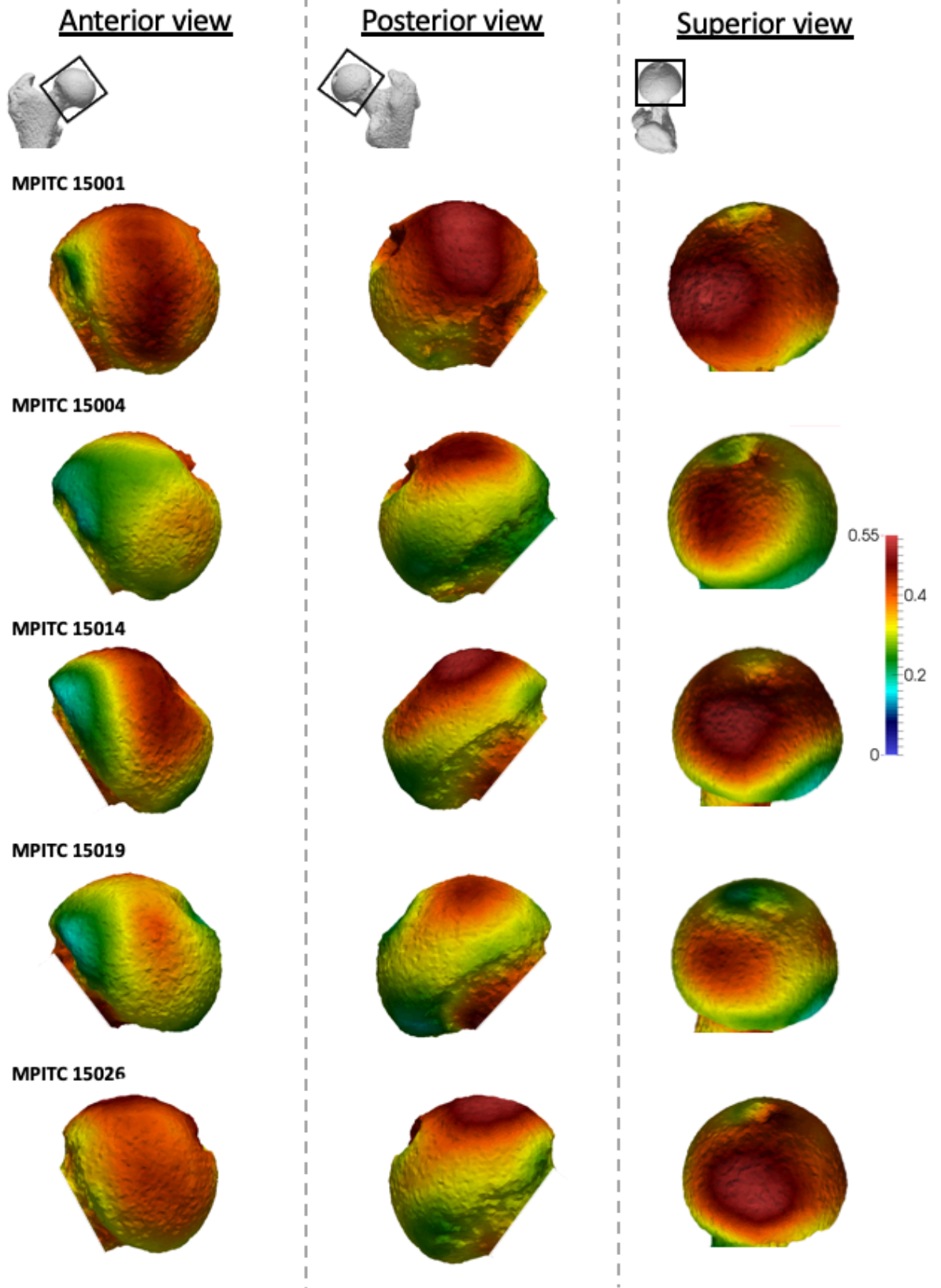
Pan troglodytes versus BV/TV distribution



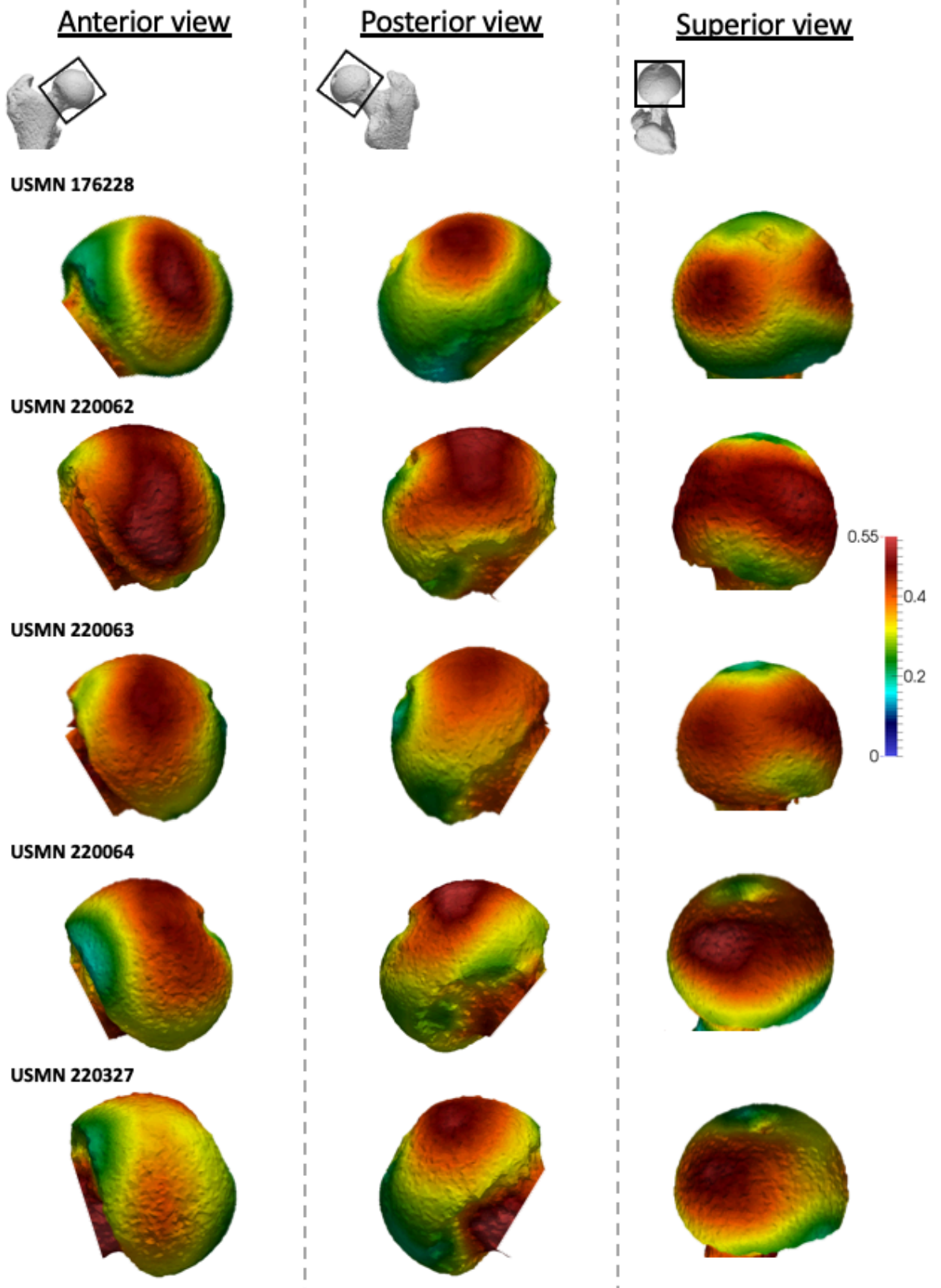
Pan troglodytes versus BV/TV distribution



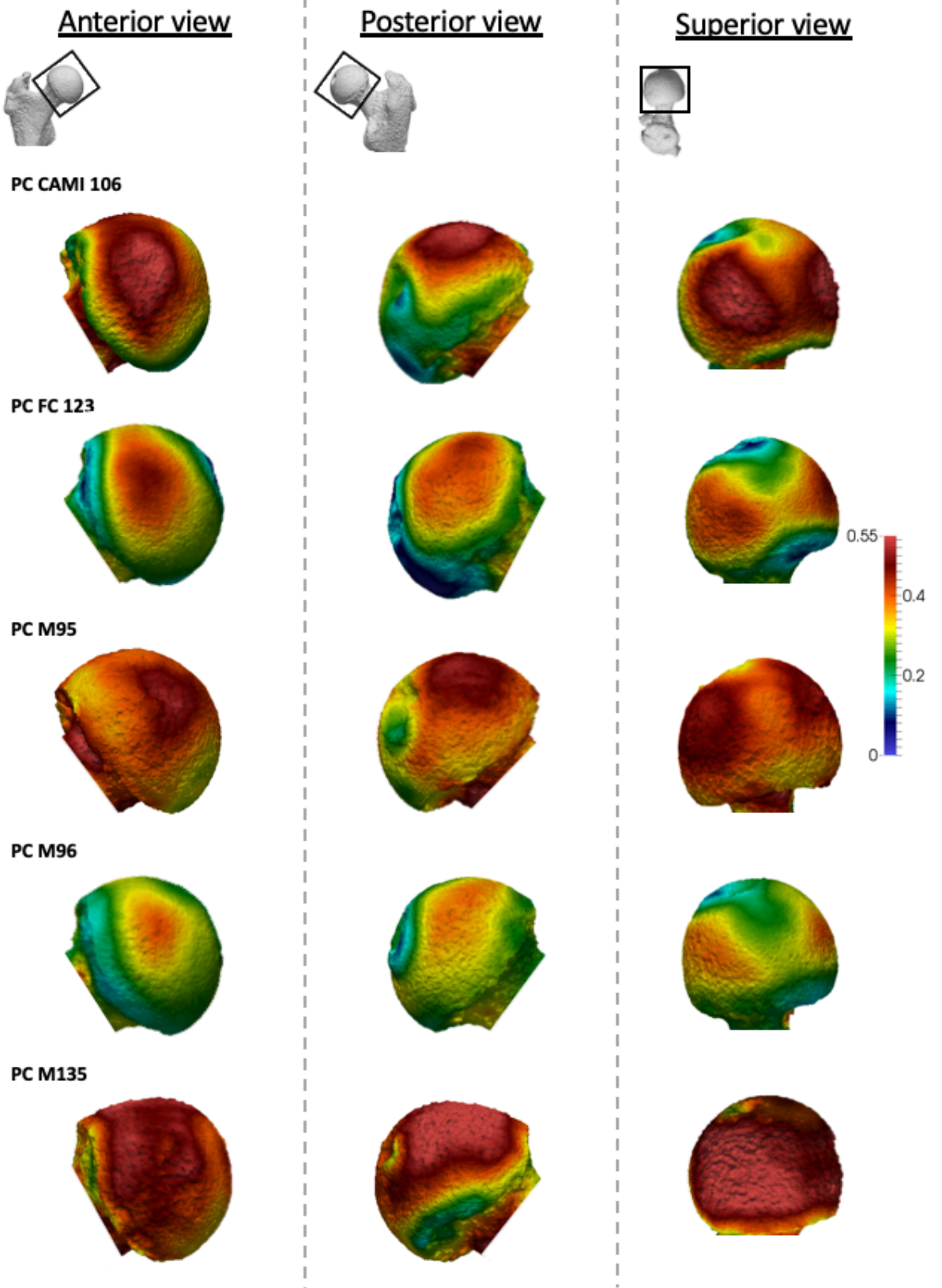
Pan troglodytes versus BV/TV distribution



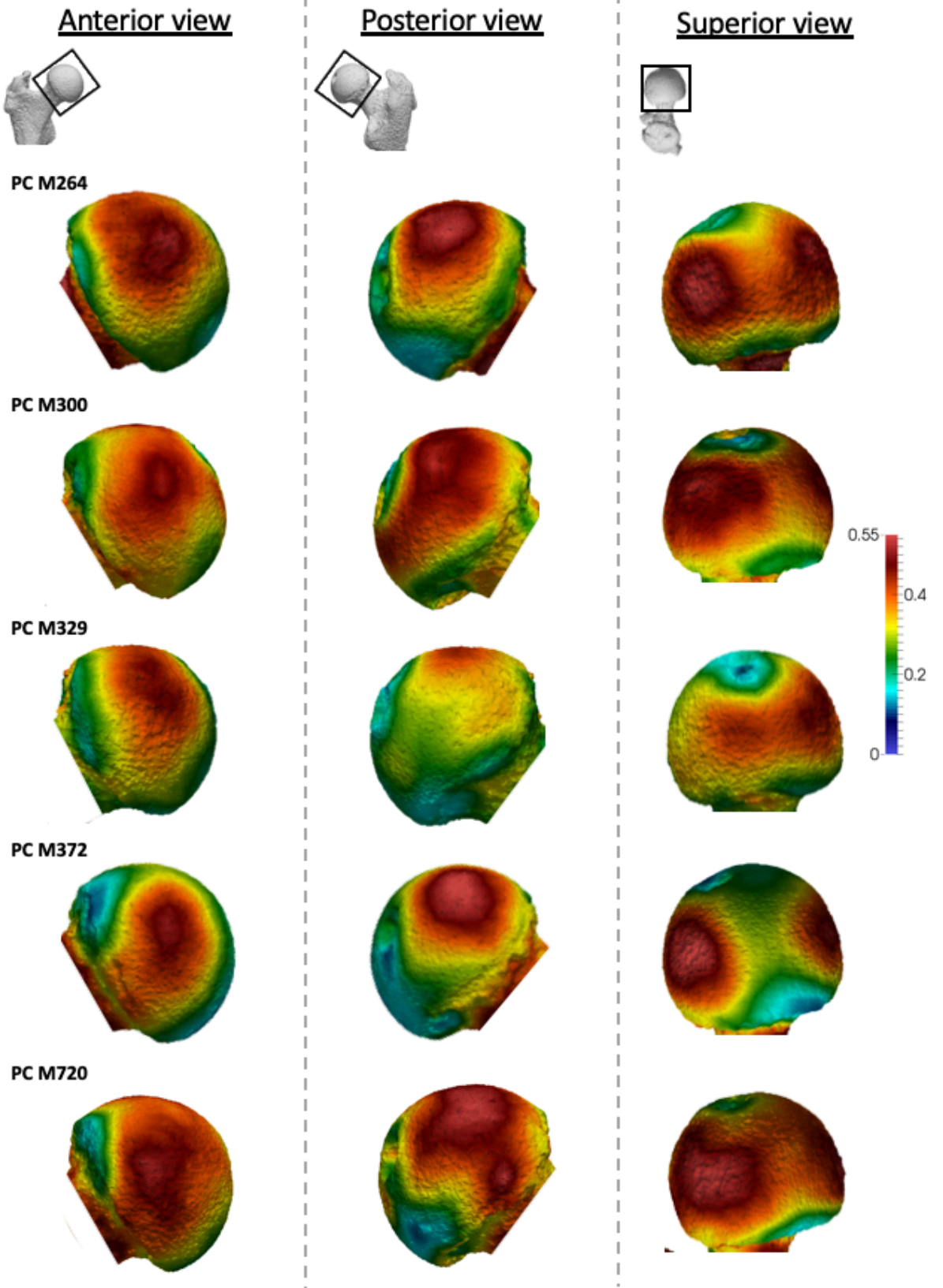
Pan troglodytes troglodytes BV/TV distribution



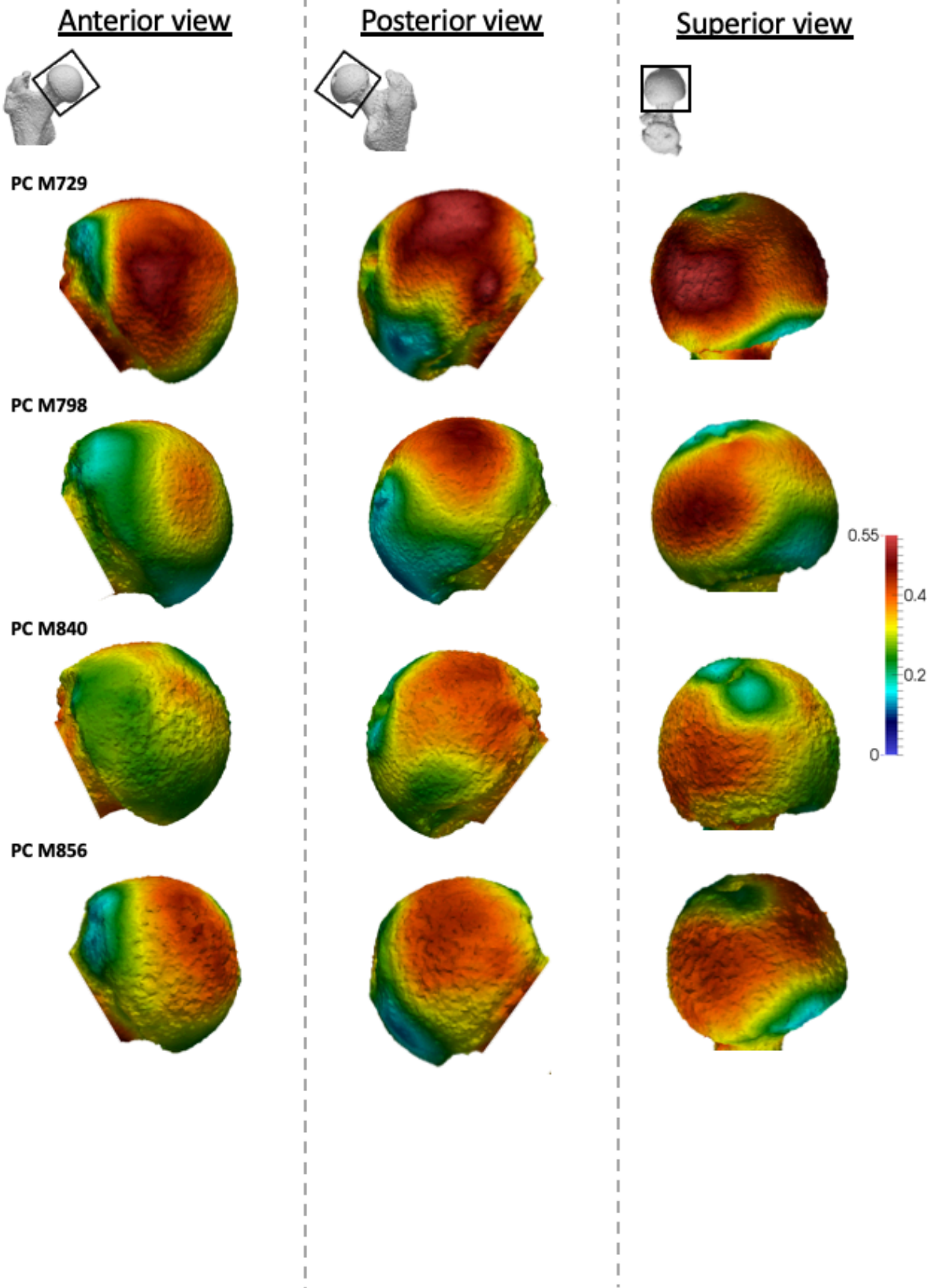
Gorilla gorilla BV/TV distribution



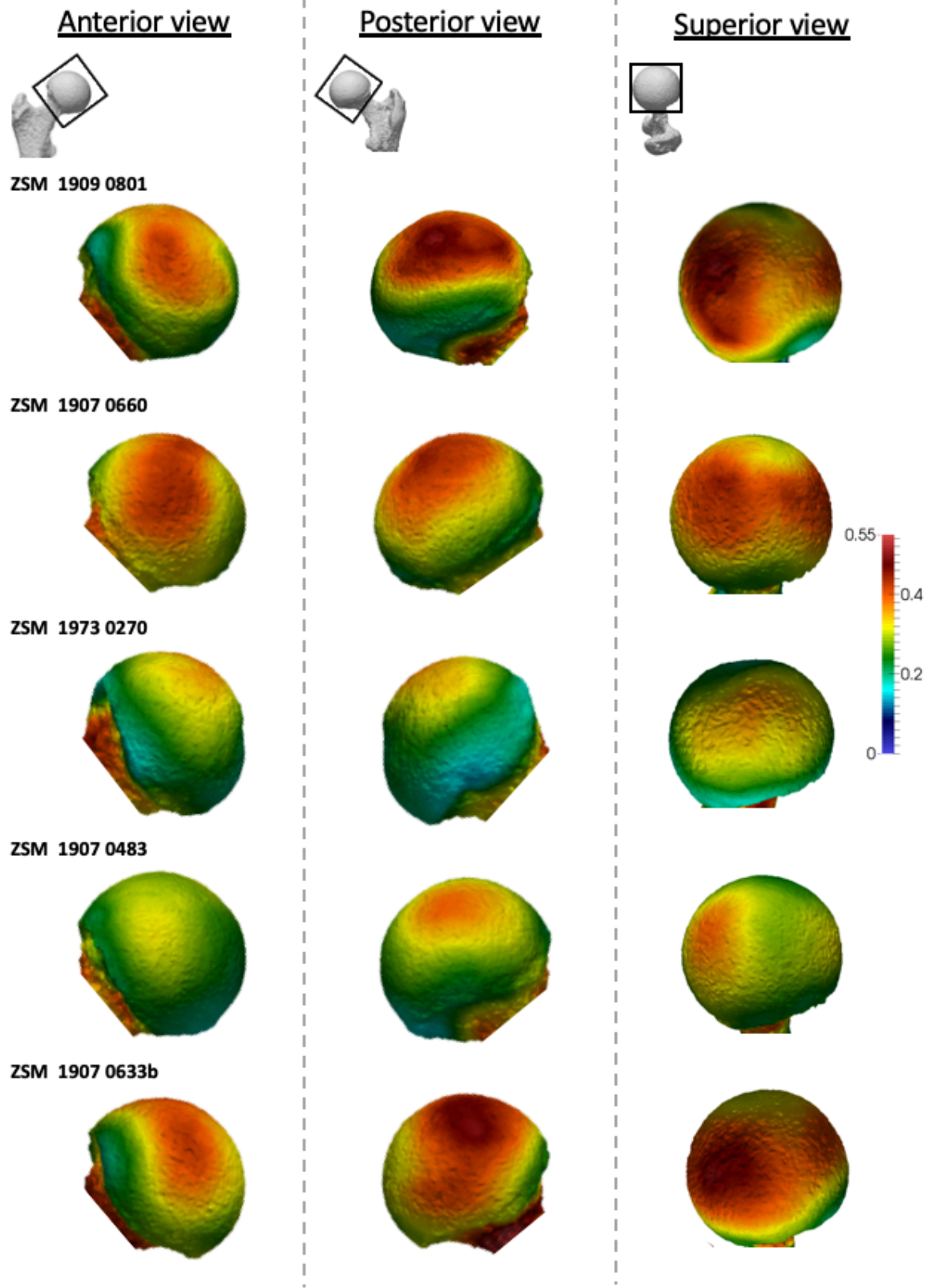
Gorilla gorilla BV/TV distribution



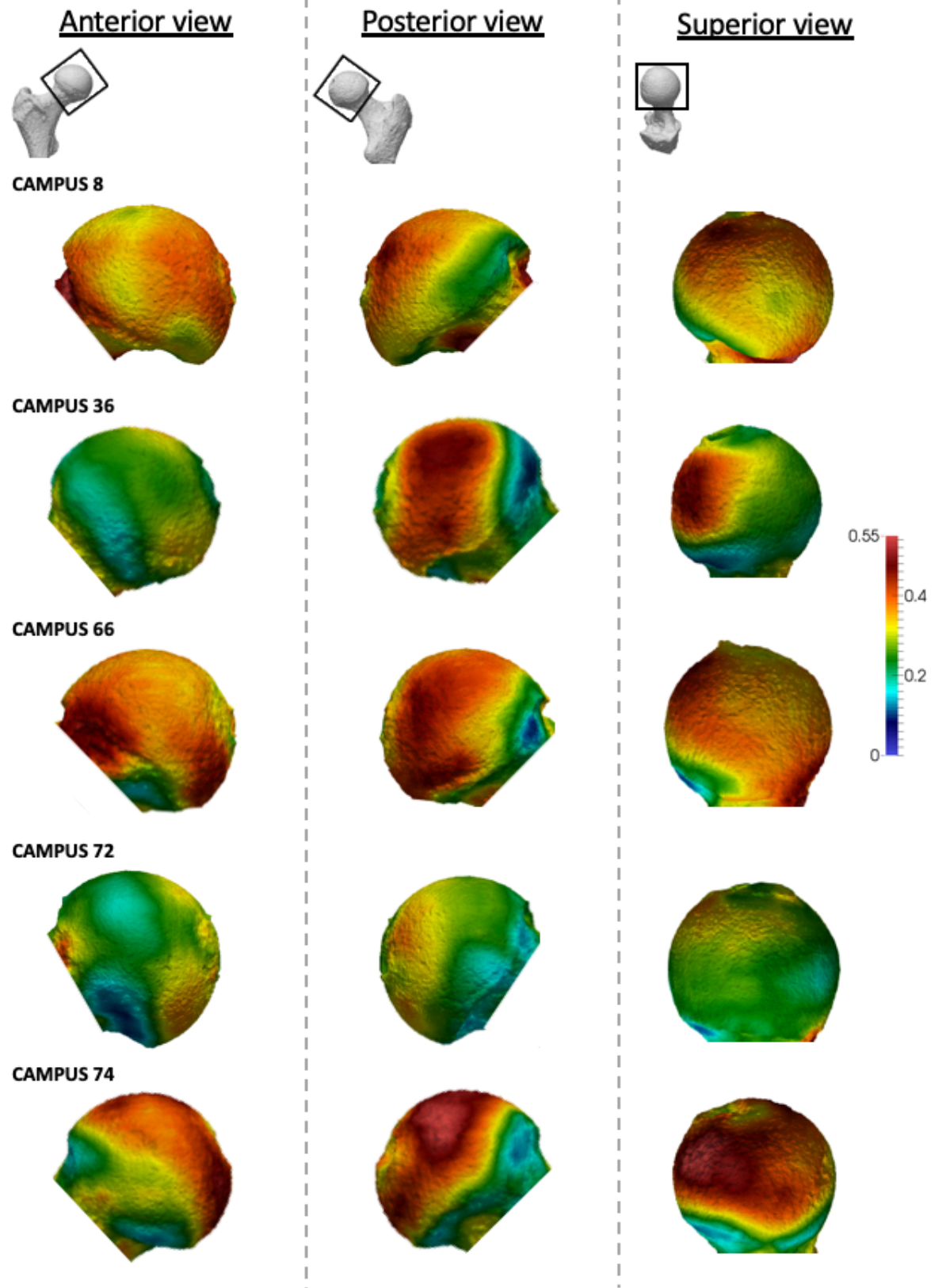
Gorilla gorilla BV/TV distribution



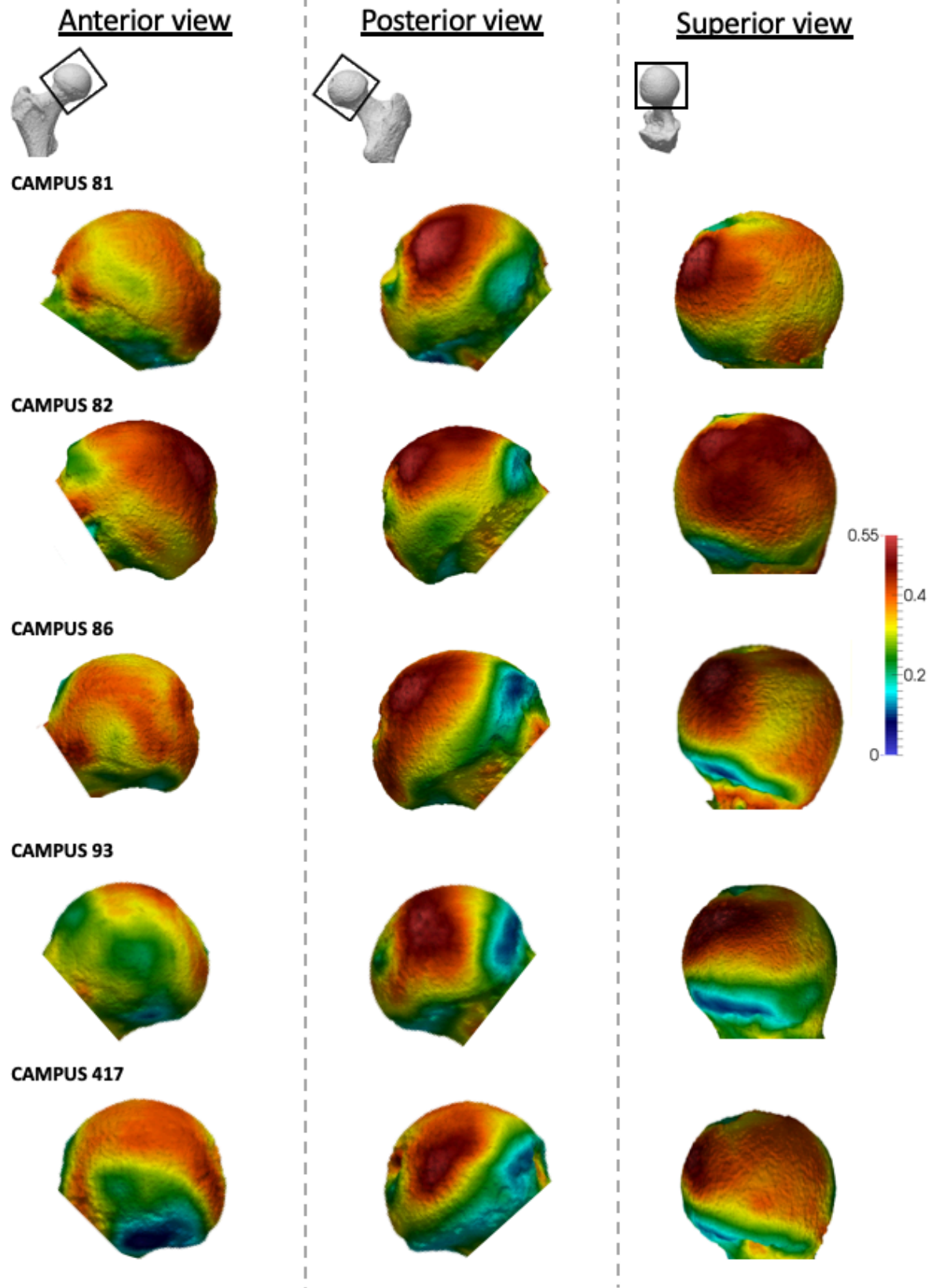
Pongo sp. BV/TV distribution



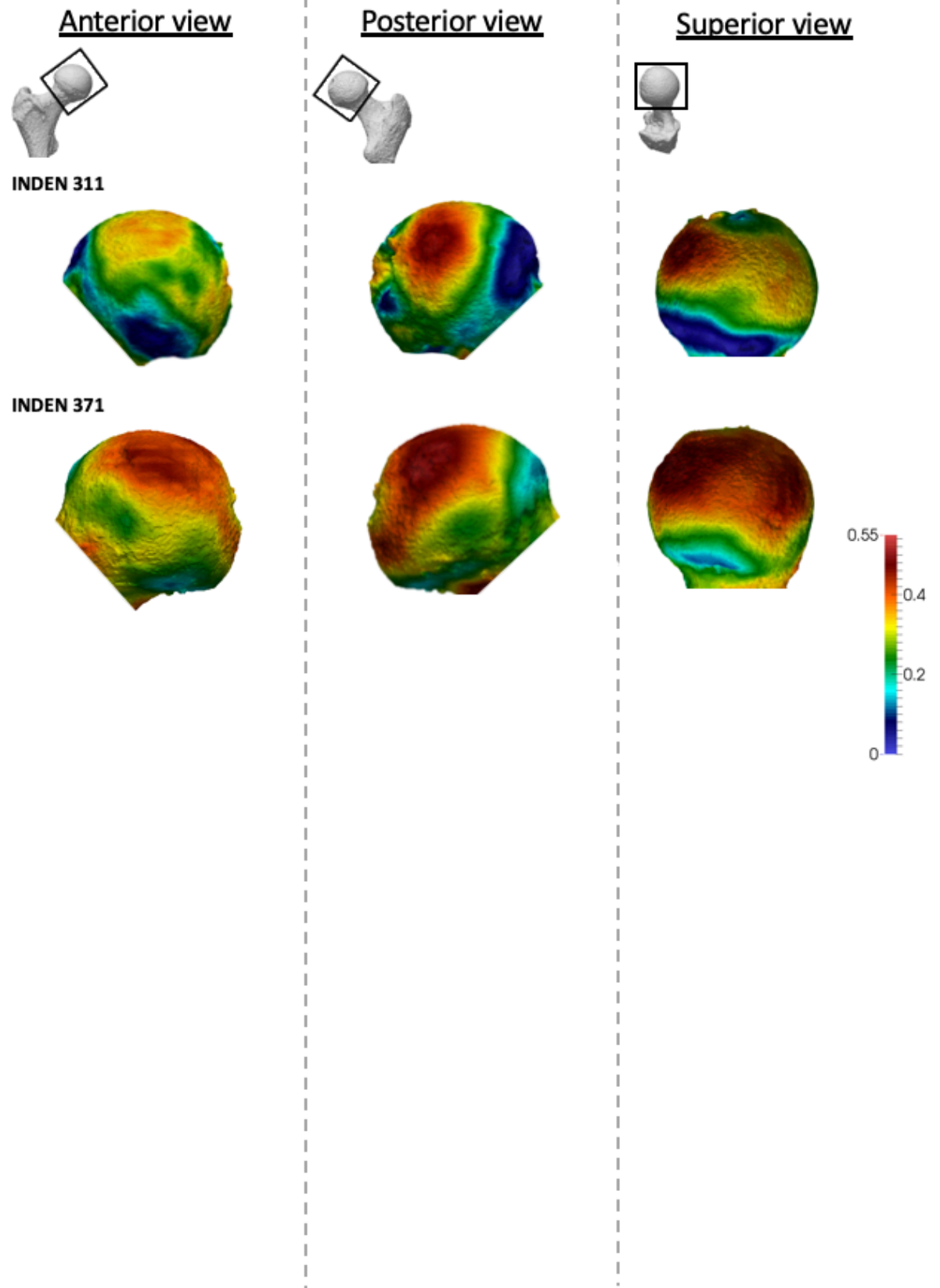
Homo sapiens BV/TV distribution



Homo sapiens BV/TV distribution

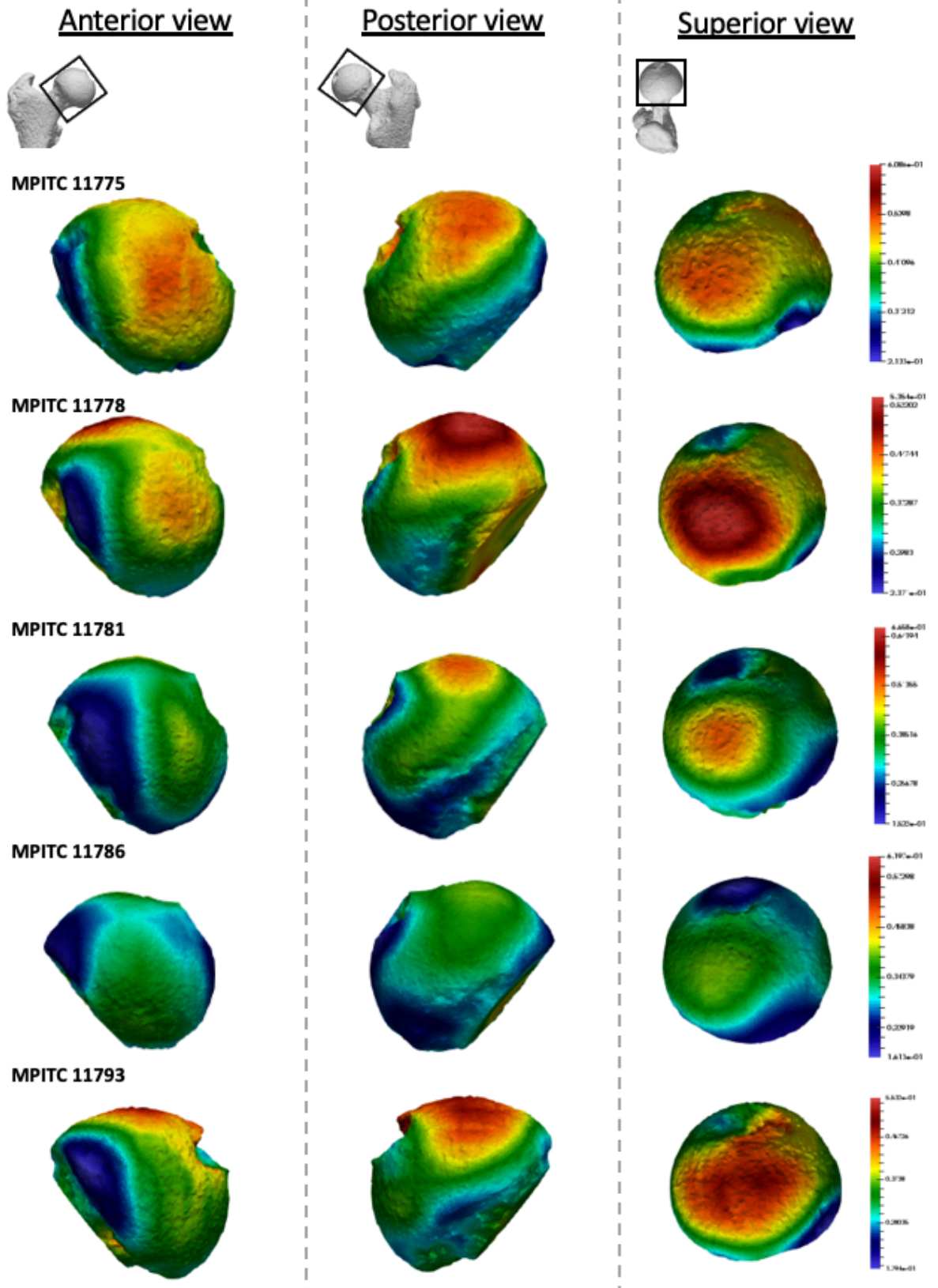


Homo sapiens BV/TV distribution

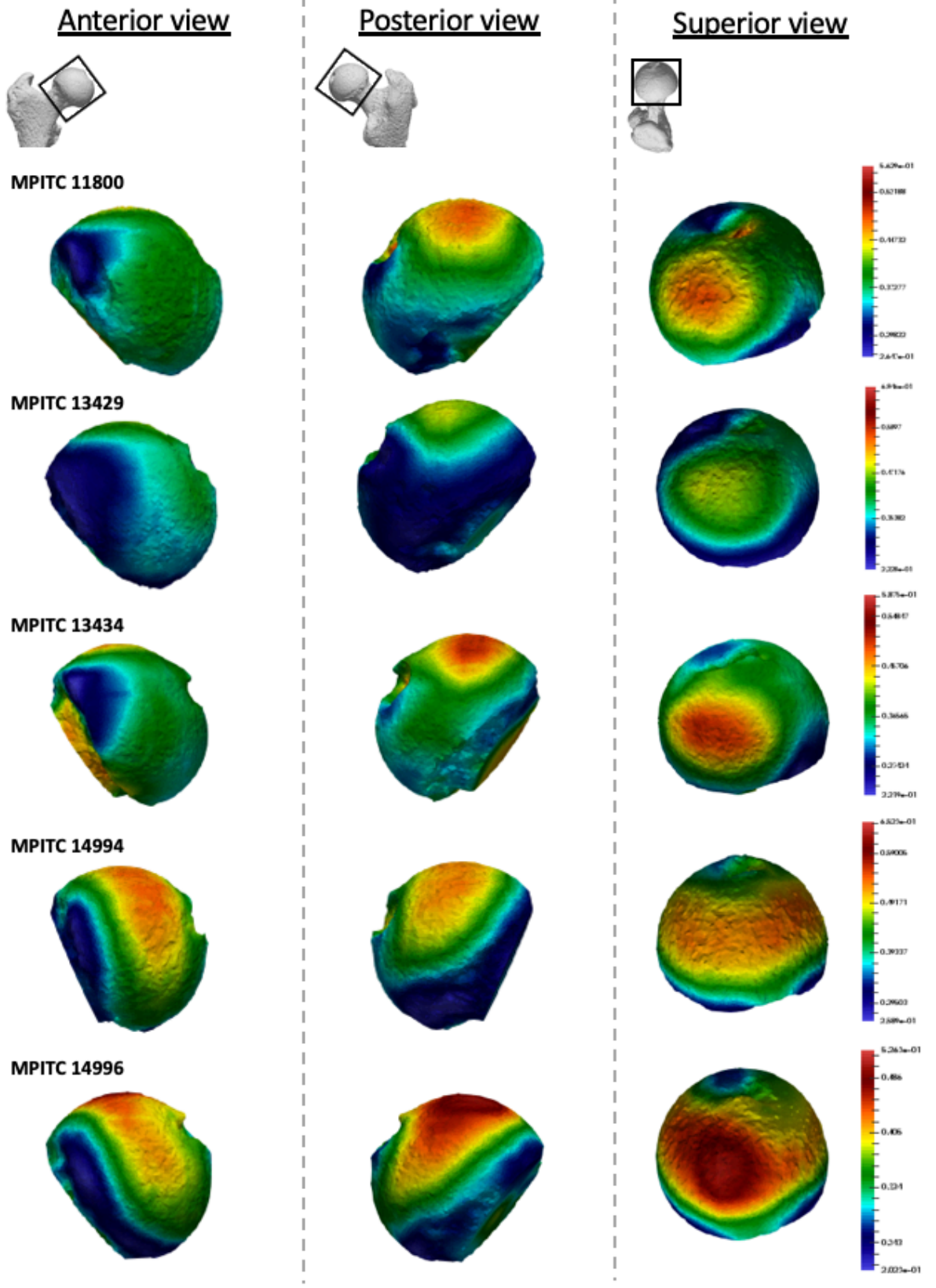


Specimens scaled to their own range

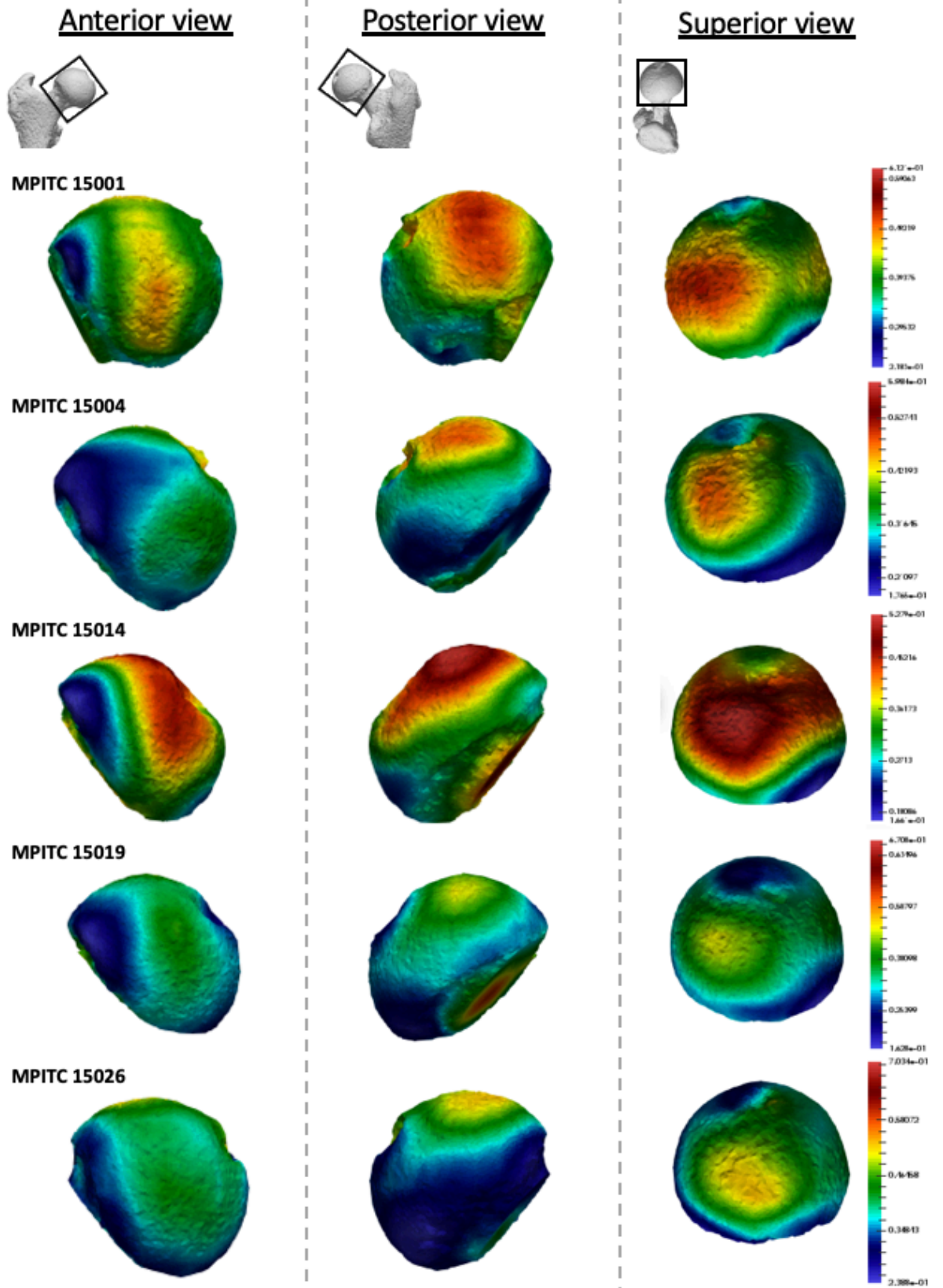
Pan troglodytes versus BV/TV distribution



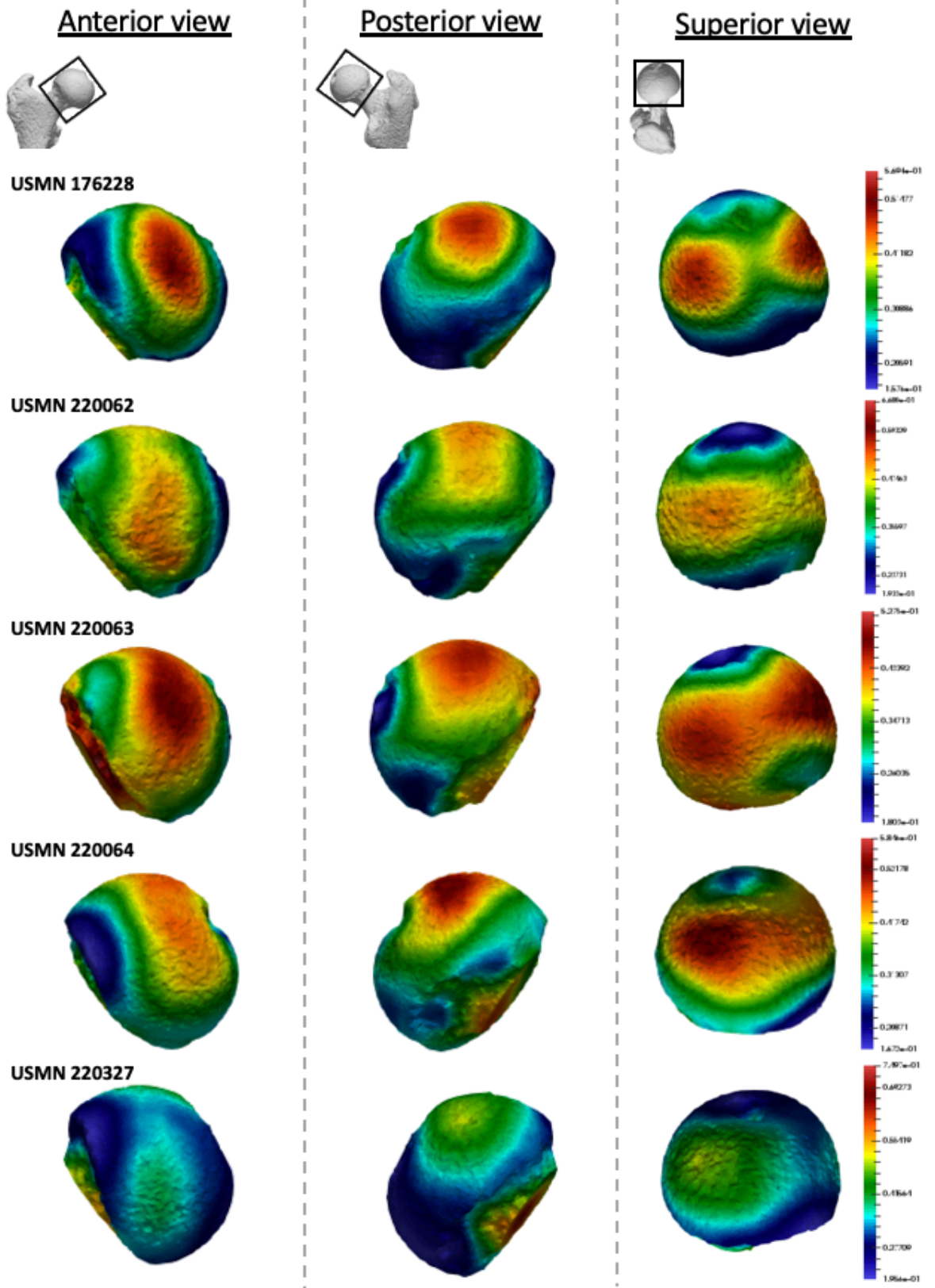
Pan troglodytes versus BV/TV distribution



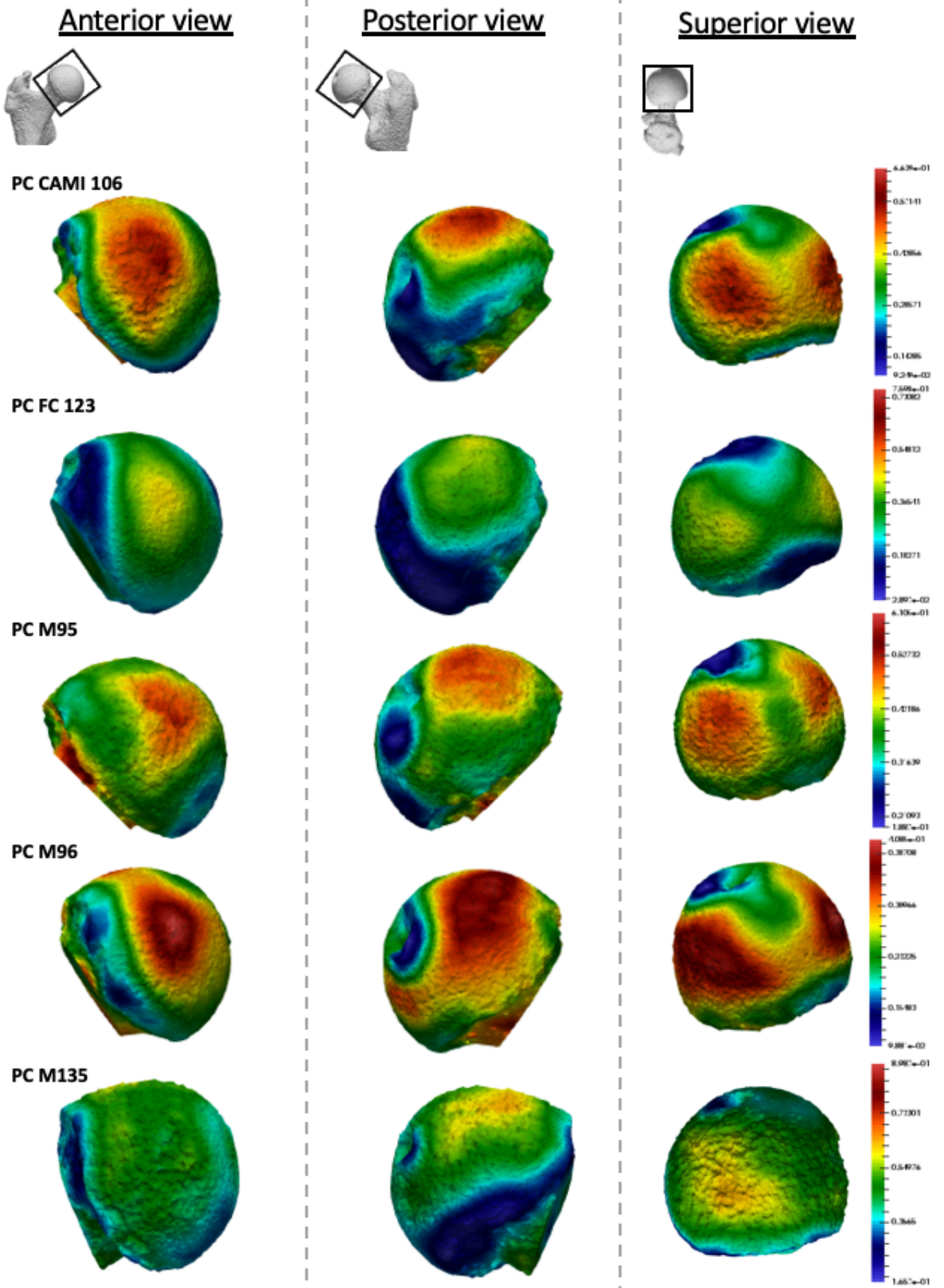
Pan troglodytes versus BV/TV distribution



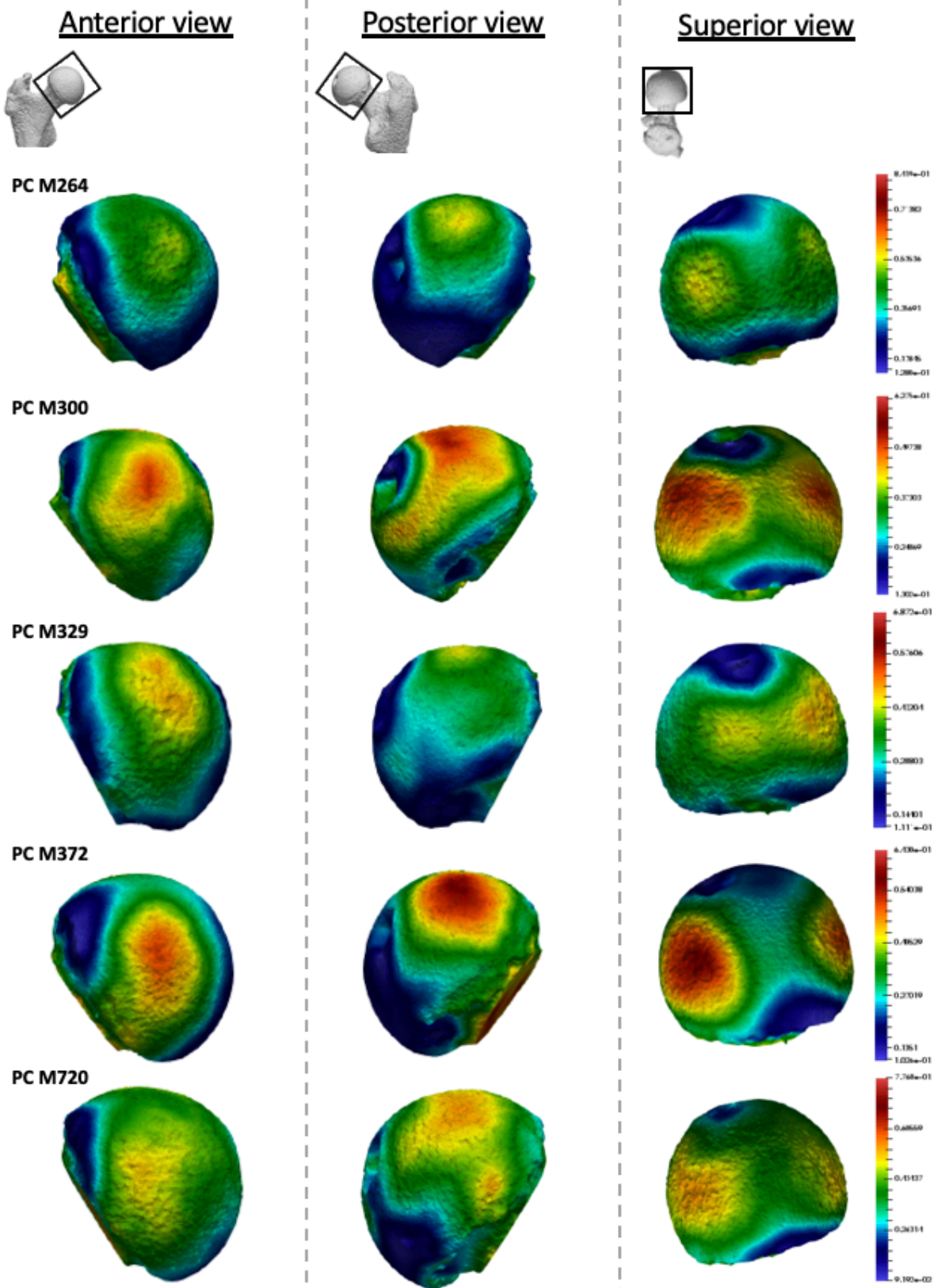
Pan troglodytes troglodytes BV/TV distribution



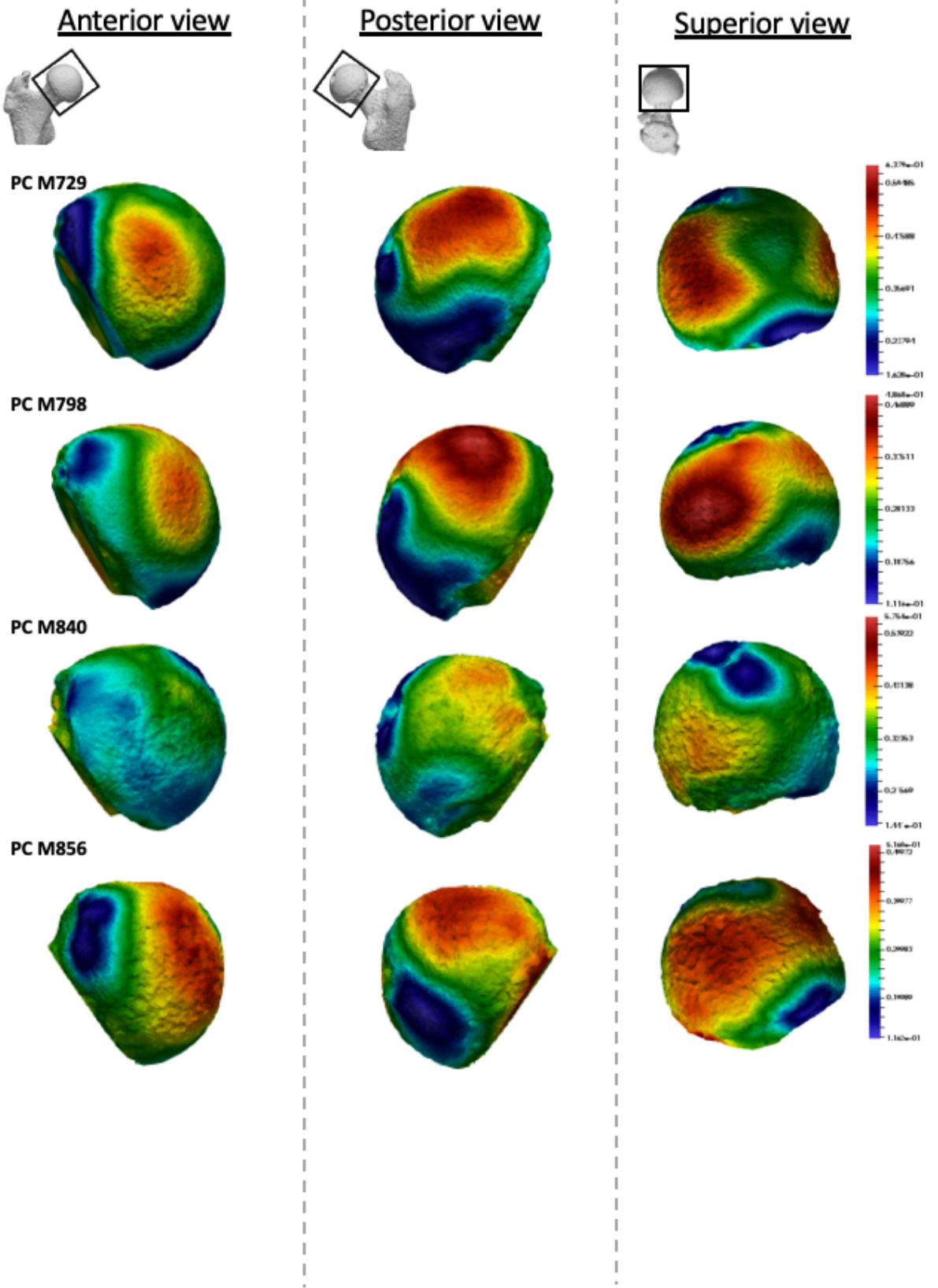
Gorilla gorilla BV/TV distribution



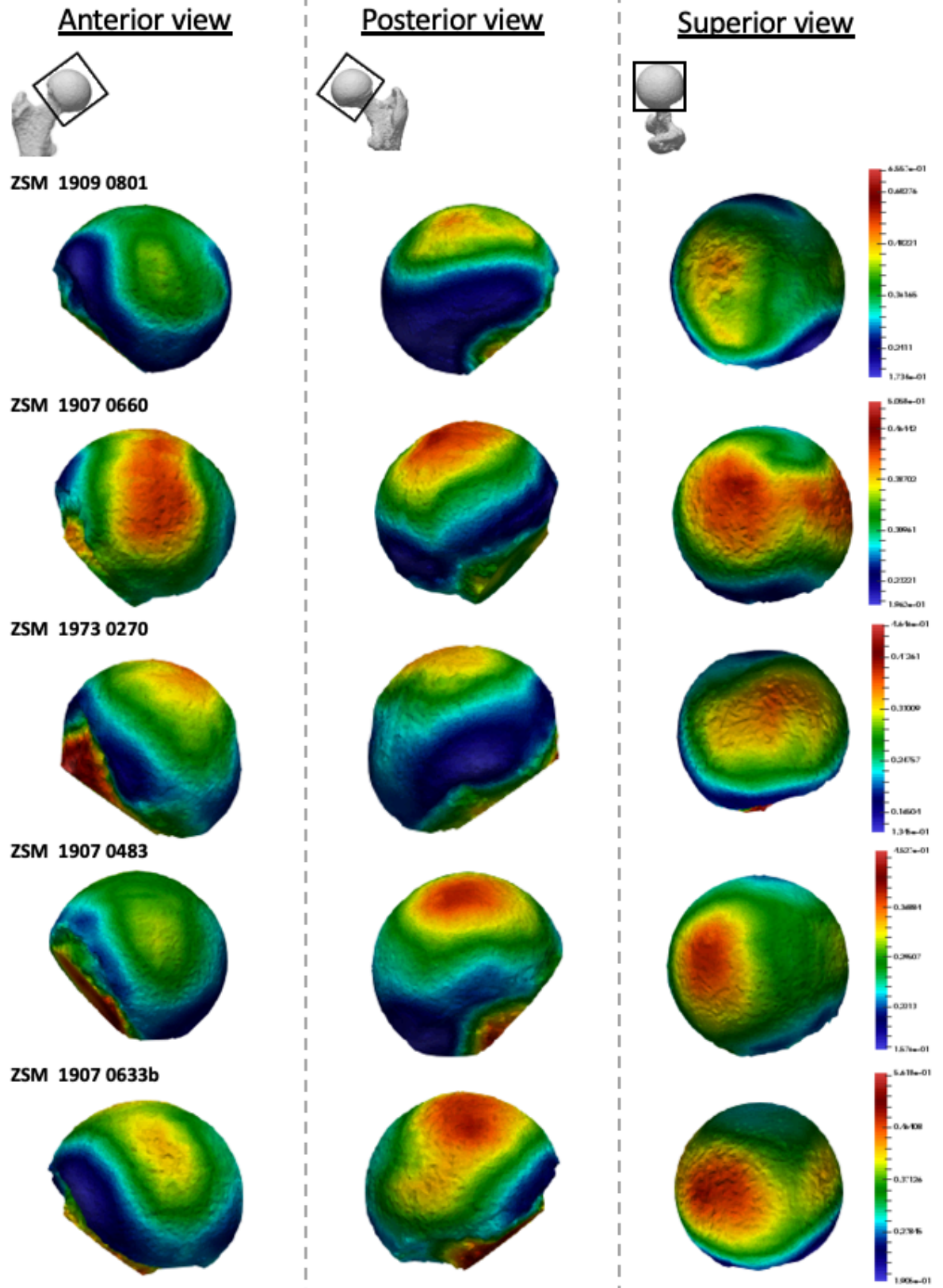
Gorilla gorilla BV/TV distribution



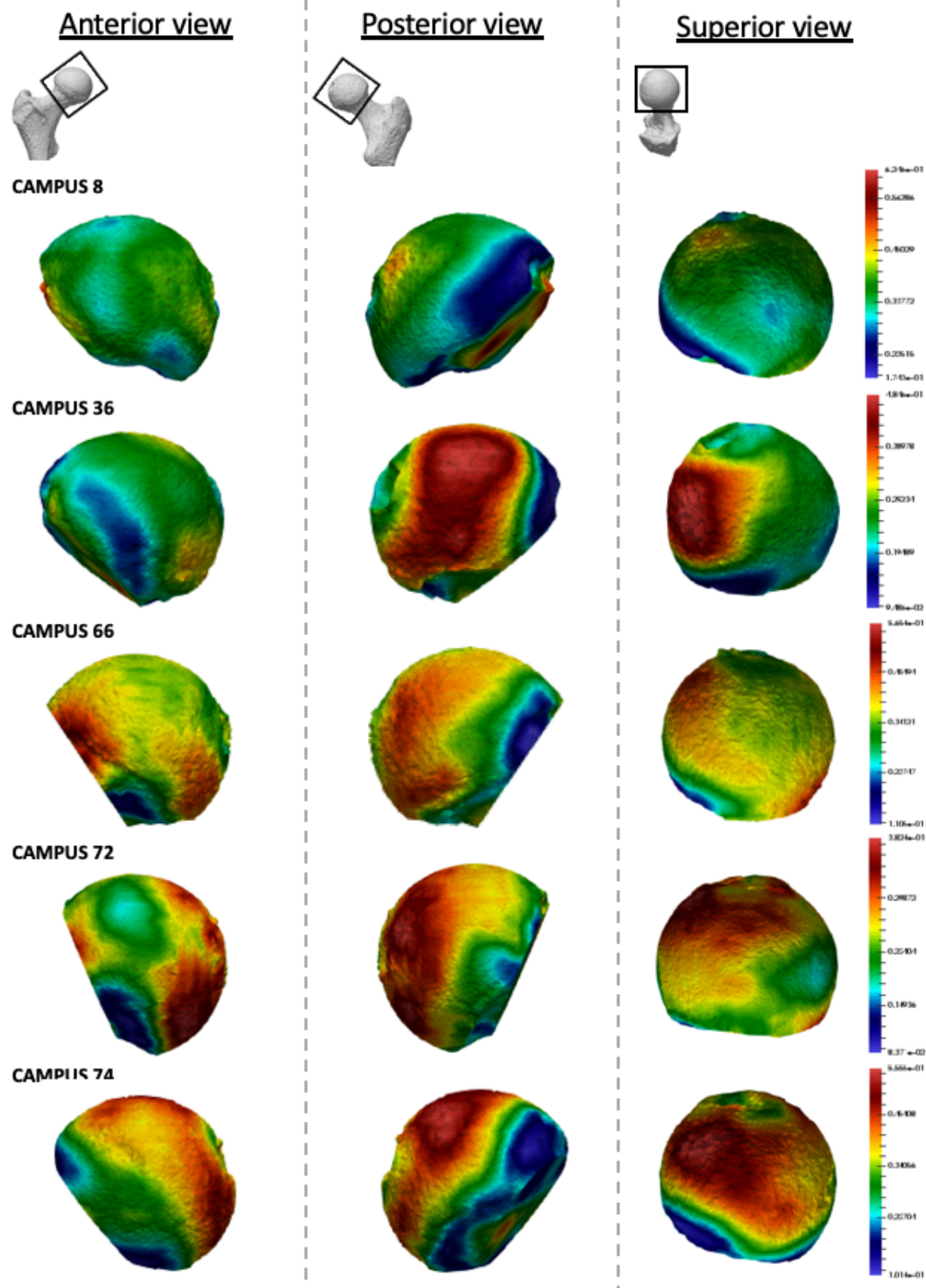
Gorilla gorilla BV/TV distribution



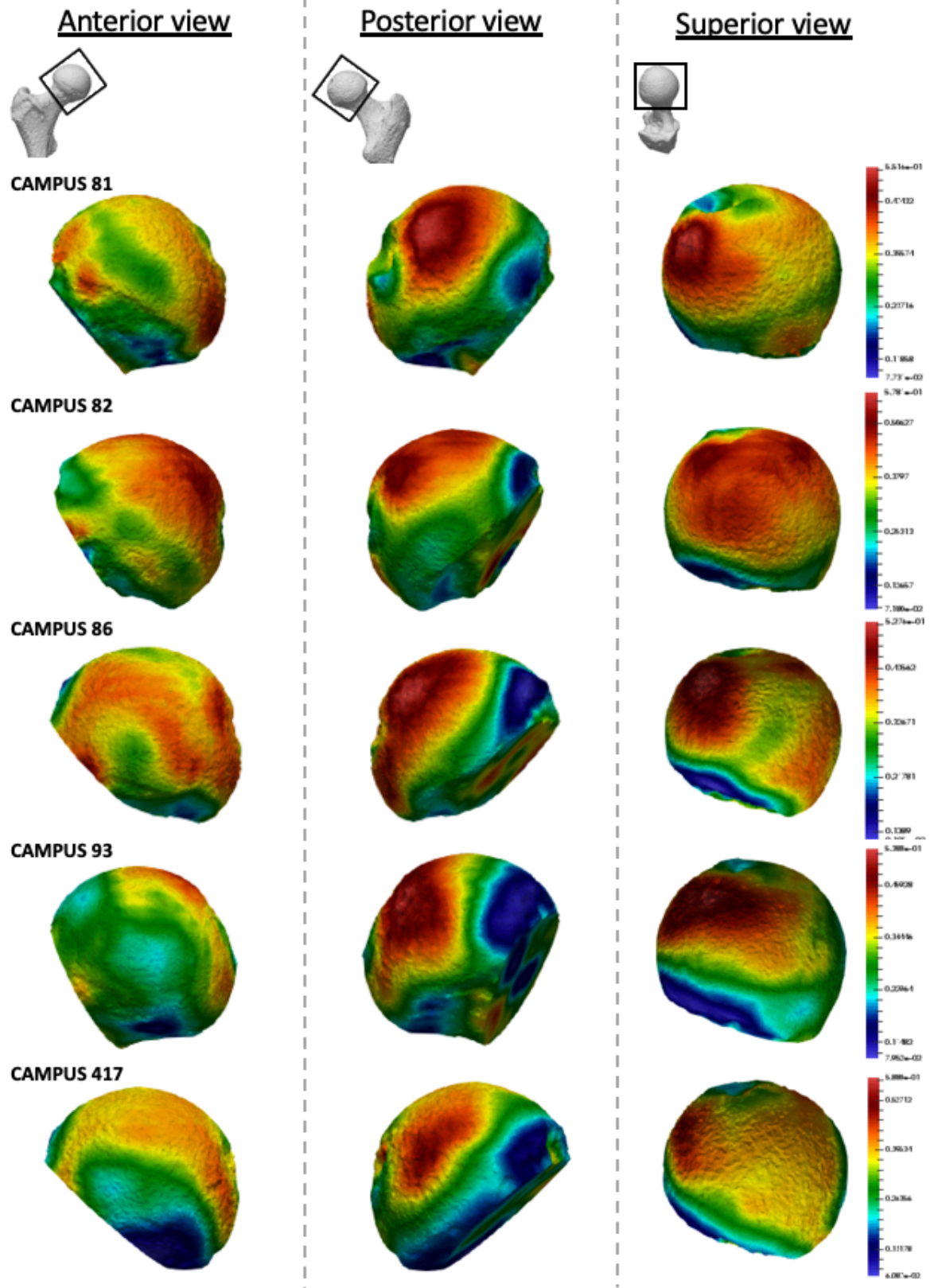
Pongo sp. BV/TV distribution



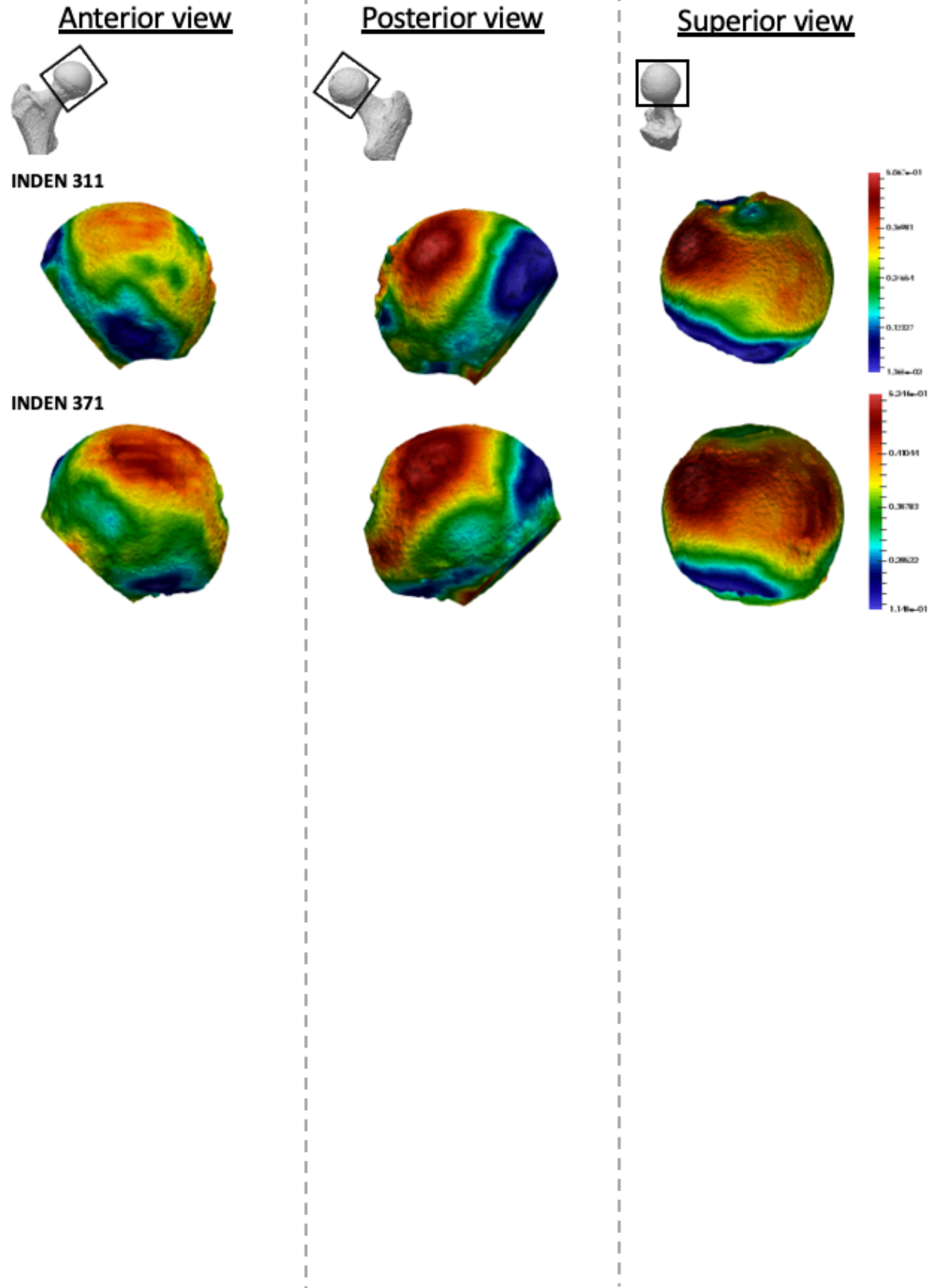
Homo sapiens BV/TV distribution



Homo sapiens BV/TV distribution



Homo sapiens BV/TV distribution



Chapter 4

Trabecular bone patterning in the hominoid distal femur

Abstract

In addition to external bone shape and cortical bone thickness and distribution, the distribution and orientation of internal trabecular bone across individuals and species has yielded important functional information on how bone adapts in response to load. In particular, trabecular bone analysis has played a key role in studies of human and nonhuman primate locomotion and has shown that species with different locomotor repertoires display distinct trabecular architecture in various regions of the skeleton. In this study, I analyse trabecular structure throughout the distal femur of extant hominoids and test for differences due to locomotor loading regime. Micro-computed tomography scans of *Homo sapiens* (n=11), *Pan troglodytes* (n=18), *Gorilla gorilla* (n=14) and *Pongo sp.* (n=7) were used to investigate trabecular structure throughout the distal epiphysis of the femur. I predicted that bone volume fraction (BV/TV) in the medial and lateral condyles in *Homo* would be distally concentrated and more anisotropic due to a habitual extended knee posture at the point of peak ground reaction force during bipedal locomotion, whereas great apes would show more posteriorly concentrated BV/TV and greater isotropy due to a flexed knee posture and more variable hindlimb use during locomotion. Results indicate some significant differences between taxa, with the most prominent being higher BV/TV in the posterosuperior region of the condyles in *Pan* and higher BV/TV and anisotropy in the posteroinferior region in *Homo*. Furthermore, trabecular number, spacing and thickness differ significantly, mainly separating *Gorilla* from the other apes. The trabecular architecture of the distal femur holds a functional signal linked to habitual behaviour; however, there was more similarity across taxa and greater intraspecific variability than expected. Specifically, there was a large degree of overlap in trabecular structure across the sample, and *Homo* was not as distinct as predicted. Nonetheless, this study offers a comparative sample of trabecular structure in the hominoid distal femur and can contribute to future studies of locomotion in extinct taxa.

4.1. Introduction

Extant great apes are often used as models to help reconstruct the origin and evolution of bipedality, and to help interpret the variable hindlimb morphology that is preserved in the hominin fossil record. The morphology of the knee in particular has played a central role in palaeoanthropological studies about the form of bipedality our ancestors adopted (Stern and Susman, 1983; Susman et al. 1984; Crompton, et al. 1998; Carey and Crompton, 2005; Lovejoy and McCollum, 2010; Raichlen et al. 2010). Some researchers propose that early hominins, such as australopiths, used bent-hip, bent-knee locomotion, similar to African ape bipedal locomotion (Stern and Susman, 1983; Susman et al. 1984), while others propose extended-hip and knee locomotion, similar to that of modern humans (Carey and Crompton, 2005; Lovejoy and McCollum, 2010; Raichlen et al. 2010). Studying the morphology of the knee joint and its links to locomotion in extant apes can help reconstruct how early hominins (e.g. australopiths, early *Homo*) walked bipedally, as well as other potential locomotor behaviours in which they may have engaged (e.g. arboreal climbing). However, inferences about the predominant joint posture and locomotion based solely on external morphology are limited by potential phylogenetic lag, in which some features are present but not necessarily functionally significant (Ward, 2002). Recent studies on trabecular bone have demonstrated that this tissue may be more informative for reconstructing joint posture and locomotion during life (e.g. Ryan and Ketcham, 2002; Ryan and Shaw, 2012; Tsegai et al. 2013; Skinner et al. 2015; Tsegai et al. 2017) and provides additional evidence that can improve our understanding of locomotor behaviour in extinct taxa. In this study, I investigate correlations between trabecular bone patterning and knee joint position during locomotion in humans and great apes.

Trabecular bone is a porous structure composed of struts, located in the epiphyses of long bones, as well as short bones, such as carpals and tarsals (Keaveny et al. 2001). It functions physiologically as a mineral reserve, contributing to

maintenance of homeostasis through resorption and deposition of bone (Rodan, 1998; Clarke, 2008). Although the mechanical function of trabecular bone is not fully understood, previous studies have demonstrated that its structure transfers joint load from subchondral bone toward the diaphyseal cortical bone (Currey, 2002; Barak et al. 2008). Through a process known as bone functional adaptation (Ruff, Holt and Trinkaus, 2006), trabecular structure has been shown to model in relation to the direction and magnitude of load, resulting in changes in overall bone volume as well as the orientation of the trabecular struts (Biewener et al. 1996; Rodan, 1997; Mitra et al. 2005; Pontzer et al. 2006; Barak et al. 2011; Harrison et al. 2011). Bone volume fraction (ratio of bone volume to total volume, or BV/TV) and degree of anisotropy (DA) can together explain up to 97% of trabecular bone strength (Goulet et al. 1994; Maquer et al. 2015). Other trabecular parameters, such as trabecular number, trabecular separation and trabecular thickness help to describe potential variation in the architecture related to trabecular bone function. Trabecular number, separation and thickness are also linked to overall trabecular bone mechanical strength (Kleerekoper et al. 1985; McCalden et al. 1997) and to bone quality, as their decline is main contributor to age-related trabecular bone loss (Parfitt et al. 1983; Weinstein and Hutson, 1987). Furthermore, these parameters, in contrast to BV/TV and DA, have been shown to scale allometrically with body size (Doube et al. 2011; Ryan and Shaw, 2013; Barak et al. 2013b) and to differ in smaller compared to larger mammals (Barak et al. 2013b).

Previous research has revealed a correlation between trabecular patterns and variation in locomotor loading in the proximal femur (Ryan and Ketcham, 2002; Scherf, 2008; Ryan and Shaw, 2012; Ryan et al. 2018), the hip and proximal tibia (Volpato et al. 2008; Mazurier et al. 2010) and the ankle of primates (Barak et al. 2013a; Tsegai et al. 2017). Longitudinal studies of trabecular bone ontogeny in humans have shown an association with bone modelling and the gait changes that occur with the development of bipedalism (Ryan and Krovitz, 2006; Gosman and Ketcham, 2009; Raichlen et al. 2015; Milovanovic et al. 2017). Looking at the knee specifically, alterations in the orientation of joint position and resulting load were found to correlate with trabecular strut alignment in guinea fowls (Pontzer et al.

2006). Furthermore, compared to a control group, the dominant knees of Olympic fencing athletes were found to have greater BV/TV and trabecular number, but lower trabecular separation, consistent with higher loading (Chang et al. 2008). Saers et al. (2016) found a correlation between mobility levels and trabecular architecture throughout the human lower limb, including the knee, across three human populations. A more recent study found sex differences in subchondral trabecular bone spacing in the knee of humans, with males having more evenly-spaced trabeculae compared to females (Sylvester and Terhune, 2017).

Despite the support for trabecular bone functional adaptation, some studies that focused on a single region of the proximal femur (Ryan and Walker, 2010; Shaw and Ryan, 2012) and the distal femoral metaphysis (Carlson et al. 2008; Wallace et al. 2013) did not detect a clear locomotor signal. These results suggest that non-mechanical factors may affect or constrain trabecular structure and that DA may not necessarily be indicative of variability in locomotor mode. There are multiple other factors that can affect trabecular structure, such as genetic or systemic differences (Paternoster et al. 2013; Tsegai et al. 2018a), age, and hormone levels (Simkin et al. 1987; Suuriniemi et al. 2004), all of which can obscure functional signals. Furthermore, it is not well understood what prompts modelling and how trabecular bone reacts when loaded (Wallace et al. 2014). However, analysing a single sub-volume may lead to non-homologous bone being sampled across species and may not capture the full structural complexity of the epiphysis (Fajardo and Müller, 2001; Kivell et al 2011; Lazenby et al 2011). Several studies have demonstrated that subchondral distribution of trabecular bone can provide important insights into bone loading that are overlooked with a centrally-placed volume of interest; particularly in morphologically complex bones and joints (Tsegai et al. 2013; Skinner et al. 2015; Stephens et al. 2016; Sylvester and Terhune, 2017; Tsegai et al. 2017). In this study, I aim to investigate the trabecular structure throughout the entire distal femoral epiphysis of humans and great apes and how potential variation in this structure might reflect differences in knee joint loading during a variety of locomotor behaviours.

4.1.1. Locomotion, morphology and predicted knee posture/loading

The most frequent locomotor behaviour in *Pan* is quadrupedal knuckle-walking, but they also engage in several other terrestrial as well as arboreal behaviours, including vertical climbing, leaping, bipedalism and suspension (e.g. Hunt, 1992; Bauer, 1977; Doran, 1993a,b; Doran, 1997; Isler, 2005), where the knee is flexed to varying degrees (D'Août et al. 2004; Isler, 2005; Ankel-Simons, 2007; Pontzer et al. 2009; Lee et al 2012). During terrestrial knuckle-walking the knee joint angle ranges from $\sim 161.4^\circ$ at foot touchdown to $\sim 117.4^\circ$ at toe-off (Finestone et al. 2018), and there is inter-individual variation in vertical ground reaction force (GRF). Some individuals show a single vertical GRF peak across the stance phase and others show two distinct peaks, one during early stance and one during late stance (Pontzer et al. 2014). During climbing and jumping they may utilise their full flexion-extension range at the knee (D'Août et al. 2002; Isler, 2005) (Figure 4.1).

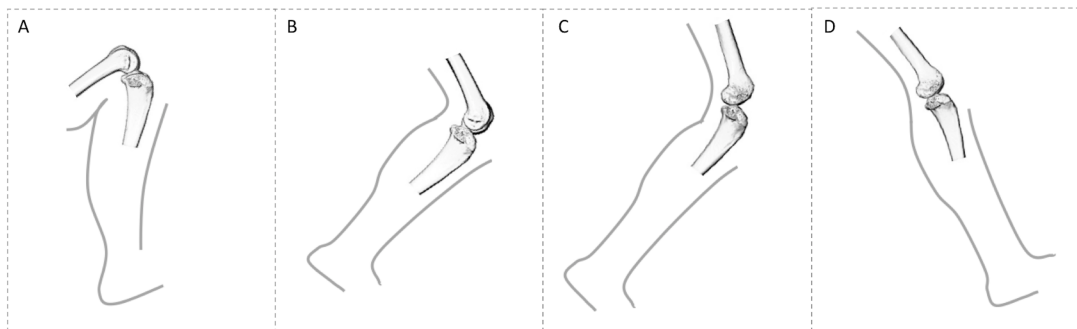


Figure 4.1. Comparison of knee posture during different habitual locomotor activities in great apes (A–B) and humans (C–D). (A) Great ape knee posture in maximum knee flexion ($\sim 50^\circ$) during climbing (Isler, 2005). (B) Great ape knee posture at toe-off ($\sim 120^\circ$) during terrestrial knuckle-walking (Finestone et al., 2018). (C) Human knee posture at toe-off ($\sim 145^\circ$). (D) Human knee posture at heel-strike ($\sim 160^\circ$). These were selected depending on when GRF is highest. In this study, all great apes are considered to show similar degrees of knee flexion during quadrupedal walking, as demonstrated by Finestone et al. (2018) and during climbing, but it should be noted that *Gorilla* has been shown to use a less flexed knee posture during vertical climbing compared with *Pan* (Isler, 2005).

Gorilla also engages most frequently in terrestrial knuckle-walking and practices variable degrees of arboreality, depending on their habitat and body size (Tutin and Fernandez, 1985; Kuroda, 1992; Remis, 1994; Doran, 1996; Doran, 1997; Isler, 2005; Crompton et al. 2010; Tocheri et al. 2011). During terrestrial knuckle-walking, knee angles vary from 163.2° at foot touchdown to ~ 126.6° at toe-off (Finestone et al. 2018) and adult females, as well as subadults of both sexes, climb with higher frequency than larger males (Isler, 2002; Isler, 2005). Additionally, flexion-extension range at the hip has been shown to differ more than 30° between sexes (Hammond, 2014), which would affect knee joint angle as well. Furthermore, range of motion at the knee joint differs between *Gorilla* and *Pan* during terrestrial locomotion and climbing with *Gorilla* practising slightly more extended knee postures (Hofstetter and Niemitz, 1998; Isler, 2005; Crompton et al. 2008; but see Finestone et al. 2018).

Pongo is the most arboreal of the great apes. They are distinguished from African apes by their greater use of torso-pronograde (i.e. quadrumanus suspension) and orthograde suspensory locomotion, and they employ a diversity of positional behaviours when navigating complex arboreal canopies (Thorpe and Crompton, 2005; Thorpe and Crompton, 2006; Thorpe et al. 2009). The frequent use of arboreal behaviours, where multiple limbs are used variously to achieve balance (Thorpe and Crompton, 2006; Payne et al 2006; Thorpe et al. 2009), alters the distribution of load across the upper and lower limb joints. *Pongo* has also been observed using bipedality and hindlimb suspension, which involves either suspension from both legs with joints extended, suspension from one leg, or suspension from one leg with support from a forelimb (Thorpe and Crompton 2005; Thorpe and Crompton, 2006). While climbing is observed in all nonhuman apes and the imposed stresses are similar to bipedal walking (Fleagle et al. 1981), the kinematics of isolated joints differ across species, with *Pongo* showing significantly larger ranges of motion in the hindlimb joints than both gorillas and bonobos (Morbeck and Zihlman, 1988; Tuttle and Cortright, 1988; Isler, 2005). However, the flexion-extension range at the knee during quadrupedal locomotion may not differ significantly to that of African apes (Finestone et al. 2018; mean values are 149.3° at touchdown and 113° at toe-off).

Humans are the only obligate bipedal ape and are unique in that both hips and knees remain relatively extended during the gait cycle (Alexander, 1991; Alexander, 2004). During the stance phase in human walking, following initial foot contact with the ground, body weight is rapidly transferred to the contacting limb and GRF reaches a maximum (Racic et al. 2009). The joint angle of the knee during foot touchdown ranges from 170° to 160° (Lafortune et al. 1992; Wallace et al. 2018) (Figure 4.1). During midstance the vertical GRF decreases, but the supporting leg carries all of the weight of the individual. While the opposite leg swings and weight is transferred forward, the heel of the supporting limb starts to rise and leads to a second peak of vertical GRF at toe-off (Racic et al. 2009). The joint angle of the knee at toe-off is approximately 140° (Lafortune et al. 1992). Humans engage in many other bipedal activities, such as running, jumping or squatting, in which and knee flexion/extension can vary considerably. Flexion angles increase during running, reaching 145° at touchdown, while the degree of flexion is greater and differs significantly to walking (Mann and Hagy, 1980). Compared with walking, there is only one (rather than two) peak of vertical GRF during a shorter stance phase and the vertical GRF are substantially higher during running (Nilsson and Thorstensson, 1989; Racic et al. 2009). Given that I do not know about the types of activities in which my human sample engaged during life, I make the assumption in this study that loading of the distal femur occurs primarily through walking, although recognise that these higher-impact activities, especially if occurring frequently, may also be reflected in the trabecular structure of the distal femur.

In addition to differences in joint kinematics and frequency of specific types of locomotion, variation in hominoid knee joint morphology may influence the distribution of load across the condyles of the distal femur and subsequently the trabecular structure. In humans the knee joint is larger relative to body size (Jungers, 1988) and the overall shape of the epiphysis is more square compared with the smaller and more mediolaterally-expanded epiphysis in other hominoids (Tardieu, 1981). Furthermore, the condyles in humans are more equally-sized and the lateral condyle is elliptical, which increases the radius of curvature and favours extension of

the knee (Heiple and Lovejoy 1971; Tardieu, 1981). In contrast, in *Gorilla*, *Pan* and *Pongo*, the articular surface of the medial condyle is larger than that of the lateral and the condyles are more circular. The disparity in relative condylar size results in increased mediolateral rotation in nonhuman apes at different stages of gait, whereas in humans mediolateral rotation is restricted to the final stage of the flexion-extension cycle, which “locks” the knee during extension (Tardieu, 1981). The varus angle of the ape femur results in higher loading of the medial condyle, while the valgus angle in humans transfers the line of load relatively closer to the lateral condyle, resulting in more equal loading of the two condyles during stance (Preuschoft and Tardieu, 1996).

4.1.2. Hypotheses

This study will investigate potential variation in the trabecular structure of the human and great ape distal femur, focusing primarily on BV/TV and DA, as well as architectural differences in trabecular number (Tb.N), trabecular separation (Tb.Sp) and trabecular thickness (Tb.Th), and how this variation relates to different locomotor and morphological traits across hominoids. Specifically, I test the following hypotheses:

1. BV/TV distribution will reflect knee joint positioning during habitual locomotion (Figure 4.1) and will differ across genera. Specifically, although *Homo* is predicted to have comparatively lower BV/TV values overall (Chirchir et al. 2015; Ryan and Shaw, 2015; Chirchir et al. 2017), BV/TV distribution will be concentrated distally beneath the condylar articular surfaces, spanning from the medial and lateral grooves to the posteroinferior region of the condyles, to reflect the habitual use of a more extended knee posture during bipedalism. Thus, I expect that high BV/TV will be detected in the distal and posteroinferior regions of the condyles. *Pan* and *Gorilla* are predicted to exhibit greater BV/TV in the posteroinferior and posterosuperior regions of the condyles to reflect more flexed knee postures during quadrupedal knuckle-walking and, particularly, climbing. Vertical climbing mechanics have been studied in

bonobos (Isler, 2005), but have not yet been quantified in chimpanzees, thus for the purpose of this study both *Pan* species are assumed to be similar. *Pongo* is predicted to have a more homogenous distribution of BV/TV throughout the condyles and high BV/TV extending from the distal to the posterosuperior region of the condyles, reflecting more variable knee joint postures and loading during their more complex locomotor repertoire.

2. DA distribution will reflect differences in habitual range of motion and loading of the knee joint in particular postures. *Homo* will display the highest DA in the distal and posteroinferior regions of the condyles, resulting from the stereotypical loading of these regions during bipedal locomotion and their overall less mobile knee joints relative to other apes (Tardieu, 1981). *Pan* and *Gorilla* will exhibit similar DA patterns, with lower values than *Homo* specifically in the posterior regions of the condyles, due to increased rotational movement of their knees during locomotion (Tardieu, 1981) and higher loading of the posterior when utilising flexed knee postures. *Pongo* will display the lowest DA within the medial and lateral condyles in all studied regions, due to their more mobile knee joints and varied locomotor loading regime, which results in varied loading of the different regions of the condyles.

3. Architectural variables Tb.N, Tb.Sp and Tb.Th will reflect variation in body size, as demonstrated in previous studies (Doube et al. 2011; Ryan and Shaw, 2013; Barak et al. 2013b), and be consistent with potential variation in BV/TV across taxa. Specifically, Tb.N is expected to be higher in smaller-bodied *Pan* and *Pongo* and lower in larger-bodied *Homo* and *Gorilla* across studied regions, while Tb.Sp and Tb.Th are expected to present the opposite pattern. Allometric relationships were not directly analysed due to small and unbalanced sample sizes of each taxon, however they are assumed to follow the same patterns found in previous studies of the femur, and other long bones, across larger samples of primates (Ryan and Shaw, 2013; Barak et al. 2013b; Tsegai et al. 2013; Fajardo et al. 2013) and mammals (Doube et al. 2011).

4.2. Materials and Methods

4.2.1. Sample and scanning

The study sample is summarised in Table 4.1. The *Pan troglodytes verus* sample (n=18) is from the Taï Forest collection of the Max Planck Institute for Evolutionary Anthropology in Leipzig, Germany. The *Gorilla gorilla gorilla* sample (n=14) is from the Powell-Cotton Museum, UK of which 13 are from Cameroon and one is from the Democratic Republic of the Congo. The *Pongo* sample (n=7) is from the Zoologische Staatssammlung München, Germany. Five individuals are *Pongo pygmaeus*, one is *Pongo abelii* and the species of one individual is unknown. The *Homo sapiens* sample (n=11) is from the anthropology collection of Georg-August-Universität Göttingen, Germany and comes from two sub-collections. One of the specimens is from an early 1900s population from a cemetery in Inden that was used between 1877 and 1924 and ten specimens are from a cemetery in Göttingen that was used between 1851 and 1889. There is no additional information on the sample. All nonhuman apes in the study sample were wild shot, except two captive *Pongo* specimens (the only male in the sample and one female). All statistical analyses were repeated excluding the two captive individuals to test for potential bias (see below). All individuals were adult, based on epiphyseal fusion of the femur and associated skeletal elements, and none showed signs of pathologies.

Table 4.1. Taxonomic composition of the study sample, voxel size range (after resampling), sex distribution and microCT scanning parameters.

Taxon	Locomotor mode	N	Voxel size (mm)	Sex	Scanning
<i>Pan troglodytes verus</i>	Arboreal/ knuckle-walker	18	0.040	11 female, 5 male, 2 unknown	kV:120-150, μ A: 80-120, 0.25 or 0.5mm brass
<i>Gorilla gorilla gorilla</i>	Terrestrial knuckle-walker	14	0.048-0.089	7 female, 7 male	kV:130-180, μ A: 100-160, 0.1-0.5mm copper
<i>Pongo sp.</i>	Arboreal/ torso-pronograde suspension	7	0.035-0.045	6 female, 1 male	kV:140, μ A: 140, 0.5mm brass
<i>Homo sapiens</i>	Bipedal	11	0.050-0.065	3 female, 7 male, 1 unknown	kV:140, μ A: 140, 0.5mm brass

Pan, *Pongo* and *Homo* samples were scanned using a BIR ACTIS 225/300 industrial microCT scanner housed in the Department of Human Evolution, Max Planck Institute for Evolutionary Anthropology. *Gorilla* specimens were scanned using a Nikon XT 225 ST microCT scanner housed in Cambridge Biotomography Centre, Department of Zoology, at the University of Cambridge. Scans were reconstructed from 1080 projections into 16-bit TIFF image stacks with isotropic voxel sizes. All scans were oriented to approximate anatomical position in AVIZO 6.3[®] (Visualization Sciences Group, SAS) to assist comparison. Subsequently, they were cropped and larger scans were re-sampled prior to segmentation to overcome computational limitations. The final range of resolution for each species is detailed in Table 4.1. The Ray Casting Algorithm (Scherf and Tilgner, 2009) was used to segment bone in all specimens (Figure 4.2A).

4.2.2. Trabecular architecture analysis

A whole-epiphysis approach was used to analyse the patterns of trabecular bone distribution in medtool v4.1 (www.dr-pahr.at) following published protocols (Gross et al. 2014). Morphological filters were applied to define and separate cortical from trabecular bone. In regions with marked depressions (or that are c-shaped), separation of the cortical shell from trabecular bone can be less reliable (see Pahr and Zysset, 2009 for explanation). In my study this was specifically an issue within the intercondyloid fossa. In specimens that presented this problem, a correction filter was applied within a manually selected bounding box. This filter re-defines cortical and trabecular bone in the selected volume by applying the algorithm iteratively. The accuracy of the separation was evaluated using AVIZO 6.3® (Visualization Sciences Group, SAS). Nonetheless, the regions of interest, and specifically the condyles, were not affected by this issue. Following the definition of the different anatomical structures, the cortical bone was removed (Figure 4.2B). Trabecular thickness values were obtained for each specimen from the isolated trabecular structure using the BoneJ plug-in (version 1.4.1, Doube et al. 2010) for ImageJ (Schneider et al. 2012) and were used to validate the size of the sphere used in the morphological filters (see Gross et al. 2014).

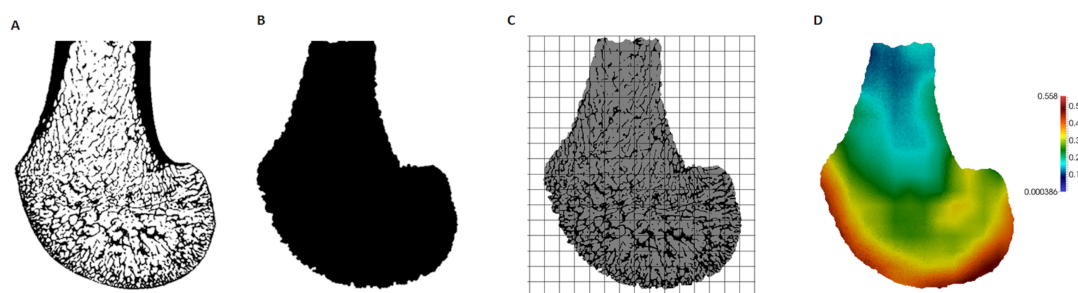


Figure 4.2. Processing steps of a *Gorilla* specimen, showing a parasagittal view through the lateral condyle. (A) Segmented microCT scan. (B) Inner trabecular area. (C) Trinary mask representing inner air, outer air and trabecular structure, as well as the 3D background grid. (D) BV/ TV distribution within this slice (scaled to its own data range).

A mask representing the inner air, outer air and trabecular structure (each with different grey values) was then produced. Both the mask representing the inner region (Figure 4.2B) and this trinary mask (Figure 4.2C) were used in the following meshing process. A 3D rectangular background grid with a grid size of 3.5mm was built around each segmented volume (Figure 4.2C) and a sampling sphere of 7.5mm in diameter was used to measure BV/TV and DA at each node using medtool v4.1. DA was calculated as $DA = 1 - [\text{smallest eigenvalue}/\text{largest eigenvalue}]$, obtained using the mean-intercept-length method (Whitehouse, 1974; Odgaard, 1997). Three-dimensional tetrahedral meshes of all specimens were created with CGAL 4.4 (CGAL, Computational Geometry, <http://www.cgal.org>), using the segmented trabecular structure and a mesh size of 0.6 mm. The values at each node were then interpolated to the tetrahedral elements and the resulting BV/TV (Figure 4.2D) and DA distribution maps were visualised using Paraview v4.0.1 (Ahrens et al. 2005).

To statistically test for regional differences in trabecular structure, three subregions of each condyle were isolated (distal, posteroinferior and posterosuperior) in a subsample of 10 individuals from each species (all seven *Pongo* were included). Condyles were defined based on the extent of the articular surface and the patello-femoral articulation was excluded (Figure 4.3A). Each condyle was divided into equal quarters using an automated script in medtool v4.1 (Figure 4.3B). The anterosuperior quarter of both condyles was excluded from the analysis, as it was not adjacent to the articular surface. Analyses of BV/TV and DA for the subregions were repeated as above and Tb.Th and Tb.Sp were calculated for these regions with an in-house script using the Hildebrand and Ruesegger (1997) method, similar to what is used in BoneJ. Tb.N was calculated as $Tb.N = 1/(Tb.Th + Tb.Sp)$.

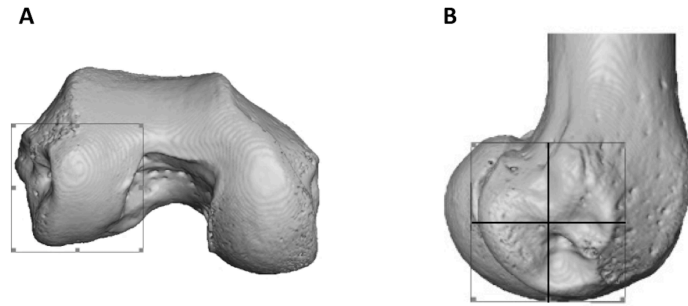


Figure 4.3. Partitioning of the lateral condyle into sub-regions in a *Pan* specimen.

(A) Selection of condyle. (B) Separation into quarters, including the distal (bottom, right), posteroinferior (bottom, left) and posterosuperior (top, left). The anterosuperior quadrant (top, right) was not analysed. The medial condyle was partitioned in the same way.

4.2.3. Statistical analysis

All statistical analyses were done in R v3.4.1 (R Core Team, 2017). The Kruskal-Wallis test was used to examine regional differences in all parameters (BV/TV, DA, Tb.N, Tb.Sp, Tb.Th) among taxa, with Wilcoxon rank sum test post-hoc analysis for pairwise comparisons. To further compare regional differences in BV/TV and DA, I calculated an “inferior ratio” comparing the distal and posteroinferior regions, as well as a “posterior ratio” comparing the posteroinferior and posterosuperior regions. These ratios were selected to examine species-specific patterns in BV/TV and DA distribution that may not be revealed when the isolated regions are directly compared between species. Furthermore, all tests were repeated excluding the captive *Pongo* specimens to test for impact of these specimens on the results. A principal components (PC) analysis was conducted to detect which trabecular parameters contribute most to inter-specific differences. DA, Tb.Sp and Tb.Th of all tested regions were included in the PC analysis. I excluded BV/TV and Tb.N from the PC analysis because multivariate regression revealed that both variables were significantly correlated with Tb.Sp and Tb.Th. This was not surprising as Tb.N was calculated using the Tb.Th and Tb.Sp values obtained directly from the specimens and BV/TV is defined by all these parameters.

4.3. Results

4.3.1. Quantitative and qualitative analysis of trabecular parameters

Quantitative and qualitative analysis of the trabecular architecture in the distal femur reveal differences across taxa. Figures 4.4-4.7 present BV/TV distribution in five individuals of each taxon and the Supplementary Online Material contains images for each specimen in the study sample. Quantitative results are shown in Figures 4.8-4.9 and are detailed in Table 4.2 and Supplementary Table 4.1. Analyses were repeated excluding the two *Pongo* captive specimens and since in most cases the results did not change, the specimens were included in the analysis (when differences were found, they are reported below).

Qualitative comparison reveals the variability in distribution patterns across taxa, while quantitative comparison reveals differences in BV/TV values in specific regions. *Pan* shows high BV/TV extending deep to the articular surface of the condyles, from the medial and lateral grooves to the posteriorsuperior margin of both condyles (Figure 4.4). This is consistent in all the specimens and is most pronounced on the medial condyle.

Table 4.2. Trabecular architecture results by condyle and region.

Taxon	Parameter	Lateral distal	CV	Lateral posteroinferior	CV	Lateral posterosuperior	CV	Medial distal	CV	Medial posteroinferior	CV	Medial posterosuperior	CV
<i>Pan</i>	BV/TV	0.29 (0.04)	13.1	0.34 (0.03)	9.8	0.33 (0.02)	6.5	0.27 (0.03)	9.3	0.32 (0.03)	10.1	0.31 (0.02)	6.3
	DA	0.31 (0.04)	4.0	0.37 (0.04)	11.7	0.33 (0.03)	9.7	0.39 (0.06)	15.2	0.43 (0.06)	13.7	0.43 (0.04)	9.8
	Tb.N (1/mm)	1.14 (0.14)	12.3	1.22 (0.12)	9.7	1.20 (0.09)	7.8	1.07 (0.12)	11.4	1.22 (0.12)	9.8	1.18 (0.10)	8.2
	Tb.Sp (mm)	0.65 (0.08)	12.7	0.57 (0.06)	10.1	0.59 (0.05)	8.8	0.70 (0.09)	12.9	0.59 (0.07)	11.3	0.61 (0.05)	8.8
	Tb.Th (mm)	0.25 (0.04)	14.4	0.25 (0.03)	13.1	0.25 (0.02)	9.1	0.24 (0.02)	9.2	0.24 (0.02)	8.4	0.24 (0.02)	7.3
<i>Gorilla</i>	BV/TV	0.27 (0.03)	10.6	0.33 (0.05)	13.6	0.29 (0.04)	12.4	0.23 (0.02)	9.6	0.29 (0.03)	9.4	0.27 (0.02)	8.5
	DA	0.35 (0.05)	4.5	0.35 (0.04)	10.5	0.34 (0.03)	10.0	0.39 (0.02)	5.8	0.41 (0.04)	10.4	0.40 (0.03)	7.6
	Tb.N (1/mm)	0.78 (0.07)	9.5	0.90 (0.10)	10.6	0.87 (0.08)	8.6	0.74 (0.08)	11.0	0.86 (0.08)	9.4	0.78 (0.08)	10.6
	Tb.Sp (mm)	0.95 (0.08)	8.4	0.78 (0.08)	9.8	0.83 (0.08)	9.5	1.06 (0.11)	10.4	0.86 (0.07)	8.4	0.95 (0.10)	10.8
	Tb.Th (mm)	0.34 (0.04)	12.6	0.34 (0.05)	15.8	0.32 (0.04)	12.0	0.32 (0.04)	13.5	0.32 (0.05)	14.7	0.34 (0.04)	12.3
<i>Pongo</i>	BV/TV	0.27 (0.04)	13.2	0.32 (0.06)	17.7	0.31 (0.05)	17.6	0.23 (0.03)	13.6	0.28 (0.06)	20.7	0.29 (0.06)	19.8
	DA	0.32 (0.06)	5.8	0.36 (0.05)	14.5	0.32 (0.05)	15.6	0.36 (0.07)	18.1	0.39 (0.06)	15.0	0.37 (0.06)	16.2
	Tb.N (1/mm)	1.07 (0.09)	8.1	1.17 (0.11)	9.8	1.05 (0.09)	8.9	0.97 (0.06)	6.0	1.09 (0.10)	9.2	1.01 (0.08)	7.6
	Tb.Sp (mm)	0.70 (0.06)	8.5	0.61 (0.07)	10.6	0.69 (0.07)	10.2	0.79 (0.06)	8.1	0.69 (0.08)	11.1	0.73 (0.07)	9.6
	Tb.Th (mm)	0.24 (0.04)	17.1	0.25 (0.05)	4.6	0.27 (0.05)	16.5	0.24 (0.03)	12.9	0.24 (0.05)	18.7	0.27 (0.04)	16.3
<i>Homo</i>	BV/TV	0.29 (0.04)	14.2	0.31 (0.04)	11.3	0.27 (0.03)	12.2	0.26 (0.04)	14.8	0.30 (0.03)	11.2	0.26 (0.03)	11.4
	DA	0.37 (0.01)	1.3	0.45 (0.02)	5.1	0.41 (0.03)	6.0	0.37 (0.04)	10.4	0.47 (0.03)	7.1	0.43 (0.02)	4.7
	Tb.N (1/mm)	0.93 (0.09)	9.6	1.12 (0.11)	9.6	0.93 (0.11)	12.3	0.83 (0.08)	9.8	1.05 (0.10)	9.5	0.91 (0.12)	12.8
	Tb.Sp (mm)	0.78 (0.09)	12.1	0.63 (0.07)	10.9	0.80 (0.12)	15.4	0.91 (0.12)	12.8	0.69 (0.09)	12.3	0.82 (0.13)	15.4
	Tb.Th (mm)	0.31 (0.03)	9.8	0.27 (0.03)	12.0	0.30 (0.03)	11.5	0.30 (0.03)	9.9	0.27 (0.02)	8.0	0.30 (0.03)	11.1

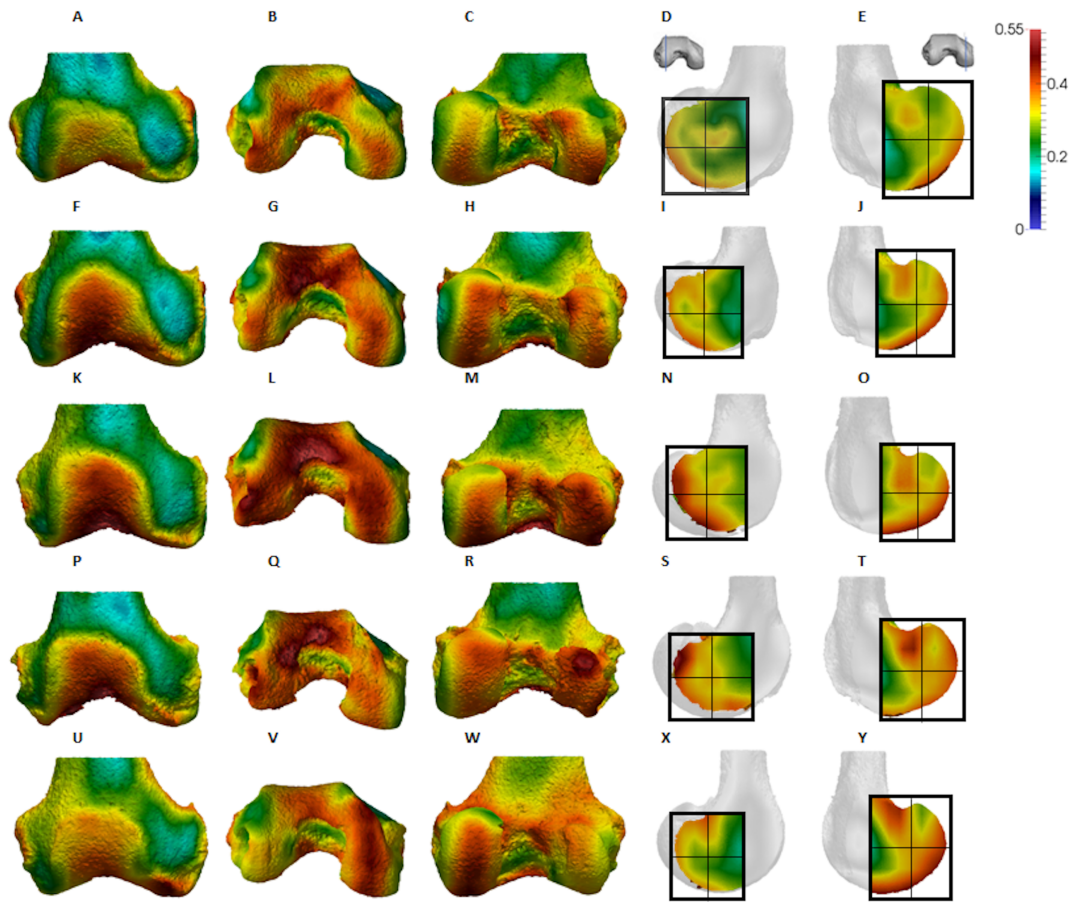


Figure 4.4. *Pan* BV/TV distribution. (A-E) Specimen MPITC 11781. (A) Anterior view. (B) Inferior view. (C) Posterior view. (D) Lateral condyle. (E) Medial condyle. (F-J) Specimen MPITC 15001. (F) Anterior view. (G) Inferior view. (H) Posterior view. (I) Lateral condyle. (J) Medial condyle. (K-O) Specimen MPITC 11786. (K) Anterior view. (L) Inferior view. (M) Posterior view. (N) Lateral condyle. (O) Medial condyle. (P-T) Specimen MPITC 11793. (P) Anterior view. (Q) Inferior view. (R) Posterior view. (S) Lateral condyle. (T) Medial condyle. (U-Y) Specimen MPITC 11778. (U) Anterior view. (V) Inferior view. (W) Posterior view. (X) Lateral condyle. (Y) Medial condyle. All specimens are from the right side. In anterior and inferior views the medial condyle is on the right. In the posterior view the medial condyle is on the left. The location of the parasagittal slice through each condyle is indicated above and the main areas of interest are outlined. Individuals are scaled to the same data range.

Gorilla and *Pongo* present a similar pattern to that of *Pan* with regions of high BV/TV that extend from the inferior margin of the patellar articulation to the posterior region of both condyles (Figure 4.5 and 4.6). However, in *Gorilla* this high

concentration does not extend as posterosuperiorly as in *Pan*. Also, in the medial condyle high BV/TV does not extend as anteriorly as it does in *Pan*. In *Gorilla*, the distribution of BV/TV along the lateral condyle is more variable across individuals.

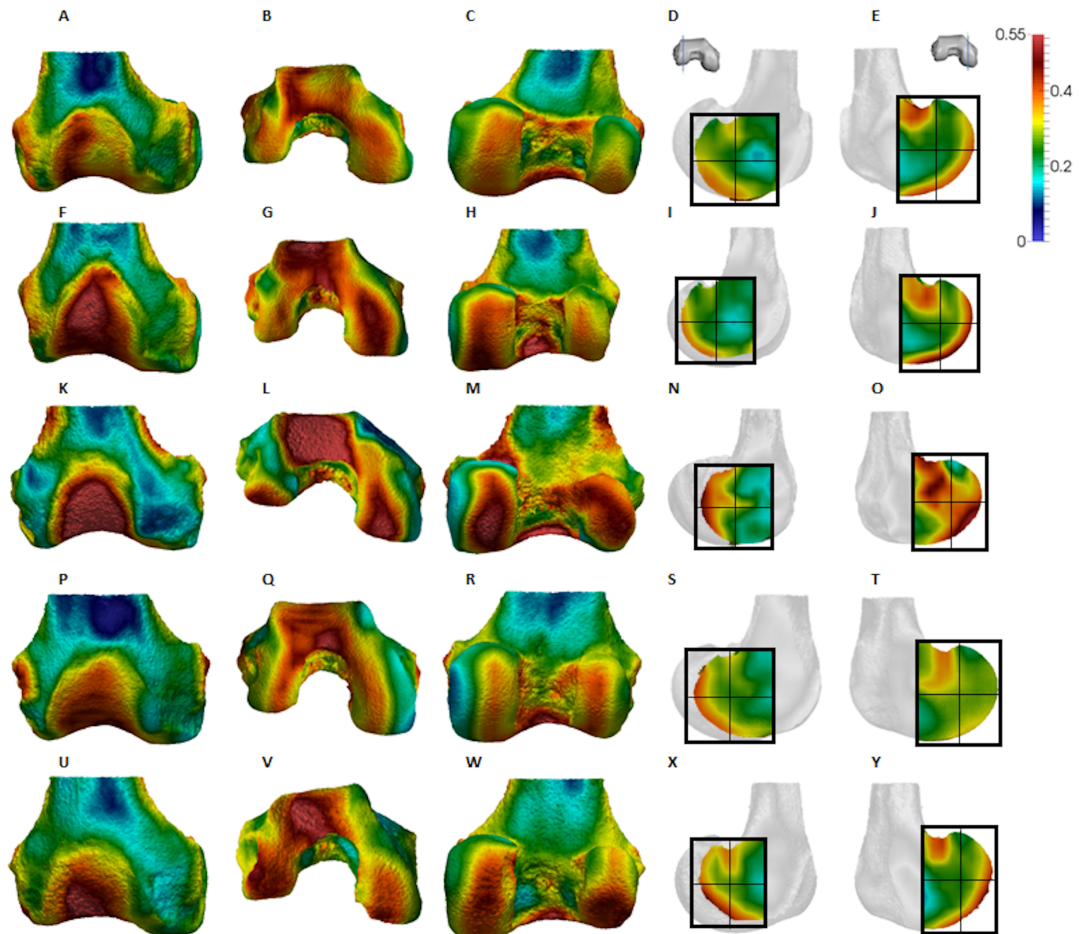


Figure 4.5. Gorilla BV/TV distribution. (A–E) Specimen M95. (A) Anterior view. (B) Inferior view. (C) Posterior view. (D) Lateral condyle. (E) Medial condyle. (F–J) Specimen M300. (F) Anterior view. (G) Inferior view. (H) Posterior view. (I) Lateral condyle. (J) Medial condyle. (K–O) Specimen M372. (K) Anterior view. (L) Inferior view. (M) Posterior view. (N) Lateral condyle. (O) Medial condyle. (P–T) Specimen M798. (P) Anterior view. (Q) Inferior view. (R) Posterior view. (S) Lateral condyle. (T) Medial condyle. (U–Y) Specimen M856. (U) Anterior view. (V) Inferior view. (W) Posterior view. (X) Lateral condyle. (Y) Medial condyle. All specimens are from the right side. In anterior and inferior views the medial condyle is on the right. In the posterior view the medial condyle is on the left. The location of the parasagittal slice through each condyle is indicated above and the main areas of interest are outlined. Individuals are scaled to the same data range.

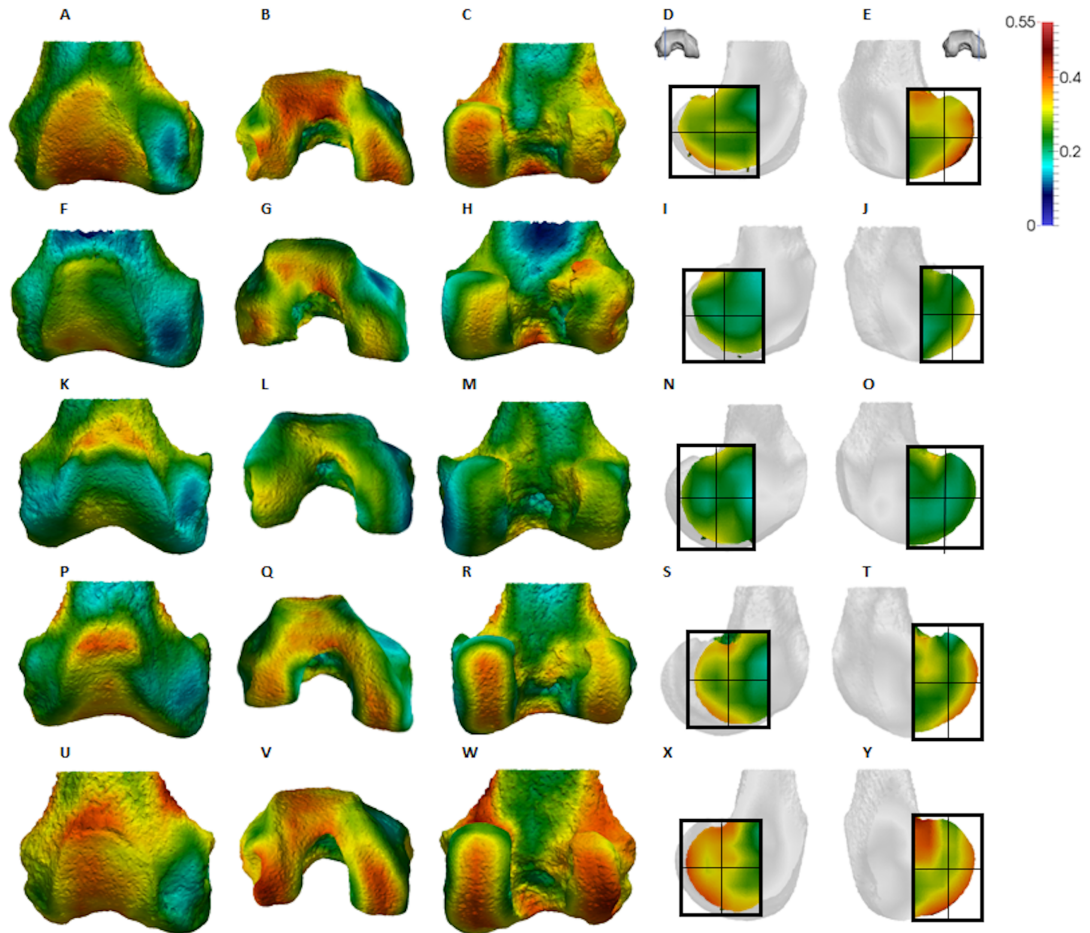


Figure 4.6. *Pongo* BV/TV distribution. (A–E) Specimen ZSM 1909 0801. (A) Anterior view. (B) Inferior view. (C) Posterior view. (D) Lateral condyle. (E) Medial condyle. (F–J) Specimen ZSM 1907 0660. (F) Anterior view. (G) Inferior view. (H) Posterior view. (I) Lateral condyle. (J) Medial condyle. (K–O) Specimen ZSM 1973 0270. (K) Anterior view. (L) Inferior view. (M) Posterior view. (N) Lateral condyle. (O) Medial condyle. (P–T) Specimen ZSM 1907 0483. (P) Anterior view. (Q) Inferior view. (R) Posterior view. (S) Lateral condyle. (T) Medial condyle. (U–Y) Specimen ZSM 1907 0633B. (U) Anterior view. (V) Inferior view. (W) Posterior view. (X) Lateral condyle. (Y) Medial condyle. All specimens are from the right side. In anterior and inferior views the medial condyle is on the right. In the posterior view the medial condyle is on the left. The location of the parasagittal slice through each condyle is indicated above and the main areas of interest are outlined. Individuals are scaled to the same data range. Captive specimens are not included in the figure but can be found in the Supplemental Files.

Homo show a greater range of BV/TV values, indicated by their higher CV (coefficient of variation) (Table 4.2), and their range overlaps with the other species. Humans generally show high BV/TV in the posteroinferior region of the condyles, which in some individuals extends further posterosuperiorly (Figure 4.7). In the lateral condyle they also show high BV/TV in the distal region. Generally, the apes appear to have lower BV/TV in the distal region of both condyles compared to humans (Figure 4.8). No differences in BV/TV are found between species in the inferior regions, but significant differences are found in the posterosuperior region in both condyles. *Pan* shows significantly higher BV/TV in this region than both *Gorilla* (lateral $p < 0.05$; medial $p < 0.01$) and *Homo* (lateral $p < 0.001$; medial $p < 0.05$), but the *Pan* range overlaps with that of *Pongo*. In the posterior regions of both condyles, *Pongo* have the highest CV values, indicating that they have the most variable trabecular structure. Qualitative analysis shows that in *Pongo*, there is a consistent distribution of high BV/TV values over the posterosuperior margin of both condyles, where the gastrocnemius heads originate (Diogo et al. 2013a); this concentration is occasionally found in African apes.

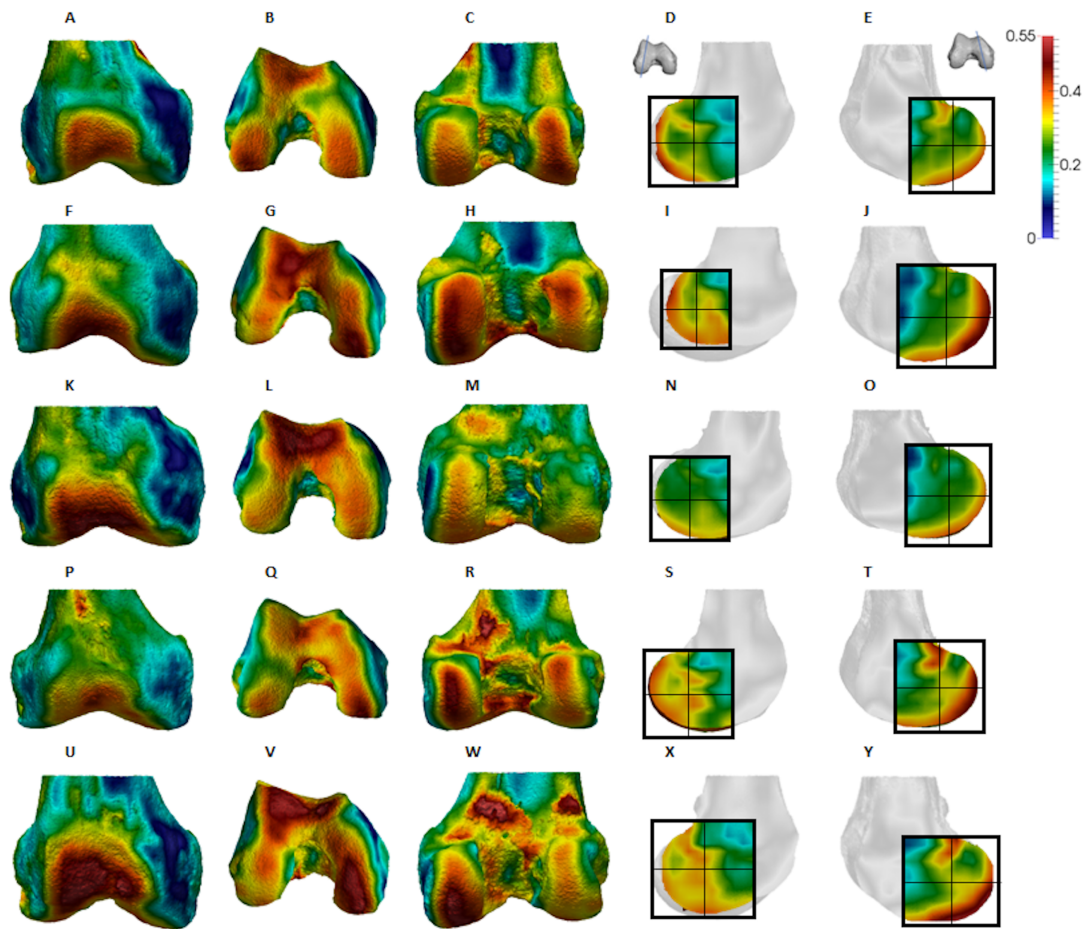


Figure 4.7. *Homo* BV/TV distribution. (A–E) Specimen Campus 66. (A) Anterior view. (B) Inferior view. (C) Posterior view. (D) Lateral condyle. (E) Medial condyle. (F–J) Specimen Campus 36. (F) Anterior view. (G) Inferior view. (H) Posterior view. (I) Lateral condyle. (J) Medial condyle. (K–O) Specimen Campus 72. (K) Anterior view. (L) Inferior view. (M) Posterior view. (N) Lateral condyle. (O) Medial condyle. (P–T) Specimen Campus 86. (P) Anterior view. (Q) Inferior view. (R) Posterior view. (S) Lateral condyle. (T) Medial condyle. (U–Y) Specimen Campus 81. (U) Anterior view. (V) Inferior view. (W) Posterior view. (X) Lateral condyle. (Y) Medial condyle. All specimens are from the right side. In anterior and inferior views the medial condyle is on the right. In the posterior view the medial condyle is on the left. The location of the parasagittal slice through each condyle is indicated above and the main areas of interest are outlined. In *Homo* the slice is angled as it follows the orientation of the condyles and runs through the centre of each condyle. Individuals are scaled to the same data range.

The qualitative data (Figures 4.4-4.7) reveal differences deep to the patellar articular surface, that were not tested for significant differences in the quantitative comparison. *Pan* shows high BV/TV concentrations centrally and inferiorly, suggesting loading of this surface during knee flexion. Farther from the articular surfaces and within the shaft, BV/TV values decrease. In *Gorilla* high values are distributed evenly across the surface, but there is not a consistent pattern of distribution across all individuals. In *Pongo* the pattern of distribution is variable, with some specimens showing high BV/TV values over the superior margin of the articulation while in others the highest BV/TV is more central and inferior. Lastly in *Homo*, some individuals show high BV/TV on the lateral patellar articular surface, in agreement with valgus knee loading, however this is not consistent across specimens.

Quantitative results also show significant between-species differences in DA (Figure 4.8). In the lateral condyle, *Homo* have significantly higher DA in the distal region than *Pan* ($p < 0.001$), but not the other taxa. In the posterior regions of this condyle, *Homo* differ significantly from all other apes (all $p < 0.001$, except the posteroinferior region with *Gorilla* and *Pongo* $p < 0.01$), showing consistently higher DA values than the other taxa. In the medial condyle, significant differences are only found in the posteroinferior region. *Homo* shows significantly higher DA in this region than both *Gorilla* ($p < 0.05$) and *Pongo* ($p < 0.05$), but not *Pan*. No significant difference is found between the nonhuman apes. *Pongo* shows the most variability in DA values across regions and consistently have the highest CV values, contrary to *Homo* which are the least variable. However, when the captive specimens are removed, the difference between *Homo* and *Pongo* is no longer significant. Variation in the DA distribution can be seen in central parasagittal slices through the condyles, provided for the whole sample in the Supplementary Material.

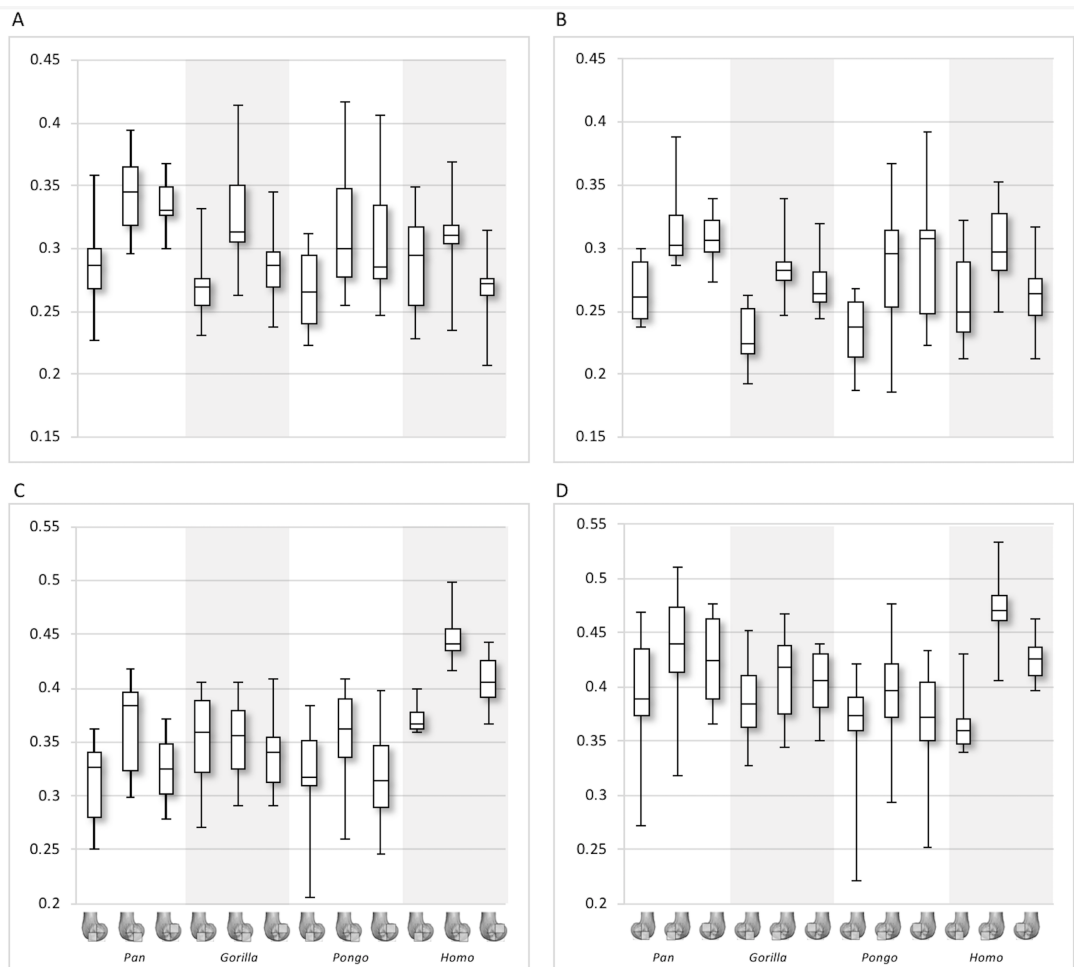


Figure 4.8. Bone volume fraction (BV/TV) and degree of anisotropy (DA) results for each region and taxon. (A) BV/TV in the lateral condyle. (B) BV/TV in the medial condyle. (C) DA in the lateral condyle. (D) DA in the medial condyle. Regions (outlined) and taxa are displayed below.

Interspecific differences are also detected in Tb.N, Tb.Sp and Tb.Th (Figure 4.9). Sexual dimorphism in some of the taxa may have a considerable effect on these trabecular parameters however unfortunately in the present study this could not be tested due to small and unbalanced samples.

In both condyles, Tb.N shows a decreasing trend from *Pan* to *Pongo* to *Homo* and to *Gorilla*, which is consistent with increases in body mass. In the lateral condyle, *Gorilla* has significantly lower Tb.N than all other apes in all regions (*Pan* $p < 0.001$, *Pongo* $p < 0.01$ in the inferior regions and $p < 0.05$ in the posterosuperior, *Homo* $p < 0.05$), except *Homo* in the posterosuperior region. *Homo* do not show significant

differences with *Pongo* in any region, but when the captive specimens are removed there is a weak but significant result ($p=0.05$) in the distal and posterosuperior regions. *Homo* also displays significantly lower Tb.N than *Pan* in the distal ($p<0.05$) and posterosuperior ($p<0.001$) regions of the lateral condyle. However, Tb.N in the posteroinferior region in *Homo* is higher than the other regions, overlapping with other taxa. Furthermore, *Pongo* has significantly lower Tb.N than *Pan* ($p<0.05$) only in the posterosuperior region of the lateral condyle. In the medial condyle, *Gorilla* similarly show significantly lower Tb.N than *Pongo* and *Pan* in all regions ($p<0.01$, and $p<0.001$ respectively), but lower Tb.N than *Homo* only in the posteroinferior region ($p<0.01$). *Pan* and *Pongo* again only differ in the posterosuperior region ($p<0.01$), with *Pongo* having a lower Tb.N. *Pongo* has significantly higher Tb.N than *Homo* in the distal region ($p<0.05$) and *Pan* shows significantly higher values than *Homo* in the distal ($p<0.05$) and posterosuperior ($p<0.001$) regions.

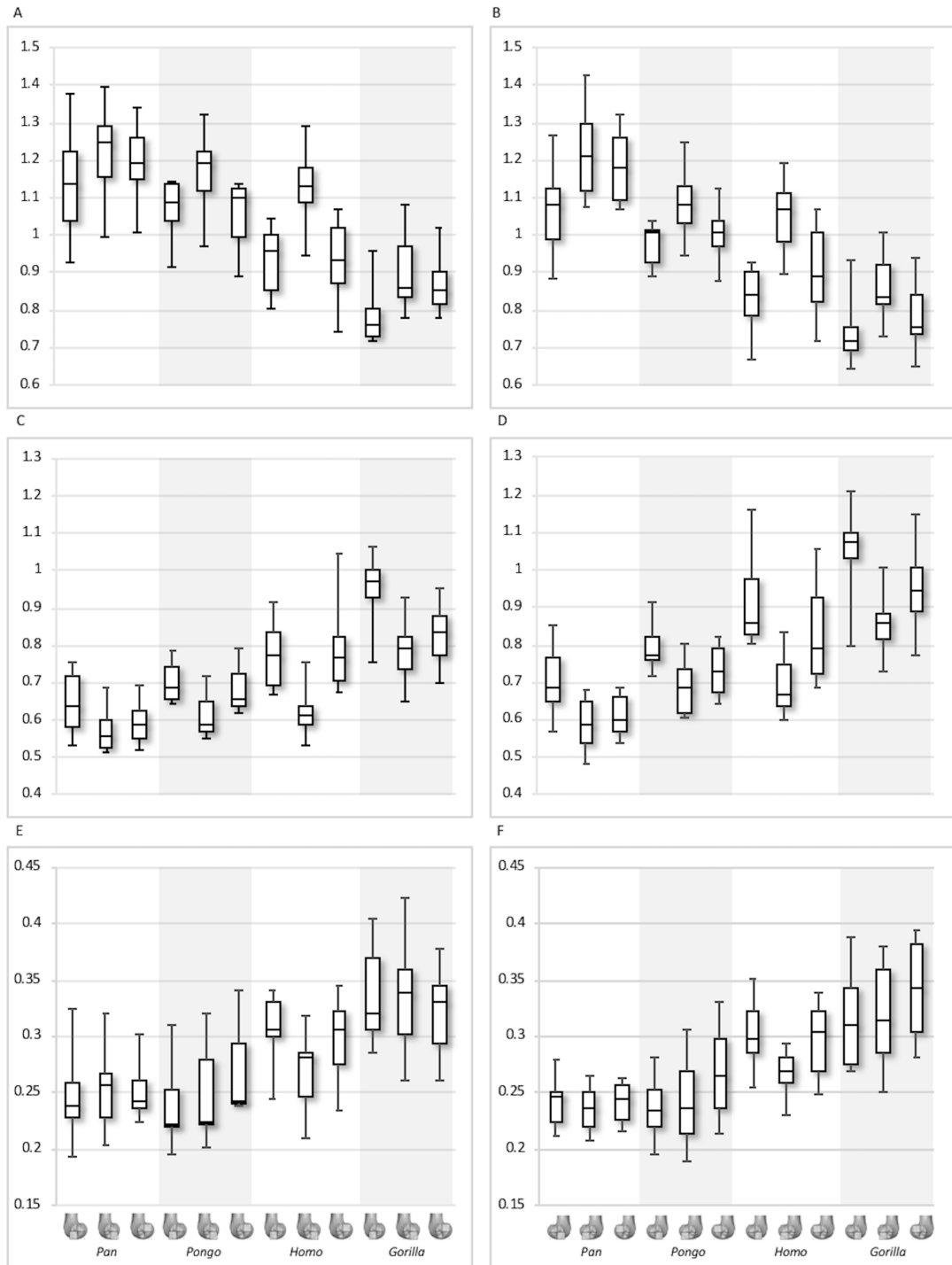


Figure 4.9. Trabecular number (Tb.N), separation (Tb.Sp) and thickness (Tb.Th) results for each region and taxon. (A) Tb.N in the lateral condyle. (B) Tb.N in the medial condyle. (C) Tb.Sp in the lateral condyle. (D) TB.Sp in the medial condyle. (E) Tb.Th in the lateral condyle. (F) Tb.Th in the medial condyle. Regions (outlined) and taxa are displayed below. Taxa are presented in order of body mass (*Pan* the smallest; *Gorilla* the largest) to better visualise any patterns potentially associated with body size.

In the lateral condyle, Tb.Sp is significantly higher in *Gorilla* than in *Pan* and *Pongo* in all regions ($p < 0.001$ and $p < 0.01$ respectively; posterosuperior with *Pongo* $p < 0.05$). Moreover, Tb.Sp is higher than in *Homo* in the inferior regions ($p < 0.01$). *Pan* and *Homo* only differ in the posterosuperior region ($p < 0.001$), where *Pan* shows significantly lower Tb.Sp. No differences are found between *Pongo* and *Pan*, or *Pongo* and *Homo*. In the medial condyle, *Gorilla* again show significantly higher Tb.Sp in all regions than *Pan* and *Pongo* ($p < 0.001$ and $p < 0.01$ respectively), but only higher Tb.Sp in the posteroinferior region than *Homo* ($p < 0.01$). *Pongo* shows significantly higher Tb.Sp than *Pan* in the posterosuperior region ($p < 0.05$), but no significant differences to *Homo*, whereas *Homo* shows significantly higher Tb.Sp than *Pan* in the distal ($p < 0.01$) and posterosuperior ($p < 0.001$) regions. CV values show that in both condyles *Pan* is the most variable in the distal region, all species show similar variation in the posteroinferior region and *Homo* shows the greatest variation in the posteriosuperior region.

In regards to Tb.Th, in the lateral condyle, *Gorilla* shows significantly higher values than *Pan* in all regions ($p < 0.01$ and $p < 0.001$ in the posterosuperior). Furthermore, *Gorilla* has significantly higher Tb.Th than *Pongo* in the inferior regions ($p < 0.05$) and, when the captive specimens are removed, a significant difference is also detected in the posterosuperior region ($p < 0.01$). The only difference detected between *Gorilla* and *Homo* is in the posteroinferior region ($p < 0.05$), where *Gorilla* has higher Tb.Th. *Pan* shows significantly lower Tb.Th than *Homo* in the distal and posterosuperior regions ($p < 0.05$), whereas *Pongo* shows significantly lower Tb.Th than *Homo* only in the distal region of this condyle ($p < 0.05$). No significant differences are detected between *Pongo* and *Pan*. In the medial condyle, *Pan* displays significantly lower Tb.Th than *Gorilla* and *Homo* in all regions (*Gorilla* $p < 0.001$ and $p < 0.01$ in the distal; *Homo* $p < 0.001$ in distal, $p < 0.05$ in posteroinferior, $p < 0.01$ in posterosuperior), but no differences with *Pongo*. Moreover, *Gorilla* shows significantly higher Tb.Th than *Pongo* in the distal and posterosuperior regions ($p < 0.05$), and when the captive specimens are removed this is extended to the posteroinferior region ($p < 0.01$). No differences are found between *Gorilla* and *Homo* in any region. Similarly to the lateral condyle, *Pongo* and *Homo* only differ in the distal

region ($p < 0.01$), with the former having lower thickness than the latter. When the captive specimens are not included, a significant result is also found in the posteroinferior region ($p < 0.05$). *Pongo* is consistently the most variable taxon across all regions of both condyles.

The PC analysis of three trabecular variables (Tb.Th, Tb.Sp and DA) from all regions of both condyles reveals good separation among the different taxa (Figure 4.10). Together, PC1 and PC2 explain 88% of the total variation (see Supplementary Table 4.2 for loadings). The first PC separates *Gorilla*, with relatively high Tb.Sp, particularly in the medial condyle, from *Pan*, with relatively low Tb.Sp, while *Homo* and *Pongo* fall out as intermediate. The second PC primarily separates *Homo* with relatively high DA in both condyles from all other apes.

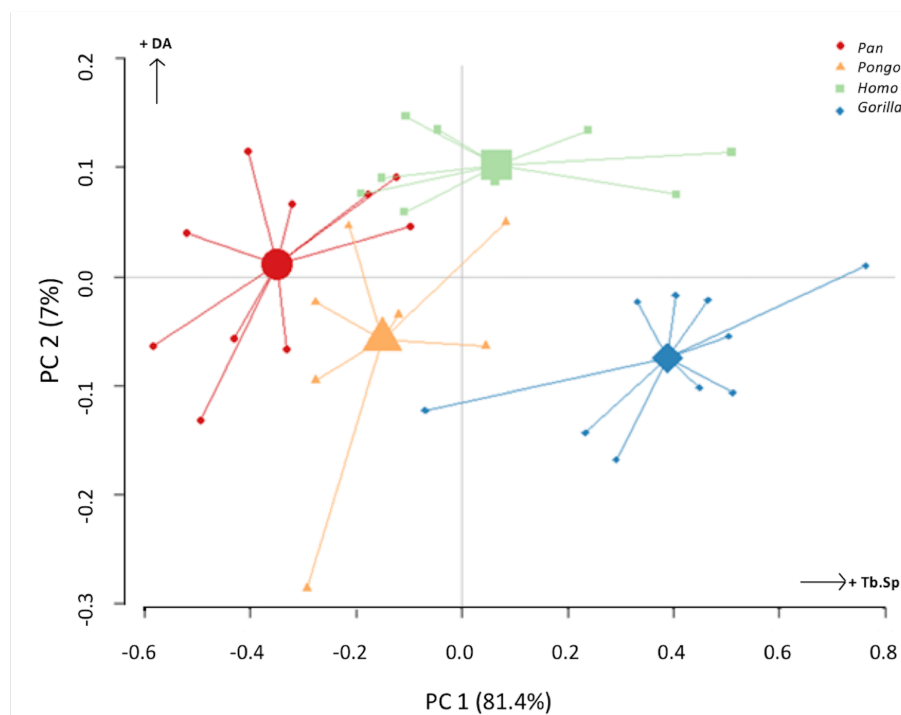


Figure 4.10. Results of principal components analysis of three trabecular variables (Tb.N, Tb.Sp, and DA) in all analysed regions. PC1 is mainly driven by variation in trabecular separation, while PC2 is driven primarily by degree of anisotropy (also see Table S2 for loadings).

4.3.2. Trabecular architecture and between-species regional relationships

Between-species variation is investigated further through two ratios that represent regional relationships in BV/TV and DA. The “inferior index” compares the distribution across the inferior regions of each condyle, where values >1 indicate higher BV/TV or DA in the distal versus the posteroinferior region. The “posterior index” compares distribution across posterior regions, where values >1 indicate higher BV/TV or DA in the posteroinferior versus the posterosuperior region. Results are displayed in Figures 4.11-4.12 and detailed in Table 4.3 and Supplementary Table 4.3. The BV/TV inferior index is <1 in all taxa and in both condyles, indicating that the posteroinferior region has consistently higher BV/TV than the distal region. However, in the lateral condyle, the *Homo* inferior index approaches 1 indicating that BV/TV is fairly equal across the inferior regions and it differs significantly from that of *Pan* ($p<0.05$) and *Gorilla* ($p<0.01$), but not *Pongo*. Thus, there is a greater disparity in BV/TV distribution between the inferior regions of the lateral condyle in African apes compared to humans. In the medial condyle no significant differences are found in the inferior index, indicating that the studied taxa have more similar relative distribution in BV/TV.

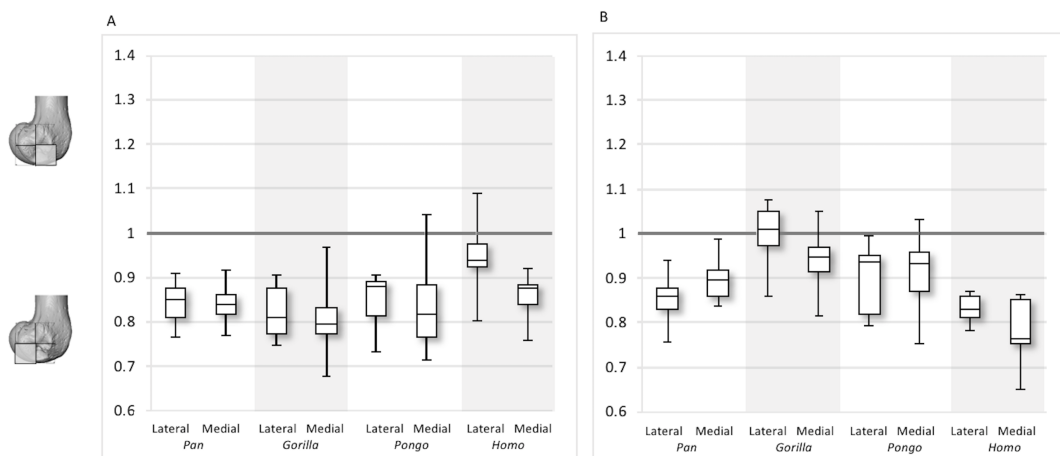


Figure 4.11. Inferior index for BV/TV and DA. (A) BV/TV. (B) DA. Index >1 indicates higher BV/TV or DA in the distal region, whereas index <1 indicates higher values in the posteroinferior region.

Table 4.3. Indices results for lateral and medial condyle.

Taxon	Parameter	Inferior lateral index	Posterior lateral index	Inferior medial index	Posterior medial index
<i>Pan</i>	BV/TV	0.84 (0.05)	1.03 (0.08)	0.84 (0.05)	1.03 (0.08)
	DA	0.86 (0.05)	1.13 (0.09)	0.90 (0.04)	1.02 (0.07)
<i>Gorilla</i>	BV/TV	0.86 (0.06)	1.15 (0.11)	0.81 (0.08)	1.06 (0.07)
	DA	1.00 (0.07)	1.04 (0.06)	0.94 (0.07)	1.01 (0.04)
<i>Pongo</i>	BV/TV	0.85 (0.06)	1.03 (0.02)	0.84 (0.11)	0.97 (0.08)
	DA	0.90 (0.08)	1.12 (0.10)	0.91 (0.09)	1.08 (0.06)
<i>Homo</i>	BV/TV	0.95 (0.08)	1.16 (0.11)	0.86 (0.05)	1.15 (0.10)
	DA	0.83 (0.03)	1.10 (0.04)	0.78 (0.07)	1.11 (0.05)

The inferior index also reveals interspecific differences in DA regional relationships. In the lateral condyle, *Homo* demonstrates the lowest ratio, indicating greater disparity in DA between the two inferior regions, with higher DA found in the posteroinferior region. In contrast, *Gorilla* has an inferior index approaching 1, indicating more equal DA across inferior regions. In the lateral condyle, the inferior index differs significantly between *Gorilla* and *Homo* ($p < 0.001$), as well as *Gorilla* and *Pan* ($p < 0.01$). In the medial condyle, all taxa show a mean inferior index < 1 , indicating that the posteroinferior has relatively greater DA than the distal region. However, one *Pongo* specimen and two *Gorilla* specimens are > 1 . *Homo* displays the greatest disparity in DA between the two regions, with a significantly lower index than *Pan* ($p < 0.01$) and *Gorilla* ($p < 0.001$). All nonhuman apes are not significantly different from each other.

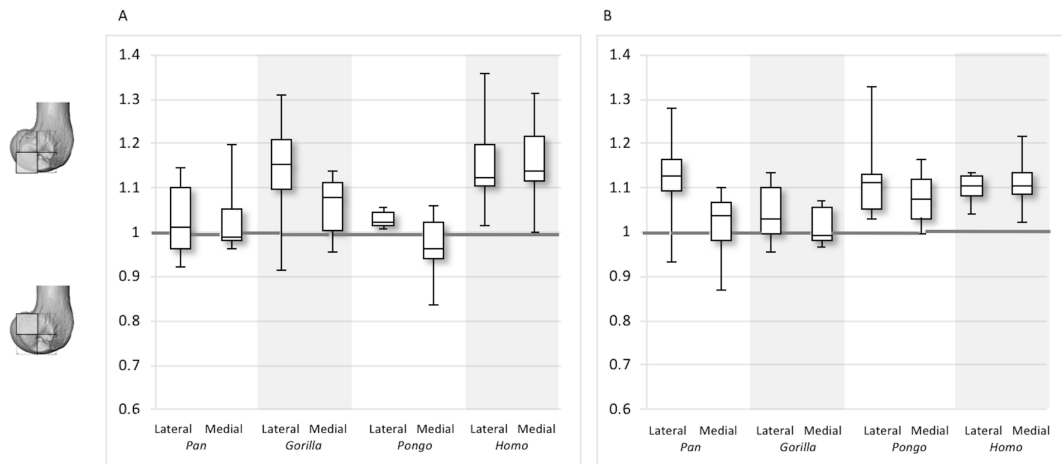


Figure 4.12. Posterior index for BV/TV and DA. (A) BV/TV. (B) DA. Index >1 indicates higher BV/TV or DA values in the posteroinferior region, whereas index <1 indicates higher values in the posterosuperior region.

For the BV/TV posterior index in the lateral condyle, *Pan* and *Pongo* have a value close to 1 indicating a relatively equal distribution of BV/TV between the posteroinferior and posterosuperior regions. In contrast, both *Homo* and *Gorilla* show an index >1, indicating relatively higher BV/TV in the posteroinferior region. In the medial condyle, *Homo* shows the highest posterior index >1, indicating relatively higher BV/TV in the posteroinferior region, while the nonhuman apes show lower indices. *Pan* and *Pongo* show relatively equal values across the two regions with indices close to 1. The posterior index is significantly higher in *Homo* compared to *Pongo* in both condyles (lateral $p < 0.05$; medial $p < 0.01$) and compared to *Pan* in the medial condyle ($p < 0.05$) only. There are no significant differences between nonhuman apes.

For the DA posterior index in the lateral condyle, *Pan*, *Pongo* and *Homo* have indices >1, indicating relatively higher DA in the posteroinferior region compared with the posterosuperior. The *Gorilla* posterior index is closer to 1, indicated that DA is similar across the posterior regions of the lateral condyle. However, there are no significant differences in the DA indices across the taxa. In the medial condyle, *Pongo* and *Homo* show greater DA in the posteroinferior than the posterosuperior region, whereas *Gorilla* and *Pan* have indices closer to 1 indicating a relatively equal DA

across these regions in African apes. Between-species comparisons of the index reveal that *Homo* has a significantly higher index than *Pan* ($p < 0.05$) and *Gorilla* ($p < 0.001$).

4.4. Discussion

This study investigated trabecular variation in the distal femur of great apes and humans. I expected variation to reflect differences in locomotion and predicted differences in habitual joint posture, as well as habitual range of motion at the knee joint. I found general support for my predictions, although variation in BV/TV distribution did not clearly distinguish taxa despite (presumably) distinct differences in knee posture and loading during locomotion. I first discuss intraspecific variation, followed by interspecific differences.

4.4.1. Within-species trabecular patterns

The *Pan* distal femur had particularly high BV/TV in the posterosuperior and posteroinferior regions of both condyles, and comparatively low BV/TV in the distal region. Higher BV/TV values extended from the subchondral surface relatively far into the epiphysis of both condyles, particularly in the medial condyle (Figure 4.4). Quantification of the trabecular architectural variables revealed that the high BV/TV in *Pan* was characterised by numerous, thin trabeculae with narrow separation. Furthermore, DA was highest in the posteroinferior region in the lateral condyle, but equally low in the two other regions. In the medial condyle DA is more equal across posterior regions, but low in the distal region. Together, these results are consistent with higher and more uniaxial loading of the distal femur in a flexed-knee posture, which is used during both quadrupedal knuckle-walking and, especially, vertical climbing (D'Août et al. 2002; D'Août et al. 2004; Isler, 2005). The more isotropic posterosuperior region may reflect the more variable loading that would occur

during climbing, as this region is (presumably) in contact with the proximal tibia only when the knee is strongly flexed (Isler, 2005; Figure 4.1).

Gorilla showed high BV/TV in the posteroinferior region, which did not always extend posterosuperiorly. The disparity between BV/TV in the posterior regions was more obvious in the lateral condyle, where the BV/TV of the posteroinferior region was visibly higher. In the medial condyle, BV/TV values were similar across the posterior regions. In both condyles BV/TV was lowest in the distal region, where trabecular separation was highest, perhaps consistent with decreased loading of this region. The BV/TV concentration did not extend far within the epiphysis. In both condyles, there was a similar degree of anisotropy across the three studied regions; however, DA in the medial condyle was generally higher than that of the lateral condyle, perhaps due to the greater loading experienced by this condyle (Preuschoft and Tardieu, 1996). Moreover, *Gorilla* displayed fewer but thicker and more widely-separated trabeculae than the other taxa in all of the analysed regions, suggesting that increasing the thickness of trabeculae is important in mitigating load.

The trabecular structure of the *Pongo* distal femur was the most variable across the sample. In general, BV/TV was lowest in the distal region of both condyles. In the lateral condyle BV/TV was highest in the posteroinferior region. However, in the medial condyle some individuals showed higher BV/TV values in the posterosuperior region while other showed fairly equal values across both posterior regions. The great range of values in all studied regions revealed high intraspecific variation in the distribution of BV/TV within the condyles. The high BV/TV was characterised by numerous trabeculae that were relatively thin and closely packed in all regions. *Pongo* showed relatively low DA values across all regions of the epiphysis, particularly in the medial condyle. Together, these results are consistent with the highly mobile knee joint (Morbeck and Zihlman, 1988; Tuttle and Cortright, 1988) that facilitates more variable loading of the distal femur during a diverse arboreal locomotor repertoire (Cant, 1987; Thorpe and Crompton, 2006; Thorpe et al. 2007; Thorpe et al. 2009). Notably, most *Pongo* specimens had a concentration of high BV/TV at the posterior shaft just superior to the femoral condyles. This region

underlies the insertion site for the heads of the gastrocnemius muscle (Prejzner-Morawska and Urbanowicz, 1981; Diogo et al. 2010; Diogo et al. 2013a; Diogo et al. 2013b). This could be the result of the gastrocnemius muscle being strongly recruited during suspension by the hindlimbs, which is more frequently practiced in *Pongo* than in African apes (Thorpe and Crompton, 2006). However, the gastrocnemius is recruited during bipedal walking and running in humans (Neptune et al. 2001; Ishikawa et al. 2006; Lichtwark et al. 2007) and is presumably also important during knuckle-walking and climbing in African apes.

The comparatively high degree of variability within *Pongo* is not necessarily surprising. Distal femur posture and loading during locomotion can vary between species (Mackinnon, 1974; Manduell et al. 2012) and between individuals due to differences in sex and/or body size (Sugardjito and van Hooff, 1986; Cant, 1987; Thorpe and Crompton, 2005). *Pongo* was the only sample in my study to comprise two species (*P. abelii* and *P. pygmaeus*), although there were no consistent differences in trabecular structure found between these species in my small sample. Furthermore, my sample also included two captive specimens; one female (*Pongo* sp.) and the other being the only male (*P. pygmaeus*) in the sample. These individuals regularly fell out as outliers in the *Pongo* sample for BV/TV, DA and Tb.Th, even though interspecific differences were not largely affected. Both showed higher BV/TV and Tb.Th than the other *Pongo* specimens in most regions, which is perhaps explained by their altered locomotion in captivity. Isler and Thorpe (2003) found that captive *Pongo* used shorter gait cycles and faster speed than wild individuals, likely because the captive environment was more predictable. Furthermore, the captive male *Pongo* specimen consistently showed the highest DA values in the sample, coupled with the lowest trabecular number in most regions, while the female displayed the lowest DA values. The trabecular architecture of the male is in line with less climbing behaviour and reflects an altered response to load in larger-sized individuals, whereas that of the female may be a result of more variable and arboreal behaviours resulting in more isotropic trabecular structure. Nonetheless, Tb.N and Tb.Sp mostly fall within the range of wild shot *Pongo* individuals. Given the limited number of *Pongo* specimens available in osteological collections, a fruitful avenue of

future research would be to systematically compare trabecular structure between wild and captive specimens, particularly if general activity patterns are known in the latter.

Homo showed highest BV/TV in the posteroinferior region. The posterosuperior region showed consistently lower values but as BV/TV in the distal region was more variable, patterns between the condyles differed. In the lateral condyle values in the distal region were generally high compared to those of the medial condyle and were higher than the values in the posterosuperior region; a pattern opposite to what is found in the medial condyle. The DA values were greatest in the posteroinferior region and lowest in the distal region of both condyles. High BV/TV in the posteroinferior region of both condyles was characterised by more numerous trabeculae that were more closely packed but less thick compared with the other regions of the *Homo* distal femur. This trabecular pattern is consistent with the region of highest loading when ground reaction forces (Racic et al. 2009) and joint reaction forces (Nordin and Frankel, 2001) are highest during the gait cycle, right before toe-off. The absence of high bone concentration in the posterosuperior region of both condyles is consistent with the relative infrequency of using a highly-flexed knee posture during habitual activities. However, the relatively high intraspecific variation in BV/TV distribution within the *Homo* sample, indicated by generally higher CV values than African apes, was somewhat surprising. Despite humans loading their knees in stereotypical ways compared with other apes, this could be the result of frequent use of behaviours not considered in the predictions of this study, including climbing stairs, sitting, squatting or running, all of which result in different flexion angles (Hardt 1978; Baltzopoulos, 1995; Simpson and Pettit, 1997; Zheng et al. 1998; Anderson and Pandy, 2001; Kellis, 2001; Nagura et al. 2002; Taylor et al. 2004). Changes in knee angle have been shown to affect joint reaction force and contact area. For example, more flexed knee postures result in higher forces on the articular surface (Taylor et al. 2004; Kutzner et al. 2010) and a larger contact area at the posterior end of the condyles (von Eisenhart-Rothe et al. 2004). In contrast, more extended knee postures result in a smaller contact area that is more centrally located on the condyles. Unfortunately, the lack of additional life-history information on the

human sample deems this speculative. Alternatively, this could be due to a lack of a clear functional signal in the trabecular structure of the human distal femur.

4.4.2. *Between-species trabecular differences*

My results revealed several interspecific differences in the trabecular structure of the distal femur across hominoids, although these differences were less pronounced than I predicted. I predicted that *Homo* would have absolutely lower BV/TV values compared with great apes and that the BV/TV distribution would be distally concentrated in the condyles reflecting a habitually extended knee posture. This prediction was not fully supported. *Homo* did not have significantly lower BV/TV in the studied regions compared to great apes, which is in contrast to recent findings that more sedentary recent humans have systemically lower BV/TV throughout various regions of the skeleton (Chirchir et al. 2015; Ryan and Shaw, 2015; Saers et al. 2016; Chirchir et al. 2017). However, my results are in line with recent findings that humans do not consistently display significantly lower BV/TV than *Pan* across skeletal sites (Tsegai et al. 2018a). Unfortunately, as I do not have information on the activity levels or professions of the human population in this study, it is difficult to interpret this result. Nonetheless, the high BV/TV values of the inferior regions and the lack of this BV/TV concentration posterosuperiorly is consistent with extended-knee locomotion.

I predicted that *Pan* and *Gorilla* would show similar, high BV/TV concentrations posterosuperiorly, reflecting the use of more flexed positions. This prediction was supported by the greater BV/TV in the posteroinferior compared to the distal region in both taxa and the high BV/TV in the posterosuperior region in *Pan* consistent with loading of the condyles in more flexed postures. *Pan* showed greater BV/TV concentration in the posterior regions than *Homo*, supporting my prediction, but differed from the pattern found in *Gorilla*. The lack of the posterosuperior concentration in *Gorilla* is consistent with their more extended-knee posture during terrestrial locomotion (Hofstetter and Niemitz, 1998; Isler, 2005; Crompton et al.

2008; but see Finestone et al. 2018), less flexion at the knee during climbing (Isler 2002, 2005) and a locomotor repertoire that includes more frequent knuckle-walking and less climbing compared with *Pan* (Tuttle and Watts, 1985; Crompton et al. 2010).

I also predicted that *Pongo* would show homogenous BV/TV distribution across all analysed regions of the distal femur, reflecting more variable knee joint loading. My results suggest that the distribution is not homogenous in *Pongo* and the pattern does not differ significantly to that of *Pan*. *Pan* and *Pongo* showed high BV/TV values across the posterior regions, consistent with the frequent adoption of both flexed and hyperflexed joint positions consistent with quadrupedal terrestrial locomotion and vertical climbing, respectively. The high degree of intraspecific variability found in *Pongo* is consistent with previous comparative trabecular studies on other skeletal elements (Schilling et al. 2014; Tsegai et al. 2013) and thus further investigation into the factors, including genetic, development, hormonal or biomechanical factors, influencing this intraspecific variability is needed.

Furthermore, I predicted that within my sample, *Homo* would show the highest DA throughout the distal femur reflecting the stereotypical loading that occurs during habitual bipedalism, while *Pan* and *Gorilla* would show similar intermediate levels of DA, and that *Pongo* would show the lowest DA values. My predictions were generally supported. *Homo* had comparatively higher DA in all regions of the distal femur compared with other great apes and the overall pattern was distinctly different from what was found in African apes and *Pongo*. These differences could be explained by variation in mediolateral motion between taxa and less variability in joint forces during locomotion in *Homo* (Preuschoft and Tardieu, 1996). Femoral movement within the tibio-femoral joint is the result of both hard and soft tissue morphology (e.g. Reynolds et al. 2017). Both cruciate ligaments prevent tibial displacement (Butler et al. 1980), whereas the collateral ligaments stop valgus or varus rotation (Shoemaker and Markolf, 1985; Gollehon et al. 1987). The quadriceps, gastrocnemius and hamstrings also assist with knee stability (Shelburne et al. 2006). "Independent rotation" is dictated by the fit with the tibia, which varies across hominoids. In *Homo*, the width of the intercondyloid notch is similar to that

of the tibial interspinal distance (Tardieu, 1981), resulting in more constriction of movement and limited independent rotation of the two elements. In the rest of the great apes this trait varies with body size (Tardieu, 1981). *Pan* has the greatest disparity in fit, followed by *Pongo* and then *Gorilla*, displaying differences in knee rotational capacity. Furthermore, the larger articular surface of the medial condyle than that of the lateral in nonhuman apes (Tardieu, 1981) assists in “combined rotation”, where rotation and flexion-extension happen simultaneously. This external rotation during extension is evident in *Pongo* and *Pan* (Lovejoy, 2007). Greater rotation in these taxa suggests that resulting forces are multi-axial, loading the knee in several directions and therefore producing less anisotropic trabecular structure within the condyles. In contrast, the *Homo* knee is more restricted and, even when flexing, there is a lack of significant mediolateral rotation. This results in more uniform loading and, consequently, a higher degree of trabecular anisotropy.

Lastly, I predicted that trabecular architectural variables would reflect differences in body size consistent with previous studies (e.g. Doube et al. 2011; Ryan and Shaw, 2013; Barak et al. 2013b). Specifically, I predicted that smaller-bodied *Pan* and *Pongo* would show higher Tb.N but lower Tb.Sp and Tb.Th, while larger-bodied *Homo* and *Gorilla* would show the opposite pattern. Although I did not directly test allometry due to the small and unbalanced sex samples within each taxon, I found some support that trabeculae of the distal femur show a similar relationship with body size as found in previous studies. The smaller-sized taxa *Pongo* and *Pan* generally showed greater Tb.N and lower Tb.Sp and Tb.Th than the other hominoids. Conversely, the larger-sized *Gorilla* generally showed greater Tb.Th and Tb.Sp, but lower Tb.N than the other taxa. These results perhaps reveal a link between certain trabecular parameters and body size that could stem from differences during the modelling process. However, further investigation of potential allometric influence on trabecular structure within each taxon is needed on larger and more balanced-sex samples.

Although I found some clear differences in trabecular structure that are consistent with my predictions based on the knee joint range of motion and loading

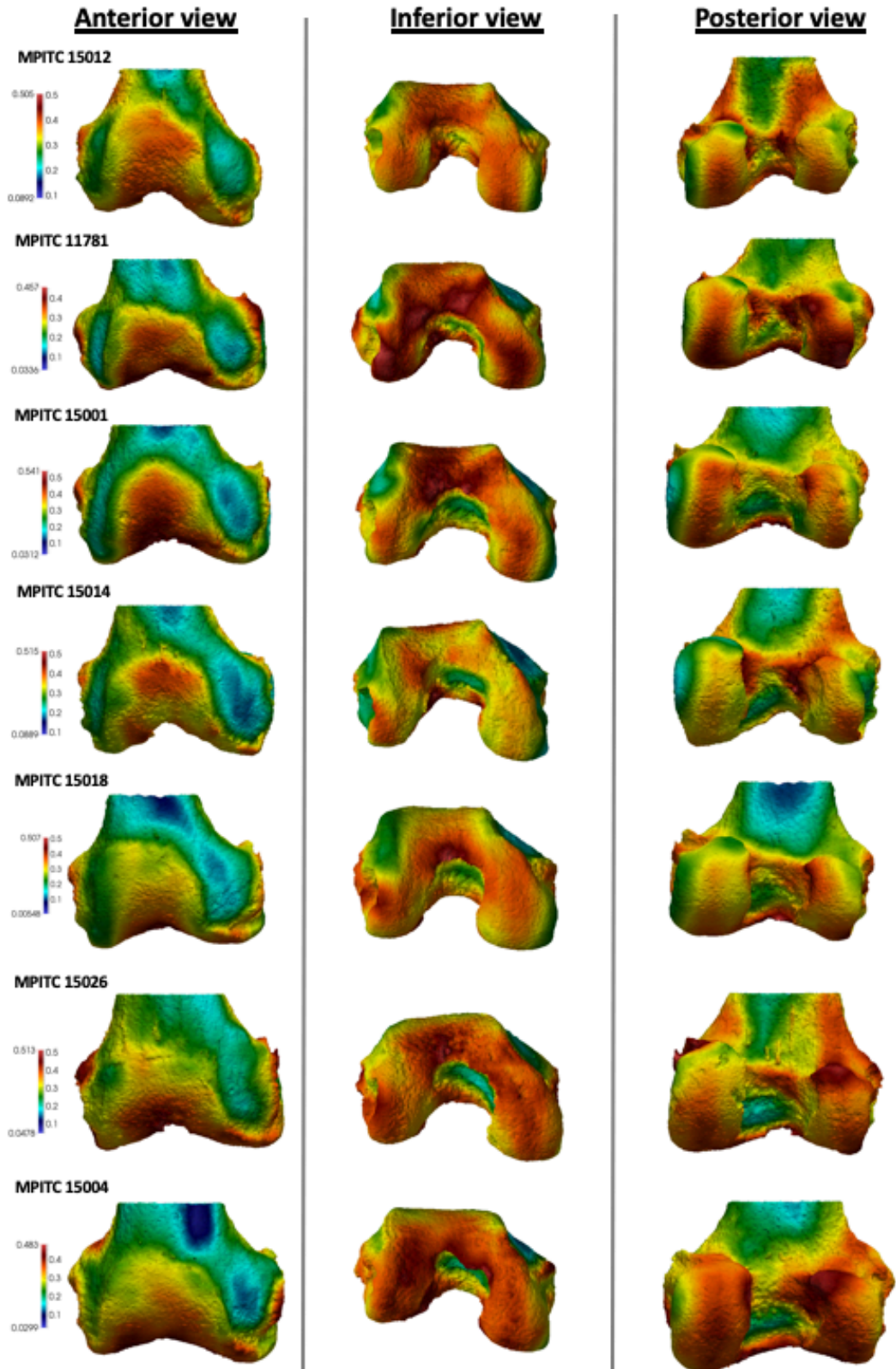
during habitual locomotion, the trabecular patterns revealed here are not necessarily straightforward. There was much greater overlap between *Homo* and other great apes than expected given their dramatic differences in knee joint posture and loading. Biomechanical inferences from trabecular structure are complex because it is not clear what triggers modelling or how trabecular and cortical bone respond to strain (Wallace et al. 2014); for example, research suggests that bone responds to high frequency, low intensity loading and low frequency, high intensity loading, as well as a range of loads that fall between the two extremes (Whalen et al. 1988; Rubin et al. 1990; Rubin et al. 2001; Judex et al. 2003; Scherf et al. 2013). Additionally, I do not know if this differs between specialist and generalist species. Furthermore, it is difficult to control for factors such as genetics, age, hormones, demands for maintaining bone homeostasis and other systemic factors that could influence the organisation of trabecular bone (e.g. Simkin et al. 1987; Lee et al. 2003; Pearson and Lieberman, 2004; Suuriniemi et al. 2004; Kivell, 2016; Wallace et al. 2017; Tsegai et al. 2018a). It has been shown that bone mineral density, as well as bone turnover are to a great extent hereditary (Smith et al. 1973; Dequeker et al. 1987; Kelly et al. 1991; Garnero et al. 1996; Harris et al. 1998). Additionally, trabecular architecture across the skeleton is regulated by different genes (Judex et al. 2009), which adds to the complexity and extrapolating from one skeletal site to another may introduce error. Genotypic variations may also influence the response to mechanical strain (Judex et al. 2002), complicating functional interpretations even further. Thus, variation in bone's response to different types of loading across skeletal sites, between sexes or pathological states (Goldstein, 1987; Keaveny et al. 2001; Yeni et al 2011), as well as the influence of non-mechanical factors suggest that the study of this tissue is complex. Hence, there is a need to understand in greater depth how the knee joint functions and how load is distributed in the different regions of the condyles across hominoids so that we can better link variation in trabecular structure to mechanical loading, particularly in extinct taxa.

4.5. Conclusion

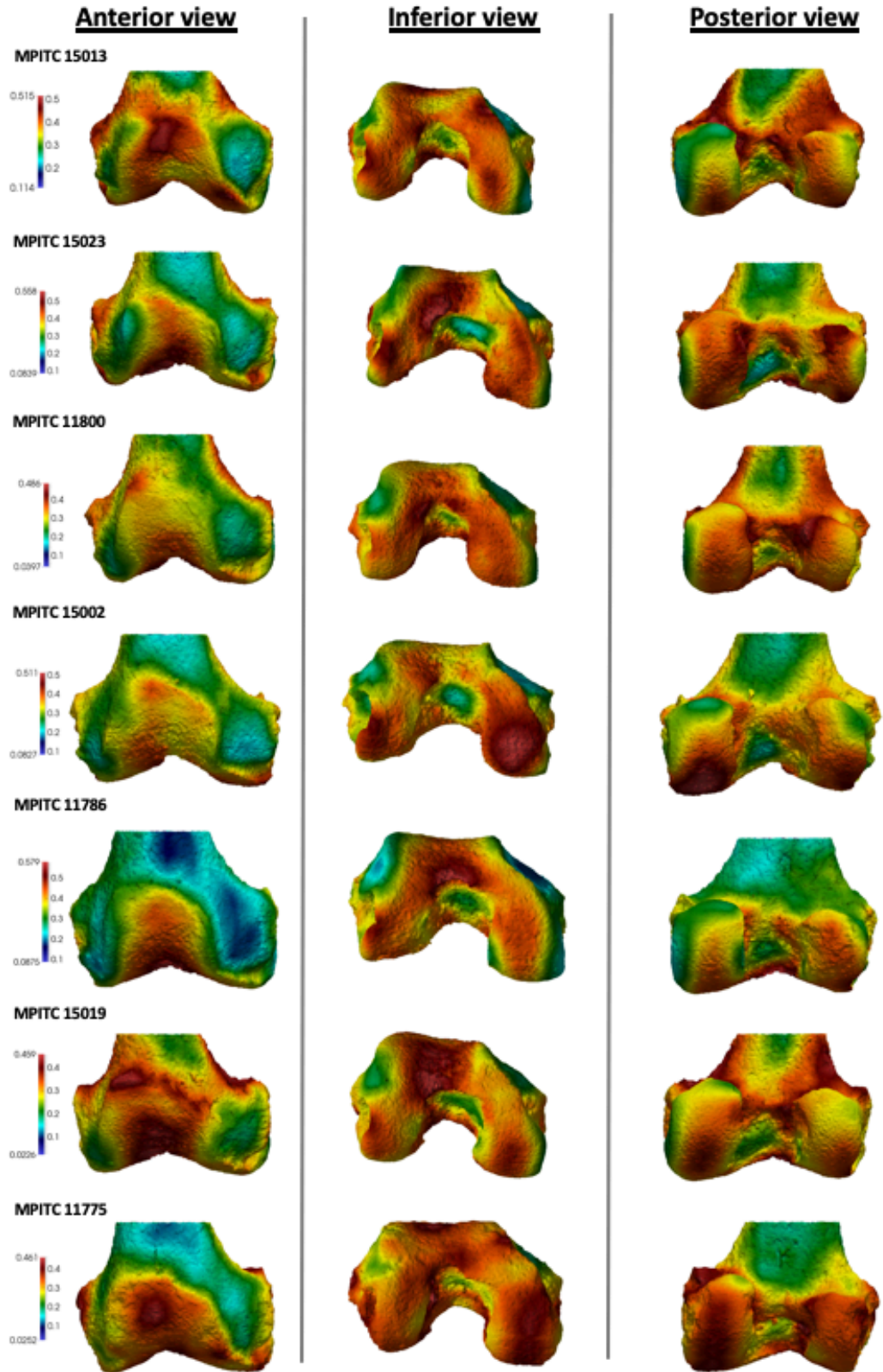
This study provided the first holistic study of trabecular bone within the hominoid distal femur. I showed that humans, despite not being as distinct as initially predicted, are characterised by higher DA than of all other hominoids and more distally concentrated BV/TV compared with *Pan* and *Pongo*, which is consistent with more stereotypical loading in an extended-knee posture during bipedalism. *Pan* and *Pongo* showed more posteriorly-concentrated BV/TV and all apes show lower DA than humans; traits that are generally consistent with more variable loading in a flexed-knee posture that is used during knuckle-walking and climbing. Variation found in this study and specifically in *Pongo*, was consistent with the limited biomechanical studies of knee posture and loading, but substantial overlap in different trabecular parameters across taxa suggest caution is needed when making inferences about behaviour in fossil taxa.

Supplementary material

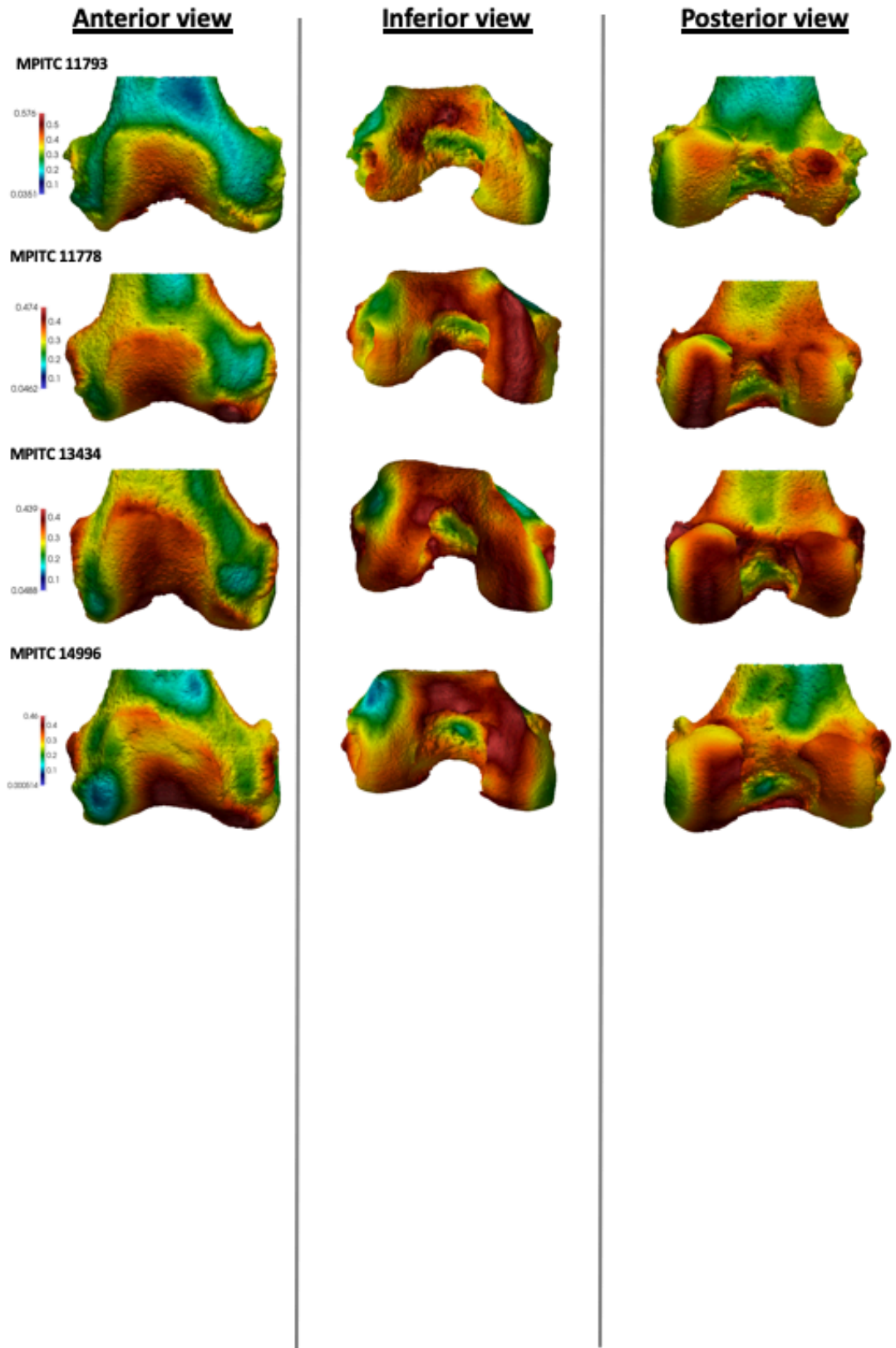
***Pan troglodytes* versus BV/TV distribution**



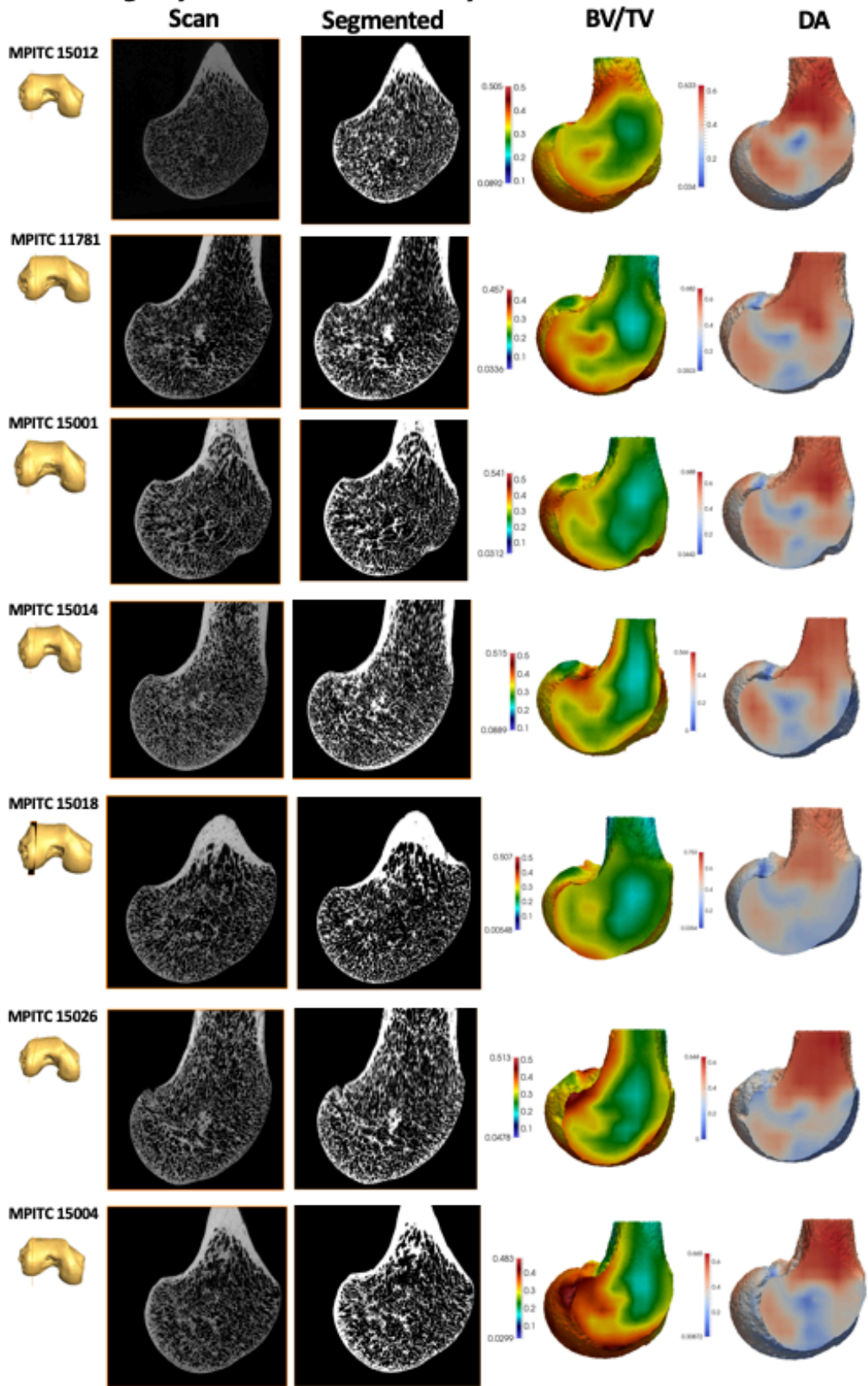
***Pan troglodytes* versus BV/TV distribution**



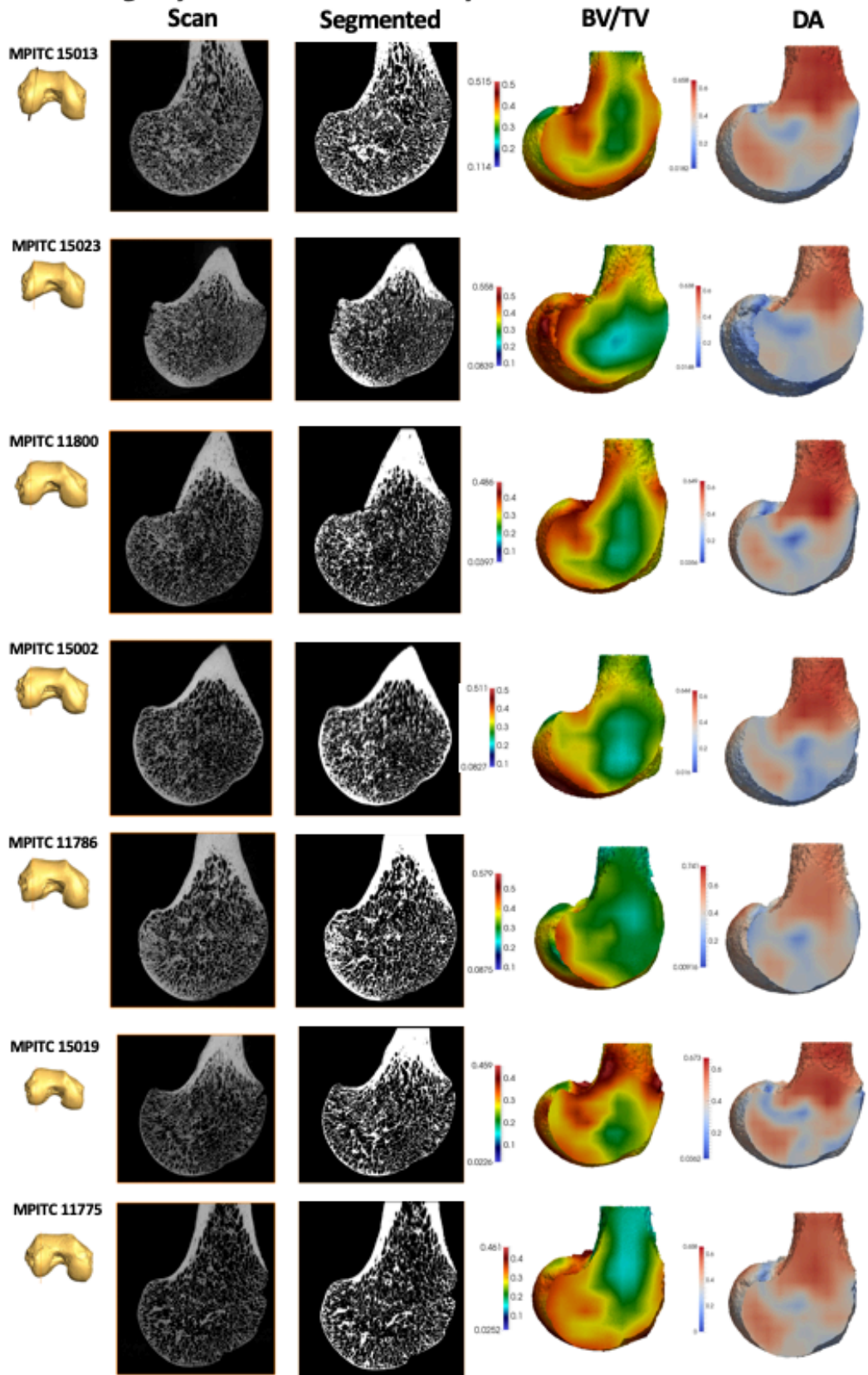
***Pan troglodytes* versus BV/TV distribution**



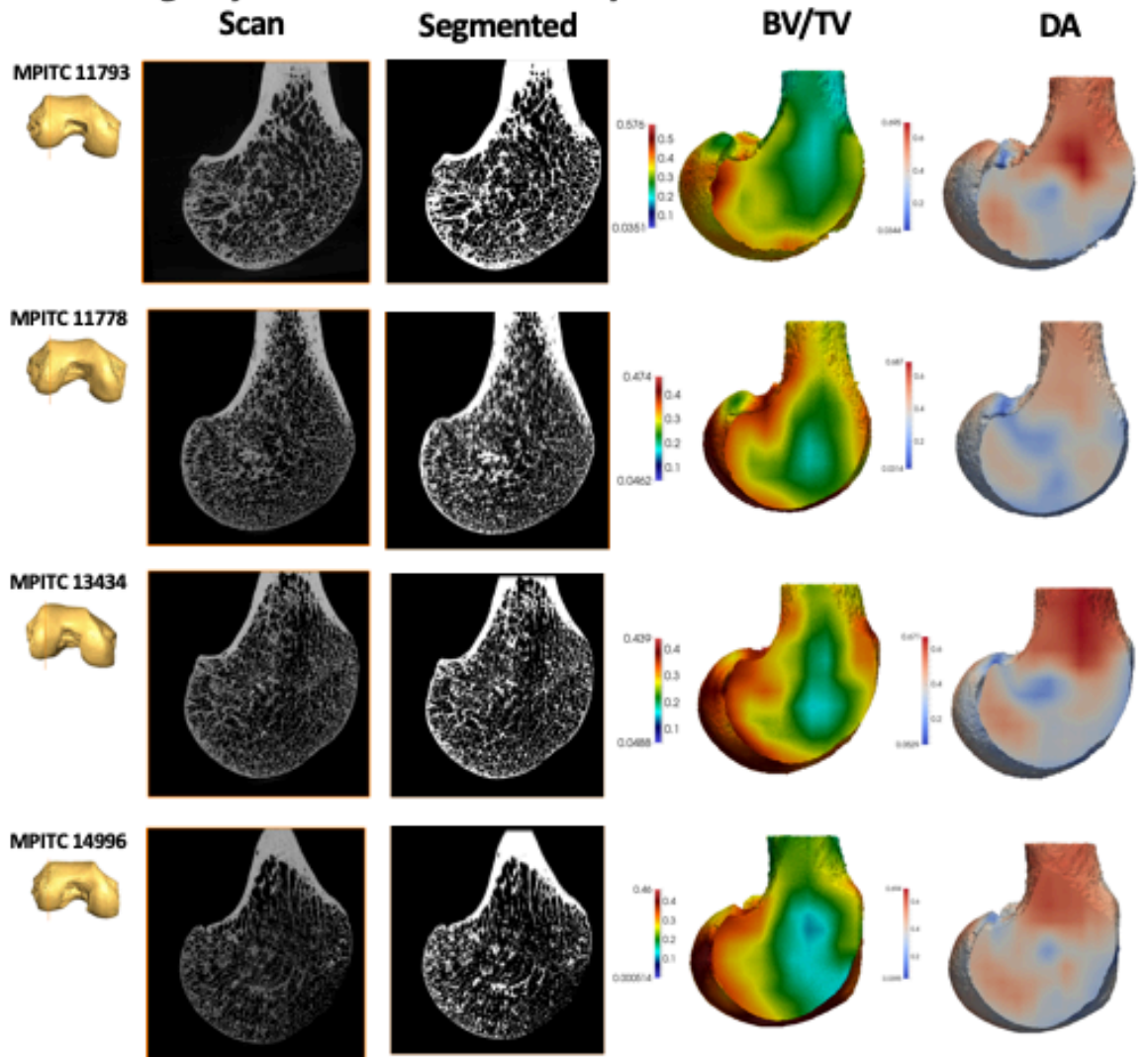
Pan troglodytes verus- Lateral condyle



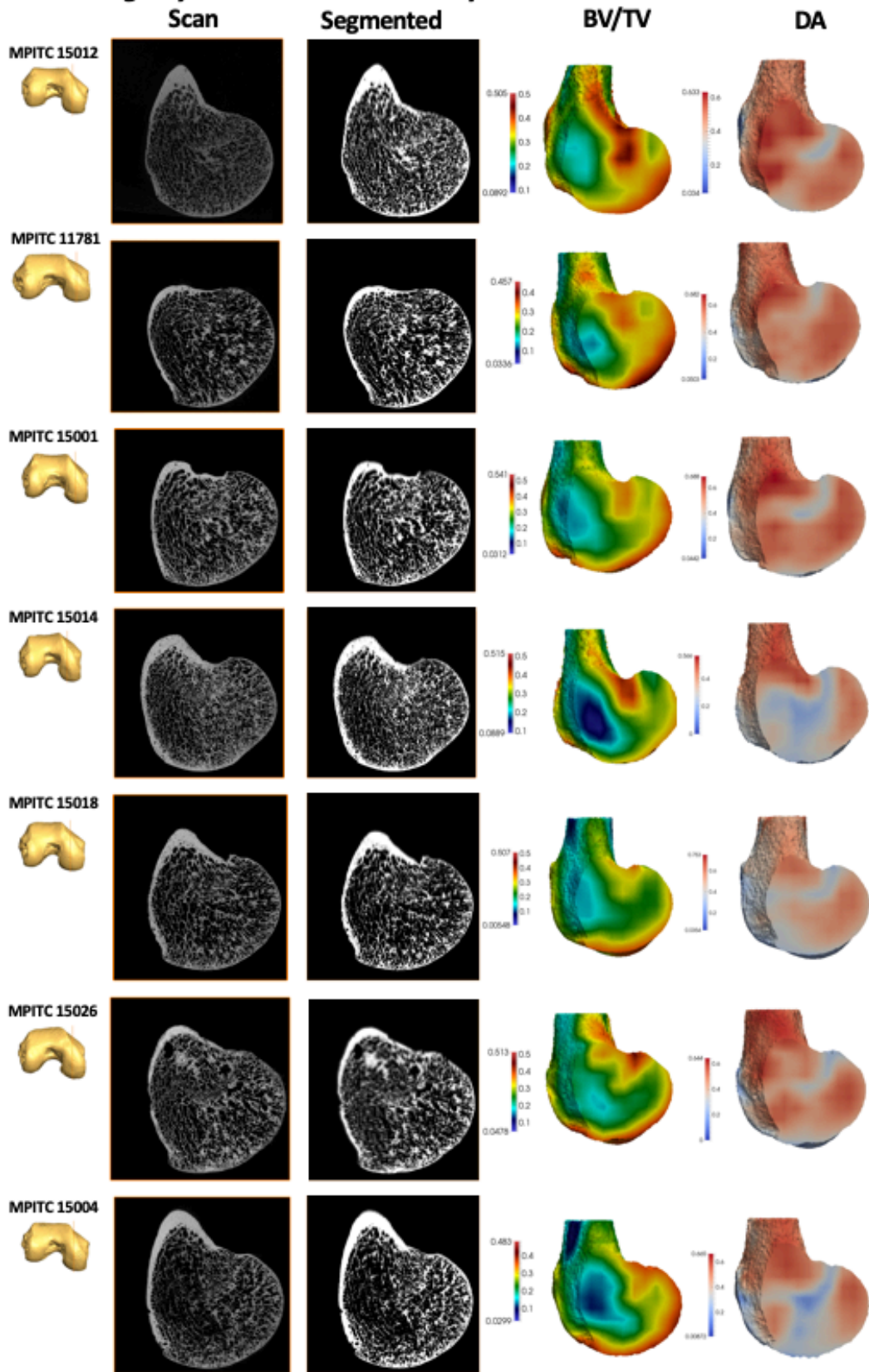
Pan troglodytes verus- Lateral condyle



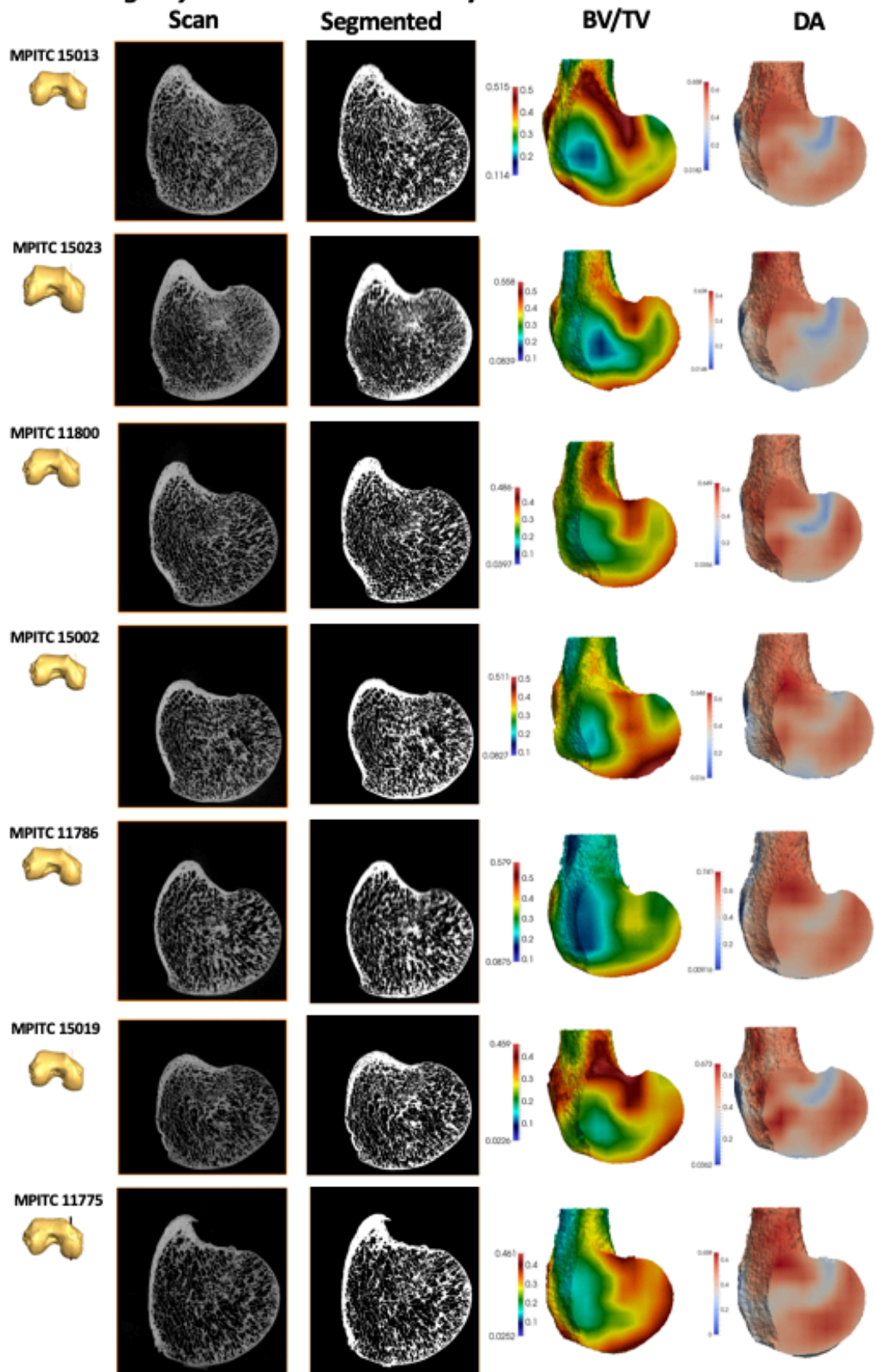
Pan troglodytes verus- Lateral condyle



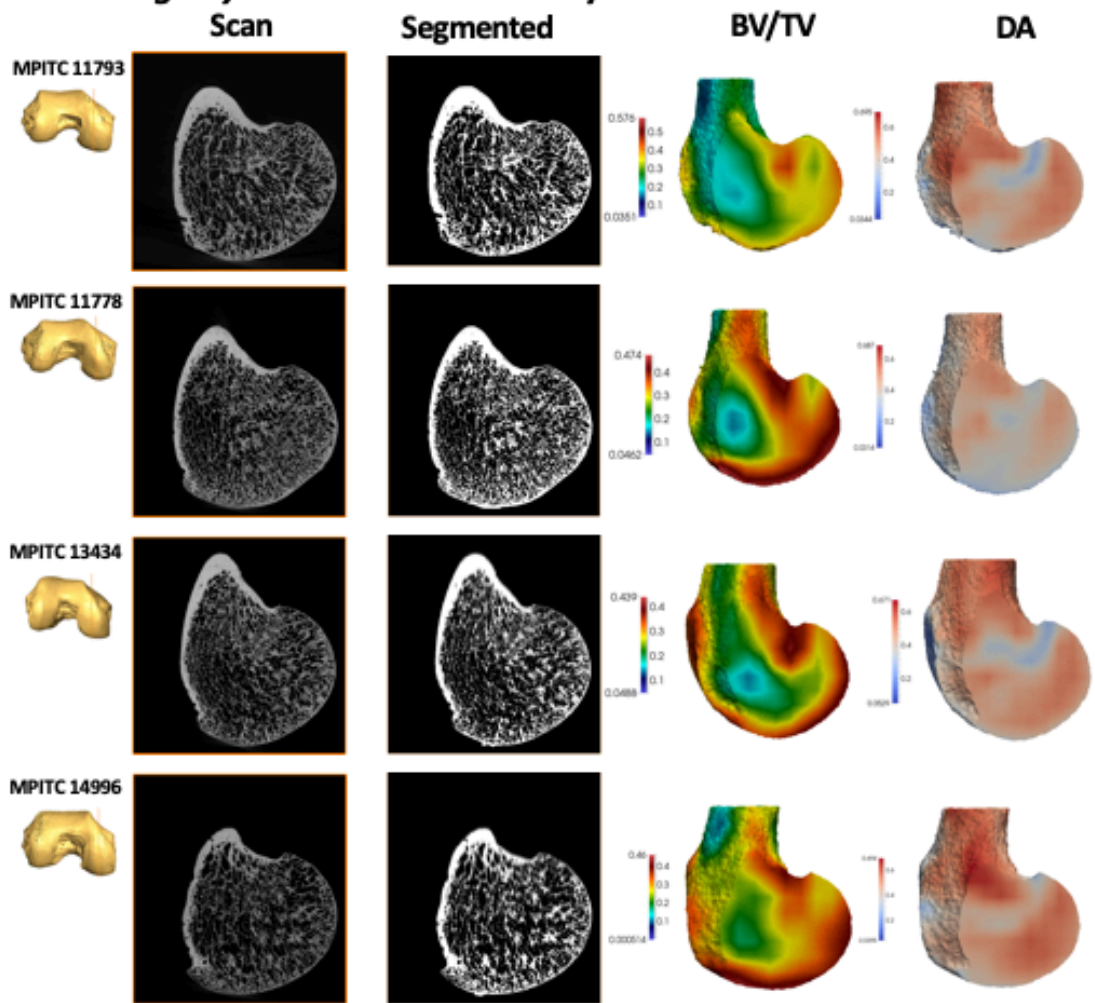
Pan troglodytes verus- Medial condyle



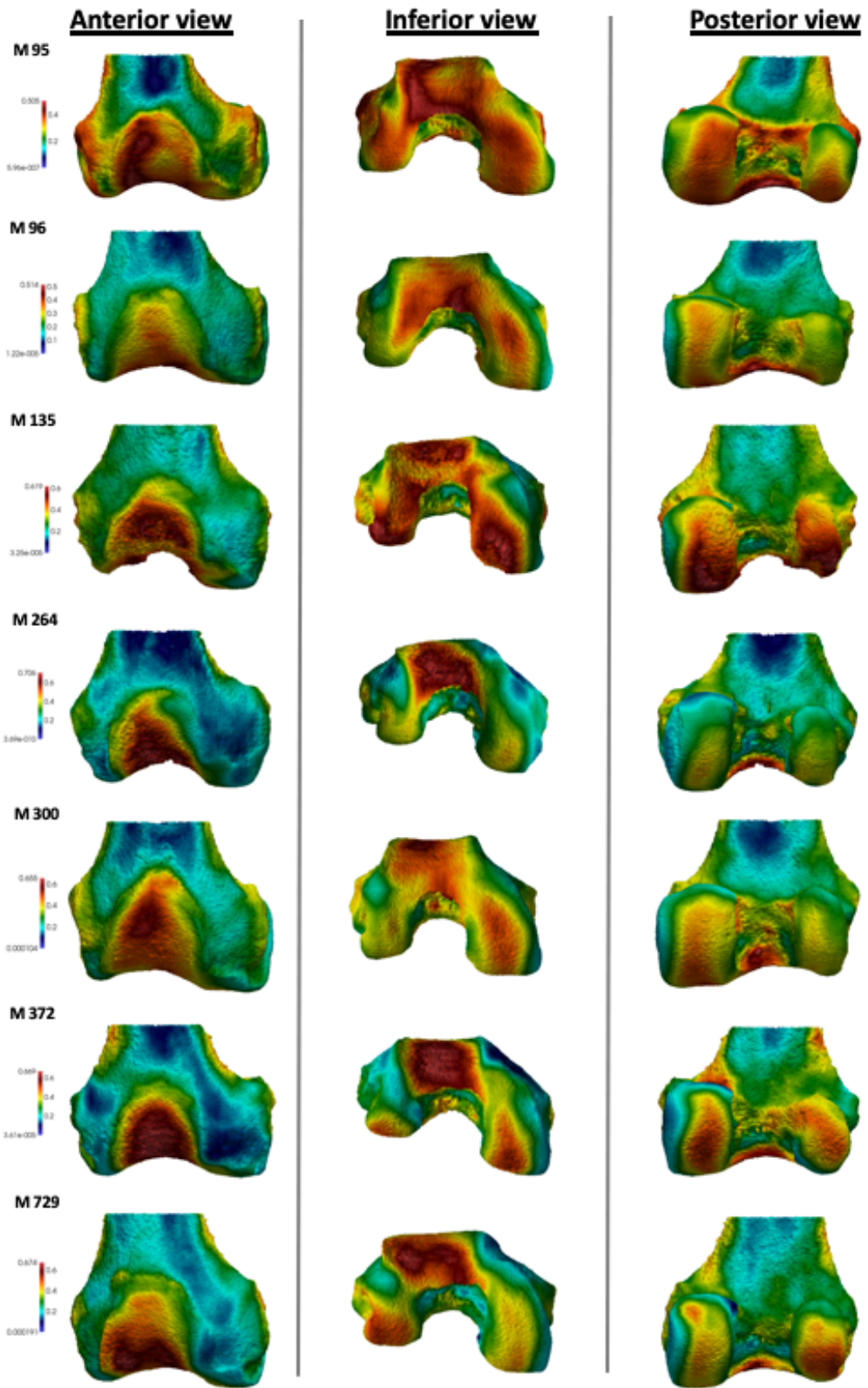
Pan troglodytes versus- Medial condyle



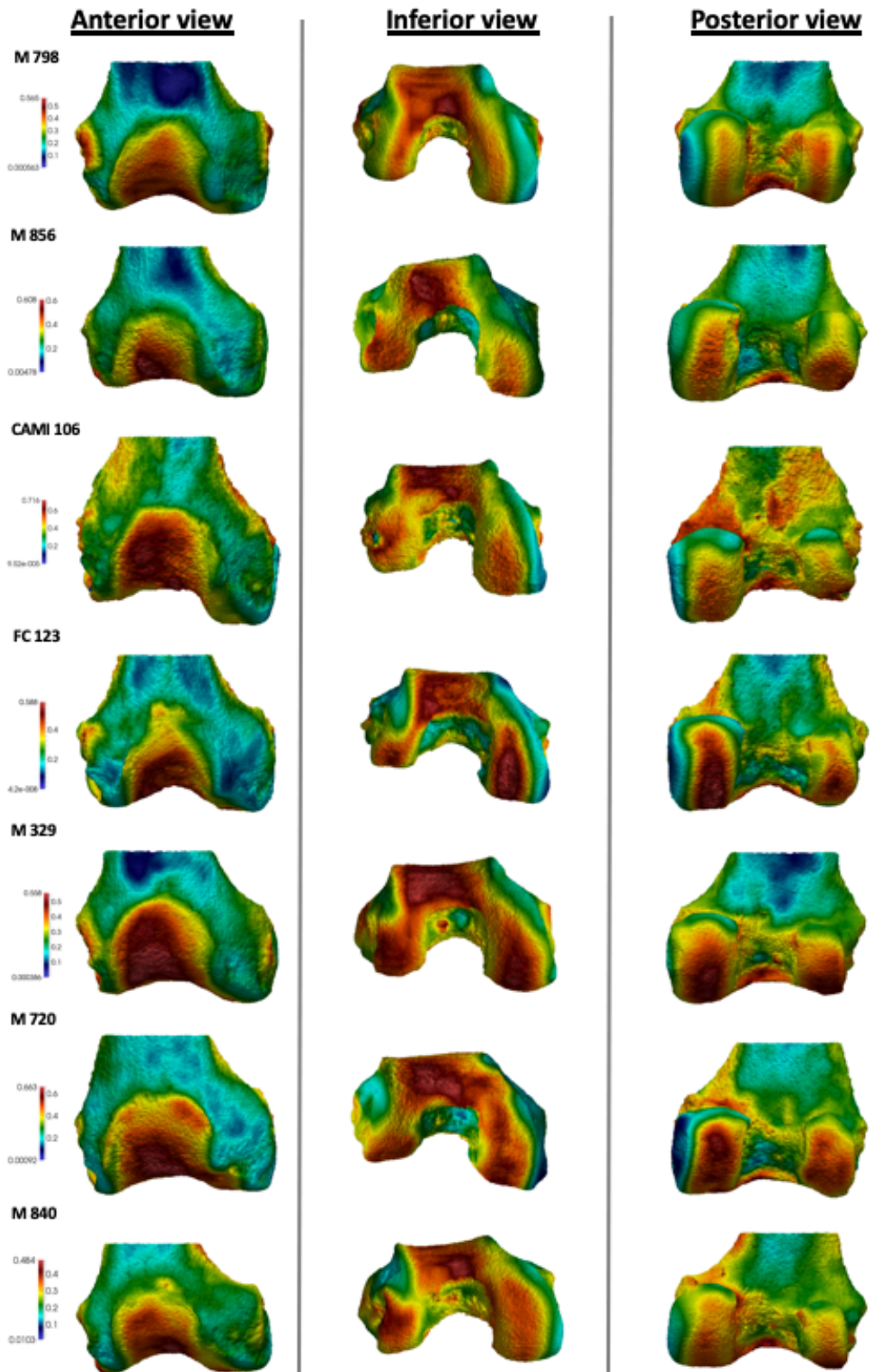
***Pan troglodytes verus*- Medial condyle**



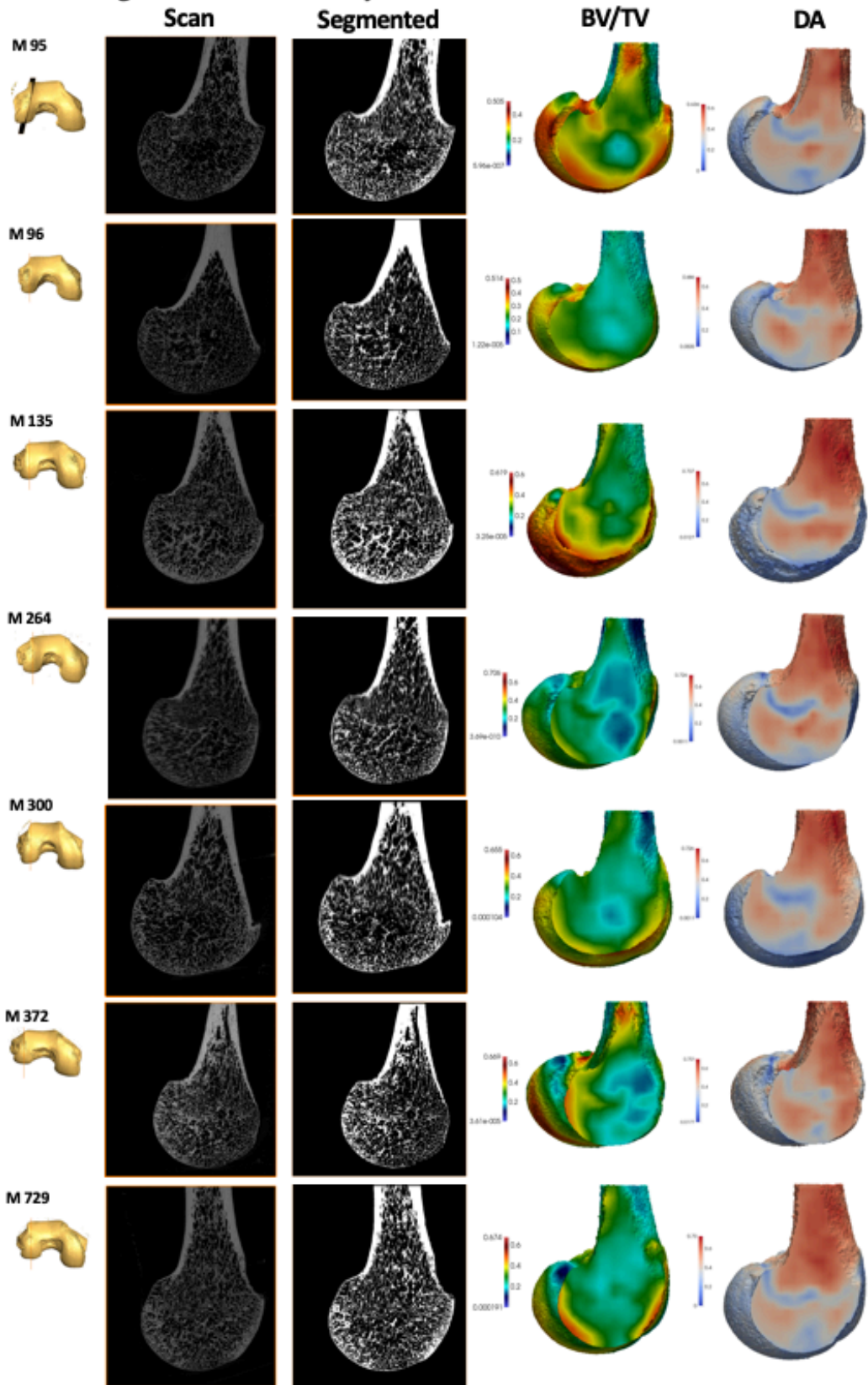
***Gorilla gorilla*- BV/TV distribution**



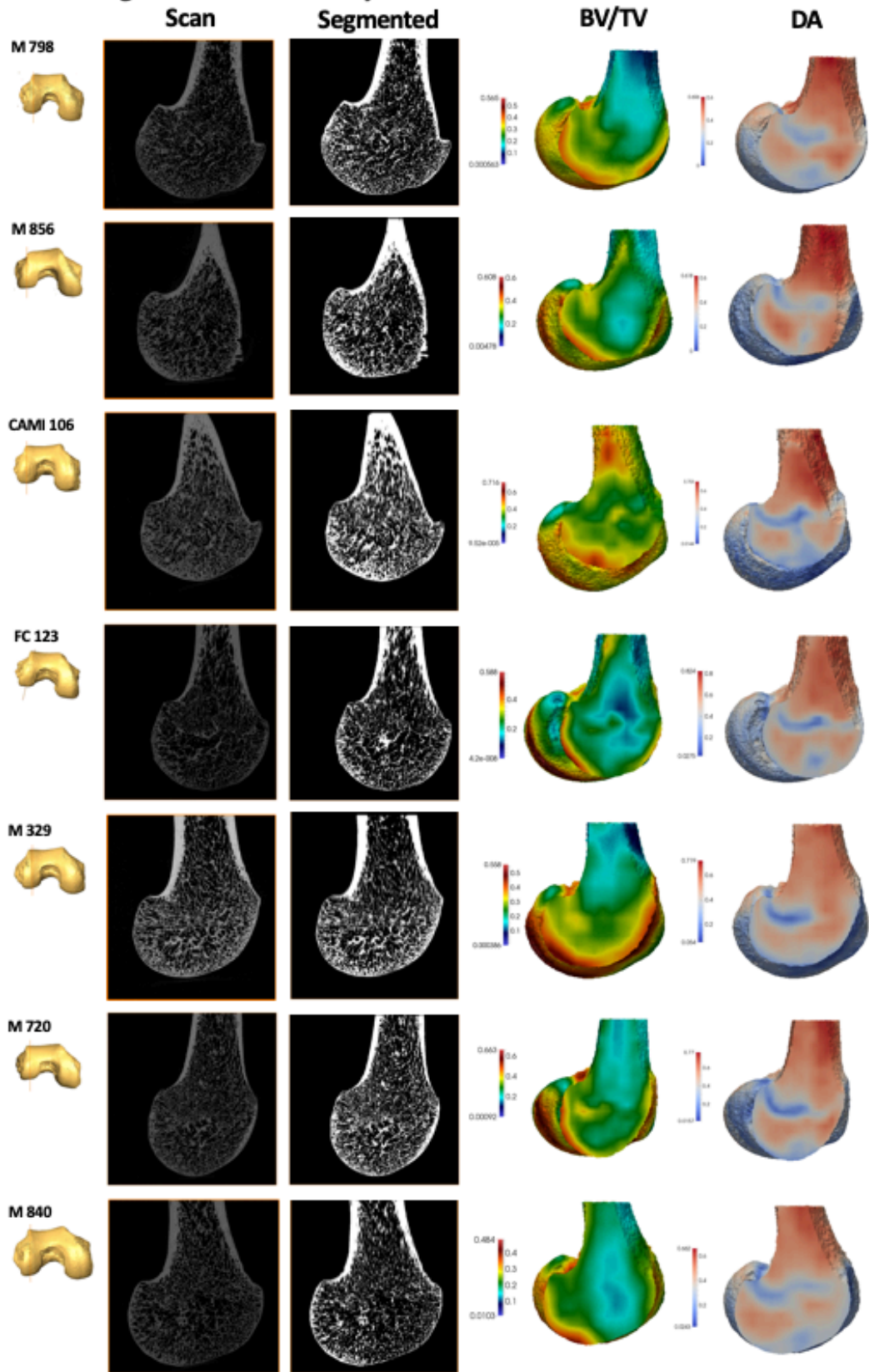
Gorilla gorilla- BV/TV distribution



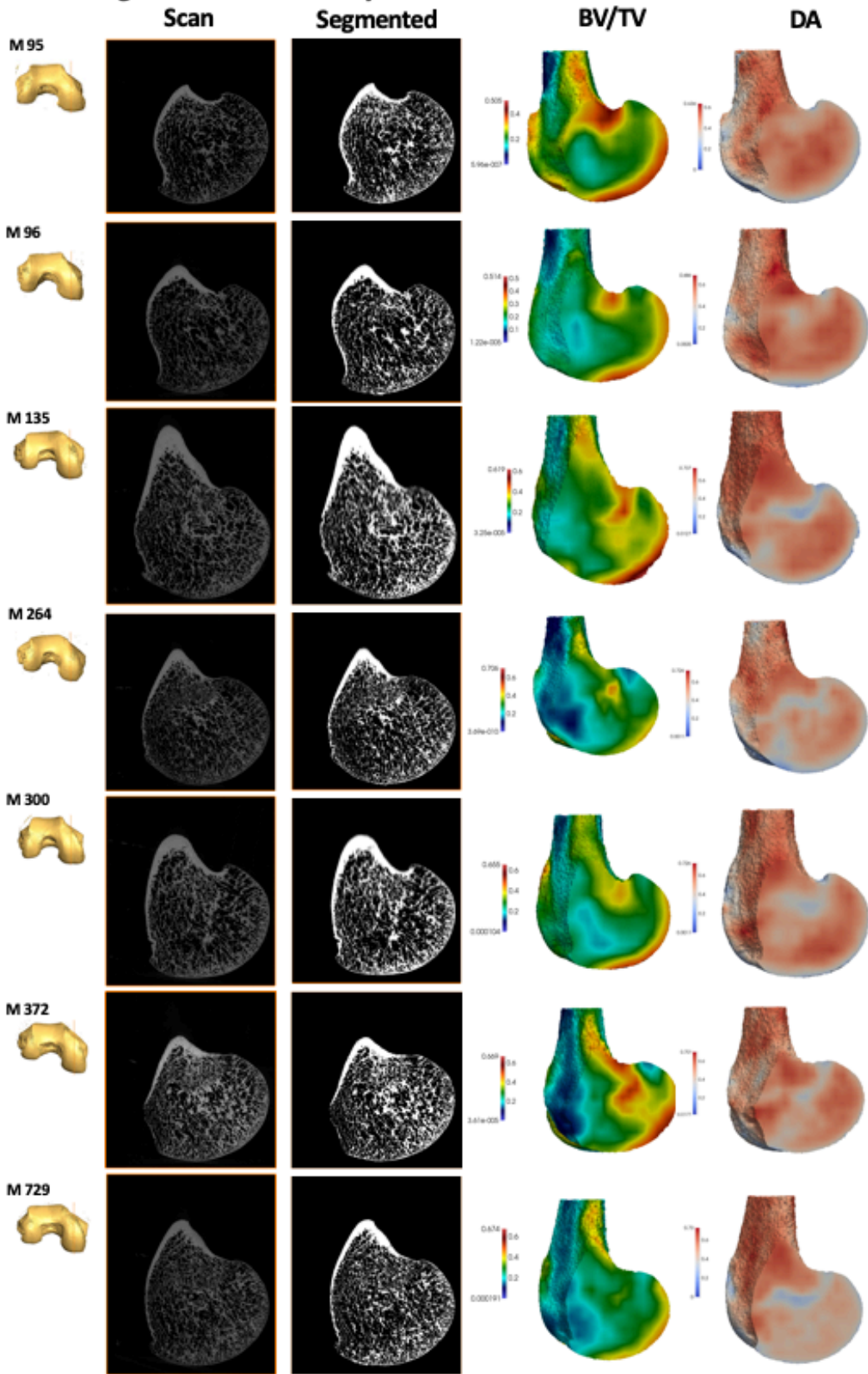
Gorilla gorilla- Lateral condyle



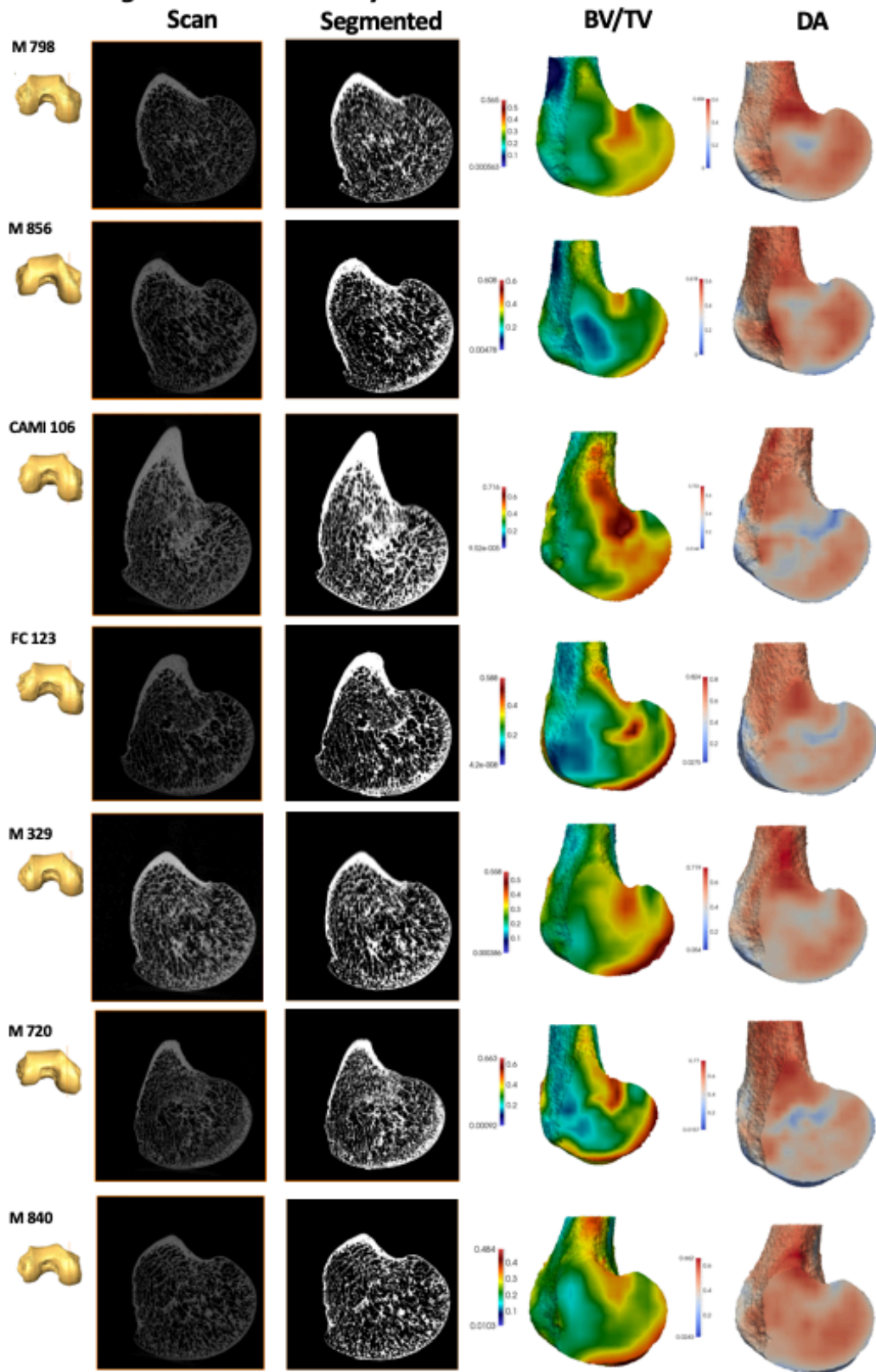
Gorilla gorilla- Lateral condyle



Gorilla gorilla- Medial condyle



Gorilla gorilla- Medial condyle



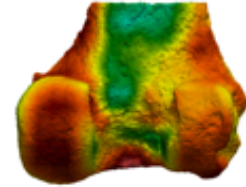
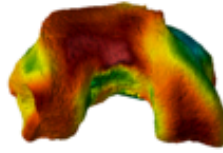
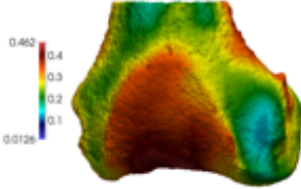
***Pongo sp-* BV/TV distribution**

Anterior view

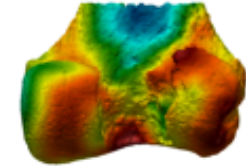
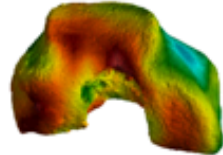
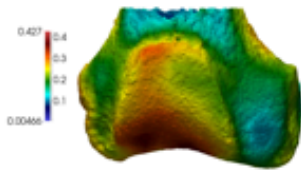
Inferior view

Posterior view

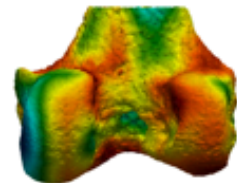
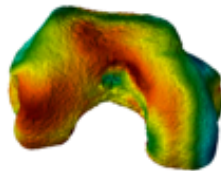
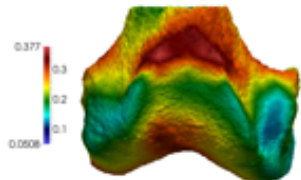
ZSM 1909 0801



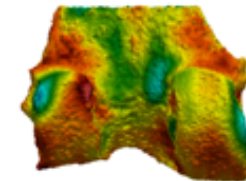
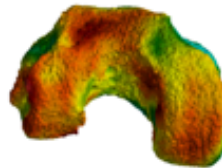
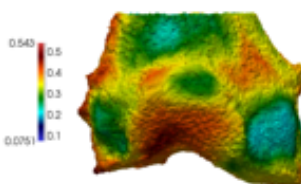
ZSM 1907 0660



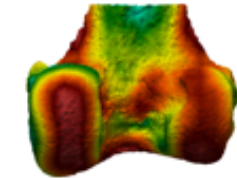
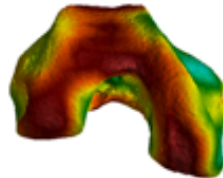
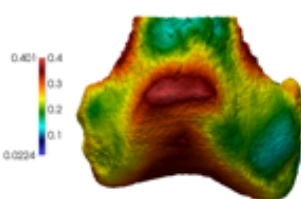
ZSM 1973 0270



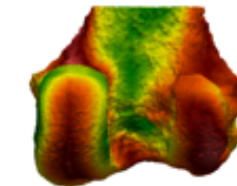
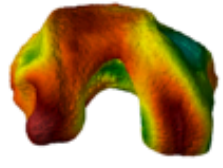
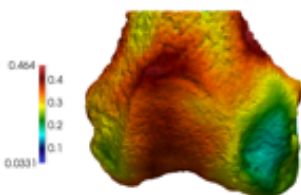
ZSM 1966 0203



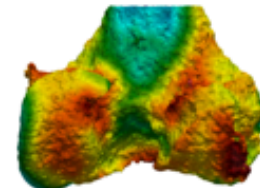
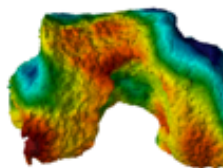
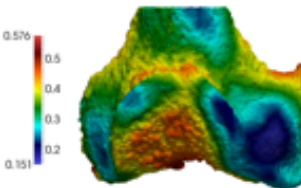
ZSM 1907 0483



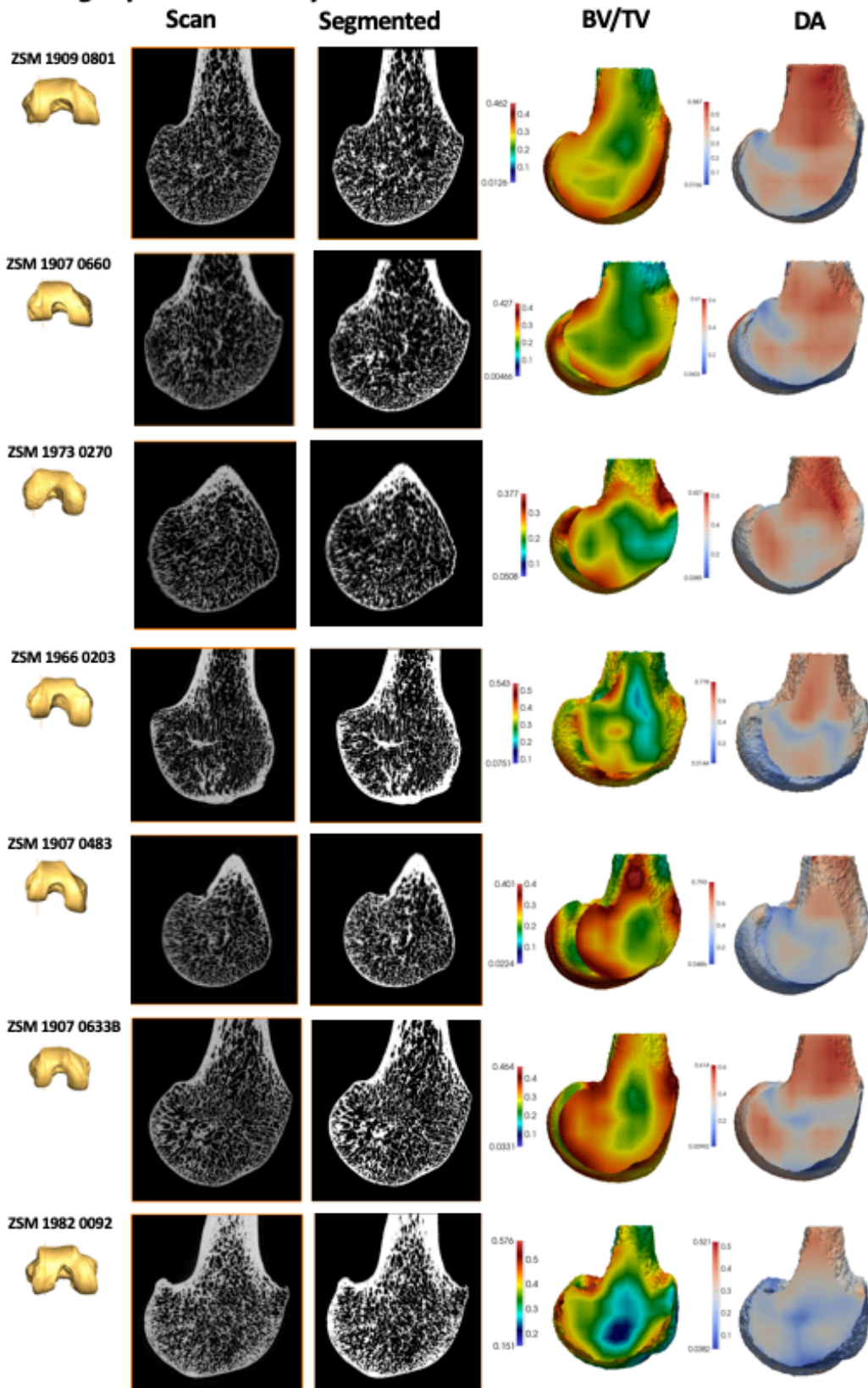
ZSM 1907 06338



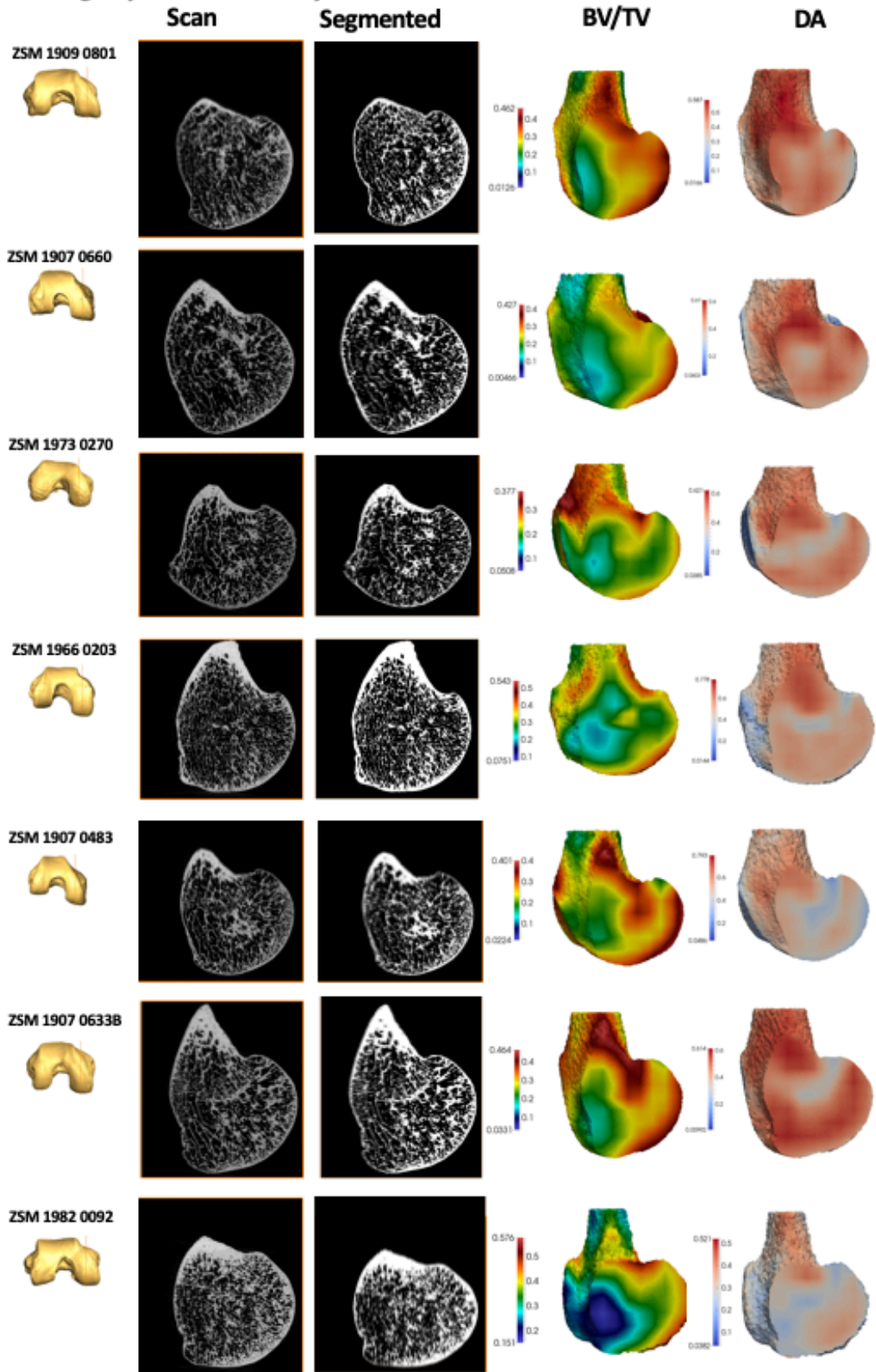
ZSM 1982 0092



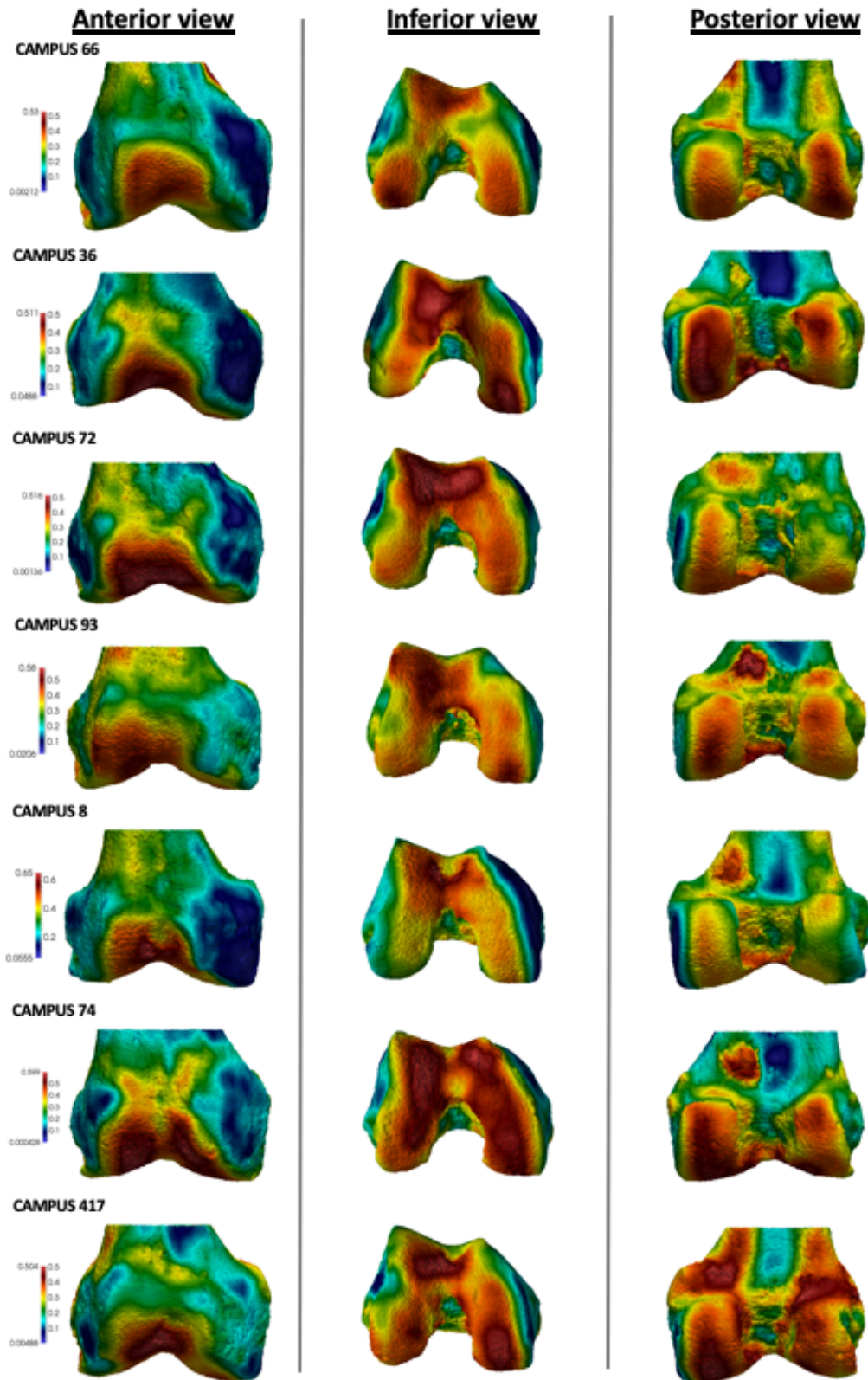
Pongo sp- Lateral condyle



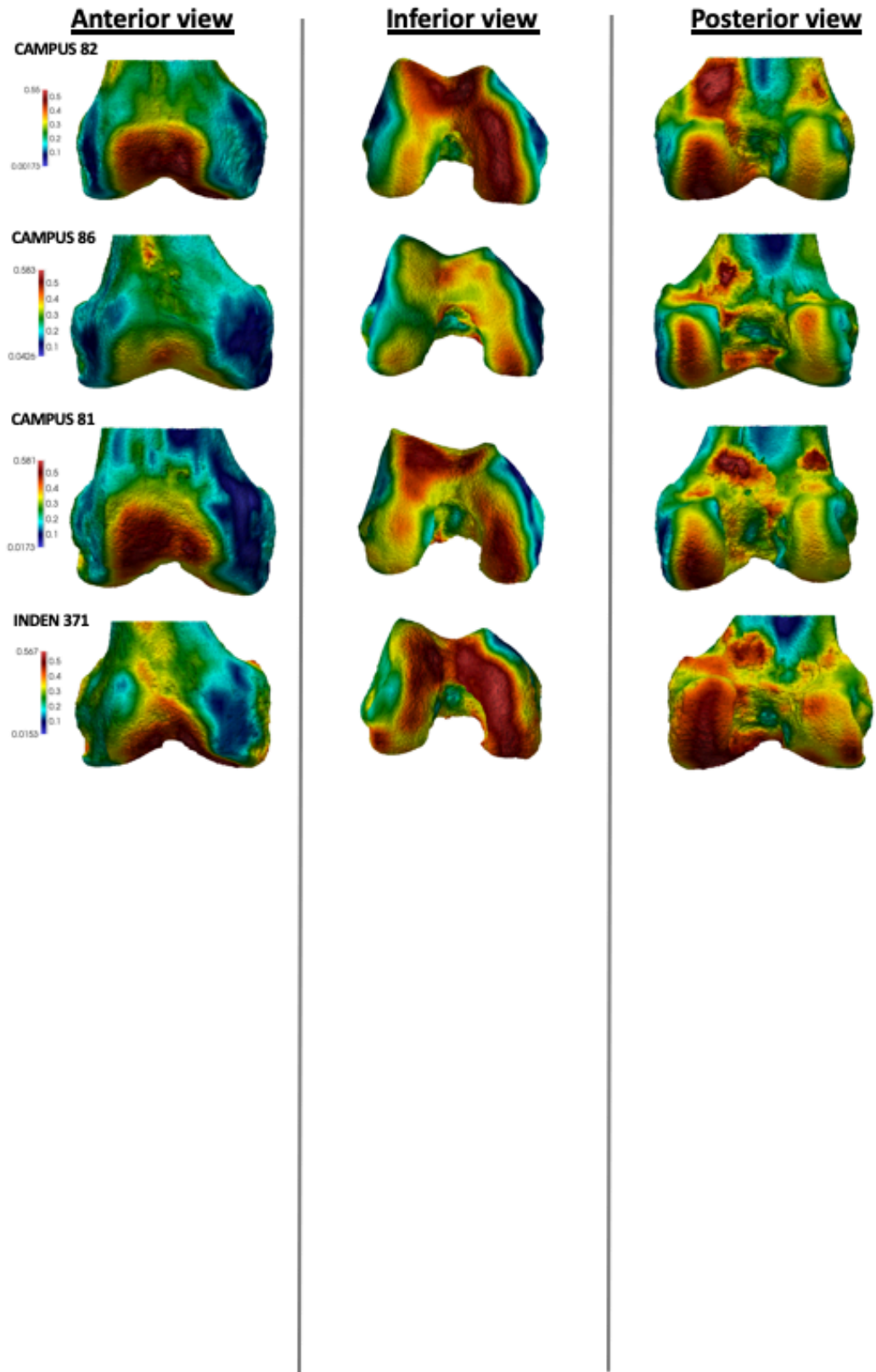
Pongo sp. - Medial condyle



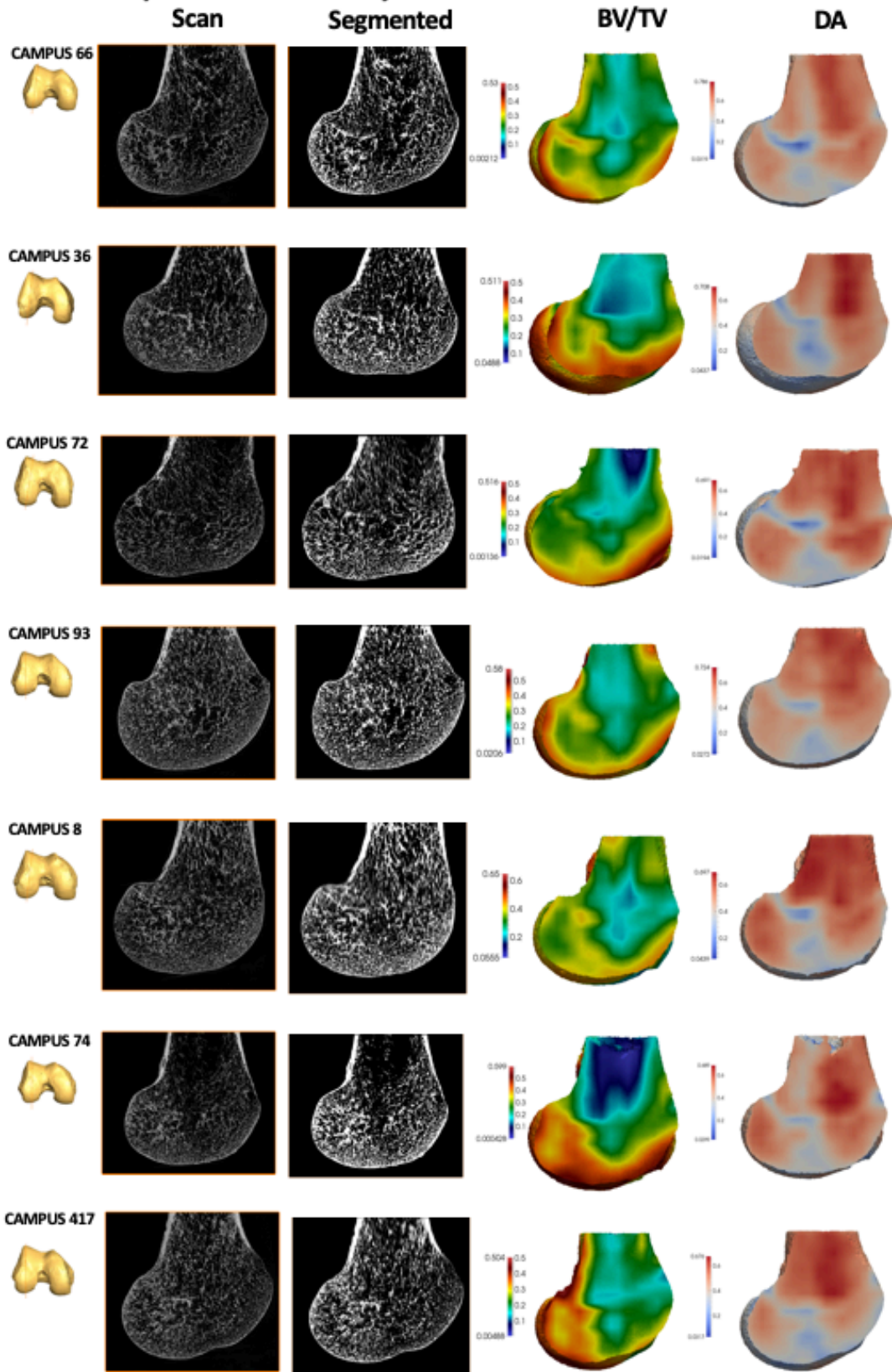
Homo sapiens- BV/TV distribution



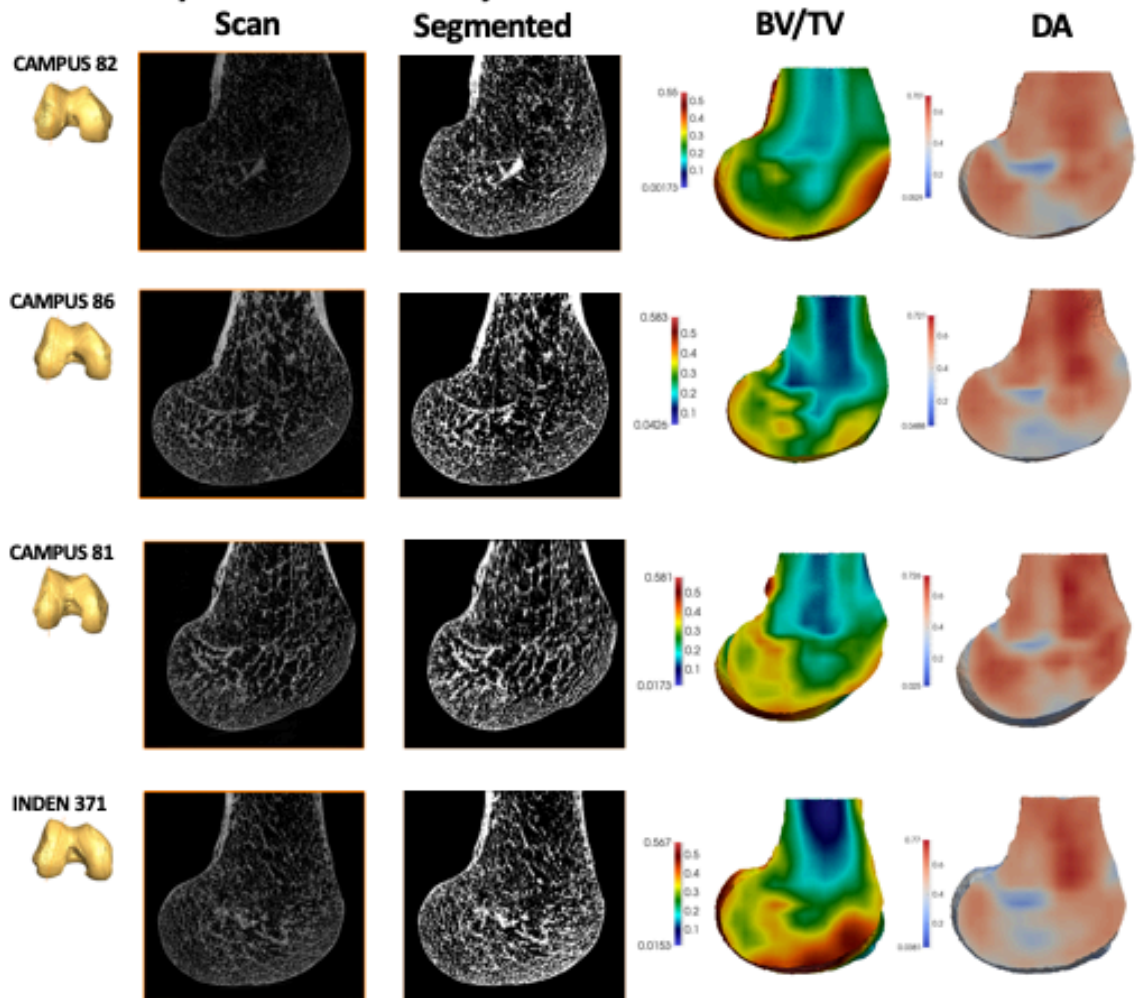
Homo sapiens- BV/TV distribution



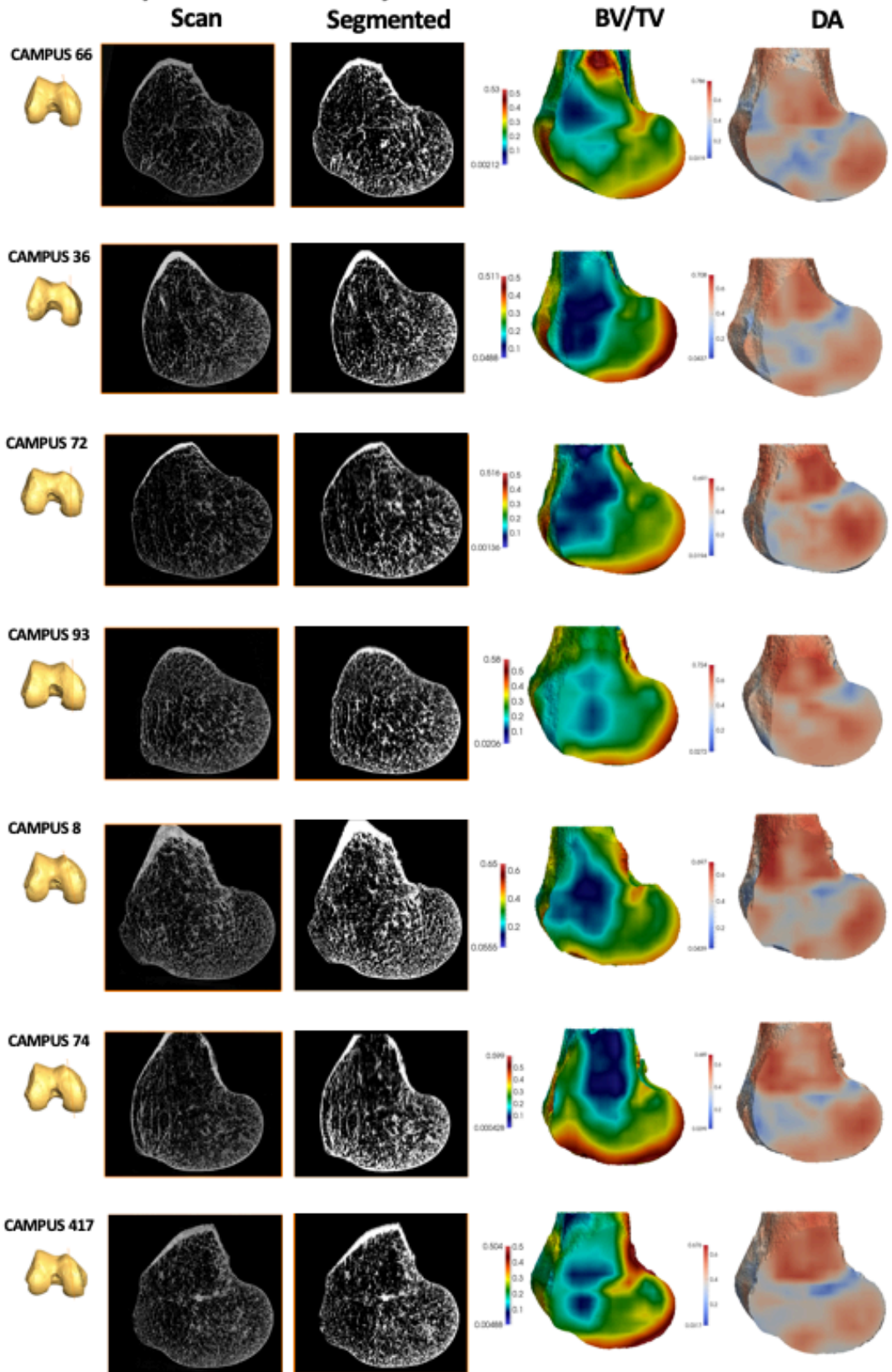
Homo sapiens- Lateral condyle



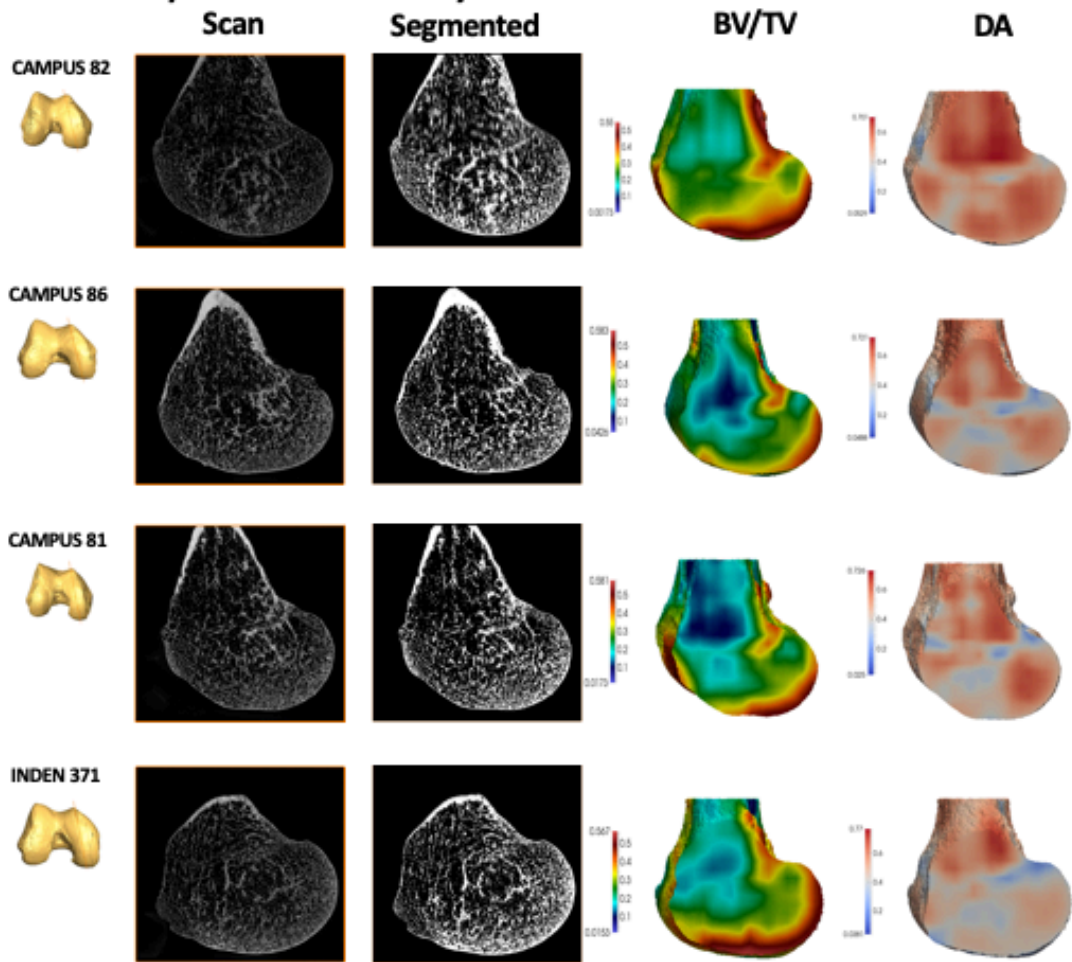
Homo sapiens- Lateral condyle



Homo sapiens- Medial condyle



***Homo sapiens*- Medial condyle**



Supplementary Table 4.1. Results (p-value) for between taxa differences in the examined regions. Captive Pongo are included.

Taxa	Parameter	Lateral distal	Lateral posteroinferior	Lateral posterosuperior	Medial distal	Medial posteroinferior	Medial posterosuperior
<i>Pan-Pongo</i>	BV/TV	N/A	N/A	N/A	N/A	N/A	N/A
	DA	N/A	N/A	N/A	N/A	N/A	N/A
	Tb.N (1/mm)	N/A	N/A	0.02777	N/A	N/A	0.00430
	Tb.Sp (mm)	N/A	N/A	N/A	N/A	N/A	0.01172
<i>Pan-Gorilla</i>	BV/TV	N/A	N/A	0.03118	N/A	N/A	0.00900
	DA	N/A	N/A	N/A	N/A	N/A	N/A
	Tb.N (1/mm)	0.00013	0.00013	0.00013	0.00026	0.00007	0.00007
	Tb.Sp (mm)	0.00007	0.00013	0.00007	0.00026	0.00007	0.00007
<i>Pan-Homo</i>	BV/TV	N/A	N/A	0.00026	N/A	N/A	0.01700
	DA	0.00078	0.00013	0.00013	N/A	N/A	N/A
	Tb.N (1/mm)	0.01254	N/A	0.00078	0.00195	0.09000	0.00007
	Tb.Sp (mm)	N/A	N/A	0.00013	0.00195	N/A	0.00013
<i>Gorilla-Pongo</i>	BV/TV	N/A	N/A	N/A	N/A	N/A	N/A
	DA	N/A	N/A	N/A	N/A	N/A	N/A
	Tb.N (1/mm)	0.00123	0.00432	0.01851	0.00247	0.00120	0.00120
	Tb.Sp (mm)	0.00250	0.00432	0.01851	0.00432	0.00430	0.00432
<i>Gorilla-Homo</i>	BV/TV	N/A	N/A	N/A	N/A	N/A	N/A
	DA	N/A	0.00007	0.00195	N/A	0.01300	N/A
	Tb.N (1/mm)	0.00435	0.00435	N/A	N/A	0.00440	N/A
	Tb.Sp (mm)	0.00290	0.00195	N/A	N/A	0.00630	N/A
<i>Pongo-Homo</i>	BV/TV	N/A	N/A	N/A	N/A	N/A	N/A
	DA	N/A	0.00062	0.00432	N/A	0.02800	N/A
	Tb.N (1/mm)	N/A	N/A	N/A	0.01851	N/A	N/A
	Tb.Sp (mm)	N/A	N/A	N/A	N/A	N/A	N/A
	Tb.Th (mm)	0.04070	N/A	N/A	0.00740	N/A	N/A

Supplementary Table 4.2. Loadings of parameters at each region to PC1 and PC2.

Parameter, region	PC1	PC2
Tb_Sp, lateral distal	16.359	0.877
Tb_Sp, lateral posteroinferior	8.388	1.494
Tb_Sp, lateral posterosuperior	12.032	1.449
Tb_Sp, medial distal	22.391	0.068
Tb_Sp, medial posteroinferior	11.886	1.996
Tb_Sp, medial posterosuperior	20.288	0.028
Tb_Th, lateral distal	1.525	0.236
Tb_Th, lateral posteroinferior	1.380	1.232
Tb_Th, lateral posterosuperior	0.956	0.089
Tb_Th, medial distal	1.022	0.558
Tb_Th, medial posteroinferior	1.018	0.271
Tb_Th, medial posterosuperior	1.421	0.201
DA, lateral distal	0.571	8.930
DA, lateral posteroinferior	0.152	24.728
DA, lateral posterosuperior	0.347	15.028
DA, medial distal	0.071	6.610
DA, medial posteroinferior	0.148	24.134
DA, medial posterosuperior	0.045	12.070

Supplementary table 4.3. Results (p-value) for between taxa differences in the indices.

Taxa	Parameter	Inferior lateral index	Posterior lateral index	Inferior medial index	Posterior medial index
<i>Pan-Pongo</i>	BV/TV	N/A	N/A	N/A	N/A
	DA	N/A	N/A	N/A	N/A
<i>Pan-Gorilla</i>	BV/TV	N/A	N/A	N/A	N/A
	DA	0.00292	N/A	N/A	N/A
<i>Pan-Homo</i>	BV/TV	0.0173	N/A	N/A	0.0173
	DA	N/A	N/A	0.00903	0.01728
<i>Gorilla-Pongo</i>	BV/TV	N/A	N/A	N/A	N/A
	DA	N/A	N/A	N/A	N/A
<i>Gorilla-Homo</i>	BV/TV	0.0063	N/A	N/A	N/A
	DA	0.00045	N/A	0.00078	0.00078
<i>Pongo-Homo</i>	BV/TV	N/A	0.012	N/A	0.0074
	DA	N/A	N/A	N/A	N/A

Chapter 5

Locomotor diversity in South African fossil hominins during the Early Pleistocene

Abstract

Bipedalism is a defining trait of the hominin lineage, associated with a transition from a more arboreal to a more terrestrial environment. While there is debate about when mechanically modern human-like bipedalism first appeared in hominins, all South African hominins show clear morphological adaptations to bipedalism and it is generally accepted that bipedalism was their dominant mode of locomotion. Here I present evidence from the internal bone structure of the femur that two different patterns of locomotion are represented by hominins at Sterkfontein. The internal trabecular structure of a proximal femur (StW 522) confidently attributed to *Australopithecus africanus* exhibits a derived, modern human-like bipedal loading pattern, suggesting bipedalism in this individual was as frequent and biomechanically similar to that of recent humans. In contrast, a geologically younger hominin femoral specimen (StW 311) possibly attributed to early *Homo* or *Paranthropus robustus*, shows a trabecular pattern that is more similar to non-human apes, indicating that both bipedalism and climbing were a dominant component of their locomotor repertoire. My results demonstrate locomotor diversity in South African hominins, suggesting an adaptive shift to climbing in younger hominins, and contribute to additional evidence from southern and eastern Africa of multiple, co-occurring forms of bipedalism among Plio-Pleistocene hominins.

5.1. Introduction

Bipedalism is one of the defining traits of the hominin lineage and skeletal adaptations for bipedal locomotion date back to at least six million years ago (e.g. Senut et al. 2001; Pickford et al. 2002; Crompton et al. 2008; Almecija et al. 2013). These bipedal adaptations are found throughout the skeleton, but those of the hip and knee are particularly important as these joints are central in determining how load is transferred through the lower limb. In modern humans, femoral adaptations for bipedalism include a relatively large femoral head and long neck proximally (McHenry and Corruccini, 1978; Lovejoy et al. 2002; Harmon, 2007), as well as flat, ellipsoid condyles and an elevated patellar lip distally (Heiple and Lovejoy, 1971; Tardieu, 1981). Conversely, in African apes the femoral head is relatively small and the neck short (McHenry and Corruccini, 1978; Harmon, 2007), while the distal condyles are relatively circular (Heiple and Lovejoy, 1971; Tardieu, 1981). Identifying bipedal adaptations in fossils helps place them on the hominin lineage, however these adaptations in the earliest fossil hominins (e.g. *Orrorin*, *Ardipithecus*) are controversial (White et al. 1994; Pickford et al. 2002; Wolpoff et al. 2002; Zollikofer et al. 2005; Crompton et al. 2008; Lovejoy et al. 2009a,b; Ohman et al. 2005; Almecija et al. 2013). More clear evidence for obligate bipedalism is found in later hominins, such as the australopiths (e.g. Ward et al. 1999; Ward et al. 2001; Lovejoy et al. 2002). *Australopithecus afarensis* presents a long femoral neck and human-like femoral muscular organisation in the proximal femur (Lovejoy, 2005a) as well as a raised patellar lip, ellipsoid condyles and a deep patellar groove in the distal femur (Lovejoy and Heiple, 1970; Tardieu, 1981) suggesting that they frequently adopted bipedality. Similar distal femoral traits are found in *Australopithecus africanus*. Furthermore, evidence for committed terrestrial bipedality is found in the foot of *A. afarensis* that suggests the presence of transverse and longitudinal arches similar to modern humans (Ward et al. 2011). Other South African fossils, including *Australopithecus sediba* MH1 and MH2 (Berger et al. 2010; Zipfel et al. 2011; DeSilva et al. 2013) and *Australopithecus* sp. StW 573 (Clarke and Tobias, 1995) further strengthen this notion

that australopiths were habitual bipeds. However, the different mosaics of human- and ape-like external traits in these australopiths has led to debate over the form of bipedalism (e.g. Stern and Susman, 1983; Susman et al. 1984; Berge, 1994; Carey and Crompton, 2005; Lovejoy and McCollum, 2010; Raichlen et al. 2010), as well as the levels of arboreality in these taxa (e.g. Ward, 2002). Although *Homo erectus* and most later *Homo* species are generally recognised as mechanically modern human-like, obligate bipeds (e.g. Day, 1971; Trinkaus, 1983; Aiello and Dean, 2002; Ruff and Walker, 1993; Lorenzo et al. 1999; Ruff, 2008, 2009; Hatala et al. 2016), the timing of the appearance of obligate bipedalism is debated (Susman and Stern, 1982; Berillon, 1999; Wood and Collard, 1999; Bramble and Lieberman, 2004; Harcourt-Smith and Aiello, 2004).

Most studies of fossil hominin bipedalism have focused on external morphological traits (e.g. Stern and Susman, 1983; Lovejoy and Heiple, 1970; Tardieu, 1981; Senut et al. 2001; Lovejoy, 2005a,b,2007; Harmon, 2009a; Lovejoy et al. 2009a,b). However, external morphology can be subject to evolutionary stasis in which features that are not functionally useful are retained, obscuring behavioural signals (Ward, 2002). Functional divergence of the upper and lower limbs may promote increased mobility in the upper limbs for climbing in contrast to increased stability in lower limb for terrestrial bipedalism (Sylvester, 2006), further complicating behaviour reconstructions based on isolated skeletal elements. Furthermore, the discovery of *A. sediba* (Berger et al. 2010), *Homo floresiensis* (Brown et al. 2004) and *Homo naledi* (Berger et al. 2015), reveal unexpected combinations of ape-like and human-like morphologies in the hominin fossil record. To better understand actual, rather than potential, behaviour in the past, morphological analyses should focus on traits that are influenced by function during development. Trabecular architecture has proven integral in reconstructing past behaviours (Macchiarelli et al. 1999; DeSilva and Devlin, 2012; Barak et al. 2013a; Tsegai et al. 2013; Skinner et al. 2015; Stephens et al. 2016; Ryan et al. 2018), as it informs about habitually acquired postures throughout the life of an individual. Trabecular bone responds to load via modelling and remodelling, mainly altering the orientation of its struts and the distribution and volume of bone across epiphyses

(e.g. Pontzer et al. 2006; Barak et al. 2011). Analysis of trabecular architecture has revealed behavioural signals in the femoral head (e.g. Ryan and Ketcham, 2002; Ryan and Shaw, 2012; Ryan et al. 2018; Georgiou et al. 2019) and less so in the distal femur (Georgiou et al. 2018) of primates. My previous work has shown that within the femoral head, trabecular bone distribution differs between humans, African apes and orangutans (Georgiou et al. 2019) and correlates with predicted loading from habitual postures. Furthermore, within the femoral head, modern humans have low bone volume (expressed as low bone volume fraction, or BV/TV), highly aligned struts (expressed as high degree of anisotropy, or DA) and distinct strut orientation compared to other apes (Ryan et al. 2018); all traits that are consistent with obligate bipedalism. Trabecular studies in the femoral head (Ryan et al. 2018) and distal tibia (Barak et al. 2013a) of *A. africanus* have shown that the trabeculae are highly aligned and oriented in a similar manner to humans and distinct from chimpanzees. However, these studies focused on sub-volumes of trabeculae and since trabecular structure is not homogeneously distributed across epiphyses (Sylvester and Terhune, 2017), analysing isolated volumes may obscure or limit our functional interpretations.

Here I conduct a comparative analysis of the 3D trabecular bone distribution beneath the subchondral layer of the proximal femoral head and distal femoral condyles, where trabecular bone strength is generally found to be highest (Harada et al. 1988), in humans, other great apes and three fossil hominin specimens from Sterkfontein, South Africa (proximal femora StW 311, StW 522 and distal femur TM 1513) using a novel, geometric morphometric, whole-epiphysis approach. The site of Sterkfontein is located in the Cradle of Humankind, alongside other hominin fossil sites, including Swartkrans, Malapa and Rising Star (e.g. Brain and Sillent, 1988; Berger et al. 2010; Berger et al. 2015). The complex stratigraphy of Sterkfontein has been divided into six different Members (Kuman and Clarke, 2000) and I analysed specimens from two of these: Members 4 and 5. Within Member 4, a large sample of craniodental and postcranial fossils attributed to *A. africanus* and a proposed second *Australopithecus* species (e.g. Clarke, 1988; Clarke, 2013) have been found, however no associated artefacts were recovered. The hominin remains include the

proximal femur StW 522 and distal femur TM 1513 analysed here, both of which have been attributed to *A. africanus* (Reed et al. 2013) based on the stratigraphic layer they were found in and associated remains. Furthermore, the body mass of StW 522 was estimated at 29.5 kg (Ruff, 2010). Dating of Member 4 has yielded various dates (Vrba, 1980; Delson, 1988; McKee, 1993; Schwarcz et al. 1994; Partridge, 2005; Pickering and Kramers, 2010), with the most recent analysis suggesting that the stratigraphic layers of this member range from 2.8 to 2.0 Ma (Herries and Shaw, 2011). Paleoenvironmental reconstructions suggest that over the time of formation of Member 4, habitats included closed forest and more open grassland in proximity (Vrba, 1974, 1975, 1980; Bamford, 1999; Avery, 2001; Sponheimer et al. 2005a,b).

Member 5 is more complex, comprising three infills that all bear hominin remains: The Member 5 StW 53 infill dated to 1.8-1.5 Ma (Herries and Shaw, 2011) includes a hominin cranium (StW 53) and juvenile maxilla (StW 75), as well as a potentially hominin ulna (StW 571) (Reynolds and Kibii, 2011). The taxonomic affinity of the cranium has been debated, with some suggesting it is *Homo habilis* (Hughes and Tobias, 1977; Prat, 2005; Curnoe and Tobias, 2006) while others consider it to be *Australopithecus* (Clarke 1985, 1998, 2008; Braga, 1998; Thackeray et al. 2000; Kuman and Clarke 2000). The Member 5 East infill, dated to 1.4-1.2 Ma (Herries and Shaw, 2011), includes *Paranthropus* dental remains as well as Oldowan and Early Acheulean tools (Kuman, 1994a,b; Kuman and Clarke, 2000). The Oldowan breccia is located in the deeper layers of Member 5 East where the *Paranthropus robustus* specimens are found, while the Early Acheulean tools appear in subsequent layers (Kuman and Clarke, 2000). The Member 5 West infill, dated to 1.3-1.1 Ma (Herries and Shaw, 2011), includes *H. erectus* craniodental remains and Early Acheulean tools (Reynolds and Kibii, 2011) consistent with being the youngest of the three infills. The StW 311 proximal femur specimen analysed has been attributed to *A. africanus* in several studies (e.g. Green et al. 2007; Harmon, 2009a). However, based on Kuman and Clarke's (2000) revision of Sterkfontein's stratigraphy, StW 311 derives from the younger Member 5 East infill and thus could be attributed to *P. robustus* or early *Homo*. The body mass of this specimen was estimated at 41.6 kg (Ruff, 2010). Unfortunately, this specimen does not preserve enough of the proximal epiphysis to

be taxonomically diagnostic and thus is attribution depends on the dating of Member 5 East and the other finds within this stratigraphic layer. All three Member 5 infills were comprised of largely open environments and differed to each other. Specifically, the StW 53 infill had dry, grassland conditions (Kuman and Clarke, 2000), the Member 5 East infill had dry, open environments but with significant tree coverage (Bishop et al. 1999; Pickering, 1999), and the Member 5 West infill had open, and/or wooded grassland (Vrba, 1975; McKee, 1991; Reed, 1997; Kuman and Clarke, 2000; Luyt and Lee-Thorp, 2003).

To investigate the potential locomotor signals within the trabecular structure of the Sterkfontein hominin femoral specimens, I combine geometric morphometrics with trabecular analysis of the whole epiphysis to quantify and compare BV/TV values at homologous locations between extant and fossil taxa (Supplementary Figure 5.1A). First, I investigate behavioural signals in the femoral head of extant non-human apes based on hindlimb postures and peak loading predictions during habitual locomotor behaviours, including terrestrial knuckle-walking and arboreal climbing in African apes (*Pan troglodytes verus* n=11, *Pan troglodytes troglodytes* n=5, *Gorilla gorilla gorilla* n=11) (Isler, 2005; Finestone et al. 2018) and diverse orthograde arboreal behaviours in orangutans (*Pongo* sp. n=5) (Isler, 2005; Thorpe and Crompton, 2006; Thorpe et al. 2009; Finestone, 2018). Second, I investigate the trabecular pattern in recent *Homo sapiens* (n=11) based on the extended hip and knee postures and peak loading predictions during bipedalism (Paul, 1976; English and Kilvington, 1979; Alexander, 1994; Yoshida et al. 2006; Abbass and Abdulrahman, 2014). I also examine the trabecular distribution in the femoral head of a fossil *H. sapiens* (Ohalo II H2) and two Neanderthals (*Homo neanderthalensis*) (Krapina 213 and Krapina 214) as obligate bipedal hominins with similar locomotion to that of modern humans. Third, I assess the trabecular bone distribution in the femoral heads of two fossil hominin specimens (StW 311, StW 522) from Sterkfontein, South Africa, to determine whether they show functional signals in the femur for ape-like, human-like or unique modes of locomotion, which external traits have failed to reconcile (See Supplementary Figure 5.2A for comparative femoral measurements). The external morphology and preserved trabecular structure of these fossils can be seen

in Supplementary Figure 5.3. Several fossil specimens were excluded from my analysis because of difficulties in obtaining an accurate representation of the trabecular structure or limited preservation that excluded homologous landmarking (Supplementary Figure 5.4). D322 15, D322 16, SK 82 and SK 97 did not preserve enough of the trabecular structure for meaningful comparisons with the extant sample, while SK 3121 and SKW 19 (when segmented) showed preferential thickening of the trabeculae toward the centre of the femoral head which obscured the patterns. Finally, I applied the same methodology to investigate trabecular distribution patterns beneath the articular surface of the distal femur in the same sample of extant apes and humans, and a distal hominin femur from Sterkfontein (TM 1513) (Supplementary Figure 5.5 for method (A) and results (B-C)). However, TM 1513 is missing part of the lateral portion of the patellar articulation, which confounds the selection of homologous landmarks between this fossil and the extant sample. Thus, these results are not discussed in detail and functional interpretations are approached with caution.

5.2. Materials and Methods

5.2.1. Sample, segmentation and trabecular architecture analysis

In this study I used micro-computed tomographic scans to analyse trabecular architecture in the femoral head and distal femur of five extant ape taxa (*Pan troglodytes verus* n=11, *Pan troglodytes troglodytes* n=5, *Pongo* sp. n=5, *Gorilla gorilla* n=11 and *H. sapiens* n=11) and six fossil specimens (StW 311, StW 522, Ohalo II H2, Krapina 213, Krapina 214 and TM 1513), detailed in Supplementary Table 5.1. Proximal and distal epiphyses for each individual of the extant sample were from the same femur, all were adult and showed no signs of pathologies. Prior to analysis, all specimens were re-oriented to approximate anatomical positions, as well as cropped and re-sampled when necessary using AVIZO 6.3[®] (Visualization Sciences Group, SAS).

Segmentation of bone from air was performed using the Ray Casting Algorithm (Scherf and Tilgner, 2009) for the extant sample and Neanderthals and the MIA-clustering algorithm (Dunmore et al. 2018) for the rest of the fossil sample. The latter was used for fossils as it allows more accurate separation of trabecular bone from surrounding inclusions. Trabecular architecture was analysed in medtool 4.1 (www.dr-pahr.at), following previously described protocol (Gross et al. 2014). Three-dimensional tetrahedral meshes with a 1mm mesh size were created using CGAL 4.4 (CGAL, Computational Geometry, <http://www.cgal.org>) and BV/TV values, which were obtained using a 7.5mm sampling sphere on a 3.5mm background grid, were interpolated onto the elements creating BV/TV distribution maps. Internal BV/TV distribution was visualised in Paraview above selected percentiles which were calculated for each femoral head using the quantile function in R v3.4.1 (R Core Team, 2017). The visualisation shows where the 15%-25% highest BV/TV values lie within the head (Supplementary Figures 5.6-5.7). This method was chosen to ensure that the selected thresholds were not affected by outliers and that isolated patterns were comparable between specimens.

The surface of the resulting 3D models was extracted and smoothed using Screened Poisson surface reconstruction in MeshLab (Cignoni et al. 2008) in preparation for landmarking.

5.2.2. Landmarking and BV/TV values extraction

Initially, fixed landmarks were selected for the proximal and distal femur. Intra-observer error for the fixed landmarks was tested by placing the landmarks on 3 specimens of the same taxon at 10 different occasions. Five fixed landmarks were identified on the femoral head; one on each direction at the head-neck border and one on the surface of the femoral head, at the midpoint of the four corner landmarks (Supplementary Figure 5.1A). Four curves were defined between the fixed landmarks, along the femoral head-neck boundary. Description of the landmarks is given in Supplementary Table 5.2. Subsequently, two hundred and eight

semilandmarks were defined on the surface of the femoral head. These were evenly spaced landmarks extending across the whole femoral articular surface. Fossil specimens, specifically Neanderthals (Krapina 213 and Krapina 214), that were broken were not landmarked, to avoid sampling non-homologous regions between taxa.

In the distal femur, nine fixed landmarks were defined around the articular surface of the distal epiphysis, following Gould (2014) and described in Supplementary Table 5.2 (Supplementary Figure 5.5A). Eight curves were then defined between the fixed landmarks, at the articular surface boundary. Since TM1513 lacks the lateral border of the patellofemoral surface, the curve extending across that lateral border was not landmarked. Two hundred and one surface semilandmarks were then defined across the articular surface of the distal femur, extending over the articulation for the patella, as well as the surface of the lateral and medial condyles.

In both epiphyses, the fixed and curve landmarks were manually defined on all specimens, while the surface semilandmarks were defined on one specimen and then projected on all other specimens using the Morpho package (Schlager, 2017) in R v3.4.1 (R Core Team, 2017). After manual inspection of the projected landmarks on each specimen the landmarks were relaxed on the surface reducing bending energy. Subsequently, the Morpho package was used to slide the surface and curve landmarks reducing Procrustes distance. A medtool 4.1 custom script was used to match the landmark coordinates to the closest neighbouring tetrahedron in the BV/TV distribution maps of each specimen and obtain the BV/TV values for each landmark. Relative BV/TV (RBV/TV) values were calculated for each landmark by dividing landmark BV/TV values by the average BV/TV of each individual. Relative values were used for the statistical analysis to ensure interspecific comparisons focused on differences in the distribution rather than systemic species differences.

5.2.3. Statistical analysis

Statistical analysis was performed in R v3.4.1 (R Core Team, 2017). A principal components (PC) analysis was used to visualise interspecific differences in RBV/TV distributions. Bonferroni-corrected pairwise permutational MANOVA tests of the first three principal components were used to test whether observed differences between the taxa in the PCA are significant. The three first components were chosen as they explained high percentages of the variation and together amounted to more than ~50%. Additionally, permutational Hotelling's T^2 tests with Bonferroni corrections were performed to evaluate differences between the distributions of each fossil specimen to the distributions of the extant taxa. The tests couldn't be performed for *Pan troglodytes troglodytes* and *Pongo* sp. due to their small sample sizes.

5.3. Results

5.3.1. Behavioural signals in the femur of non-human apes

Variation in the distribution of BV/TV within the subchondral trabecular bone of the femoral head in non-human great apes (Figure 5.1; Table 5.1; for average distribution maps for each taxon, see Supplementary Figure 5.1B) was consistent with my predictions.

Table 5.1. Intertaxon pairwise permutational MANOVA tests of the first three principal components. Bonferroni corrected p-values are given for each comparison in the femoral head and the distal femur.

Element	Taxon	<i>P.t. verus</i>	<i>P.t. troglodytes</i>	<i>G. gorilla</i>	<i>Pongo sp.</i>
Proximal	<i>P.t. verus</i>	-	-	0.001	-
	<i>P.t. troglodytes</i>	0.253	-	0.997	-
	<i>Pongo sp.</i>	0.034	1	0.012	-
	<i>H. sapiens</i>	0.001	0.002	0.001	0.01
Distal	<i>P.t. verus</i>	-	-	0.001	-
	<i>P.t. troglodytes</i>	0.464	-	0.038	-
	<i>Pongo sp.</i>	0.029	0.78	0.002	-
	<i>H. sapiens</i>	0.001	0.004	0.002	0.001

Extant non-human apes show two concentrations of high BV/TV across the femoral head (Figure 5.1B; Georgiou et al. 2019 see Figure 5.2 for contrast with *Homo*) that extend internally as two “pillars” or inverted cones (Supplementary Figure 5.6). Average BV/TV distributions in the subchondral BV/TV reveal significant variation between taxa (Supplementary Figure 5.1B). *Gorilla* has the most well-separated regions of high BV/TV, followed by the *Pan* subspecies which only differ slightly, while *Pongo* has the least separated concentrations. *Gorilla* is clearly separated from the other apes in the PCA (Figure 5.3). The presence of the anterior concentration in all non-human apes is consistent with loading during vertical climbing when hips are highly flexed (Isler, 2005; Nakano et al. 2006), while the posterior concentration is consistent with the more extended hip posture used during terrestrial locomotion (Figure 5.1A). *Pan* and *Pongo* have a more extensive concentration of high BV/TV along the superior aspect of the head indicating more frequent and/or higher magnitude loading of this region than in *Gorilla*, which is consistent with their more frequent arboreality and the need to navigate complex forest canopies using a variety of locomotor behaviours (Hunt, 1991a,b; Doran, 1993b; Thorpe and Crompton, 2006; Thorpe et al. 2009). The distinct high BV/TV concentrations in *Gorilla*, suggests a more dichotomous loading pattern from less variable hip postures, perhaps associated with reduced arboreality and/or larger body size (Remis, 1995, 1999; Doran, 1997; Isler, 2005).

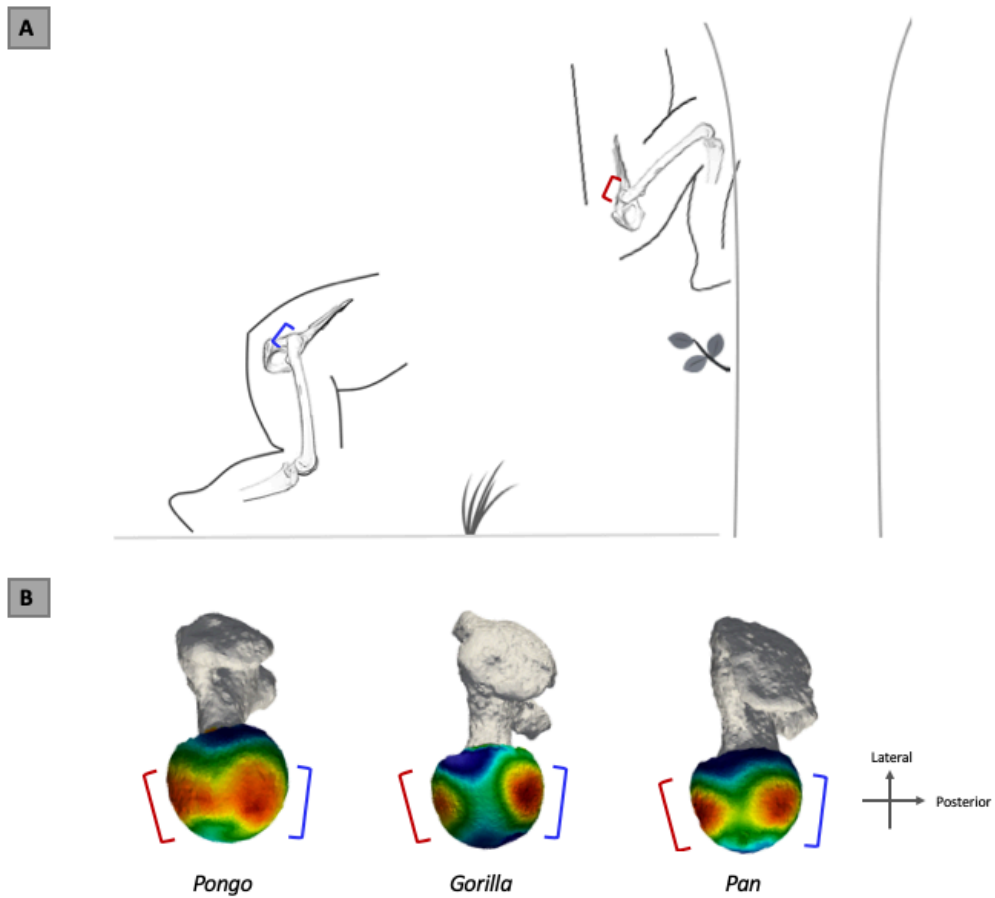


Figure 5.1. Non-human great ape hip flexion angles during terrestrial quadrupedalism and vertical climbing, and BV/TV distribution in the femoral head. (A) Great ape hip posture at toe-off ($\sim 110^\circ$) during terrestrial knuckle-walking (Finestone et al. 2018), as well as joint posture in maximum flexion ($\sim 55^\circ$ - 60°) during climbing (Isler, 2005). (B) BV/TV distribution in the femoral head of *Pongo*, *Gorilla* and *Pan*. Brackets indicate regions of predicted peak pressure during vertical climbing (red) and terrestrial locomotion (blue).

The use of vertical climbing is also reflected in the trabecular patterns of the distal femur of *Pan* and *Pongo* (Supplementary Figure 5.5B). These taxa are characterised by high BV/TV in the posterosuperior region of the lateral condyle and the inferior region of the articulation for the patella, both of which are consistent with loading during flexed knee postures (Hefzy et al. 1991; Isler, 2005). In the PCA plot they cluster together and are clearly separated from the other apes (Figure 5.4). In contrast, *Gorilla* shows high BV/TV across the entire articulation for the patella and has low BV/TV in the posterosuperior region of the lateral condyle. These traits

reflect both the use of a more extended knee during locomotion (Isler, 2005; Crompton et al. 2008; but see Finestone et al. 2018), where the patella is pushed against the articulation, while the posterosuperior region of the lateral condyle is not highly loaded (von Eisenhart-Rothe et al. 2004; Lovejoy, 2007) and separate *Gorilla* in the PCA plot (Figure 5.4). None of the apes show high BV/TV values in the posterosuperior region of the medial condyle, perhaps due to its greater surface area allowing wider load distribution.

5.3.2. Behavioural signals in obligate bipedal taxa

The pattern found in the femoral head of recent and fossil *H. sapiens* is distinct from that of other great apes and consistent with previous studies (Lubovsky et al. 2011; Wright et al. 2011; Treece and Gee, 2014; Georgiou et al. 2019), showing one superior region of high BV/TV, located posteriorly and medially on the femoral head (Figure 5.2; Supplementary Figure 5.1B). Recent *H. sapiens* and Ohalo II H2, cluster together and away from non-human apes in the PCA (Figure 5.3). The region of high BV/TV corresponds to the region of highest pressure during a bipedal gait (Paul, 1976; English and Kilvington, 1979; Yoshida et al. 2006). In the average distribution (Supplementary Figure 5.1B), intermediate BV/TV values continue along the inferior aspect of the femoral head, reflecting contact between this region and the acetabulum while the femur is at a valgus angle. Furthermore, the extended range of intermediate values across the head is also consistent with hip loading from positions of moderate flexion towards moderate extension (van den Bogert et al. 1999; Giarmatzis et al. 2015). *H. sapiens* shows the distinct feature of a single pillar of high BV/TV extending beneath the posterior-superior concentration towards the femoral neck (Supplementary Figure 5.6). In the distal femur (Supplementary Figure 5.5B-C) *H. sapiens* has lower BV/TV in the posterosuperior region of the lateral condyle than *Pan* and *Pongo*, reflecting the less frequent use of highly flexed knee postures. Furthermore, *H. sapiens* is differentiated from other apes by an extended area of high BV/TV across the medial condyle and a lack of high BV/TV in the distal region of the lateral condyle (Figure 5.4). This reflects differences in relative condyle

size across apes, in which *H. sapiens* have similarly-sized condyles with reduced medial and enlarged lateral condyles relative to other apes (Tardieu, 1981).

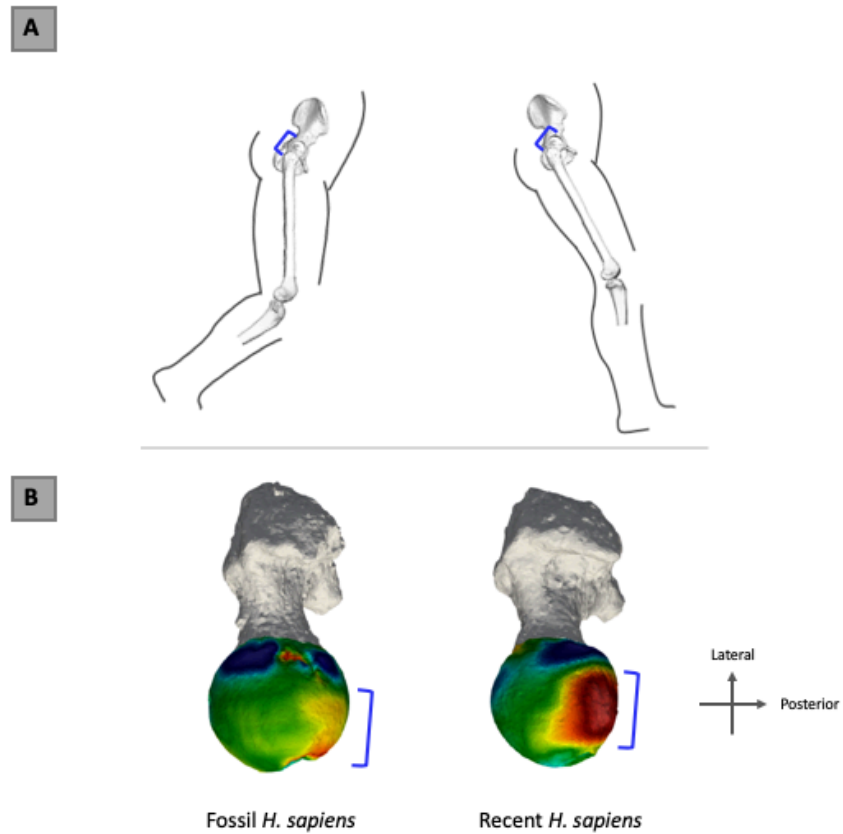


Figure 5.2. Human hip flexion angles during bipedal locomotion and BV/TV distribution in the femoral head of *Homo*. (A) Modern human hip posture during bipedal walking at toe-off ($\sim 175^\circ$) and heel-strike ($\sim 160^\circ$), when ground reaction force is highest (Lafortune et al. 1992). (B) BV/TV distribution in the femoral head of *H. neanderthalensis*, fossil *H. sapiens* and a representative extant *H. sapiens* specimen. Blue brackets indicate regions of peak pressure during bipedal walking.

The single BV/TV concentration, extending through the femoral head, is also present in the Neanderthal individuals (Krapina 213 and 214) (Figure 5.5; Supplementary Figure 5.7). In Neanderthals (and less so in Ohalo II H2) this BV/TV concentration is anteroposteriorly broader, perhaps suggesting higher, more variable loading of the hip joint than in recent humans, which is not unexpected for hunter-gatherers. Nonetheless, both trabecular structure and external femoral morphology of Neanderthals, which is generally similar to modern *H. sapiens*

(Trinkaus, 1976; Hershkovitz et al. 1995; Trinkaus and Jelínek, 1997; De Groote, 2011), suggest that they used a modern human-like bipedal gait.

Table 5.2. Permutational Hotelling's T² results. Bonferroni corrected p-values are given for each comparison of the fossils and the extant taxa.

Fossil	<i>P.t. verus</i>	<i>G. gorilla</i>	<i>H. sapiens</i>
Ohalo II H2	0.01	0.0155	0.871
StW 311	0.013	0.022	0.3945
StW 522	0.013	0.033	0.502
TM 1513	0.028	0.033	0.094

5.3.3. Trabecular distribution patterns and locomotion of hominins at Sterkfontein

The femoral head of StW 522 attributed to *A. africanus* presents a similar trabecular distribution pattern to that of *H. sapiens* (Figure 5.3; Table 5.2; Supplementary Figure 5.1C). StW 522 shows one high BV/TV concentration along the superior aspect of the femoral head that extends internally as a single pillar, as well as intermediate values which continue inferiorly (Figure 5.5). The high superior values are located medially, close to the fovea capitis, resembling *H. sapiens*, but are slightly more anterior. Although in the PCA analysis StW 522 falls just outside the range of variation in modern humans and mean femoral head trabecular parameters (e.g., DA, trabecular number and thickness) are within the extant ape range (Supplementary Figure 5.2B), the trabecular distribution of StW 522 is distinctly human-like and lacks the anterior concentration found in other apes. Therefore, I suggest that *A. africanus* used a more extended hip joint posture during bipedalism similar to that of humans.

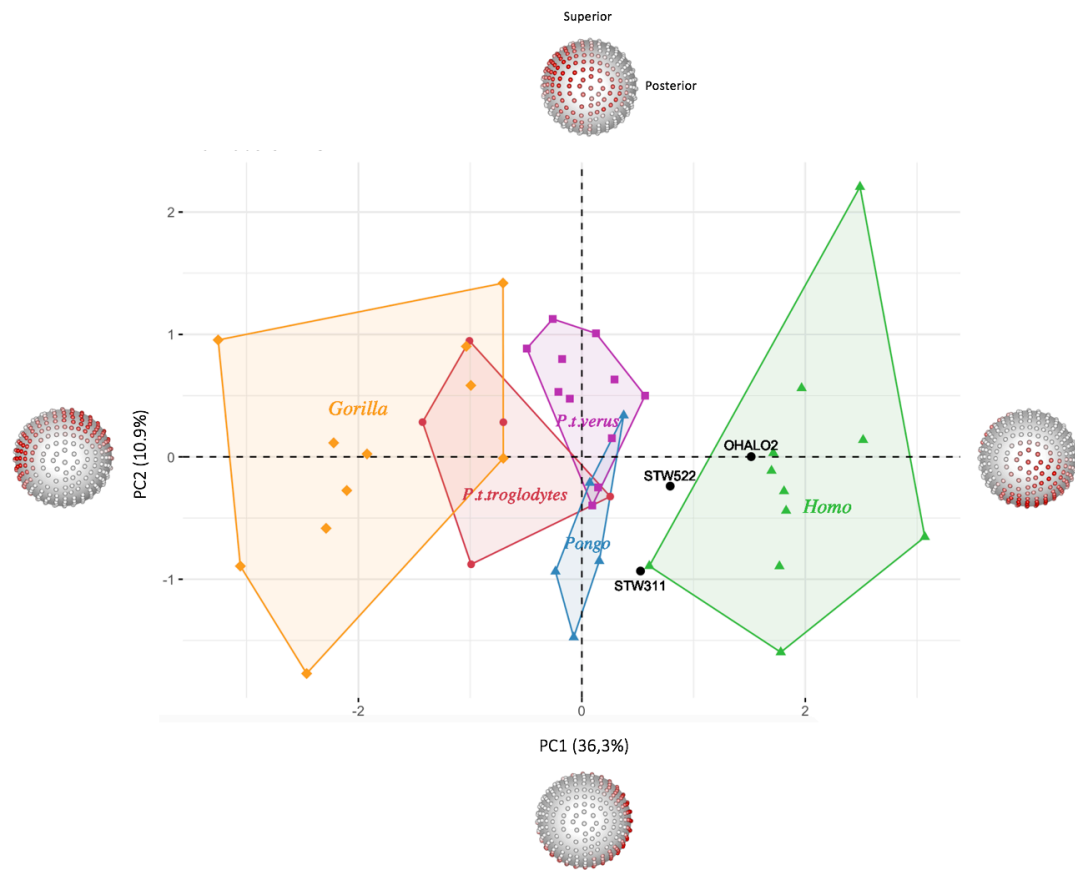


Figure 5.3. PCA of the relative BV/TV distribution in the femoral head. 2D

stereoplots show in red the landmarks that have the highest loading on each axis. BV/TV values in landmarks on the inferior aspect of the head have the highest positive loading on PC1, (separating *Homo* from the non-human apes through its high BV/TV in this region) and BV/TV values in landmarks on two regions across the superior aspect of the head have the highest negative loading (separating *Gorilla* from the other apes through its two distinct high BV/TV concentrations). Furthermore, BV/TV values in landmarks along the anterior aspect of the head have the highest positive loading on PC2, while BV/TV values in landmarks along the posterior aspect of the head have the highest negative loading. The *H. neanderthalensis* specimens (Krapina 213 and Krapina 214) were not included in the PC analysis as gaps in their subchondral trabecular structure prohibited the selection of homologous landmarks for interspecies comparisons.

This functional interpretation is further supported by the BV/TV distribution pattern in the TM 1513 distal femur. This specimen lacks the high BV/TV in the posterosuperior border of the lateral condyle found in *Pan* and *Pongo* (Supplementary Figure 5.5C), suggesting use of highly flexed knee postures that are

required during climbing were infrequent in this individual. Furthermore, TM 1513 shows high BV/TV in the lateral aspect of the patellofemoral articulation, similar to humans. Combined with preserved external morphology of this specimen indicating a high bicondylar angle and elevated patellar lip, both of which are associated with modern human extended-knee bipedalism (Heiple and Lovejoy, 1971; Tardieu, 1981), this concentration reveals frequent loading from the patella during extended knee postures. Although in the PCA this specimen falls out as intermediate between *Pan* and *H. sapiens* (Figure 5.4), its BV/TV distribution pattern does not significantly differ to *H. sapiens* (Table 5.2). Nonetheless, although preservation of TM 1513 prevents a confident assessment of its complete trabecular structure, the morphology that is well-preserved in combination with the distinctly human-like trabecular pattern of StW 522, suggests that *A. africanus* was a habitual biped whose locomotion did not include habitual climbing.

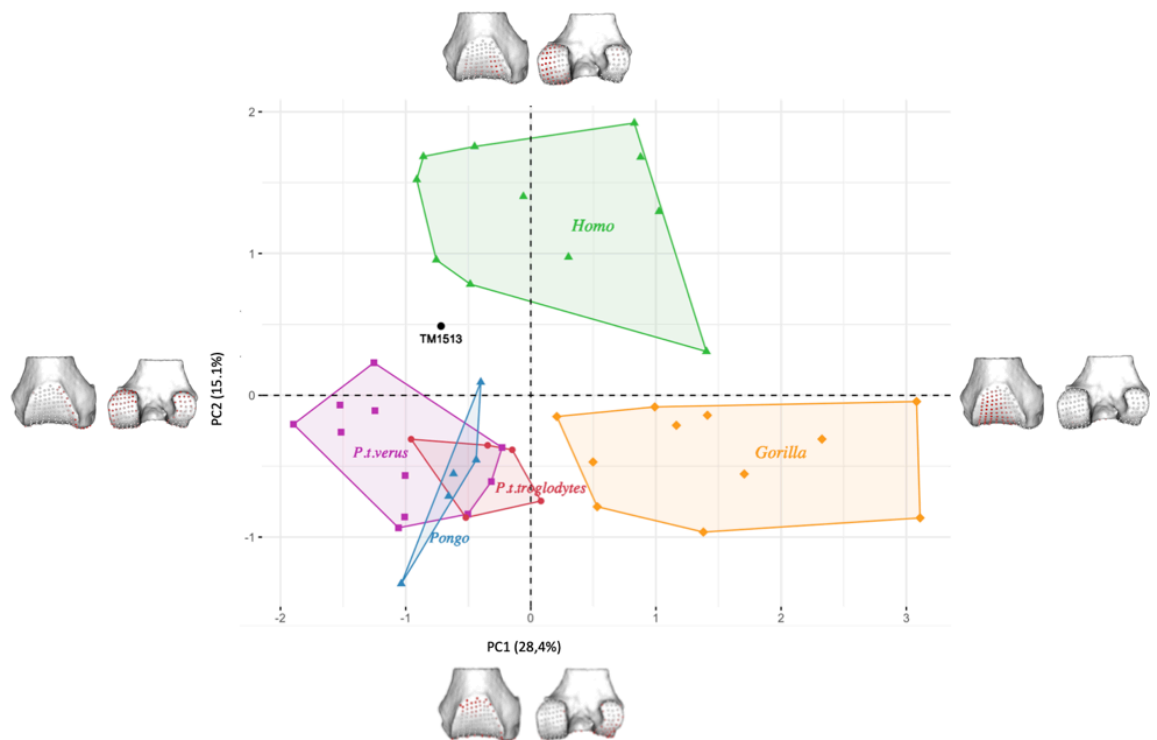


Figure 5.4. PCA of the relative BV/TV distribution in the distal femur. Femoral models show in red the landmarks that have the highest loading on each axis. BV/TV values in landmarks on the articulation for the patella have the highest positive loading on PC1 (separating *Gorilla* from the other non-human apes through its high BV/TV in this region)

and BV/TV values in landmarks on the posterosuperior regions of both condyles have the highest negative loading (separating *Pan* and *Pongo*). *Homo* overlaps with both *Gorilla* and *Pan/Pongo* along PC1. Furthermore, BV/TV values in landmarks along the posterior aspect of medial condyle have the highest positive loading (separating *Homo* from the non-human apes), while BV/TV values in landmarks in the distal region of the lateral condyle have the highest negative loading on PC2.

In contrast to StW 522 and TM 1513, the geologically younger proximal femur StW 311 shows a more ape-like trabecular pattern. This individual has two high BV/TV concentrations along the superior aspect of the femoral head that extend internally towards the neck, a trait distinct to non-human apes (Figure 5.5). The ape-like anterior concentration suggests that, in addition to bipedalism, there was high loading during frequent, marked flexion of the hip, such that which occurs during climbing. Furthermore, in contrast to previous finds (Ryan et al. 2018), mean femoral head trabecular parameters fall consistently within the *Pan* range (Supplementary Figure 5.2B). For example, there is low anisotropy and high bone volume, compared to the typical pattern in *H. sapiens* (Chirchir et al. 2017; Ryan et al. 2018). Furthermore, StW 311 perhaps had distinct hip kinematics during climbing, as it does not fall within the distribution of any of the non-human apes but is between apes and *H. sapiens* (Figure 5.3). It appears closer to *H. sapiens* as a result of its similarity to one particular human specimen with an extended range of high BV/TV along the anterior aspect of the head and its distribution does not differ significantly to *H. sapiens* (Table 5.2).

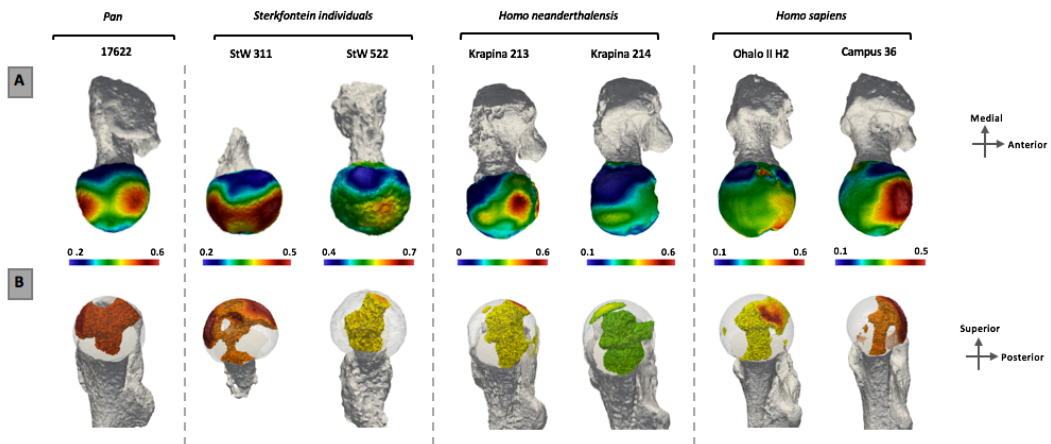


Figure 5.5. BV/TV distribution in the subchondral layer of the femoral head (A) and within the femoral head (B) in the fossil taxa. Internal concentrations are visualised for BV/TV above the 80th percentile. This threshold was chosen to visualise the regions where the highest BV/TV is found within each specimen. Specimens are scaled to their own data range.

5.4. Discussion

In this study, I demonstrate distinct patterns within the trabecular bone distribution of the femoral head that clearly distinguish extended-hip bipedal humans from more flexed-hip quadrupedal climbing great apes. In non-human great apes, body size influences the frequency of behaviours (e.g. larger individuals climb less frequently), as well as joint kinematics (e.g. larger individuals climb more cautiously) (Doran, 1993b; Isler, 2005), but apes primarily load their hindlimbs during terrestrial locomotion and vertical climbing, their most frequent activities (Doran, 1993a,b; Thorpe and Crompton, 2006). This is demonstrated very clearly in the trabecular bone distribution of their femoral head in the two distinct regions of high BV/TV. Modern humans on the other hand are different and display a single region of high BV/TV on the femoral head which corresponds to the region most loaded during bipedal locomotion (Paul, 1976; English and Kilvington, 1979; Yoshida et al. 2006). These behavioural signals are less clear in the distal femur, however there is evidence for the use of a more flexed knee in the extant apes. *Pan* and *Pongo* show high BV/TV

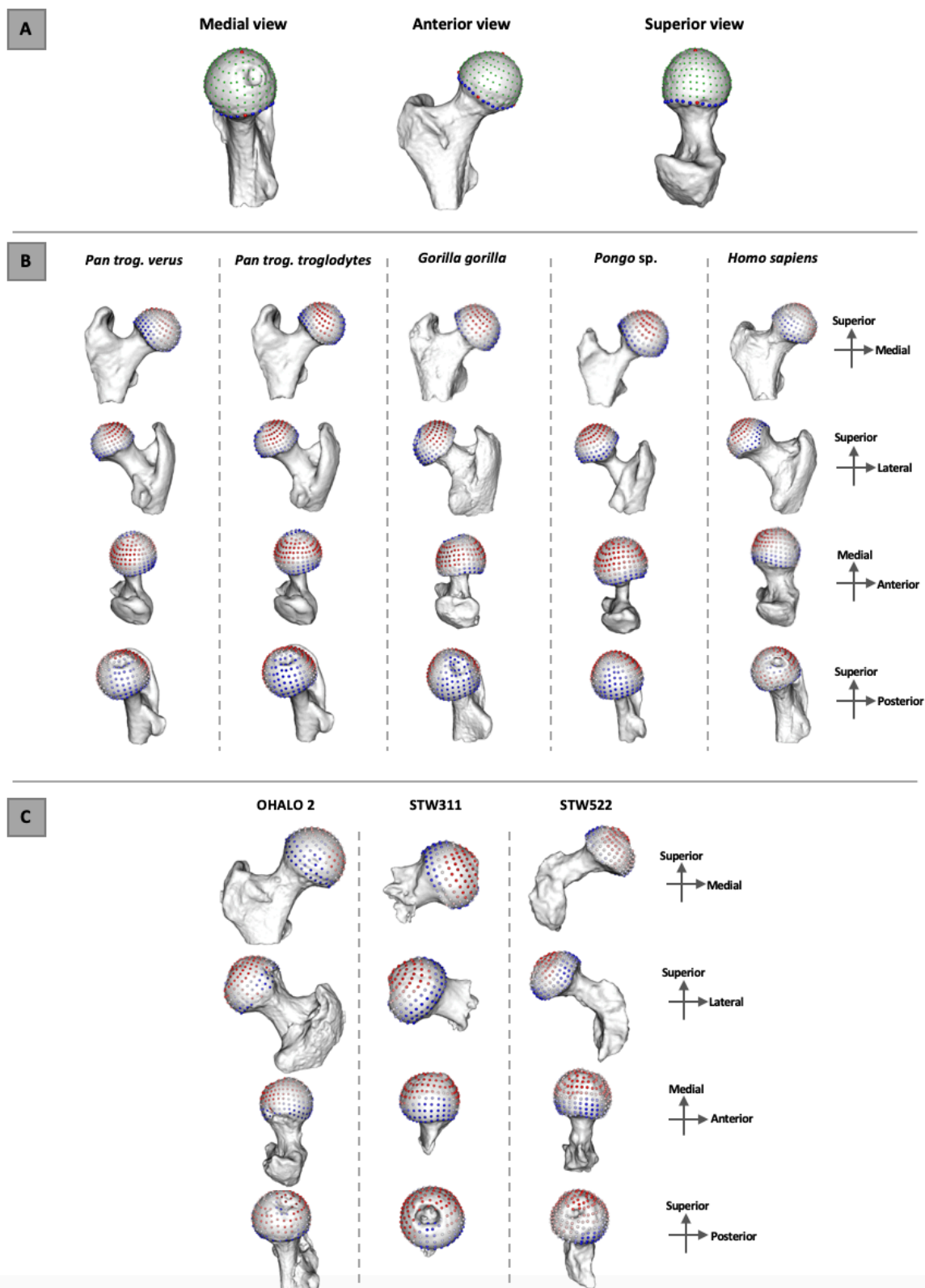
values along the posterosuperior region of the condyles, as well as along the inferior portion of the articulation for the patella, traits which consistent with the use of flexed knee positions during locomotion. These are missing from the distributions of *Gorilla* and *H. sapiens*, consistent with the use of more extended knee postures during locomotion.

To date, research on external morphology has failed to resolve the debate about the mode and evolution of hominin bipedalism (e.g. Stern and Susman, 1983; Susman et al. 1984; Ward, 2002; Carey and Crompton, 2005; Ohman et al. 2005; Lovejoy et al. 2009a,b; Lovejoy and McCollum, 2010; Raichlen et al. 2010). Here I show that trabecular bone can provide novel insight into reconstructing past behaviours. My findings suggest that the locomotion of South African hominins in the early Pleistocene was diverse. The trabecular bone distribution of StW 522 and TM 1513 reveals that these *A. africanus* individuals were obligate bipeds, in accordance to prior literature (Ward et al. 1999; Ward et al. 2001; Lovejoy et al. 2002). However, my study provides evidence for the lack of frequent and/or high loading of flexed hip in these individuals, suggesting that climbing was not a significant component of the locomotor repertoire. This interpretation is consistent with the more human-like morphology of the pelvis and knee of *A. africanus* (Napier, 1964; Lovejoy and Heiple, 1970; Tardieu, 1981; Häusler and Berger, 2001; Haeusler, 2002), and suggests that the more ape-like features, such as the limb-size proportions (Richmond et al. 2002; Green et al. 2007) and highly mobile big toe (Clarke and Tobias, 1995) are evolutionary retentions.

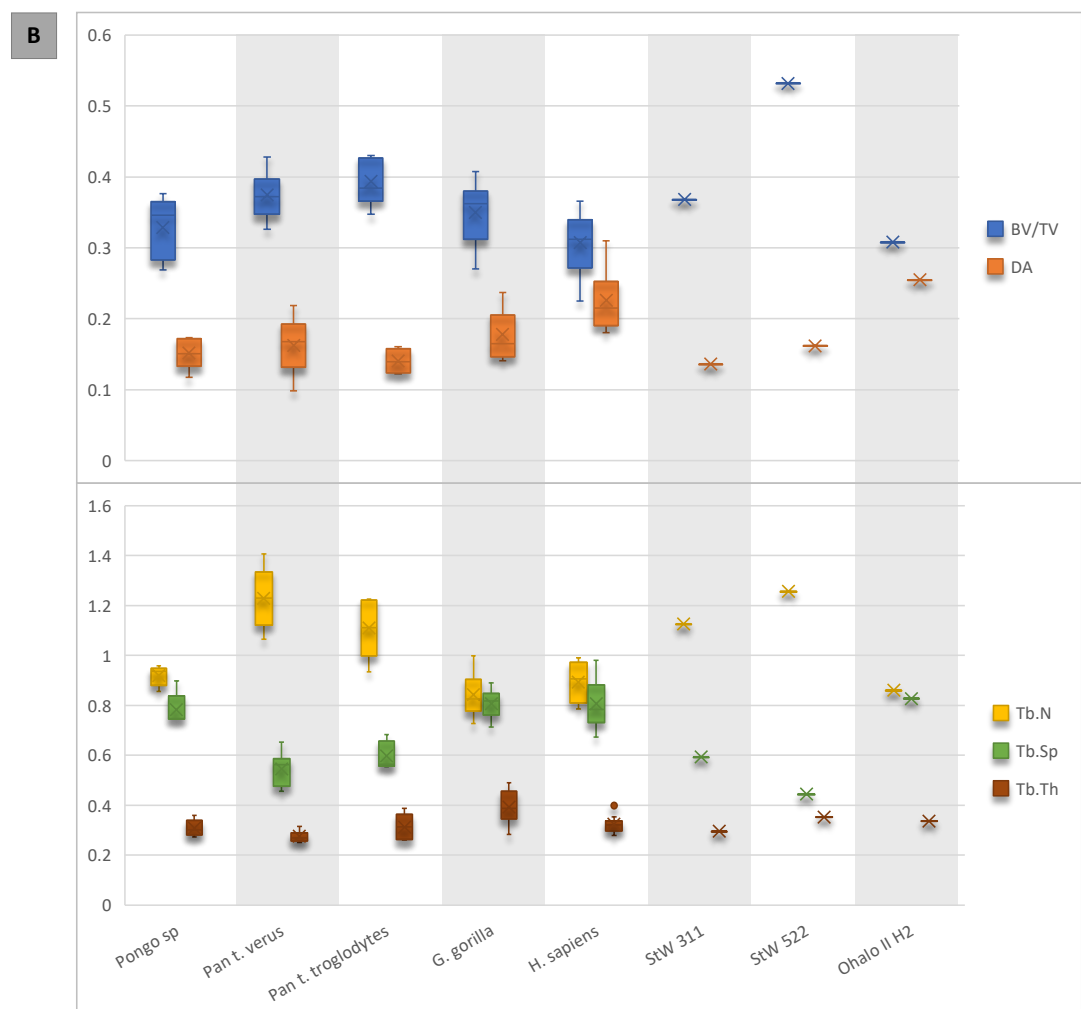
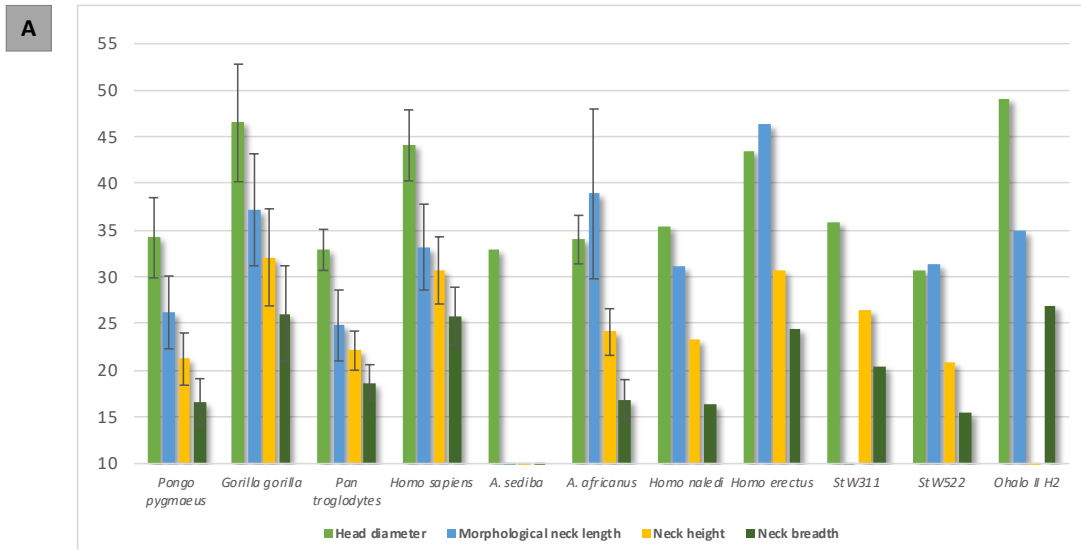
Furthermore, I present evidence that a younger hominin at Sterkfontein frequently engaged in climbing. The larger femoral size and estimated body mass of StW 311 (41.6 kg) compared to StW 522 (29.5 kg) are consistent with it belonging to younger taxon, however it is not clear if body size had any influence on this individual's locomotion. The evidence for climbing is consistent with paleoenvironmental reconstructions showing significant tree coverage (Reynolds and Kibij, 2011) and cycles of wet as well as dry phases (Pickering et al. 2018) at Sterkfontein during the Early Pleistocene, however is inconsistent with results from

the trabecular analysis of a distal tibia specimen from the Member 5 East infill (StW 567). Barak and colleagues (2013a) found that this individual had human-like trabecular orientation that differs to chimpanzees reflecting the use of less dorsiflexed ankles. However, mean trabecular parameters were not clearly human-like. BV/TV in the two studied VOIs of StW 567 was higher than *H. sapiens* as well as *P. troglodytes*, whereas Tb.N, Tb.Sp and ConnD were between the *H. sapiens* and *P. troglodytes* values. Additionally, Tb.Th was more similar to *H. sapiens*, while DA was more similar to *P. troglodytes*. The lack of certainty on the taxonomic affinity of StW 567 introduces difficulties in the interpretation of these results, as we do not know it belongs to the same taxon as StW 311 and the Member 5 East infill contains *Paranthropus robustus* fossils as well as early *Homo*. Nonetheless, I present here strong evidence in the femoral head trabecular distribution of StW 311 for frequent vertical climbing. My results imply that Sterkfontein hosted hominins with a diversity of locomotor types at the various times of occupation and provide morphological evidence that *A. africanus* was a non-climbing obligate biped while later hominins were frequently engaging in vertical climbing.

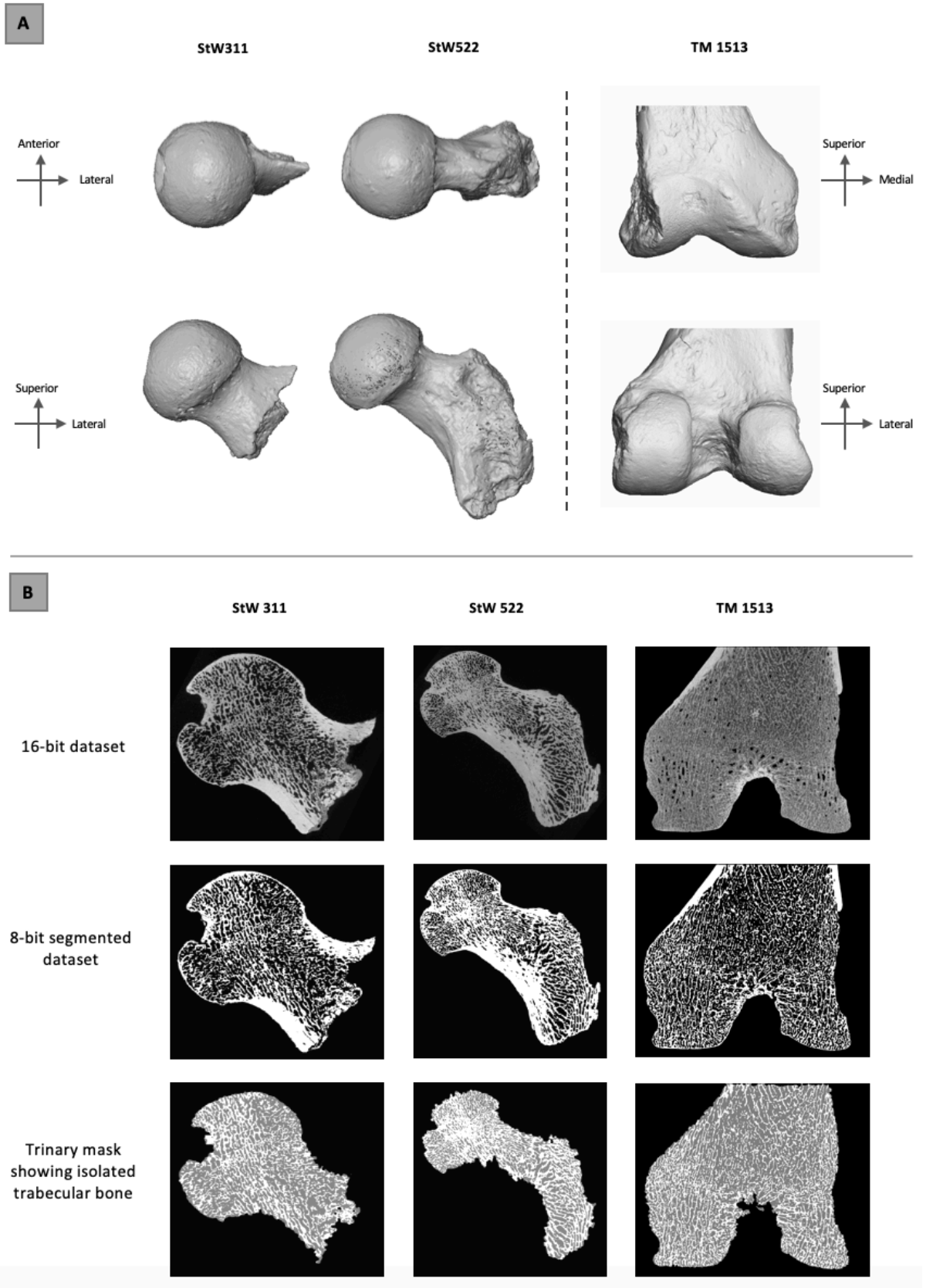
Supplementary material



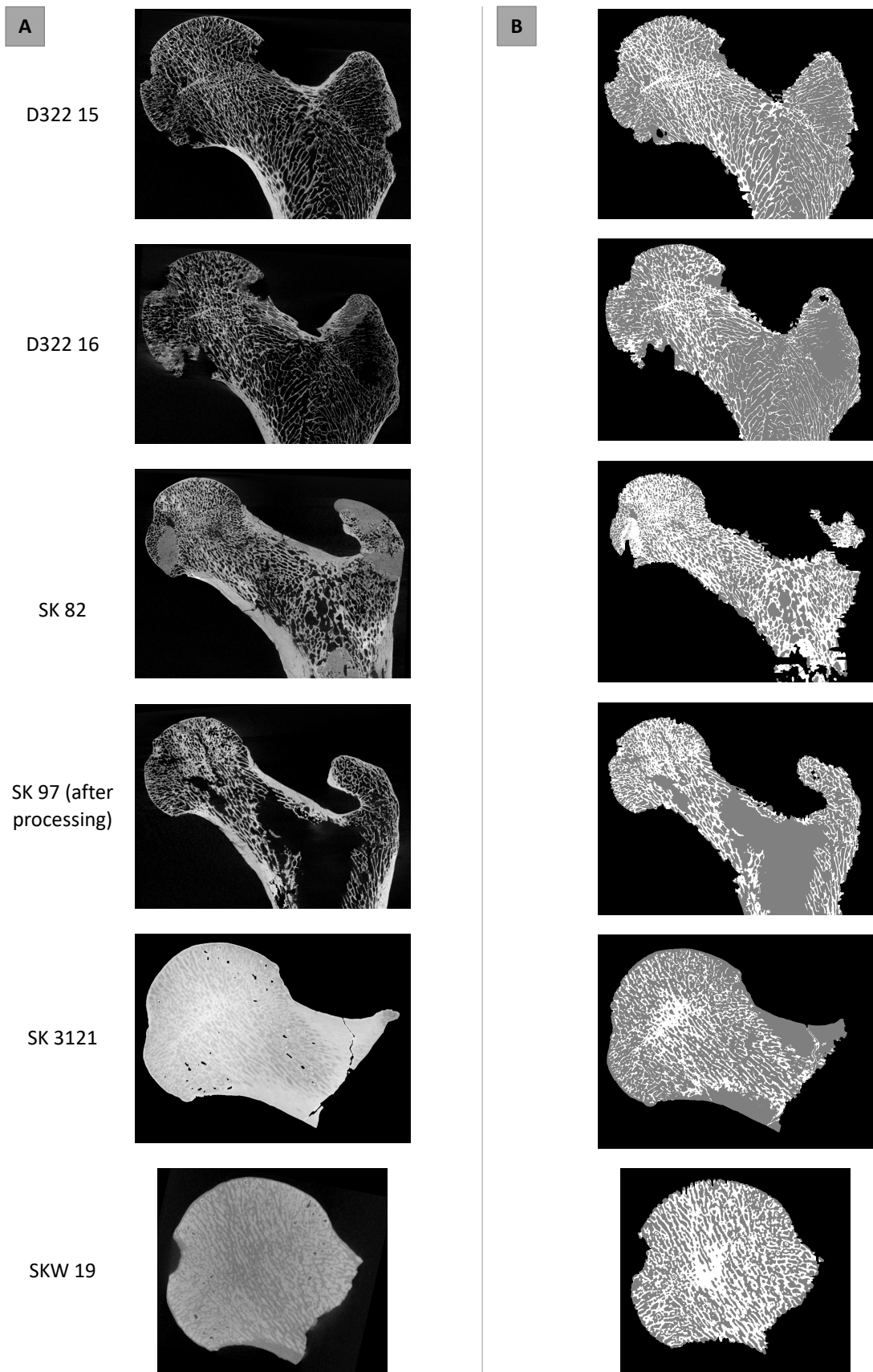
Supplementary Figure 5.1. Landmarking and results for the femoral head. (A) Landmarks used for the analysis femoral head trabecular structure. Fixed landmarks are indicated in red, curve landmarks are indicated in blue and surface semilandmarks are indicated in green. (B) Average relative BV/TV distributions over the femoral head in the extant taxa. (C) Relative BV/TV distributions over the femoral head in the fossils.



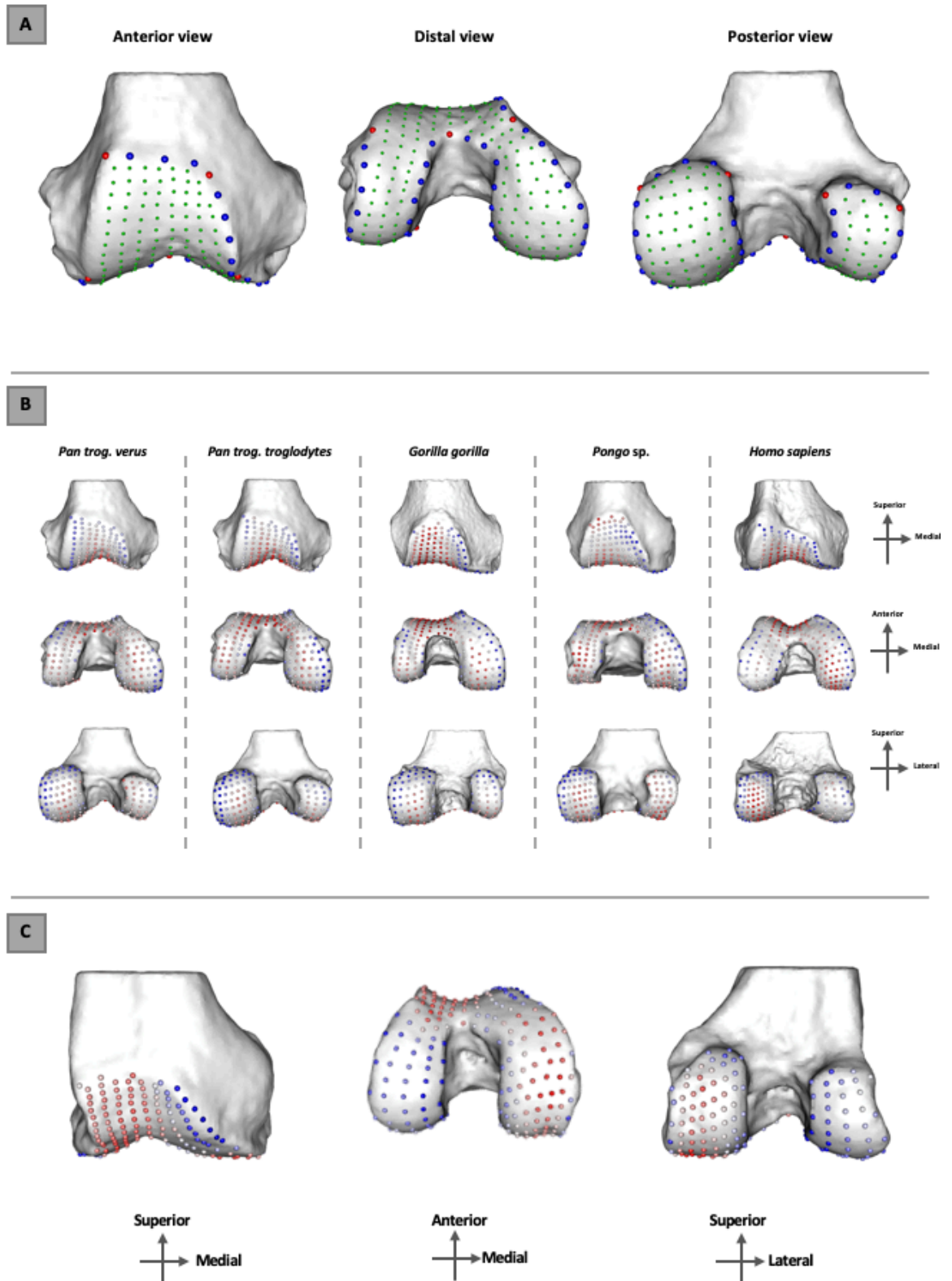
Supplementary Figure 5.2. Comparative femoral measurements for extant and extinct taxa (A) and trabecular parameters for the sample (B). (A) Columns represent mean values for each femoral measurement and error bars represent the standard deviation. Comparative femoral measurements were taken from Harmon, 2009, except for *A. sediba* which were taken from DeSilva et al. 2013 SOM, *H. naledi* and *H. erectus* which were taken from Marchi et al. 2016 and Ohalo II H2 which were taken from Hershkovitz et al. 1995. (B) Trabecular parameters quantified over the entire femoral head for the extant taxa and the fossils.



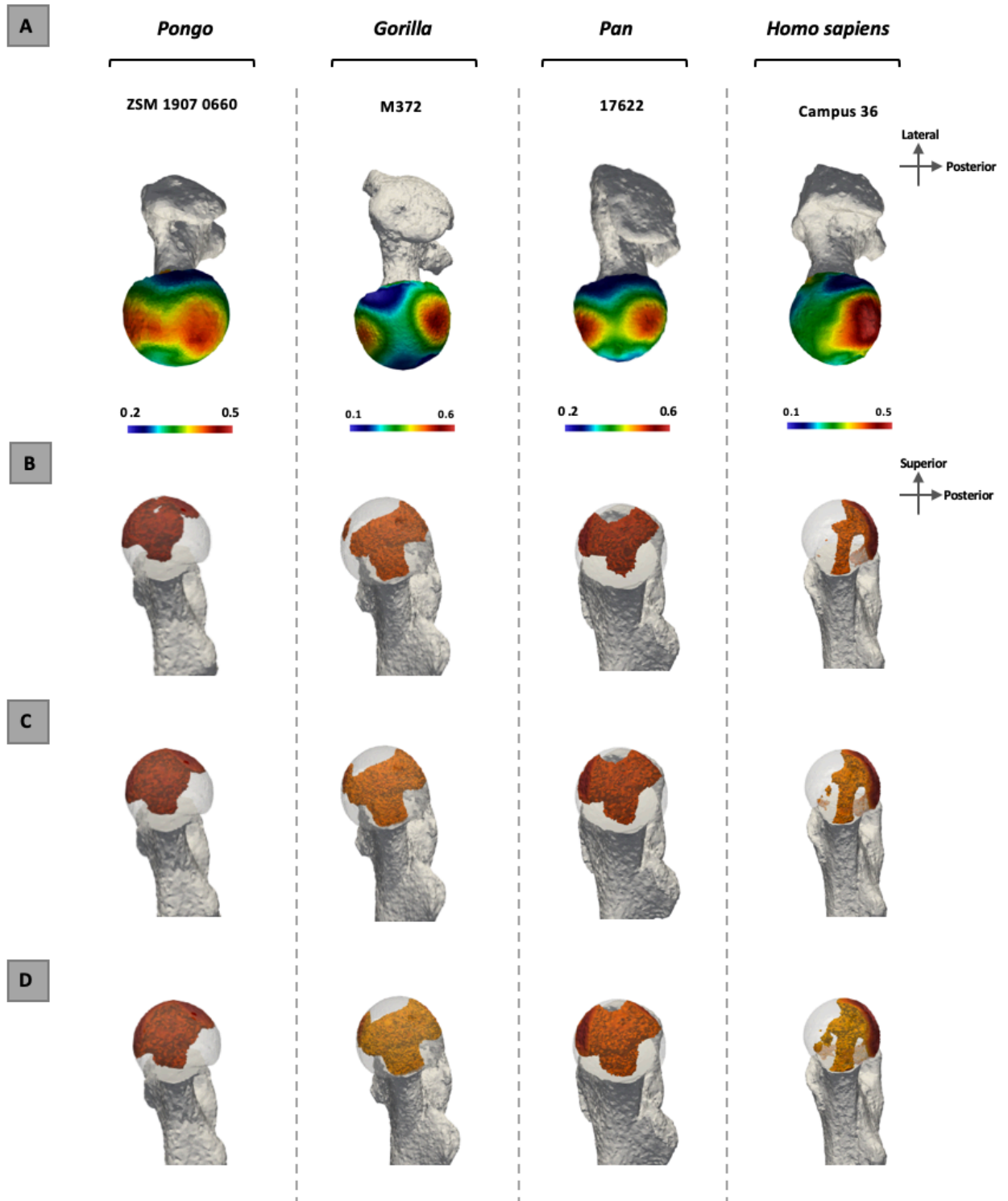
Supplementary Figure 5.3. External (A) and internal (B) morphology of StW 311, StW 522 and TM 1513. (A) Three-dimensional models showing the superior (top) and posterior (bottom) views of StW 311 and StW 522, as well as the anterior (top) and posterior (bottom) views of TM 1513. (B) Preserved trabecular structure (top), segmented bone (middle) and trinary mask showing isolated trabecular structure (bottom).



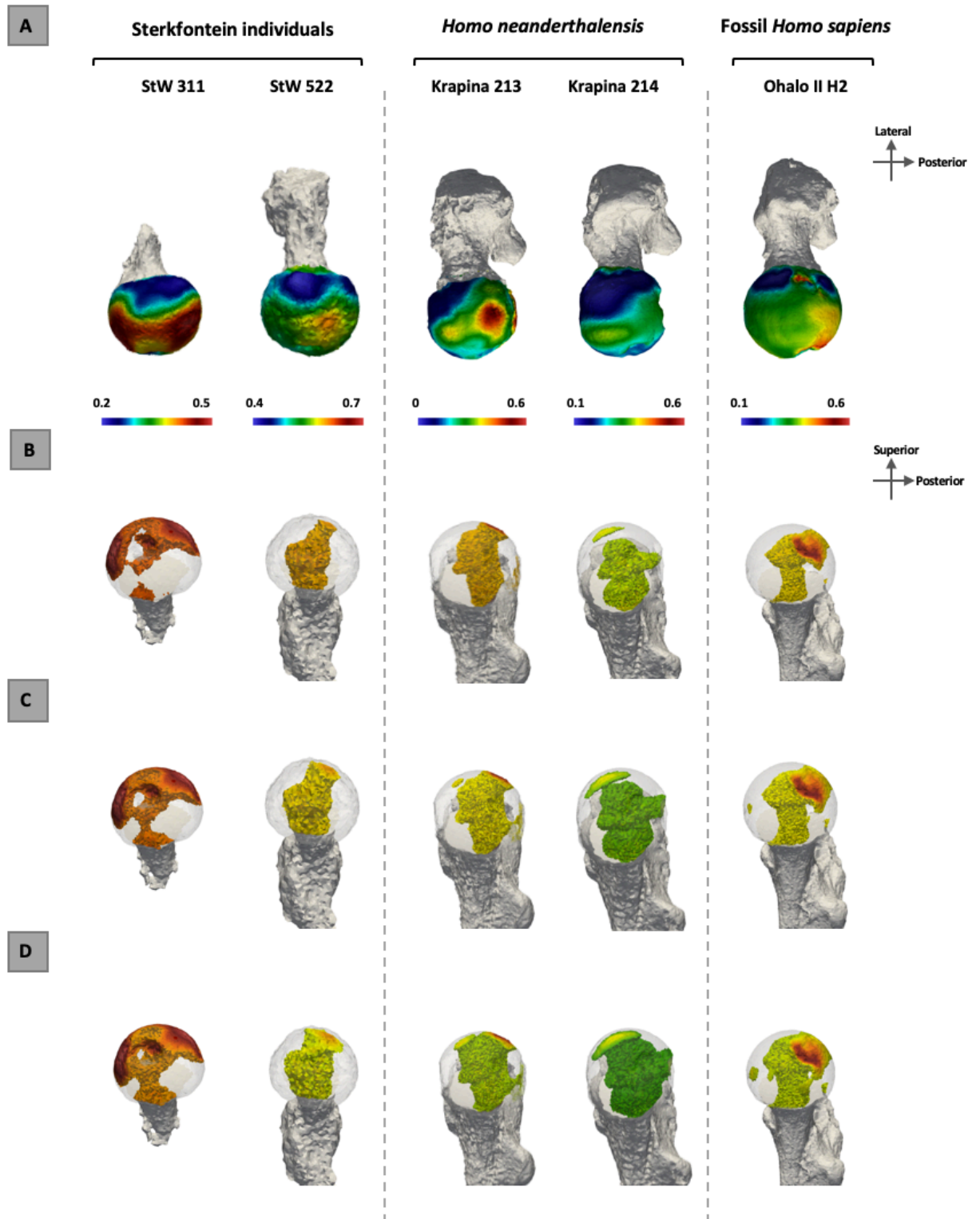
Supplementary Figure 5.4. Fossil which were not used in the analysis but were processed. (A) Original scan. (B) Trinary mask.



Supplementary Figure 5.5. Landmarking and results for the distal femur. (A) Landmarks used for the analysis of the distal femoral articular surface trabecular structure. Fixed landmarks are indicated in red, curve landmarks are indicated in blue and surface semilandmarks are indicated in green. (B) Average relative BV/TV distributions over the distal articular surface in the extant taxa. (C) Relative BV/TV distributions over the distal articular surface in TM 1513.



Supplementary Figure 5.6. BV/TV distribution in the subchondral layer of the femoral head (A) and within the femoral head (B-D) in the extant taxa. Internal high BV/TV is shown above the 85th (B), 80th (C) and 75th (D) percentile in each individual. Specimens are scaled to their own range.



Supplementary Figure 5.7. BV/TV distribution in the subchondral layer of the femoral head (A) and within the femoral head (B-D) in the fossil taxa. Internal high BV/TV is shown above the 85th (B), 80th (C) and 75th (D) percentile in each individual. Specimens are scaled to their own range.

Supplementary Table 5.1. Study sample composition, sex and resampled voxel size range in both epiphyses.

Taxon	N	Sex	Proximal voxel size (mm)	Distal voxel size (mm)	Collection or Site, Institution
<i>Pan troglodytes verus</i>	11	7 female, 4 male	0.04-0.05	0.04	Tai Forest collection, Max Planck Institute for Evolutionary Anthropology, Leipzig, Germany.
<i>Pan troglodytes troglodytes</i>	5	3 female, 2 male	0.05	0.04	Smithsonian National Museum of Natural History in Washington, DC, USA.
<i>Gorilla gorilla gorilla</i>	11	6 female, 5 male	0.05-0.08	0.045-0.09	Powell-Cotton Museum, UK.
<i>Pongo</i> sp.	5	5 female	0.04-0.045	0.035	Zoologische Staatssammlung München, Germany.
<i>H. sapiens</i>	11	3 female, 7 male, 1 N/A	0.06-0.07	0.05-0.06	Georg-August-Universität Göttingen, Germany.
<i>H. sapiens</i> : Ohalo II H2	1	N/A	0.06	-	Tel Aviv University, Israel.
<i>H. neanderthalensis</i> : Krapina 213 & 214	2	N/A	0.055-0.06	-	Croatian Natural History Museum
<i>Unknown</i> : StW 311	1	N/A	0.035	-	Sterkfontein, University of the Witwatersrand, South Africa.
<i>Australopithecus africanus</i> : StW 522	1	N/A	0.04	-	Sterkfontein, University of the Witwatersrand, South Africa.
<i>Australopithecus africanus</i> : TM 1513	1	N/A	-	0.045	Sterkfontein, Ditsong National Museum of Natural History, South Africa.

Supplementary Table 5.2. Description of landmarks.

Epiphysis	Landmark	Description	Type
Proximal	1	Medial point on head-neck border at neck midline	III
	2	Lateral point on head-neck border at neck midline	III
	3	Posterior point on head-neck border at neck midline	III
	4	Anterior point on head-neck border at neck midline	III
	5	Superior point at midpoint of the head	III
	6-12	Curve between fixed landmarks 1 and 3	IV
	13-19	Curve between fixed landmarks 3 and 2	IV
	20-26	Curve between fixed landmarks 2 and 4	IV
	27-33	Curve between fixed landmarks 4 and 1	IV
	34-242	Surface semilandmarks	Semilandmarks
Distal	1	Point where superior border meets medial edge of patellar groove	III
	2	Point where medial border of patellar groove meets medial border of medial condyle	II
	3	Medialmost point of superior border of medial condyle	III
	4	Lateralmost point of superior border of medial condyle	III
	5	Deepest point of intercondylar notch	II
	6	Medialmost point of superior border of lateral condyle	III
	7	Lateralmost point of superior border of lateral condyle	III
	8	Point where lateral border of patellar groove meets lateral border of lateral condyle	II
	9	Point where superior border meets lateral edge of patellar groove	III
	10-14	Curve between fixed landmarks 1 and 2	IV
	15-23	Curve between fixed landmarks 2 and 3	IV
	24-26	Curve between fixed landmarks 3 and 4	IV
	27-34	Curve between fixed landmarks 4 and 5	IV
	35-41	Curve between fixed landmarks 5 and 6	IV
	42-43	Curve between fixed landmarks 6 and 7	IV
	44-49	Curve between fixed landmarks 7 and 8	IV
	50-52	Curve between fixed landmarks 9 and 1	IV
53-253	Surface semilandmarks	Semilandmarks	

Chapter 6

General Discussion, Conclusion, Limitations and Future Directions

6.1. General Discussion

The aim of this thesis was to investigate the trabecular bone architecture in the femur of extant hominids and its links to locomotion, with the ultimate goal to infer locomotion in extinct hominins. Trabecular bone analysis can provide additional evidence to external morphology and inform about actual behaviour in extinct taxa as it remodels throughout life in response to load (e.g. Pontzer et al. 2006; Volpato et al. 2008; Barak et al. 2011). Therefore, analysing the trabecular bone patterns in extant apes and establishing connections to locomotor behaviour is vital for understanding the behaviours of extinct hominin taxa. Extant great apes are arguably the best analogues we have for understanding extinct hominins, as they are genetically our closest living relatives (e.g. Prüfer et al. 2012) and use a variety of terrestrial and arboreal locomotor modes, including bipedalism (e.g. Tuttle, 1969; Doran, 1996, 1997; Videan and McGrew, 2001; Isler, 2005; Thorpe and Crompton, 2005, 2006).

In this dissertation, novel analytical tools were used to examine trabecular architecture in the femoral head and distal femoral epiphysis in a holistic way. The aim of this thesis was achieved in three chapters:

- First, the trabecular architecture of the femoral head in extant apes was analysed to identify locomotor-related patterns in the hip.
- Second, the trabecular architecture of the distal femoral epiphysis in extant apes was analysed to identify locomotor-related patterns in the knee.
- Third, the trabecular patterns of the femoral head and distal femur in the extant apes were used to infer locomotion in extinct South African hominins from Sterkfontein. Geometric morphometrics were combined with holistic trabecular analysis to statistically analyse trabecular bone distribution patterns beneath the subchondral layer. This allowed a more comprehensive

evaluation of the trabecular architecture and provided the first statistical comparison of the three-dimensional trabecular patterns beneath both articulations of the femur in these extant and extinct hominids.

Below I review and discuss the key findings from these chapters and how they together inform our broader understanding of the evolution of hominin bipedalism.

6.1.1. Does the femoral trabecular architecture of extant non-human apes hold locomotor signals?

Chapters 3 and 4 of this dissertation showed that trabecular patterns of the femur in non-human apes generally reflect their most frequent activities, although differences between taxa were not always as pronounced as predicted. *Pan troglodytes* individuals mostly use quadrupedal knuckle-walking when locomoting terrestrially, though they also frequently climb and engage in several arboreal behaviours (Hunt, 1991b; Doran, 1992, 1993a). The trabecular bone distribution of the femoral head reflects locomotion. There are two distinct regions of high BV/TV across the femoral head, one anterior and one posterior. High BV/TV at these regions correlates to high load at highly flexed hip angles during vertical climbing (Isler, 2005; Nakano et al. 2006) and less flexed angles during terrestrial knuckle-walking (Finestone et al. 2018). A strip of slightly less dense bone that was found between the two concentrations is correlated with intermediate hip flexion angles used during the various other activities of *Pan*. In the distal femur, *Pan* has particularly high BV/TV in the posterosuperior region of the condyles and high BV/TV in the inferior region of the patellofemoral articulation reflecting the frequent use of highly flexed knee postures. Within both epiphyses, the trabeculae of *Pan* are relatively isotropic, consistent with the variable hip and knee joint positioning during chimpanzee locomotion. Individuals have numerous, thin and closely packed trabeculae, traits that may reflect body size-related mechanisms for adjusting BV/TV (e.g. Barak et al. 2013b) or species-specific systemic patterns (e.g. Tsegai et al. 2018a), therefore these properties (i.e. Tb.N, Tb.Sp and Tb.Th) are not as informative as the other parameters about mechanical loading.

Gorilla was expected to have very similar trabecular architecture to *Pan*, as their locomotor repertoire largely consists of the same behaviours (Remis, 1995; Crompton et al. 2010). They are also terrestrial, quadrupedal knuckle-walkers and frequent climbers; however, their trabecular architecture shows some differences to *Pan*. In the femoral head *Gorilla* has two high BV/TV concentrations, similar to *Pan*,

though these are more well-separated. The lack of slightly lower BV/TV values between the two main regions of high BV/TV suggests that *Gorilla* individuals do not frequently load their hips at intermediate flexion angles like *Pan* individuals do. Furthermore, in the distal femur *Gorilla* lacks the high BV/TV in the posterosuperior region of the condyles found in *Pan* and shows high BV/TV across the patellofemoral articulation. While the trabecular bone distribution in the femoral head of *Gorilla* reflects loading during hip postures associated with terrestrial knuckle-walking (Finestone et al. 2018) and vertical climbing (Isler, 2005), the trabecular bone distribution in the distal femur does not reflect loading at highly flexed knee postures. The pattern of the distal femur is perhaps indicative of different knee kinematics during vertical climbing in *Gorilla* compared to *Pan*, which involves a relatively more extended knee (Isler, 2005). Despite differences in the BV/TV distribution patterns of *Pan* and *Gorilla*, these taxa are close in DA values in both epiphyses, which is perhaps indicative of a similar level of variation in their joint positioning during locomotion. However, these taxa differ in other trabecular parameters. Contrary to *Pan* individuals, *Gorilla* individuals generally have relatively few, thick and widely spaced trabeculae in both femoral epiphyses, which again could reflect non-mechanical factors or body size-related mechanisms that affect trabecular structure.

Pongo is the most arboreal of the hominids and that is generally reflected in their femoral trabecular architecture. In the femoral head they also show two main concentrations of high BV/TV, however these are the least well-separated amongst the apes. Similar to what is found in *Pan*, a strip of less dense bone connects these two areas. While the two separate regions of high BV/TV are consistent with peak loading during vertical climbing and terrestrial locomotion, the extended region of dense bone across the superior reflects the variable hip joint positioning in *Pongo* individuals during locomotion (Cant, 1987; Isler and Thorpe, 2003; Thorpe and Crompton, 2006; Thorpe et al. 2009). This is further supported by the high variability of trabecular parameters across the *Pongo* sample. In the distal femur *Pongo* resembles *Pan* in distribution, with individuals having high BV/TV at the inferior aspect of the patellofemoral articulation as well as the posterosuperior region of the

condyles, though the latter is not as extended as in the *Pan* individuals. Contrary to the prediction that *Pongo* would be the most isotropic, this taxon shows a similar degree of isotropy to that of African apes in both epiphyses. This implies that their highly variable joint positioning is not clearly reflected in the degree of trabecular strut orientation. Additionally, similarly to *Pan*, they have relatively numerous, thin and closely packed trabeculae in both epiphyses perhaps reflecting the similar body size range of the *Pan* and *Pongo* individuals in this dissertation.

Together these findings suggest that the trabecular bone of the femoral head of non-human apes holds a strong functional signal which can be linked to habitual locomotor behaviours, but also that of the distal femur shows a less clear functional signal. Of course, it is important to consider variation in cortical structure when interpreting trabecular results. Cross-sectional dimensions possibly influence trabecular patterns, as cross-sectional properties (e.g. Rafferty, 1998; Ruff, 2002; Carlson, 2005) and the relative size of articulations to diaphyseal proportions (e.g. Ruff, 2002) in apes vary with locomotor mode. Even though in the femur the two tissues adapt differently in response to load (Shaw and Ryan, 2012), both contribute to overall mechanical efficiency. The lack of a strong signal in the distal femur could be the result of increased cortical response, either in the form of diaphyseal cross-sectional geometry or epiphyseal size. Unfortunately, as femoral cross-sectional geometry was outside the scope of this dissertation it cannot be discussed in further detail.

This dissertation is the first to describe these 3D trabecular patterns in both the proximal and distal femur of great apes and identify locomotor-related traits in BV/TV distribution. Prior research has analysed the trabecular structure within isolated volume in the femoral head, but not the distal femoral epiphysis of apes. My findings for the femoral head are generally consistent with previous studies (e.g. Ryan and Shaw, 2015; Georgiou et al. 2018; Ryan et al. 2018; Tsegai et al. 2018a). *Pan*'s trabecular architecture is the most distinct, showing the highest BV/TV and Tb.N, as well as the lowest Tb.Sp and Tb.Th, similar to what was found by Ryan and Shaw (2015). However, my results suggest that mean femoral head trabecular

parameters are not good predictors of locomotor behaviour, as they do not distinguish between *Gorilla* and *Pongo*, and analysis should focus on the three-dimensional distribution of trabecular parameters.

6.1.2. *Is Homo sapiens femoral trabecular pattern unique?*

Homo sapiens is the only obligate bipedal extant ape and many of the femoral trabecular traits of *H. sapiens* individuals reflect this locomotion. Perhaps the most characteristic human trait is their highly aligned trabeculae in both the proximal and distal epiphyses, reflecting the stereotypical loading of both the hip and the knee during bipedal locomotion. This is consistent with previous research showing that taxa with specialised locomotion have more highly aligned and organised trabecular struts than taxa with more variable locomotion (Ryan and Ketcham, 2002; Scherf, 2008). Furthermore, in the femoral head *H. sapiens* has a unique pattern of trabecular bone distribution with one (instead of two) high BV/TV concentration on the posterosuperior aspect of the femoral head. This concentration coincides with the region most frequently loaded during bipedalism (Paul, 1976; English and Kilvington, 1979; Yoshida et al. 2006). The human femoral head pattern also lacks the anterior high bone volume concentration found in African apes and *Pongo*, which is consistent with loading of a flexed hip during vertical climbing, though this is not surprising as most *H. sapiens* individuals do not habitually climb. Furthermore, BV/TV in the human femoral head is lower than other apes, consistent with previous findings (Maga et al. 2006; Cotter et al. 2009; Scherf et al. 2013; Tsegai et al. 2013; Tsegai et al. 2017; Tsegai et al. 2018a). It is interesting that the walking signal is very clear in the *H. sapiens* femoral head distribution despite the diversity of human activities that involve various hip flexion angles and loads, including running which involves greater hip flexion and hip loading (e.g. Van der Bogert et al. 1999; Yoshida et al. 2006; Giarmatzis et al. 2015). Therefore, my findings indicate that the femoral head trabecular network is important in transmitting load particularly during walking in humans. This is perhaps because other activities which result in higher loading of the hip (e.g. running) (van den Bogert et al. 1999) are not frequent enough to elicit

trabecular reorganisations or the cost of those activities is not high enough to overcome the benefit of having a trabecular network adapted to the most frequent activity.

In the distal femur, the trabecular pattern is not as distinct in *H. sapiens* compared to other apes. The most noteworthy feature is the lack of high BV/TV in the posterosuperior region of the condyles, which is consistent with the use of more extended knee postures throughout gait. However, *Gorilla* also lacks this concentration therefore it is not a distinctly human trait. Some of the differences in trabecular traits between humans and other apes can be explained by shape variation in the condyles. The lateral condyle of *H. sapiens* is relatively enlarged compared to other apes (Tardieu, 1981), resulting in a greater area for load distribution. This perhaps explains why, beneath the subchondral layer, BV/TV in this condyle is relatively lower in humans than other apes. The opposite is true for the medial condyle. This condyle is relatively reduced in *H. sapiens* compared to other apes (Tardieu, 1981) and BV/TV is relatively greater beneath its subchondral layer. However, in this epiphysis the mean BV/TV of different regions is not markedly lower in *H. sapiens* than other apes, which is perhaps surprising given prior findings (e.g. Maga et al. 2006; Cotter et al. 2009; Scherf et al. 2013; Tsegai et al. 2013; Tsegai et al. 2017; Tsegai et al. 2018a). This may be partially explained by the microarchitecture. In this epiphysis, trabecular thickness in *H. sapiens* is comparable to that of *Gorilla* and is higher than *Pan* and *Pongo*, while in the femoral head it is more comparable to that of *Pan* and *Pongo* and is lower than *Gorilla*. Therefore, the lack of significantly lower BV/TV in the distal femur of *H. sapiens* compared to other apes is perhaps explained by the relatively thick trabeculae of the distal femoral epiphysis. In both epiphyses, trabeculae are relatively few and widely spaced, therefore Tb.N and Tb.Sp probably do not contribute as much to this as Tb.Th does.

Nonetheless, generally results suggest that humans have distinct trabecular architecture and that their trabecular bone distribution, especially in the femoral head, is linked to obligate bipedalism.

6.1.3. *Can the trabecular patterns of the femur be used to infer locomotion in extinct hominins?*

In this dissertation I have shown that the trabecular bone of the femur in extant apes holds a functional signal that is linked to habitual locomotion. Findings presented here indicate that *H. sapiens* is distinct in its femoral head trabecular pattern, showing traits clearly linked to obligate bipedalism, while African apes and *Pongo* are more similar to each other and show traits linked to both vertical climbing as well as terrestrial quadrupedalism. The distinctive human pattern with a single high BV/TV concentration in the femoral head differs to the non-human ape pattern that has an additional anterior high BV/TV concentration, owing to the use of highly flexed hip postures. These patterns provide strong evidence for a locomotor signal in the trabecular structure of the femoral head in hominids. On the contrary, if there is a functional signal in the distal femur that separates humans from other extant apes, it is more difficult to decipher. The extant apes do not show vast differences and, even though results generally follow predictions, *H. sapiens* is not as distinct as would be expected based on their different form of locomotion. Knee kinematics are not well understood, especially in non-human apes, therefore trabecular results are difficult to interpret. The close resemblance between the distributions of the taxa may be due to similar kinematics in the knee joint across apes or the result of less responsive trabecular bone to applied load in this joint, however this cannot be said with certainty. Adding to that the structural complexity of this joint makes trabecular patterns of the knee difficult to explain and therefore less useful in inferences of behaviour in extinct hominins. Since the trabecular patterns of the distal femur appear to be less functionally informative in hominids than those of the femoral head, the latter can be used to more accurately predict locomotion in extinct human relatives. This can provide insight into the evolution of bipedalism in the hominin lineage, which has been of great interest in paleoanthropological research (e.g. Stern and Susman, 1983; Susman et al. 1984; White et al. 1994; Crompton, et al. 1998; Ward et al. 1999; Senut et al. 2001; Ward et al. 2001; Lovejoy et al. 2002; Pickford et al. 2002; Wolpoff et al. 2002; Zollikofer et al. 2005; Crompton et al 2008; Carey and

Crompton, 2005; Ohman et al. 2005; Harmon, 2009a,b; Lovejoy et al. 2009a,b; Lovejoy and McCollum, 2010; Raichlen et al. 2010; Ward et al. 2011; Almecija et al. 2013; DeSilva et al. 2013).

6.1.4. How do the trabecular patterns of the extinct hominins compare to those of the extant taxa?

In Chapter 5, I analysed trabecular patterns in the femur of extinct hominins, with a particular focus on three femoral specimens from Sterkfontein, South Africa. The main goal of this chapter was to examine the trabecular structure in comparison to that of extant apes and humans and ultimately make inferences about the locomotion of these hominin individuals. Subchondral trabecular bone in both articulations was analysed statistically using holistic trabecular analysis and geometric morphometrics. Additionally, the internal distribution of high bone volume was examined within the femoral head of both the extant and extinct taxa, to gain insight into the three-dimensional distribution of trabecular bone. This chapter focused more on the trabecular distribution patterns of the femoral head, as this was shown in previous chapters to preserve a stronger functional signal than the distal femoral epiphysis.

The trabecular patterns in the femoral head of one fossil *H. sapiens* (Ohalo II H2) and two *H. neanderthalensis* specimens (Krapina 213 and Krapina 214) were initially examined for comparison with modern humans. These specimens, as expected, presented a similar trabecular distribution pattern to modern *H. sapiens*, validating that this pattern is linked to obligate bipedal locomotion. These specimens, along with the modern *H. sapiens*, showed a single pillar of high BV/TV within the femoral head, a trait which is linked to stereotypical loading during specialised bipedal locomotion and is unique to the *Homo* specimens. Findings from this chapter, as well as the previous ones, support that the femoral head trabecular pattern of obligate bipedal taxa is unique amongst apes.

Among the Sterkfontein fossils, different trabecular patterns were found suggesting variation in locomotor behaviour among these individuals. StW 522, a specimen from Member 4 attributed to *A. africanus*, showed the single subchondral concentration in the posterosuperior aspect of the femoral head as found in *H. sapiens*, which continued internally forming a single pillar of high bone volume. This distribution pattern suggests that this individual, and potentially *A. africanus*, was frequently bipedal. Despite some variation between the *H. sapiens* and *A. africanus* pattern, the findings presented here reveal that this individual did not engage frequently in a strongly flexed hip posture that is found during great ape climbing. The distribution pattern clearly lacks an anterior high bone volume concentration, which in extant apes was shown to correlate to hip postures used during vertical climbing. The distal femoral epiphysis of *A. africanus* (TM 1513) that came from the same member at Sterkfontein as StW 522 also revealed some *H. sapiens*-like trabecular distribution traits. This specimen lacks the high BV/TV found in the posterosuperior region of the condyles of *Pan*, suggesting they did not frequently use highly flexed knee postures. However, this specimen is missing part of the patellar articulation which complicates the selection of homologous landmarks and it decreases the confidence in the statistical analysis of its trabecular distribution. In contrast to StW 522 and TM 1513, the StW 311 proximal femoral specimen from Member 5 presented a different pattern to that of *H. sapiens*, despite being a geologically younger specimen. The trabecular distribution pattern both beneath the subchondral layer and within the femoral head most closely resembled that of extant apes, showing two high bone volume concentrations on the femoral head that continued internally forming two separate pillars. This trabecular distribution pattern suggests that this individual frequently engaged in both locomotion that involves relatively extended hip postures, as well as locomotor behaviours, such as climbing, that involve strongly flexed hip postures.

If both StW 522 and TM 1513 are indeed accurately attributed to *A. africanus* then the findings here are perhaps unsurprising, as previous research has suggested that australopiths had human-like bipedal locomotion (e.g. Lovejoy and Heiple, 1970;

Tardieu, 1981; Ward et al. 1999; Ward et al. 2001; Lovejoy et al. 2002; Lovejoy, 2005a; Ward et al. 2011; Ryan et al. 2018). My findings suggest that the habitual hip postures used by *A. africanus* and *H. sapiens* were not remarkably different, as evident by the closeness in the location of the single high BV/TV concentration on the femoral head of the two taxa. Results do not support the use of a bent-hip in *A. africanus* locomotion, contributing to the longstanding debate over the form of bipedal locomotion used by australopiths (Stern and Susman, 1983; Susman et al. 1984; Ward, 2002; Carey and Crompton, 2005; Lovejoy and McCollum, 2010; Raichlen et al. 2010). Furthermore, the BV/TV distributions of StW 522 and TM 1513 clearly demonstrate a lack of strongly flexed hip and knee postures in *A. africanus* locomotion and therefore that climbing was potentially absent from their locomotor repertoire. No prior study has provided such strong evidence for the lack of climbing in australopith locomotion (Ward, 2002a).

Results from the Sterkfontein individuals confirm that hominins with different types of locomotion existed in the Pleistocene. However, interpretation of the StW 311 result in an evolutionary context is challenging as the taxonomy of this specimen is not clear. Member 5 East has yielded hominin fossils attributed to *Paranthropus robustus* and potentially early *Homo*, as well as Oldowan and Early Acheulean tools industries (Reynolds and Kibii, 2011; Barak et al. 2013a). If StW 311 is *P. robustus* it means that this taxon had different locomotion to *A. africanus* and engaged in frequent climbing. Perhaps this suggests that the *Paranthropus* genus was generally more arboreal than *Australopithecus*, since recent findings also suggest that *P. boisei* may have engaged in suspensory behaviours based on its the scapular anatomy (Green et al. 2018). Alternatively, if StW 311 is early *Homo* it means that climbing was used frequently in the genus *Homo* after obligate bipedalism had evolved in *Australopithecus*. Understanding the stratigraphy of Sterkfontein in greater depth is integral in determining this individual's taxonomy and subsequently the evolutionary meaning of my result. This will potentially have important implications on the evolution of locomotion in the genus *Paranthropus* or *Homo* and will help understand the evolution of locomotion in the hominin clade.

This thesis outlines the importance of analysing trabecular architecture across an entire epiphysis. Previous research has focused on the trabecular structure within isolated sub-volumes (e.g. Ryan and Ketcham, 2002; Scherf, 2008; Ryan and Shaw, 2002; Ryan et al. 2018) and specifically within the femoral head a few studies failed to find distinct locomotor signals (e.g. Ryan and Walker, 2010; Shaw and Ryan, 2012). However, this dissertation is an example for how much additional information you can gain from looking at the distribution of trabecular parameters across an epiphysis. Specifically in Chapter 6, when the whole femoral head is treated as one VOI the mean femoral head parameters of StW 522 and StW 311 cannot definitively appoint the fossils to one locomotor group. Furthermore, their mean values are not necessarily comparable to the taxa with which they share a similar trabecular distribution pattern and presumably locomotor mode. This thesis therefore makes a compelling argument for holistic analysis of trabecular structure, where analysis focuses on the distribution of trabecular parameters rather than mean values within a VOI, as previous research has demonstrated (Skinner et al. 2015; Tsegai et al. 2013; Tsegai et al. 2017; Tsegai et al. 2018a,b), and presents new evidence for locomotor signals in the femoral architecture of extant and extinct hominids.

6.2. Conclusion

This dissertation found clear locomotor signals in the trabecular bone of the femoral head of extant hominids, and less so in that of the distal femoral epiphysis. In the femoral head trabecular bone distribution patterns correlate to habitual hip postures in extant apes, which in non-human apes include those of terrestrial locomotion and vertical climbing while in humans include those of bipedal locomotion. Correlations are also found in the distal femoral epiphysis, however the patterns in this epiphysis are more complex and links are not as obvious. Furthermore, findings of this dissertation suggest that South African hominins used a variety of locomotor modes. The *Australopithecus africanus* trabecular pattern is

most similar to modern humans indicating they were obligate bipeds. Though the slight variation between the patterns of modern taxa and *A. africanus* suggests that their joint kinematics may have differed. Furthermore, the trabecular architecture of a younger specimen from Sterkfontein suggests that this individual was frequently climbing indicating that the locomotion of this taxon was different to *A. africanus*. This dissertation provides insight into the locomotion of extinct human relatives, with particular implications on the evolution of South African hominins, and represents yet another example of fruitful holistic trabecular analysis.

6.3. Limitations and future directions

In this dissertation the samples were relatively small, even for the extant taxa. Specifically, the *Pongo* sample consisted of 7 individuals, 5 of which were wildshot and 2 were captive. The captive individuals were only included in the analysis of the distal femoral trabecular architecture, as they did not significantly affect statistical comparisons, however even then the 2 specimens complicated interpretations. Understanding the *Pongo* pattern was difficult, and this was partially due to the high intraspecific variability in the *Pongo* patterns, but that could have been improved with a larger sample. Additionally, larger and balanced samples of the extant apes would have allowed intraspecific comparisons between the sexes. While the *Gorilla* sample was comprised of the same number of males and females, the *Pongo* wildshot individuals were all female and the *Pan* sample included more females than males, therefore limiting comparisons between the sexes. Since locomotor behaviour, joint positioning and body size differ between male and female gorillas (e.g. Isler, 2005), as well as male and female chimpanzees (e.g. Doran, 1993b), more information would have been potentially gleaned from the patterns if they could have been compared between the sexes. Furthermore, the statistical power of my analysis would have increased with larger samples. In the human sample the biggest limitation was the lack of information on the individuals, as no data was available about their professions or lifestyles. This limitation would have been overcome if the

additional human specimens I had processed did not present issues. The collection curated at the University of Kent possesses information on the individuals that could have provided further understanding of their locomotor behaviour and therefore would have perhaps been useful when interpreting the human femoral pattern. Another limitation of all trabecular studies is that, to this point, there has not been a published method for statistically comparing the three-dimensional trabecular structure between specimens. In my thesis, this restricts interpretations to the observations made from the distribution of BV/TV (and DA), and mean parameters over specific region. However, this is not as robust as statistically comparing the spatial distribution of trabecular parameters. Finally, the extant and fossil samples were scanned using different scanners and parameters which could potentially have an effect on the representation of the trabecular structure.

Future research will focus on analysing the three-dimensional femoral trabecular structure of larger and more varied samples, using more statistically robust methods. Comparisons between sexes in non-human apes, as well as between ages, will provide a more comprehensive picture of the locomotor signals identified in this study. Furthermore, comparing femoral trabecular structure between species of *Pan* (e.g. bonobos vs. chimpanzees), subspecies of *Gorilla* (e.g. western lowland gorillas vs. mountain gorillas) or between human populations that exploit different habitats will further our understanding of trabecular functional signals in the femur.

References

- Abbass, S.J., Abdulrahman, G. (2014) Kinematic analysis of human gait cycle. *Nahrain University College of Engineering Journal (NUCEJ)*, 16 (2), pp. 208-222.
- Abitbol, M.M. (1987a) Evolution of the lumbosacral angle. *American Journal of Physical Anthropology*, 72, pp. 361-372.
- Abitbol, M.M. (1987b) Evolution of the sacrum in hominoids. *American Journal of Physical Anthropology*, 74, pp. 65-81.
- Adolph, K.E. (2003) Learning to keep balance. *Advances in Child Development and Behavior*, 30, pp. 1-40.
- Ahrens, J., Geveci B., Law C. (2005) 'ParaView: An end-user tool for large data visualization', in Hansen C.D., Johnson C.R. (eds). *Visualization handbook*. Burlington, MA: Butterworth-Heinemann, pp. 717-731.
- Aiello, L.C., Dean, C. (1990) *An Introduction to Human Evolutionary Anatomy*. London: Academic Press.
- Alexander, C.J. (1994) Utilisation of joint movement range in arboreal primates compared with human subjects: an evolutionary frame for primary osteoarthritis. *Annals of the Rheumatic Diseases*, 53 (11), pp. 720-725.
- Alexander, R.McN. (1991). 'Characteristics and advantages of human bipedalism' in Rayner J.M.V., Wooton R.J., (eds). *Biomechanics in Evolution*. Cambridge: Cambridge University Press, pp. 225–266.
- Alexander, R.McN. (1993) Optimization of structure and movement of the legs of animals. *Journal of Biomechanics*, 26 (Suppl. 1), pp. 1-6.
- Alexander, R.McN. (2004) Bipedal animals, and their differences from humans. *Journal of Anatomy*, 204, pp. 321–330.
- Alexander, R.McN., Jayes, A.S., Maloiy, G.M.O., Wathuta, E.M. (1981) Allometry of the leg muscles of mammals. *Journal of Zoology London Series A*, 194, pp. 227-267.
- Almécija, S., Tallman, M., Alba, D.M., Pina, M., Moyà-Solà, S., Jungers, W.L. (2013) The femur of *Orrorin tugenensis* exhibits morphometric affinities with both Miocene apes and later hominins. *Nature Communications*, 4, pp. 2888.
- Amson, E., Arnold, P., van Heteren, A.H., Canoville, A., Nyakature, J.A. (2017) Trabecular architecture in the forelimb epiphyses of extant xenarthrans (Mammalia). *Frontiers in Zoology*, 14, pp. 52.
- Anderson, F.C, Pandy, M.G. (2001) Static and dynamic optimization solutions for gait are practically equivalent. *Journal of Biomechanics*, 34, pp. 153-161.
- Ankel-Simons, F. (2007) *Primate Anatomy: an introduction*. Burlington: Academic Press.
- Arnason, U., Gullberg, A., Janke, A. (1998) Molecular timing of primate divergences as estimated by two nonprimate calibration points. *Journal of Molecular Evolution*, 47, pp. 718-727.
- Avery, D.M. (2001) The Plio-Pleistocene vegetation and climate of Sterkfontein and Swartkrans, South Africa, based on micromammals. *Journal of Human Evolution*, 41, pp. 113-132.

- Baltzopoulos, V. (1995) Muscular and tibiofemoral joint forces during isokinetic concentric knee extension. *Clinical Biomechanics*, 10, pp. 208-214.
- Bamford, M. (1999) Pliocene fossil woods from an early hominid cave deposit, Sterkfontein, South Africa. *South African Journal of Science*, 95, pp. 231-237.
- Barak, M.M., Lieberman, D.E., Hublin, J.-J. (2011) A Wolff in sheep's clothing: trabecular bone adaptation in response to changes in joint loading orientation. *Bone* 49, pp. 1141-1151.
- Barak, M.M., Lieberman, D.E., Raichlen, D., Pontzer, H., Warrener, A.G., Hublin, J.-J. (2013a) Trabecular Evidence for a Human-Like Gait in *Australopithecus africanus*. *PLoS ONE*, 8: e77687.
- Barak, M.M., Lieberman, D.E., Hublin, J. (2013b) Of mice, rats and men: Trabecular bone architecture in mammals scales to body mass with negative allometry. *Journal of structural biology*, 183, pp. 123-131.
- Barak, M.M., Sherratt, E., Lieberman, D.E. (2017) Using principal trabecular orientation to differentiate joint loading orientation in the 3rd metacarpal heads of humans and chimpanzees. *Journal of Human Evolution*, 113, pp. 173-182.
- Barak, M.M., Weiner, S., Shahar, R. (2008) Importance of the integrity of trabecular bone to the relationship between load and deformation in rat femora: an optical metrology study. *Journal of Materials Chemistry*, 18, pp. 3855-3864.
- Bartholomew, G.A., Birdsell, J.B. (1953) Ecology and the protohominids. *American Anthropology*, 55, pp. 481-498.
- Basmajian, J.V. (1965) *Muscles alive: their functions revealed by electromyography*. Baltimore: Wilkins and Wilkins Co.
- Bauer, H.R. (1977). Chimpanzee bipedal locomotion in the Gombe National Park, East Africa. *Primates*, 18, pp. 913-921.
- Berge, C. (1994) How did the australopithecines walk? A biomechanical study of the hip and thigh of *Australopithecus afarensis*. *Journal of Human Evolution*, 26, pp. 259-273.
- Berger, L.R., de Ruiter, D.J., Churchill, S.E., Schmid, P., Carlson, K.J., Dirks, P.H.G.M., Kibii, J.M. (2010) *Australopithecus sediba*: A New Species of *Homo*-Like Australopithecine from South Africa. *Science*, 328 (5975), pp. 195-204.
- Berger, L.R., Hawks, J., de Ruiter, D.J., Churchill, S.E., Schmid, P., Deleuzene, L.K., Kivell, T.L., Garvin, H.M., Williams, S.A., DeSilva, J.M., Skinner, M.M., Musiba, C.M., Cameron, N., Holliday, T.W., Harcourt-Smith, W., Ackermann, R.R., Bastir, M., Bogin, B., Bolter, D., Brophy, J., Cofran, Z.D., Congdon, K.A., Deane, A.S., Dembo, M., Drapeau, M., Elliot, M.C., Feuerriegel, E.M., Garcia-Martinez, D., Green, D.J., Gurtov, A., Irish, J.D., Kruger, A., Laird, M.F., Marchi, D., Meyer, M.R., Nalla, S., Negash, E.W., Orr, C.M., Radovic, D., Schroeder, L., Scott, J.E., Throckmorton, Z., Tocheri, M.W., VanSickle, C., Walker, C.S., Wei, P., Zipfel, B. (2015) *Homo naledi*, a new species of the genus *Homo* from the Dinaledi Chamber, South Africa. *eLife* 4:e09560.
- Berger, L.R. (1994). *The functional morphology of the hominoid shoulder girdle, past and present*, Ph.D. Dissertation, University of the Witwatersrand.

- Bergmann, G., Deuretzbacher, G., Heller, M., Graichen, F., Rohlmann, A., Strauss, J., Duda, G.N. (2001) Hip forces and gait patterns from routine activities. *Journal of Biomechanics*, 34, pp. 859–71.
- Bergmann, G., Graichen, F., Rohlmann, A., Holger, L. (1997) Hip joint forces during load carrying. *Clinical Orthopaedics and Related Research*, 335, pp. 190-201.
- Berillon, G. (1999) Geometric pattern of the hominoid hallucal tarsometatarsal complex. Quantifying the degree of hallux abduction in early hominids. *Comptes-Rendus de l'Académie des Sciences, Paris, Série IIa*, 328, pp. 627-633.
- Bertram, J.E.A., Swartz, S.M. (1991) The law of bone transformation: a case of crying Wolff? *Biological Reviews*, 66, pp. 245-273.
- Biewener, A.A., Fazzalari, N.L., Konieczynski, D.D., Baudinette, R.V. (1996) Adaptive changes in trabecular architecture in relation to functional strain patterns and disuse. *Bone*, 19, pp. 1-8.
- Bishop, L.C., Pickering, T.R., Plummer, T., Thackeray, J.F. (1999) Paleoenvironment setting for the Oldowan Industry at Sterkfontein (abstract). Paper for presentation at the XV International Union for Quaternary Research (INQUA), Durban, South Africa.
- Bonneau, N., Baylac, M., Gagey, O., Tardieu, C. (2014) Functional integrative analysis of the human hip joint: The three-dimensional orientation of the acetabulum and its relation with the orientation of the femoral neck. *Journal of Human Evolution*, 69, pp. 55-69.
- Bonneau, N., Gagey, O., Tardieu, C. (2012) Biomechanics of the human hip joint. *Computer Methods in Biomechanics and Biomedical Engineering*, 15, pp. 197-199.
- Bookstein F. L. (1996) Biometrics, biomathematics and the morphometric synthesis. *Bulletin of Mathematical Biology*, 58 (2), pp. 313–365.
- Bookstein, F.L. (1991) *Morphometric Tools for Landmark Data: Geometry and Biology*. Cambridge, UK: Cambridge University Press.
- Bookstein, F.L. (1997) Landmark methods for forms without landmarks: morphometrics of group differences in outline shape. *Medical Image Analysis*, 1, pp. 225-243.
- Boyle, C., Kim, I.Y. (2011) Three-dimensional micro-level computational study of Wolff's law via trabecular bone remodeling in the human proximal femur using design space topology optimization. *Journal of Biomechanics*, 44, pp. 935-942.
- Braga, J. (1998) Chimpanzee variation facilitates the interpretation of the incisive suture closure in South African Plio-Pleistocene hominids. *American Journal of Physical Anthropology*, 105, pp. 121-135.
- Brain, C.K., Sillent, A. (1988) Evidence from the Swartkrans cave for the earliest use of fire. *Nature*, 336, pp. 464-466.
- Bramble, D.M., Lieberman, D.E. (2004) Endurance running and the evolution of *Homo*. *Nature*, 432, pp. 345-352.

- Brock, S.L., Ruff, C.B. (1988) Diachronic patterns of change in structural properties of the femur in the prehistoric American Southwest. *American Journal of Physical Anthropology*, 75, pp. 113-127.
- Brown, P., Sutikna, T., Morwood, M.J., Soejono, R.P., Jatmiko, Wayhu Saptomo, E., Awe Due, R. (2004) A new small-bodied hominin from the Late Pleistocene of Flores, Indonesia. *Nature*, 431, pp. 1055-1061.
- Burr, D.B., Piotrowski, G., Martin, R.B., Cook, P.N. (1982) Femoral mechanics in the lesser bushbaby (*Galago senegalensis*): Structural adaptations to leaping in primates. *Anatomical Record*, 202, pp. 419-429.
- Burr, D.B., Ruff, C.B., Johnson, C. (1989) Structural adaptations of the femur and humerus to arboreal and terrestrial environments in three species of macaque. *American Journal of Physical Anthropology*, 79, pp. 357-367.
- Butler, D., Noyes, F., Grood, E. (1980) Ligamentous restraints to anterior-posterior drawer in the human knee. *The Journal of Bone and Joint Surgery. American Volume*, 62 (2), pp. 259-270.
- Cant, J.G.H. (1987) Positional behavior of female Bornean orangutans (*Pongo pygmaeus*). *American Journal of Primatology*, 12, pp. 71-90.
- Carey, T.S., Crompton, R.H. (2005) The metabolic costs of 'bent hip, bent knee' walking in humans. *Journal of Human Evolution*, 48, pp. 25-44.
- Carlson, K.J. (2005) Investigating the form-function interface in African apes: Relationships between principal moments of area and positional behaviors in femoral and humeral diaphyses. *American Journal of Physical Anthropology*, 127, pp. 312-334.
- Carlson, K.J., Judex, S. (2007) Increased non-linear locomotion alters diaphyseal bone shape. *Journal of Experimental Biology*, 210, pp. 3117-3125.
- Carlson, K.J., Lublinsky, S., Judex, S. (2008) Do different locomotor modes during growth modulate trabecular architecture in the murine hindlimb? *Integrative and Comparative Biology*, 48, pp. 385-393.
- Carter, D.R., van der Meulen, M.C.H., Beaupré, G.S. (1996) Mechanical factors in bone growth and development. *Bone*, 18, pp. 5-10.
- Cartmill, M., Hylander, W.L., Shafland, J. (1987) *Human structure*. Cambridge, MA: Harvard University Press.
- Cavagna, G.A., Thys, H., Zamboni, A. (1976). Sources of external work in level walking and running. *Journal of Physiology London*, 262, pp. 639-657.
- Chang, G., Pakin, S.K., Schweitzer, M.E., Saha, P.K., Regatte, R.R. (2008) Adaptations in trabecular bone microarchitecture in Olympic athletes determined by 7T MRI. *Journal of Magnetic Resonance Imaging*, 27, pp. 1089-1095.
- Chen, H., Zhou, X., Shoumura, S., Emura, S., Bunai, Y. (2010) Age- and gender-dependent changes in three-dimensional microstructure of cortical and trabecular bone at the human femoral neck. *Osteoporosis International*, 21, pp. 627-636.

- Chevallier, A. (1977) Origine des ceintures scapulaires et pelviennes chez l'embryon d'oiseau. *Journal of Embryology and Experimental Morphology*, 42, pp. 275-292.
- Chirchir, H., Kivell, T.L., Ruff, C.B., Hublin, J.-J., Carlson, K.J., Zipfel, B., Richmond, B.G. (2015) Recent origin of low trabecular bone density in modern humans. *Proceedings of the National Academy of Sciences* 112 (2), pp. 366-371.
- Chirchir, H., Ruff, C.B., Helgen, K.M., Potts, R. (2016) Trabecular Bone mass and Daily Travel Distance in Mammals. *The FASEB Journal* 30:1_supplement, 779.15-779.15
- Chirchir, H., Ruff, C.B., Junno, J.-A., Potts, R. (2017) Low trabecular bone density in recent sedentary modern humans. *American Journal of Physical Anthropology*, 162, pp. 550-560.
- Choi, K., Goldstein, S.A. (1992) A comparison of the fatigue behavior of human trabecular and cortical bone tissue. *Journal of Biomechanics*, 25, pp. 1371-1381.
- Ciarelli, T.E., Fyhrie, D.P., Schaffler, M.B., Goldstein, S.A. (2000) Variations in three-dimensional cancellous bone architecture of the proximal femur in female hip fractures and in controls. *Journal of Bone and Mineral Research*, 15, pp. 32-40.
- Cignoni, P., Corsini, M., Ranzuglia, G. (2008) Meshlab: an open-source 3d mesh processing system. *ERCIM News*, 73, pp. 45-46.
- Clarke, B. (2008) Normal Bone Anatomy and Physiology. *Clinical Journal of the American Society of Nephrology*, 3, pp. 131-139.
- Clarke, R.J. (1985) 'Early Acheulean with *Homo habilis* at Sterkfontein', in Tobias, P.V (ed.). *Hominid Evolution: Past, Present and Future*. New York: Alan R. Liss, pp. 287-298.
- Clarke, R.J. (1988) 'A new *Australopithecus* cranium from Sterkfontein and its bearing on the ancestry of *Paranthropus*', in Grine, F. (ed.). *Evolutionary History of the 'Robust' Australopithecines*. New York, Aldine de Gruyter, pp. 287-292.
- Clarke, R.J. (1998) The first ever discovery of a well-preserved skull and associated skeleton of *Australopithecus*. *South African Journal of Science*, 94, pp. 460-463.
- Clarke, R.J. (2008) Latest information on Sterkfontein's *Australopithecus* skeleton and a new look at *Australopithecus*. *South African Journal of Science*, 104, pp. 443-449.
- Clarke, R.J. (2013) *Australopithecus* from Sterkfontein Caves, South Africa', in Reed K., Fleagle J., Leakey R. (eds). *The Paleobiology of Australopithecus. Vertebrate Paleobiology and Paleoanthropology*. Dordrecht: Springer.
- Clarke, R.J., Tobias, P.V. (1995) Sterkfontein member 2 foot bones of the oldest South African hominid. *Science*, 269 (5223), pp. 521-524.
- Cooke, S.B., Terhune, C.E. (2015) Form, function and geometric morphometrics. *The Anatomical Record*, 298, pp. 5-28.
- Cotter, M.M., Simpson, S.W., Latimer, B.M, Hernandez, C.J. (2009) Trabecular microarchitecture of hominoid thoracic vertebrae. *The Anatomical Record*, 292, pp. 1098-1106.

- Crelin, E.S. (1988) Ligament of the head of the femur in the orangutan and Indian elephant. *The Yale journal of biology and medicine*, 61 (5), pp. 383-388.
- Crompton, R.H., Li, Y., Wang, W., Günther, M., Savage, R. (1998) The mechanical effectiveness of erect and 'bent-knee, bent-hip' bipedal walking in *Australopithecus afarensis*. *Journal of Human Evolution*, 35, pp. 55-74.
- Crompton, R.H., Sellers, W.I., Thorpe, S.K.S. (2010) Arboreality terrestriality and bipedalism. *Philosophical Transactions of the Royal Society B: Biological Sciences*, 365 (1556), pp. 3301-3314.
- Crompton, R.H., Vereecke, E.E., Thorpe, S.K.S. (2008) Locomotion and posture from the common hominoid ancestor to fully modern hominins, with special reference to the last common panin/hominin ancestor. *Journal of Anatomy*, 212, pp. 501-543.
- Cunningham, C.A., Black, S.M. (2009a). Iliac cortical thickness in the neonate – the gradient effect. *Journal of Anatomy*, 215, pp. 364-370.
- Cunningham, C.A., Black, S.M. (2009b). Development of the fetal ilium – challenging concepts of bipedality. *Journal of Anatomy*, 214, pp. 91-99.
- Cunningham, C.A., Black, S.M. (2009c) Anticipating bipedalism: trabecular organization in the newborn ilium. *Journal of Anatomy* 214, pp. 817-829.
- Curnoe, D., Tobias, P.V.T. (2006) Description, new reconstruction comparative anatomy, and classification of the Stw 53 cranium, with discussions about the taxonomy of other southern African early *Homo* remains. *Journal of Human Evolution*, 50, pp. 36-77.
- Currey, J.D. (2002) *Bones: Structure and Mechanics*. Princeton: Princeton University Press.
- D'Août, K., Aerts, P., De Clercq, D., De Meester, K., Van Elsacker, L. (2002) Segment and joint angles of hind limb during bipedal and quadrupedal walking of the bonobo (*Pan paniscus*). *American Journal of Physical Anthropology*, 119, pp. 37-51.
- D'Août, K., Vereecke, E., Schoonaert, K., De Clercq, D., Van Elsacker, L., Aerts, P. (2004) Locomotion in bonobos (*Pan paniscus*): differences and similarities between bipedal and quadrupedal terrestrial walking, and a comparison with other locomotor modes. *Journal of Anatomy*, 204, pp. 353-361.
- Dart, R.A. (1925) *Australopithecus africanus*: the man-ape of South Africa. *Nature*, 115, pp. 195–199.
- Dart, R.A. (1959) *Adventures with the missing link*. New York: Harper and Brothers.
- Darwin, C. (1871) *The decent of man, and selection in relation to sex*. London: John Murray (Reprinted in 1981 by Princeton University).
- Day, M.H. (1971) Postcranial Remains of *Homo erectus* from Bed IV, Olduvai Gorge, Tanzania. *Nature*, 232, pp. 383-387.
- Day, W.H., Swanson, S.A.V., Freeman, M.A.R. (1975) Contact pressures in the loaded human cadaver hip. *Journal of Bone and Joint Surgery, British*, 57, pp. 302-313.
- De Groote, I. (2011) The Neanderthal lower arm. *Journal of Human Evolution*, 61, pp. 396-410

- Della Croce, U., Riley, P.O., Lelas, J.L., Kerrigan, D.C., (2001) A refined view of the determinants of gait. *Gait & Posture*, 14, pp. 79-84.
- Delson, E. (1988) 'Chronology of South African australopith site units', in Grine, F.E. (ed.). *Evolutionary History of the "Robust" Australopith ecines*. New York: Aldine, pp. 317-324.
- Demes, B., Larson, S.G., Stern, J.T. Jr, Jungers, W.L., Biknevicius, A.R., Schmitt, D. (1994) The kinetics of primate quadrupedalism: "hindlimb drive" reconsidered. *Journal of Human Evolution* 26, pp. 353-374.
- Demes, B., Stern Jr., J.T., Hausman, M.R., Larson, S.G., McLeod, K.J., Rubin, C.T. (1998) Patterns of strain in the macaque ulna during functional activity. *American Journal of Physical Anthropology*, 106, pp. 87-100.
- Dempster, D.W. (1992) 'Bone remodeling', in Coe F.L., Favus M.J. (eds.). *Disorders of Bone and Mineral Metabolism*. New York: Raven Press, pp. 355-380.
- Dequeker, J., Nijis, J., Verstaeten, A., Geusen, P., Gevers, G. (1987) Genetic determinants of bone mineral content at the spine and radius: A twin study. *Bone*, 8, pp. 207-209.
- DeSilva, J.M., Devlin, M.J. (2012) A comparative study of the trabecular bony architecture of the talus in humans, non-human primates, and *Australopithecus*. *Journal of Human Evolution*, 63, pp. 536-551.
- DeSilva, J.M., Holt, K.G., Churchill, S.E., Carlson, K.J., Walker, C.S., Zipfel, B., Berger, L.R. (2013) The lower limb and mechanics of walking in *Australopithecus sediba*. *Science*, 340, pp. 6129.
- Ding, M. (2000) Age variations in the properties of human tibial trabecular bone and cartilage. *Acta Orthopaedica Scandinavica Suppl.*, 292, pp. 1-45.
- Diogo, R., Potau, J.M., Pastor, J.F., de Paz, F.J., Ferrero, E.M., Bello, G., Barbosa, M., Aziz, M.A., Arias-Martorell, J., Wood, B.A. (2013a). *Photographic and descriptive musculoskeletal atlas of orangutans: with notes on the attachments, variations, innervations, function and synonymy and weight of the muscles*. Florida: CRC Press.
- Diogo, R., Potau, J.M., Pastor, J.F., de Paz, F.J., Ferrero, E.M., Bello, G., Barbosa, M., Aziz, M.A., Burrows, A.M., Arias-Martorell, J., Wood, B.A. (2013b). *Photographic and descriptive musculoskeletal atlas of chimpanzees: with notes on the attachments, variations, innervation, function and synonymy and weight of the muscles*. Florida: CRC Press.
- Diogo, R., Potau, J.M., Pastor, J.F., de Paz, F.J., Ferrero, E.M., Bello, G., Barbosa, M., Wood, B.A. (2010) *Photographic and Descriptive Musculoskeletal Atlas of Gorilla: With Notes on the Attachments, Variations, Innervation, Synonymy and Weight of the Muscles*. Florida: CRC Press.
- Doran, D.M, McNeilage, A. (1998) Gorilla ecology and behavior. *Evolutionary Anthropology: Issues, News, and Reviews*, 6, pp. 120-131.
- Doran, D.M. (1992) The ontogeny of chimpanzee and pygmy chimpanzee locomotor behavior: a case study of pedomorphism and its behavioral correlates. *Journal of Human Evolution*, 23 (2), pp. 139-157.

- Doran, D.M. (1993a) Comparative locomotor behavior of chimpanzees and bonobos: The influence of morphology on locomotion. *American Journal of Physical Anthropology*, 91 (1), pp. 83-98.
- Doran, D.M. (1993b) Sex differences in adult chimpanzee positional behavior: the influence of body size on locomotion and posture. *American Journal of Physical Anthropology*, 91, pp. 99-115.
- Doran, D.M. (1996) 'Comparative positional behavior of the African apes' in McGrew, W., Marchant, L., Nishida, T. (eds). *Great Ape Societies*. Cambridge: Cambridge University Press, pp. 213–224.
- Doran, D.M. (1997) Ontogeny of locomotion in mountain gorillas and chimpanzees. *Journal of Human Evolution*, 32 (4), pp. 323-344.
- Doube, M., Kłosowski, M.M., Arganda-Carreras, I., Cordelières, F.P., Dougherty, R.P., Jackson, J.S., Schmid, B., Hutchinson, J.R., Shefelbine, S.J. (2010) BoneJ: Free and extensible bone image analysis in ImageJ. *Bone*, 47(6), pp. 1076-1079.
- Doube, M., Kłosowski, M.M., Wiktorowicz-Conroy, A., Hutchinson, J., Shefelbine, S. (2011) Trabecular bone scales allometrically in mammals and birds. *Proceedings of the Royal Society B: Biological Sciences*, 278 (1721), pp. 3067-3073.
- Dryden I.L., Mardia K.V. (1998) *Statistical Shape Analysis*. London, Chichester: John Wiley & Sons.
- Ducher, G., Prouteau, S., Courteix, D., Benhamou, C. (2004) Cortical and trabecular bone at the forearm show different adaptation patterns in response to tennis playing. *Journal of Clinical Densitometry*, 7, pp. 399-405.
- Dumont, M., Laurin, M., Jacques, F., Pellé, E., Dabin, W., de Buffrénil, V. (2013) Inner architecture of vertebral centra in terrestrial and aquatic mammals: A two-dimensional comparative study. *Journal of Morphology*, 274, pp. 570-584.
- Dunmore, C.J., Wollny, G., Skinner, M.M. (2018) MIA-Clustering: a novel method for segmentation of paleontological material. *PeerJ*, 6, e4374
- Eiseley, L.C. (1953) Fossil man. *Scientific American*, 189, pp. 65-72.
- Eizirik, E., Murphy, W.J., Springer, M.S., O'Brien, S.J. (2004) 'Molecular phylogeny and dating of early primate divergences', in Ross, C.F., Kay, R.F. (eds). *Anthropoid Origins: New Visions*. New York: Kluwer Academic/Plenum Publishers, pp. 45-64.
- Elftman, H., Manter, J. (1935) The evolution of the human foot, with special reference to the joints. *Journal of Anatomy*, 70, pp. 56-67.
- English, T.A, Kilvington, M. (1979) In vivo records of hip loads using a femoral implant with telemetric output (a preliminary report). *Journal of Biomedical Engineering*, 1 (2), pp. 111-115.
- Eriksen, E.F. (1986) Normal and pathological remodeling of human trabecular bone: three dimensional reconstruction of the remodeling sequence in normals and in metabolic bone disease. *Endocrine Reviews*, 7, pp. 379-408.
- Eriksen, E.F. (2010) Cellular mechanisms of bone remodelling. *Reviews in Endocrine and Metabolic Disorders*, 11, pp. 219-227.

- Etkin, W. (1954) Social behavior and the evolution of man's faculties. *The American Naturalist*, 88, pp. 129-142.
- Fajardo, R.J., DeSilva, J.M., Manoharan, R.K., Schmitz, J.E., Maclatchy, L.M., Boussein, M.L. (2013) Lumbar vertebral body bone microstructural scaling in small to medium-sized strepsirhines. *The Anatomical Record*, 296, pp. 210-226.
- Fajardo, R.J., Müller, R. (2001) Three-dimensional analysis of nonhuman primate trabecular architecture using micro-computed tomography. *American Journal of Physical Anthropology*, 115, pp. 327-336.
- Fajardo, R.J., Müller, R., Ketcham, R.A., Colbert, M. (2007) Nonhuman anthropoid primate femoral neck trabecular architecture and its relationship to locomotor mode. *The Anatomical Record: Advances in Integrative Anatomy and Evolutionary Biology*, 290, pp. 422-436.
- Feldkamp, L.A., Goldstein, S.A., Parfitt, A.M., Jesion, G., Kleerekoper, M. (1989). The direct examination of three-dimensional bone architecture in vitro by computed tomography. *Journal of Bone and Mineral Research* 4, pp. 3-11.
- Finestone, E.M., Brown, M.H., Ross, S.R., Pontzer, H. (2018) Great ape walking kinematics: Implications for hominoid evolution. *American Journal of Physical Anthropology* 166 (1), pp. 43-55.
- Fleagle, J.G., Stern, J.T. Jr, Jungers, W.L., Susman, R.L., Vangor, A.K., Wells, J.P. (1981) Climbing: a biomechanical link with brachiation and with bipedalism. *Symposia of the Zoological Society of London*, 48, pp. 359-375.
- Ford, C.M., Keaveny, T.M. (1996) The dependence of shear failure properties of bovine tibial trabecular bone on apparent density and d trabecular orientation. *Journal of Biomechanics*, 29, pp. 1309-1317.
- Forsberg, H. (1985) Ontogeny of human locomotor control I. Infant stepping, supported locomotion and transition to independent locomotion. *Experimental Brain Research*, 57, pp 480-493.
- Frost, H.M. (2004) A 2003 update of bone physiology and Wolff's law for clinicians. *The Angle Orthodontist*, 74, pp. 3-15.
- Frost, H.M., Ferretti, J.L., Jee, W.S.S. (1998) Perspectives: some roles of mechanical usage, muscle strength, and the mechanostat in skeletal physiology, disease, and research. *Calcified Tissue International*, 62, pp. 1-7.
- Fyhrie, D.P., Hamid, M.S. (1993) The probability distribution of trabecular level strains for vertebral cancellous bone. Transactions of the 39th Annual Meeting of the Orthopaedic Research Society, San Francisco.
- Garnero, P., Arden, N.K., Griffiths, G., Delmas, P.D., Spector, T.D. (1996) Genetic influence on bone turnover in postmenopausal twins. *The Journal of Clinical Endocrinology and Metabolism*, 81, pp. 140-146.
- Gebo, D.L. (1992) Plantigrady and foot adaptation in African apes: Implications for hominid origins. *American Journal of Physical Anthropology*, 89, pp. 29-58.

- Georgiou, L., Kivell, T.L., Pahr, D.H., Buck, L.T., Skinner, M.M. (2019) Trabecular architecture of the great ape and human femoral head. *Journal of Anatomy*, doi:10.1111/joa.12957.
- Georgiou, L., Kivell, T.L., Pahr, D.H., Skinner, M.M. (2018) Trabecular bone patterning in the hominoid distal femur. *PeerJ*, 6, e5156.
- Giarmatzis, G., Jonkers, I., Wesseling, M., Van Rossom, S., Verschueren, S. (2015) Loading of hip measured by hip contact forces at different speeds of walking and running. *Journal of Bone and Mineral Research*, 30 (8), pp. 1431-1440.
- Gibson, L.J., (1985) The mechanical behavior of cancellous bone. *Journal of Biomechanics*, 18, pp. 317-328.
- Goldstein, S.A. (1987) The mechanical properties of trabecular bone: dependence on anatomic location and function. *Journal of Biomechanics*, 20, pp. 1055-1061.
- Goldstein, S.A., Goulet, R., McCubbrey, D. (1993) Measurement and significance of three-dimensional architecture to the mechanical integrity of trabecular bone. *Calcified Tissue International*, 53, pp. 127-133.
- Gollehon, D., Torzilli, P., Warren, R. (1987) The role of the posterolateral and cruciate ligaments in the stability of the human knee. A biomechanical study. *Journal of Bone and Joint Surgery American Volume*, 69, pp. 233-242.
- Gosman, J., Ketcham, R. (2009) Patterns in ontogeny of human trabecular bone from Sunwatch village in prehistoric Ohio Valley: general features of microarchitectural change. *American Journal of Physical Anthropology*, 138, pp. 318-332.
- Gould, F.D.H. (2014) To 3D or not to 3D, that is the question: Do 3D surface analyses improve the ecomorphological power of the distal femur in placental mammals? *PLOS ONE*, 9, e91719.
- Goulet, R.W., Goldstein, S.A., Ciarelli, M.J., Kuhn, J.L., Brown, M.B., Feldkamp, L.A. (1994) The relationship between the structural and orthogonal compressive properties of trabecular bone. *Journal of Biomechanics*, 27, pp. 375-389.
- Green, D.J., Chirchir, H., Mbua, E., Harris, J.W.K., Braun, D.R., Griffin, N.L., Richmond, B.G. (2018) Scapular anatomy of *Paranthropus boisei* from Ileret, Kenya. *Journal of Human Evolution*, 152, pp. 181-192.
- Green, D.J., Gordon, A.D., Richmond, B.G. (2007) Limb-size proportions in *Australopithecus afarensis* and *Australopithecus africanus*. *Journal of Human Evolution*, 52, pp. 187-200.
- Griffin, N.L., D'Août, K., Richmond, B., Gordon, A., Aerts, P. (2010a) Comparative in vivo forefoot kinematics of *Homo sapiens* and *Pan paniscus*. *Journal of Human Evolution*, 59, pp. 608-619.
- Griffin, N.L., D'Aout, K., Ryan, T., Richmond, B., Ketcham, R., Postnov, A. (2010b). Comparative forefoot trabecular bone architecture in extant hominids. *Journal of Human Evolution*, 59, pp. 202-213.

- Gross, T., Kivell, T.L., Skinner, M.M., Nguyen, N.H., Pahr, D.H. (2014) A CT-image-based framework for the holistic analysis of cortical and trabecular bone morphology. *Palaeontologia Electronica*, 17, pp. 1-13.
- Gunness-Hey, M., Hock, J.M. (1984) Increased trabecular bone mass in rats treated with human synthetic parathyroid hormone. *Metabolic Bone Disease and Related Research* 5 (4), pp. 177-181.
- Gunz P., Mitteroecker P., Bookstein F.L. (2005) 'Semilandmarks in Three Dimensions', in Slice D.E. (ed) *Modern Morphometrics in Physical Anthropology*. Developments in Primatology: Progress and Prospects. Boston, MA: Springer.
- Haeusler, M. (2002) New insights into the locomotion of *Australopithecus africanus* based on the pelvis. *Evolutionary Anthropology: Issues, News, and Reviews*, 11, pp. 53-57.
- Haile-Selassie, Y. (2001) Late Miocene hominids from the Middle Awash, Ethiopia. *Nature*, 412, pp. 178–181.
- Haile-Selassie, Y., Saylor, B.Z., Deino, A., Levin, N.E., Alene, M., Latimer, B.M. (2012) A new hominin foot from Ethiopia shows multiple Pliocene bipedal adaptations. *Nature*, 483, pp. 565-569.
- Hall, B.K. (1972) Immobilization and cartilage transformation into bone in the embryonic chick. *The Anatomical Record*, 173, pp. 391-404.
- Hammond, A.S. (2014) In vivo baseline measurements of hip joint range of motion in suspensory and nonsuspensory anthropoids. *American Journal of Physical Anthropology*, 153 (3), pp. 417-434.
- Hanna, J.B., Granatosky, M.C., Rana, P., Schmitt, D. (2017) The evolution of vertical climbing in primates: Evidence from reaction forces. *Journal of Experimental Biology*, 20, pp. 3039-3052.
- Harada, Y., Wevers, H.W., Cooke, T.D.V. (1988) Distribution of bone strength in the proximal tibia. *The Journal of arthroplasty*, 3, pp. 167-175.
- Harcourt-Smith, W., Aiello, L.C. (2004) Fossils, feet and the evolution of human bipedal locomotion. *Journal of Anatomy*, 204, pp. 403-416.
- Hardt, D.E. (1978) Determining muscle forces in the leg during normal human walking—an application and evaluation of optimization methods. *ASME. Journal of Biomechanical Engineering*, 100(2), pp. 72-78.
- Harmon, E.H. (2007) The shape of the hominoid proximal femur: a geometric morphometric analysis. *Journal of Anatomy*, 210 (2), pp. 170-185.
- Harmon, E.H. (2009a) Size and shape variation in the proximal femur of *Australopithecus africanus*. *Journal of Human Evolution* 56 (6), pp. 551-559.
- Harmon, E.H. (2009b) The shape of the early hominin proximal femur. *American Journal of Physical Anthropology* 139 (2), pp. 154-171.
- Harrigan, T.P., Jasty, M., Mann, R.W., Harris, W.H. (1988) Limitations of the continuum assumption in cancellous bone. *Journal of Biomechanics*, 21, pp. 269-275.

- Harris, M., Nguyen, T.V., Howard, G.M., Kelly, P.J., Eisman, J.A. (1998) Genetic and environmental correlations between bone formation and bone mineral density: A twin study. *Bone* 22 (2), pp. 141-145.
- Harrison, L.C.V., Nikander, R., Sikio, M., Luukaala, T., Helminen, M.T., Ryymin, P., Soimakallio, S., Eskola, H.J., Dastidar, P., Sievanen, H. (2011) MRI texture analysis of femoral neck: detection of exercise load-associated differences in trabecular bone. *Journal of Magnetic Resonance Imaging*, 34, pp. 1359-1366.
- Harrison, T.J. (1961) The influence of the femoral head on pelvic growth and acetabular form in the rat. *Journal of Anatomy*, 95, pp. 12-24.
- Hatala, K.G., Roach, N.T., Ostrofsky, K.R., Wunderlich, R.E., Dingwall, H.L., Villmoare, B.A., Green, D.J., Harris, J.W.K., Braun, D.R., Richmond, B.G. (2016) Footprints reveal direct evidence of group behavior and locomotion in *Homo erectus*. *Scientific Reports*, 6, pp. 28766.
- Hauser, D.L., Fox, J.C., Sukin, D., Mudge, B., Coutts, R.D. (1997) Anatomic variation of structural properties of periacetabular bone as a function of age: A quantitative computed tomography study. *The Journal of Arthroplasty*, 12 (7), pp. 804-811.
- Häusler, M., Berger, L. (2001) Stw 441/465: a new fragmentary ilium of a small-bodied *Australopithecus africanus* from Sterkfontein, South Africa. *Journal of Human Evolution*, 40, pp. 411-417.
- Havill, L.M., Allen, M.R., Bredbenner, T.L, Burr, D.B., Nicoletta, D.P., Turner, C.H., Warren, D.M., Mahaney, M.C. (2010) Heritability of lumbar trabecular bone mechanical properties in baboons. *Bone*, 46, pp. 835-840.
- Hefzy, M.S., Jackson, W.T., Saddemi, S.R., Hsieh, Y.F. (1992) Effects of tibial rotations on patellar tracking and patello-femoral contact areas. *Journal of Biomedical Physics and Engineering*, 14, 329-343.
- Heiple, K.G., Lovejoy, C.O. (1971) The distal femoral anatomy of *Australopithecus*. *American Journal of Physical Anthropology*, 35, pp. 75-84.
- Herries, A.I.R., Shaw, J. (2011) Palaeomagnetic analysis of the Sterkfontein palaeocave deposits: implications for the age of the hominin fossils and stone tool industries. *Journal of Human Evolution*, 60, pp. 523-539.
- Herskovitz, I., Speirs, M.S., Frayer, D., Nadel, D., Wish-Baratz, S., Arensburg, B. (1995) Ohalo II H2: A 19,000-year-old skeleton from a water-logged site at the Sea of Galilee, Israel. *American Journal of Physical Anthropology*, 96, pp. 215-234.
- Hewes, G.W. (1961) Food transport and the origin of hominid bipedalism. *American Anthropologist*, 63, pp. 687-710.
- Hildebrand, T., Rügsegger, P. (1997) A new method for the model-independent assessment of thickness in three-dimensional images. *Journal of microscopy*, 185 (1), pp. 67-75.
- Hipp, J. A., Rosenberg, A. E., Hayes, W. C. (1992) Properties of Trabecular Bone Within and Adjacent to Osseous Metastases. *J. Bone Miner. Res.*, 7: 1165-1171.

- Hoffler, C.E., McCreadie, R., Smith, E.A., Goldstein, S.A. (2000) 'A hierarchical approach to exploring bone mechanical properties', in An Y.H., Draughn R.A. (Eds.). *Mechanical Testing of Bone and the Bone-Implant Interface*. Boca Raton: CRC Press, pp. 133-149.
- Hofstetter, A.M., Niemitz, C. (1998) Comparative gait analyses in apes [abstract]. *Folia Primatologica*, 69, pp. 233–234.
- Hogervorst, T., Bouma, H.W., de Vos, J. (2009) Evolution of the hip and pelvis. *Acta Orthopaedica*, 80, pp. 1-39.
- Hollister, S.J., Brennan, J.M., Kikuchi, N. (1994) A homogenization sampling procedure for calculating trabecular bone effective stiffness and tissue level stress. *Journal of Biomechanics*, 27, pp. 433-444.
- Hordon, L.D., Raisi, M., Aaron, J.E., Paxton, S.K., Beneton, M., Kanis, J.A. (2000) Trabecular architecture in women and men of similar bone mass with and without vertebral fracture: I. Two-dimensional histology. *Bone*, 27:271-276. 497
- Hughes, A.R., Tobias, P.V. (1977) A fossil skull probably of the genus *Homo* from Sterkfontein, Transvaal. *Nature*, 265, pp. 310.
- Huiskes R, Ruimerman R, van Lenthe GH, Janssen, J.D. (2000) Effects of mechanical forces on maintenance and adaptation of form in trabecular bone. *Nature*, 405, pp. 704-706.
- Hunt, K.D. (1991a). Mechanical implications of chimpanzee positional behavior. *American Journal of Physical Anthropology*, 86, pp. 521–536.
- Hunt, K.D. (1991b) Positional behavior in the Hominoidea. *International Journal of Primatology*, 12, pp. 95-118.
- Hunt, K.D. (1992) Positional behavior of *Pan troglodytes* in the Mahale Mountains and Gombe Stream National Parks, Tanzania. *American Journal of Physical Anthropology*, 87, pp. 83-105.
- Hunt, K.D. (1996). The postural feeding hypothesis: an ecological model for the evolution of bipedalism. *South African Journal of Science*, 92, pp. 77-90.
- Inman, V.T., Ralston, H.J., Todd, F. (1981) *Human Walking*. Baltimore: Williams and Wildens.
- Ishikawa, M., Pakaslahti, J., Komi, P.V. (2006) Medial gastrocnemius muscle behavior during human running and walking. *Gait & Posture*, 25, pp. 380-384.
- Isler, K. (2002) Characteristics of vertical climbing in African apes. *Senckenburg Lethaea*, 82, pp. 115–124.
- Isler, K. (2005) 3D-Kinematics of vertical climbing in hominoids. *American Journal of Physical Anthropology*, 126, pp. 66–81.
- Isler, K., Thorpe, S.K.S. (2003) Gait parameters in vertical climbing of captive, rehabilitant and wild Sumatran orang-utans (*Pongo pygmaeus abelii*). *Journal of Experimental Biology*, 206, pp. 4081-4096.
- Jablonski, N.G., Chaplin, G. (1993) Origin of habitual terrestrial bipedalism in the ancestor of the Hominidae. *Journal of Human Evolution*, 24, pp. 259-280.

- Jenkins, F.A. (1972) Chimpanzee bipedalism: cineradiographic analysis and implications for the evolution of gait. *Science* 178 (4063), pp. 877-879.
- Jolly, C.J. (1970) The seed-eaters: a new model for hominoid differentiation based on a baboon analogy. *Man* 5, pp. 1-26.
- Jones, H.H., Priest, J.D., Hayes, W.C., Tichenor, C.C., Nagel, D.A. (1977) Humeral hypertrophy in response to exercise. *Journal Of Bone And Joint Surgery, American volume*, 59, pp. 204-208.
- Judex, S., Boyd, S., Qin, Y.X., Turner, S., Ye, K., Muller, R., Rubin, C. (2003) Adaptations of trabecular bone to low magnitude vibrations result in more uniform stress and strain under load. *Annals of Biomedical Engineering*, 31, pp. 12-20.
- Judex, S., Donahue, L.R., Rubin, C. (2002) Genetic predisposition to low bone mass is paralleled by an enhanced sensitivity to signals anabolic to the skeleton. *The FASEB Journal*, 16, pp. 1280-1282.
- Judex, S., Garman, R., Squire, M., Donahue, L., Rubin, C. (2004) Genetically Based Influences on the Site-Specific Regulation of Trabecular and Cortical Bone Morphology. *Journal of Bone and Mineral Research*, 19, pp. 600-606.
- Jungers, W.L. (1988) Relative joint size and hominoid locomotor adaptations with implications for the evolution of hominid bipedalism. *Journal of Human Evolution*, 17, pp. 247-265.
- Keaveny, T.M., Hayes, W.C. (1993) A 20-Year Perspective on the Mechanical Properties of Trabecular Bone. *Journal of Biomechanical Engineering*, 115, pp. 534-542.
- Keaveny, T.M., Morgan, E.F., Niebur, G.L., Yeh, O.C. (2001) Biomechanics of trabecular bone. *Annual Review of Biomedical Engineering*, 3, pp. 307-333.
- Keaveny, T.M., Wachtel, E.F., Ford, C.M., Hayes, W.C. (1994) Differences between the tensile and compressive strengths of bovine tibial trabecular bone depend on modulus. *Journal of Biomechanics* 27, pp. 1137-1146.
- Kellis, E. 2001. Tibiofemoral joint forces during maximal isokinetic eccentric and concentric efforts of the knee flexors. *Clinical Biomechanics*, 16, pp. 229-236.
- Kelly, P.J., Hopper, J.L., Macaskill, G.T., Pocock, N.A., Sambrook, P.N., Eisman, J.A. (1991) Genetic factors in bone turnover. *The Journal of Clinical Endocrinology and Metabolism*, 72, pp. 808-813.
- Kharb, A., Saini, V., Jain, Y.K., Dhiman, S. (2011) A review of gait cycle and its parameters. *IJCEM*, 13, pp 78-83.
- Kibii, J.M., Churchill, S.E., Schmid, P., Carlson, K.J., Reed, N.D., de Ruiter, D.J., Berger, L.R. (2011) A Partial Pelvis of Australopithecus sediba. *Science*, 333, pp. 1407-1411.
- Kim, I.Y., Kwak, B.M. (2002) Design space optimization using a numerical design continuation method. *Journal for Numerical Methods in Engineering*, 53, pp. 1979-2002.
- Kirschmann, E. (1999) Das Zeitalter der Werfer—eine neue Sicht des Menschen. Kirschmann, Hannover.

- Kivell, T.L. (2016) A review of trabecular bone functional adaptation: what have we learned from trabecular analyses in extant hominoids and what can we apply to fossils? *Journal of Anatomy*, 228 (4), pp. 569-594.
- Kivell, T.L., Skinner, M.M., Lazenby, R., Hublin, J.-J. (2011) Methodological considerations for analyzing trabecular architecture: an example from the primate hand. *Journal of Anatomy* 218, pp. 209-225.
- Kleerekoper, M., Villanueva, A.R., Stanciu, J., Rao, D.S., Parfitt, A.M. (1985) The role of three-dimensional trabecular microstructure in the pathogenesis of vertebral compression fractures. *Calcified Tissue International*, 37, pp. 594-597.
- Kopperdahl, D.L., Keaveny, T.M. (1998) Yield strain behavior of trabecular bone. *Journal of Biomechanics*, 31, pp. 601-608.
- Kuman, K. (1994a) The archaeology of Sterkfontein: preliminary findings on site formation and cultural change. *South African Journal of Science*, 90, pp. 215-219.
- Kuman, K. (1994b) The archaeology of Sterkfontein-past and present. *Journal of Human Evolution*, 27, pp. 471-495.
- Kuman, K., Clarke, R.J. (2000) Stratigraphy, artefact industries and hominid associations for Sterkfontein, Member 5. *Journal of Human Evolution*, 38, pp. 827-847.
- Kuo, S., Desilva, J.M., Devlin, M.J., McDonald, G., Morgan, E.F. (2013) The Effect of the Achilles Tendon on Trabecular Structure in the Primate Calcaneus. *The Anatomical Record*, 296, pp. 1509-1517.
- Kuroda, S. (1992) 'Ecological interspecies relationships between gorillas and chimpanzees in the Ndoki-Nouabale Reserve, Northern Congo' in Itoigawa N., Sugiyama Y., Sackett G., Thompson R.K.R., (eds). *Topics in Primatology, vol. 2: Behavior Ecology and Conservation*. Tokyo: University of Tokyo Press, pp. 385-394.
- Kutzner, I., Heinlein, B., Graichen, F., Bender, A., Rohlmann, A., Halder, A., Beier, A., Bergmann, G. (2010) Loading of the knee joint during activities of daily living measured in vivo in five subjects. *Journal of Biomechanics*, 43, pp. 2164-2173.
- Lafortune, M.A., Cavanagh, P.R., Sommer, H.J. III, Kalenak, A. (1992) Three-dimensional kinematics of the human knee during walking. *Journal of biomechanics*, 25, pp. 347-357.
- Lazenby, R.A., Skinner, M.M., Hublin, J., Boesch, C. (2011a) Metacarpal trabecular architecture variation in the chimpanzee (*Pan troglodytes*): Evidence for locomotion and tool-use? *American Journal of Physical Anthropology*, 44, pp. 215-225.
- Lazenby, R.A., Skinner, M.M., Kivell, T.L., Hublin, J.-J. (2011b) Scaling VOI size in 3D μ CT studies of trabecular bone: a test of the over-sampling hypothesis. *American Journal of Physical Anthropology*, 144, pp. 196-203.
- Le Damany, P. (1905) L'adaptation de l'homme à la station debout. *Journal of Anatomy Physiol.*, 2, pp. 133-170.
- Lee, C.R., Farley, C.T. (1998). Determinants of the center of mass trajectory in human walking and running. *Journal of Experimental Biology*, 201, pp. 2935-2944.

- Lee, K., Jessop, H., Suswillo, R., Zaman, G., Lanyon, L. (2003). Endocrinology: bone adaptation requires oestrogen receptor-alpha. *Nature*, 424, pp. 389.
- Lee, L.F., O'Neill, M.C., Demes, B., LaBoda, M.D., Thompson, N.E., Larson, S.G., Stern, J.T. Jr, Umberger, B.R. (2012) Joint kinematics in chimpanzee and human bipedal walking [abstract]. *Hip*, 20, pp. 10.
- Lee, M.C., Ebersson, C.P. (2006) Growth and development of the child's hip. *Orthopedic Clinics of North America*, 37, pp. 119-132.
- Lewton, K.L. (2015) In vitro bone strain distributions in a sample of primate pelvises. *Journal of Anatomy*, 226, pp. 458-477.
- Lichtwark, G.A., Bougoulias, K., Wilson, A.M. (2007) Muscle fascicle and series elastic element length changes along the length of the human gastrocnemius during walking and running. *Journal of Biomechanics*, 40, pp. 157-164.
- Lieberman, D.E., Pearson, O.M., Polk, J.D., Demes, B., Crompton, A.W. (2003) Optimization of bone growth and remodeling in response to loading in tapered mammalian limbs. *Journal of Experimental Biology*, 206, pp. 3125-3138.
- Lieberman, D.E., Raichlen, D.A., Pontzer, H., Bramble, D.M., Cutright-Smith, E. (2006) The human gluteus maximus and its role in running. *Journal of Experimental Biology*, 209, pp. 2143-2155.
- Lorenzo, C., Arsuaga, J-L., Carretero, J-M. (1999) Hand and foot remains from the Gran Dolina Early Pleistocene site (Sierra de Atapuerca, Spain). *Journal of Human Evolution*, 37, pp. 501-522.
- Lovejoy, C.O. (1975) 'Biomechanical perspectives on the lower limb of early hominids', in Tuttle R.H. (editor). *Primate Functional Morphology and Evolution*. The Hague: Mouton, pp. 291-326.
- Lovejoy, C.O. (1981) The origin of man. *Science*, 211, pp. 341-350.
- Lovejoy, C.O. (1988) Evolution of human walking. *Scientific American*, 259, pp. 118-125.
- Lovejoy, C.O. (2005a) The natural history of human gait and posture: Part 1. Spine and pelvis. *Gait & posture*, 21, pp. 95-112.
- Lovejoy, C.O. (2005b) The natural history of human gait and posture: Part 2. Hip and thigh. *Gait & posture* 21, pp. 113-124.
- Lovejoy, C.O. (2007) The natural history of human gait and posture: Part 3. The knee. *Gait & posture*, 25, pp. 325-341.
- Lovejoy, C.O., Heiple, K.G. (1970) A reconstruction of the femur of *Australopithecus africanus*. *American Journal of Physical Anthropology*, 32, pp. 33-40.
- Lovejoy, C.O., McCollum, M.A. (2010) Spinopelvic pathways to bipedality: why no hominids ever relied on a bent-hip-bent-knee gait. *Philosophical Transactions of the Royal Society of London B: Biological Sciences*, 365, pp. 3289-3299.
- Lovejoy, C.O., Meindl, R.S., Ohman, J.C., Heiple, K.G., White, T.D. (2002) The Maka femur and its bearing on the antiquity of human walking: applying contemporary

concepts of morphogenesis to the human fossil record. *American Journal of Physical Anthropology*, 119, pp. 97-133.

Lovejoy, C.O., Suwa, G., Simpson, S.W., Matternes, J.H., White, T.D. (2009a) The great divides: *Ardipithecus ramidus* reveals the postcrania of our last common ancestors with African apes. *Science*, 326, pp. 73-106.

Lovejoy, C.O., Suwa, G., Spurlock, L., Asfaw, B., White, T.D. (2009b) The pelvis and femur of *Ardipithecus ramidus*: the emergence of upright walking. *Science*, 326, pp. 71e1-71e6.

Lubovsky, O., Wright, D., Hardisty, M., Kiss, A., Kreder, H.J., Whyne, C. (2011) Importance of the dome and posterior wall as evidenced by bone density mapping in the acetabulum. *Clinical Biomechanics*, 26, pp. 262-266.

Luyt, C.J., Lee-Thorp, J.A. (2003) Carbon isotope ratios of Sterkfontein fossils indicate a marked shift to open environments c. 1.7 Myr ago. *South African Journal of Science*, 99, pp. 271-273.

Macchiarelli, R., Bondioli, L., Galichon, V., Tobias, P.V. (1999) Hip bone trabecular architecture shows uniquely distinctive locomotor behaviour in South African australopithecines. *Journal of human evolution*, 36, pp. 211-232.

Mackinnon, JR. (1974) The behaviour and ecology of wild orang-utans (*Pongo pygmaeus*). *Animal Behavior*, 22, pp. 3-74.

MacLatchy, L., Muller, R. (2002) A comparison of the femoral head and neck trabecular architecture of *Galago* and *Perodicticus* using micro-computed tomography (μ CT). *Journal of Human Evolution* 43, pp. 89-105.

Maga, M., Kappelman, J., Ryan, T.M., Ketcham, R.A. (2006) Preliminary observations on the calcaneal trabecular microarchitecture of extant large-bodied hominoids. *American Journal of Physical Anthropology*, 129, pp. 410-417.

Manduell, K. L., Harrison, M.E., Thorpe, S.K.S (2012). Forest structure and support availability influence orangutan locomotion in Sumatra and Borneo.(Report). *American Journal of Primatology*, 74, pp. 1128-1142.

Mann, R.A., Hagy, J. (1980) Biomechanics of walking running and sprinting. *The American Journal of Sports Medicine*, 8 (5), pp. 345-350.

Maquer, G., Musy, S.N., Wandel, J., Gross, T., Zysset, P.K. (2015) Bone volume fraction and fabric anisotropy are better determinants of trabecular bone stiffness than other morphological variables. *Journal of Bone and Mineral Research*, 30, pp. 1000-1008.

Marangalou, J.H., Ito, K., Taddei, F., Van Rietbergen, B. (2014) Inter-individual variability of bone density and morphology distribution in the proximal femur and T12 vertebra. *Bone*, 60, pp. 213-220.

Marchi, D. (2005) The cross-sectional geometry of the hand and foot bones of the Hominoidea and its relationship to locomotor behaviour. *Journal of Human Evolution*, 49, pp. 743-761.

- Marks, S., Hermey, D.C. (1996) 'The structure and development of bone', in Bilezikian J.P., Raisz L.G., Rodan G.A. (Eds.). *Principles of Bone Biology*. New York: Academic Press, pp. 3-14.
- Martinón-Torres, M. (2003) Quantifying trabecular orientation in the pelvic cancellous bone of modern humans, chimpanzees, and the Kebara 2 Neanderthal. *American Journal of Human Biology*, 15, pp. 647-661.
- Matarazzo, S.A. (2015) Trabecular Architecture of the Manual Elements Reflects Locomotor Patterns in Primates. *PLoS ONE*, 10, e0120436.
- Mazurier, A., Nakatsukasa, M., Macchiarelli, R. (2010) The inner structural variation of the primate tibial plateau characterized by high-resolution microtomography. Implications for the reconstruction of fossil locomotor behaviours. *Comptes Rendus Palevol*, 9, pp. 349-359.
- McCalden, R.W., McGeough, J.A., Court-Brown, C.M. (1997) Age-related changes in the compressive strength of cancellous bone. The relative importance of changes in density and trabecular architecture. *Journal of Bone and Joint Surgery*, 79, pp. 421-427.
- McHenry, H.M., Corruccini, R.S. (1975) Multivariate analysis of early hominid pelvic bones. *American Journal of Physical Anthropology*, 43, pp. 263-270.
- McHenry, H.M., Corruccini, R.S. (1978) The femur in early human evolution. *American Journal of Physical Anthropology*, 49 (4), pp. 473-487.
- Mckee, J.K. (1991) Palaeo-ecology of the Sterkfontein hominids: a review and synthesis. *Palaeontologia Africana*, 28, pp. 41-51.
- Mckee, J.K. (1993) Faunal dating of the Taung hominid fossil deposit. *Journal of Human Evolution*, 25, pp. 363-376.
- McMahon, T.A. (1984) *Muscles, Reflexes, and Locomotion*. Princeton, N.J.: Princeton University Press.
- Mielke, M., Wolfer, J., Arnold, P., van Hetern, A. H., Amson, E., Nyakatura, J.A. (2018) Trabecular architecture in the sciuriform femoral head: allometry and functional adaptation. *Zoological letters* 4, pp. 10.
- Milovanovic, P., Djonic, D., Hahn, M., Amling, M., Busse, B., Djuric, M. (2017) Region-dependent patterns of trabecular bone growth in the human proximal femur: A study of 3D bone microarchitecture from early postnatal to late childhood period. *American Journal of Physical Anthropology* 164 (2), pp. 281-291.
- Mitteroecker P., Gunz P. (2009) Advances in Geometric Morphometrics. *Evolutionary Biology*, 36, pp. 235-247.
- Mittra, E., Rubin, C., Qin, Y. (2005) Interrelationship of trabecular mechanical and microstructural properties in sheep trabecular bone. *Journal of Biomechanics*, 38, pp. 1229-1237.
- Miyakoshi, N. (2004) Effects of parathyroid hormone on cancellous bone mass and structure in osteoporosis. *Current Pharmaceutical Design*, 10 (21), pp. 2615-2627.

- Mizrahi, J., Solomon, L., Kaufman, B., Duggan, T.O.D. (1981) An experimental method for investigating load distribution in the cadaveric human hip. *Journal of Bone and Joint Surgery, British*, 63, pp. 610-613.
- Moorjani, P., Amorim, C.E.G., Arndt, P.F., Przeworski, M. (2016) Variation in the molecular clock of primates. *Proceedings of the National Academy of Sciences*, 113, pp. 10607-10612.
- Morbeck, M.E., Zihlman, A.L. (1988) 'Body composition and limb proportions', in Schwartz J.H. (editor). *Orangutan biology*. Oxford: Oxford University Press, pp. 285–297.
- Myatt, J.P., Crompton, R.H., Thorpe, S.K.S. (2011) Hindlimb muscle architecture in non-human great apes and a comparison of methods for analysing inter-species variation. *Journal of Anatomy*, 219, pp. 150-166.
- Myers, C.A., Register, B.C., Lertwanich, P, Ejnisman, L., Pennington, W.W., Giphart, J.E., LaPrade, R.F., Philippon, M.J. (2011) Role of the acetabular labrum and the iliofemoral ligament in hip stability: an in vitro biplane fluoroscopy study. *The American Journal of Sports Medicine*, 39 (1), pp. 85-91.
- Nagura, T., Dyrby, C.O., Alexander, E.J., Andriacchi, T.P. (2002). Mechanical loads at the knee joint during deep flexion. *Journal of Orthopaedic Research*, 20, pp. 881-886.
- Nakano, Y., Hirasaki, E., Kumakura, H. (2006) 'Patterns of vertical climbing in primates', in Ishida H., Tuttle R., Pickford M., Ogihara N., Nakatsukasa M., (eds). *Human Origins and Environmental Backgrounds Developments in Primatology: Progress and Prospects*. Boston, MA: Springer, pp. 97-104.
- Napier, J.R. (1964) The evolution of bipedal walking in the hominids. *Archives of Biology (Liege)*, 75, 673-708.
- Napier, J.R. (1967) The antiquity of human walking. *Scientific American*, 216, pp 56-66.
- Neptune, R.R., Kautz, S.A., Zajac, F.E. (2001) Contributions of the individual ankle plantar flexors to support, forward progression and swing initiation during walking. *Journal of Biomechanics*, 34, pp. 1387-1398.
- Nikita, E., Ysi Siew, Y., Stock, J., Mattingly, D., Mirazón Lahr, M. (2011) Activity patterns in the Sahara Desert: An interpretation based on cross-sectional geometric properties. *American Journal of Physical Anthropology*, 146. pp. 423-434.
- Nikodem, A. (2012) Correlations between structural and mechanical properties of human trabecular femur bone. *Acta of Bioengineering and Biomechanics*, 24, pp. 37-46.
- Nilsson, J., Thorstensson, A. 1989. Ground reaction forces at different speeds of human walking and running. *Acta Physiologica Scandinavica*, 136, pp. 217-227.
- Nordin, M., Frankel, V.H. (2001) *Basic Biomechanics of the Musculoskeletal System*. 3rd ed. Philadelphia, Pa: Lippincott Williams & Wilkins.
- Novacheck, T.F. (1998) The biomechanics of running. *Gait & Posture*, 7, pp. 77-95.

- O'Neill, M.C., Lee, L., Demes, B., Thompson, N.E., Larson, S.G., Stern Jr., J.T., Umberger, B.R. (2015) Three-dimensional kinematics of the pelvis and hindlimbs in chimpanzee (*Pan troglodytes*) and human bipedal walking. *Journal of human evolution*, 86, pp. 32-42.
- Odgaard, A. (1997) Three-dimensional methods for quantification of cancellous bone architecture. *Bone*, 20 (4), pp. 315-328.
- Ohman, J.C., Krochta, T.J., Lovejoy, C.O., Mensforth, R.P., Latimer, B. (1997) Cortical bone distribution in the femoral neck of hominoids: Implications for the locomotion of *Australopithecus afarensis*. *American Journal of Physical Anthropology*, 104, pp. 117-131.
- Ohman, J.C., Lovejoy, C.O., White, T.D. (2005) Questions About Orrorin Femur. *Science*, 307, (5711), pp. 845-845.
- Ott, S.M. (1996) 'Theoretical and methodical approach', in Bilezikian J.P., Raisz L.G., Rodan G.A. (Eds.). *Principles of Bone Biology*. New York: Academic Press, pp. 231-241.
- Ounpuu, S. (1990) The biomechanics of running: a kinematic and kinetic analysis. *AAOS Instructional Course Lectures*, 39, pp. 305-318.
- Ounpuu, S. (1994) The biomechanics of walking and running. *Clinics in Sports Medicine*, 13 (4), pp. 843-863.
- Pahr, D.H., Zysset, P.K. (2009) From high-resolution CT data to finite element models: development of an integrated modular framework. *Computer Methods in Biomechanics and Biomedical Engineering*, 12 (1), pp. 45-57.
- Parfitt, A.M., Mathews, C.H., Villanueva, A.R., Kleerekoper, M., Frame, B., Rao, D.S. (1983) Relationships between surface, volume, and thickness of iliac trabecular bone in aging and in osteoporosis. Implications for the microanatomic and cellular mechanisms of bone loss. *Journal of Clinical Investigation*, 72 (4), pp. 1396-1409.
- Parr, W.C.H., Chamoliemail U., Jonesemail, A., Walshemail W.R., Wroemail, S. (2013) Finite element micro-modelling of a human ankle bone reveals the importance of the trabecular network to mechanical performance: New methods for the generation and comparison of 3D models. *Journal of Biomechanics*, 46, pp. 200-205.
- Partridge, T.C. (2005) Dating of the Sterkfontein hominids: progress and possibilities. *Transactions of the Royal Society of South Africa*, 60, pp. 107-110.
- Paul, J.P. (1976) Approaches to design- Force actions transmitted by joints in the human body. *Proceedings of the Royal Society of London B*, 192, 163-172.
- Payne, R.C. (2001) Musculoskeletal adaptations for climbing in hominoids and their role as exaptations for the acquisition of bipedalism. PhD thesis, The University of Liverpool.
- Payne, R.C., Crompton, R.H., Isler, K., Savage, R., Vereecke, E.E., Günther, M.M., D'Août, K. (2006a) Morphological analysis of the hindlimb in apes and humans. I. Muscle architecture. *Journal of Anatomy*, 208, pp 709-724.

- Payne, R.C., Crompton, R.H., Isler, K., Savage, R., Vereecke, E.E., Günther, M.M., D'Août, K. (2006b) Morphological analysis of the hindlimb in apes and humans. II. Moment arms. *Journal of Anatomy*, 208, pp. 725-742.
- Pearson, O.M. (2000) Activity, climate, and postcranial robusticity: implications for modern human origins and scenarios of adaptive change. *Current anthropology*, 41, pp. 569-607.
- Pearson, O.M., Lieberman, D.E. (2004) The aging of Wolff's law: Ontogeny and responses to mechanical loading in cortical bone. *American Journal of Physical Anthropology*, 125 (39), pp. 63-99.
- Pedersen, D.R., Brand, R.A., Davy, D.T. (1997) Pelvic muscle and acetabular contact forces during gait. *Journal of Biomechanics*, 30 (9), pp. 959-965.
- Pettersson, U., Nilsson, M., Sundh, V., Mellström, D., Lorentzon, M. (2010) Physical activity is the strongest predictor of calcaneal peak bone mass in young Swedish men. *Osteoporosis International*, 21, pp. 447-455.
- Phillips, A.T.M., Pankaj, P., Howie, C.R., Usmani, A.S., Simpson, A.H.R.W. (2007) Finite element modelling of the pelvis: Inclusion of muscular and ligamentous boundary conditions. *Medical Engineering and Physics*, 29, pp. 739-748.
- Pickering, T.R. (1999) *Taphonomic interpretations of the Sterkfontein early hominid site (Gauteng, South Africa) reconsidered in light of recent evidence*. Ph.D. thesis, University of Wisconsin, Madison.
- Pickering, R., Herries, A.I.R., Woodhead, J.D., Hellstrom, J.C., Green, H.E., Paul, B., Ritzman, T., Strait, D.S., Schoville, B.J., Hancox, P.J. (2018) ²³⁸U–²¹⁰Pb-dated flowstones restrict South African early hominin record to dry climate phases. *Nature letter*.
- Pickering, R., Kramers, J.D. (2010) Re-appraisal of the stratigraphy and determination of new U-Pb dates for the Sterkfontein hominin site, South Africa. *Journal of Human Evolution*, 59, pp. 70-86.
- Pickford, M., Senut, B. (2001a) The geological and faunal context of late Mioene hominid remains from Lukeino, Kenya. *Comptes rendus de l'Académie des Sciences, Paris Series IIA*, 332, pp. 145-152.
- Pickford, M., Senut, B. (2001b) 'Millenium Ancestor' a 6-million year old bipedal hominid from Kenya. *South African Journal of Science*, 97, pp. 22.
- Pickford, M., Senut, B., Gommery, D., Treil, J. (2002) Bipedalism in Orrorin tugenensis revealed by its femora. *Comptes Rendus Palevol*, 1, pp. 191-203.
- Pitsillides, A.A. (2006) Early effects of embryonic movement: 'a shot out of the dark'. *Journal of Anatomy* 208, pp. 417-431.
- Polk, J.D., Blumenfeld, J., Ahlumwalia, D. (2008) Knee posture predicted subchondral apparent density in the distal femur: an experimental validation. *The Anatomical Record*, 291, pp. 293-302.
- Pomikal, C., Streicher, J. (2010) 4D-analysis of early girdle development in the mouse (*Mus musculus*). *Journal of Morphology*, 271, pp. 116-126.

- Pontzer, H., Lieberman, D.E., Momin, E., Devlin, M.J., Polk, J.D., Hallgrímsson, B., Cooper, D.M. (2006) Trabecular bone in the bird knee responds with high sensitivity to changes in load orientation. *Journal of Experimental Biology*, 209, pp. 57-65.
- Pontzer, H., Raichlen, D.A., Rodman, P.S. (2014) Bipedal and quadrupedal locomotion in chimpanzees. *Journal of Human Evolution*, 66, pp. 64-82.
- Pontzer, H., Raichlen, D.A., Sockol, M.D. (2009) The metabolic cost of walking in humans, chimpanzees, and early hominins. *Journal of Human Evolution*, 56, pp. 43-54.
- Potts, R. (1998) Environmental hypotheses of hominin evolution. *American Journal of Physical Anthropology*, 107, pp. 93-136.
- Prat, S. (2005) 'Characterising early *Homo*: cladistic, morphological and metric analyses of the original Plio-Pleistocene specimens', in d'Errico, F., Backwell, L.R. (eds). *From Tools to Symbols. From Early Hominids to Modern Humans*. Johannesburg: Wits University Press, pp. 198-228.
- Prejzner-Morawska, A., Urbanowicz, M. (1981) 'Morphology of some of the lower limb muscles in primates', in Chiarelli A., Corruccini R., (eds). *Primate evolutionary biology*. New York: Springer-Verlag, pp. 60-67.
- Preuschoft, H., Tardieu, C. (1996) Biomechanical reasons for the divergent morphology of the knee joint and the distal epiphyseal suture in hominoids. *Folia Primatologica*, 66, pp. 82-92.
- Prüfer, K., Munch, K., Hellmann, I., Akagi, K., Miller, J.R., Walenz, B., Koren, S., Sutton, G., Kodira, C., Winer, R., Knight, J.R., Mullikin, J.C., Meader, S.J., Ponting, C.P., Lunter, G., Higashino, S., Hobolth, A., Dutheil, J., Karakoç, E., Alkan, C., Sajjadian, S., Catacchio, C.C., Ventura, M., Marques-Bonet, T., Eichler, E.E., André, C., Atencia, R., Mugisha, L., Junhold, J., Patterson, N., Siebauer, M., Good, J.M., Fischer, A., Ptak, S.E., Lachmann, M., Symer, D.E., Mailund, T., Schierup, M.H., Andrés, A.M., Kelso, J., Pääbo, S. (2012) The bonobo genome compared with the chimpanzee and human genomes. *Nature*, 486, pp. 527-531.
- R Development Core Team (2017) R: A language and environment for statistical computing. Vienna, Austria: The R Foundation for Statistical Computing.
- Racic, V., Pavic, A., Brownjohn, J.M.W. (2009) Experimental identification and analytical modelling of walking forces: a literature review. *Journal of Sound and Vibration*, 326, pp. 1-49.
- Rafferty, K.L. (1998) Structural design of the femoral neck in primates. *Journal of Human Evolution*, 34 (4), pp. 361-383.
- Rafferty, K.L., Ruff, C.B. (1994) Articular structure and function in *Hylobates*, *Colobus* and *Papio*. *American Journal of Physical Anthropology*, 94 (3), pp. 395-408.
- Raichlen, D.A., Gordon, A.D., Foster, A.D., Webber, J.T., Sukhdeo, S.M., Scott, R.S., Gosman, J.H., Ryan, T.M. (2015) An ontogenetic framework linking locomotion and trabecular bone architecture with applications for reconstructing hominin life history. *Journal of Human Evolution*, 81, pp. 1-12.

- Raichlen, D.A., Gordon, A.D., Harcourt-Smith, W.E.H., Foster, A.D., Haas, W.R., Jr (2010) Laetoli Footprints Preserve Earliest Direct Evidence of Human-Like Bipedal Biomechanics. *Public Library of Science*, 3, e9769.
- Rajan, K. (1985) Linear elastic properties of trabecular bone: a cellular solid approach. *Journal of Materials Science Letters*, 4, pp. 609-611.
- Reed, K.E. (1997) Early hominid evolution and ecological change through the African Plio-Pleistocene. *Journal of Human Evolution*, 32, pp. 289-322.
- Reed, K., Fleagle, J., Leakey, R. (2013) *The Paleobiology of Australopithecus. Vertebrate Paleobiology and Paleoanthropology*. Dordrecht: Springer.
- Reissis, D., Abel, R.L. (2012) Development of fetal trabecular micro-architecture in the humerus and femur. *Journal of Anatomy* 220 (5), pp. 496-503.
- Remis, M.J. (1994). Feeding ecology and positional behavior of western gorillas (*Gorilla gorilla gorilla*) in the Central African Republic. Ph.D. Dissertation: Yale University.
- Remis, M.J. (1995). Effects of body size and social context on the arboreal activities of lowland gorillas in the Central African Republic. *American Journal of Physical Anthropology* 97, pp. 413-433.
- Remis, M.J. (1999) Tree structure and sex differences in arboreality among western lowland gorillas (*Gorilla gorilla gorilla*) at Bai Hokou, Central African Republic. *Primates*, 40, pp. 383-396.
- Reynolds, R.J., Walker, P.S., Buza, J. (2017) Mechanisms of anterior-posterior stability of the knee joint under load-bearing. *Journal of Biomechanics*, 57, pp. 39-45.
- Reynolds, S.C., Kibii, J.M. (2011) Sterkfontein at 75: review of paleoenvironments, fauna, dating and archaeology from the hominin site of Sterkfontein (Gauteng Province, South Africa). *Palaeontologia africana*, 55, 59-88.
- Richmond, B.G., Aiello, L.C., Wood, B.A. (2002) Early hominin limb proportions. *Journal of Human Evolution*, 43, pp. 529-548.
- Richmond, B.G., Jungers, W.L. (2008) *Orrorin tugenensis* femoral morphology and the evolution of hominin bipedalism. *Science*, 319, pp. 1662-1665.
- Robinson, J.T. (1972) *Early Hominid Posture and Locomotion*. Chicago: University of Chicago Press.
- Rodan, G.A. (1997) Bone mass homeostasis and bisphosphonate action. *Bone*, 20, pp. 1-4.
- Rodan, G.A. (1998) Bone homeostasis. *Proceedings of the National Academy of Sciences of the United States of America*, 95 (23), pp. 13361-13362.
- Rohlf F.J., Slice D., (1990) Extensions of the Procrustes method for the optimal superimposition of landmarks. *Systematic Zoology*, 39, pp. 40-59.
- Rook, L., Bondioli, L., Köhler, M., Moyà-Solà, S., Macchiarelli, R. (1999) *Oreopithecus* was a bipedal ape after all: Evidence from the iliac cancellous architecture. *Proceedings of the National Academy of Sciences of the United States of America*, 96, pp. 8795-8799.

- Rose, M.D. (1976) Bipedal behavior of the olive baboon (*Papio anubis*) and its relevance to an understanding of the evolution of human bipedalism. *American Journal of Physical Anthropology*, 4, pp. 247-261.
- Rubin, C., Turner, A.S., Bain, S., Mallinckrodt, C., McLeod, K. (2001) Low mechanical signals strengthen long bones. *Nature*, 412, pp. 603-604.
- Rubin, C.T., McLeod, K.J., Bain, S.D. (1990) Functional strains and cortical bone adaptation: epigenetic assurance of skeletal integrity. *Journal of Biomechanics*, 23, pp. 43-54.
- Ruff, C.B. (1987) Structural allometry of the femur and tibia in Hominoidea and *Macaca*. *Folia Primatologica*, 48, pp. 9-49.
- Ruff, C.B. (1995) Biomechanics of the hip and birth in early *Homo*. *American Journal of Physical Anthropology*, 98 (4), pp. 527-574.
- Ruff, C.B. (2002) Long bone articular and diaphyseal structure in Old World Monkeys and apes. I: Locomotor effects. *American Journal of Physical Anthropology*, 119, pp. 305-342.
- Ruff, C.B. (2008) Femoral/humeral strength in early African *Homo erectus*. *Journal of Human Evolution*, 54, pp. 383-390.
- Ruff, C.B. (2009) Relative limb strength and locomotion in *Homo habilis*. *American Journal of Physical Anthropology*, 138, pp. 90-100.
- Ruff, C.B. (2010) Body size and body shape in early hominins - implications of the Gona Pelvis. *Journal of Human Evolution*, 58 (2), pp. 166-178.
- Ruff, C.B., Hayes, W.C. (1983) Cross-sectional geometry of Pecos Pueblo femora and tibiae-A biomechanical investigation: II. Sex, age, and side differences. *American Journal of Physical Anthropology*, 60, pp. 383-400.
- Ruff, C.B., Higgins, R. (2013) Femoral neck structure and function in early hominins. *American Journal of Physical Anthropology*, 150 (4), pp. 512-525.
- Ruff, C.B., Holt, B., Trinkaus, E. (2006) Who's afraid of the big bad Wolff? "Wolff's law" and bone functional adaptation. *American Journal of Physical Anthropology*, 129, pp. 484-498.
- Ruff, C.B., Runestad, J.A. (1992) Primate limb bone structural adaptations. *Annual Review of Anthropology*, 21, pp. 407-433.
- Ruff, C.B., Scott, W.W., Liu, A.Y-C. (1991) Articular and diaphyseal remodeling of the proximal femur with changes in body mass in adults. *American Journal of Physical Anthropology*, 86, pp. 397-413.
- Ruff, C.B., Trinkaus, E., Walker, A., Larsen, C.S. (1993) Postcranial robusticity in *Homo*. I: Temporal trends and mechanical interpretation. *American Journal of Physical Anthropology*, 91, pp. 21-53.
- Ruff, C.B., Walker, A. 'Body size and body shape' in Walker, A.C., Leakey, R.E. (eds). *The Nariokotome Homo Erectus Skeleton*. Cambridge, MA: Harvard Press, pp. 234-265.

- Ruff, C.B., Walker, A., Trinkaus, E. (1994) Postcranial robusticity in *Homo*. III: ontogeny. *American Journal of Physical Anthropology*, 93, pp. 35-54.
- Ryan, T.M., Carlson, K.J., Gordon, A.D., Jablonski, N., Shaw, C.N., Stock, J.T. (2018) Hyman-like hip joint loading in *Australopithecus africanus* and *Paranthropus robustus*. *Journal of Human Evolution*, 121, pp. 12-24.
- Ryan, T.M., Ketcham, R.A. (2002) The three-dimensional structure of trabecular bone in the femoral head of strepsirrhine primates. *Journal of Human Evolution*, 43, pp. 1-26.
- Ryan, T.M., Ketcham, R.A. (2005) Angular orientation of trabecular bone in the femoral head and its relationship to hip joint loads in leaping primates. *Journal of Morphology*, 265, pp. 249-263.
- Ryan, T.M., Krovitz, G.E. (2006) Trabecular bone ontogeny in the human proximal femur. *Journal of Human Evolution*, 51, pp. 591-602.
- Ryan, T.M., Shaw, C.N. (2012) Unique suites of trabecular bone features characterize locomotor behavior in human and non-human anthropoid primates. *PLoS ONE*, 7, e41037.
- Ryan, T.M., Shaw, C.N. (2013) Trabecular bone microstructure scales allometrically in the primate humerus and femur. *Proceedings of the Royal Society B: Biological Sciences*, 280, 20130172.
- Ryan, T.M., Shaw, C.N. (2015) Gracility of the modern *Homo sapiens* skeleton is the result of decreased biomechanical loading. *Proceedings of the National Academy of Sciences of the United States of America*, 112, pp. 372-377.
- Ryan, T.M., Walker, A. (2010) Trabecular Bone Structure in the Humeral and Femoral Heads of Anthropoid Primates. *The Anatomical Record: Advances in Integrative Anatomy and Evolutionary Biology*, 293, pp. 719-729.
- Saers, J.P.P., Cazorla-Bak, Y., Shaw, C.N., Stock, J.T., Ryan, T.M. (2016) Trabecular bone structural variation throughout the human lower limb. *Journal of Human Evolution*, 97, pp. 97-108.
- San Millán, M., Kaliontzopoulou, A., Rissech, C., Turbón, D. (2015) A geometric morphometric analysis of acetabular shape of the primate hip joint in relation to locomotor behaviour. *Journal of Human Evolution*, 83, pp. 15-27.
- Sarringhaus, L.A., MacLatchy, L.M., Mitani, J.C. (2014) Locomotor and postural development of wild chimpanzees. *Journal of Human Evolution*, 66, pp. 29-38.
- Saunders, J.B., Inman, V.T., Eberhart, H.D. (1953) The major determinants in normal and pathological gait. *Journal of Bone and Joint Surgery. American volume*, 35-A, pp. 543-558.
- Scherf, H. (2008) 'Locomotion-related femoral trabecular architectures in primates-high resolution computed tomographies and their implications for estimations of locomotor preferences of fossil primates' in Endo H., Frey R. (eds). *Anatomical Imaging: Towards a New Morphology*. Japan, Tokyo: Springer, pp. 39-59.

- Scherf, H., Harvati, K., Hublin, J-J (2013) A comparison of proximal humeral cancellous bone of great apes and humans. *Journal of Human Evolution*, 65 (1), pp. 29-38.
- Scherf, H., Tilgner R (2009) A new high-resolution computed tomography (CT) segmentation method for trabecular bone architectural analysis. *American Journal of Physical Anthropology*, 140 (1), pp. 39-51.
- Schilling, A., Tofanelli, S., Hublin, J., Kivell, T.L. (2014) Trabecular bone structure in the primate wrist. *Journal of Morphology*, 275, pp. 572-585.
- Schlager, S. (2017) 'Morpho and Rvcg – Shape Analysis in R', in Zheng, G., Li, S., Szekely, G. (eds.). *Statistical Shape and Deformation Analysis*. Academic Press pp. 217-256.
- Schneider, C.A., Rasband, W.S., Eliceiri, K.W. (2012) NIH Image to ImageJ: 25 years of Image Analysis. *Nature methods*, 9 (7), pp. 671-675.
- Schultz, A.H. (1969) Observations on the Acetabulum of Primates. *Folia Primatologica*, 11 (3), pp. 181-199.
- Schwarcz, H.P., Grün, R., Tobias, P.V. (1994) ESR dating studies of the australopithecine site of Sterkfontein, South Africa. *Journal of Human Evolution*, 26, pp. 175-181.
- Sellers, W. I., Dennis, L. A., Wang, W.-J., Crompton, R. H. (2004) Evaluating alternative gait strategies using evolutionary robotics. *Journal of Anatomy*, 204 (5), pp. 343-351.
- Senut, B. (1981) Humeral outlines in some hominoid primates and in Plio-Pleistocene hominids. *American Journal of Physical Anthropology*, 56, pp. 275-283.
- Senut, B. (2003) Palaeontological approach to the evolution of hominid bipedalism: the evidence revisited. *Cour Forsch-Inst Senkenberg*, 243, pp. 125-134.
- Senut, B. (2006) 'Arboreal origin of bipedalism', in Ishida H., Tuttle R., Pickford M., Ogiwara N., Nakatsukasa M. (eds). *Human Origins and Environmental Backgrounds*. Developments in Primatology: Progress and Prospects. Boston, MA: Springer.
- Senut, B., Pickford, M. (2004) La dichotomie grands singes-homme revisitée. *Comptes Rendu Palevol*, 3, pp. 265-276.
- Senut, B., Pickford, M., Gommery, D., Mein, P., Cheboi, K., Coppens, Y. (2001) First hominid from the Miocene (Lukeino formation, Kenya). *Comptes rendus de l'Académie des Sciences, Paris Series IIA*, 332, pp. 137-144.
- Serrat, M.A., Reno, P.L., McCollum, M.A., Meindl, R.S., Lovejoy, C.O. (2007) Variation in mammalian proximal femoral development: comparative analysis of two distinct ossification patterns. *Journal of Anatomy*, 210, pp. 249-258.
- Shaw, C.N., Ryan, T.M. (2012) Does skeletal anatomy reflect adaptation to locomotor patterns? cortical and trabecular architecture in human and nonhuman anthropoids. *American Journal of Physical Anthropology*, 147, pp. 187-200.
- Shaw, C.N., Stock, J.T. (2009a) Habitual throwing and swimming correspond with upper limb diaphyseal strength and shape in modern human athletes. *American Journal of Physical Anthropology*, 140, pp. 160-172.

- Shaw, C.N., Stock, J.T. (2009b) Intensity, repetitiveness, and directionality of habitual adolescent mobility patterns influence the tibial diaphysis morphology of athletes. *American Journal of Physical Anthropology*, 140, pp. 149-159.
- Shaw, C.N., Stock, J.T. (2013) Extreme mobility in the Late Pleistocene? Comparing limb biomechanics among fossil *Homo*, varsity athletes and Holocene foragers. *Journal of Human Evolution*, 64, 242-249.
- Shelburne, K.B., Torry, M.R., Pandy, M.G. (2006) Contributions of muscles, ligaments, and the ground-reaction force to tibiofemoral joint loading during normal gait. *Journal of Orthopaedic Research*, 24, pp. 1983-1990.
- Shoemaker, S., Markolf, K. (1985) Effects of joint load on the stiffness and laxity of ligament- deficient knees, an in vitro study of the anterior cruciate and medial collateral ligaments. *The Journal of Bone and Joint Surgery, American Volume*, 67, pp. 136-146.
- Sigmon, B.A. (1974) A functional analysis of pongid hip and thigh musculature. *Journal of Human Evolution*, 3, pp. 161-185.
- Simkin, A., Ayalon, J., Leichter, I. (1987) Increased trabecular bone density due to bone- loading exercises in postmenopausal osteoporotic women. *Calcified Tissue International*, 40, pp. 59-63.
- Simpson, K.J., Pettit, M. (1997) Jump distance of dance landings influencing internal joint forces: II. Shear forces. *Medicine and Science in Sports and Exercise*, 29, pp. 928-936.
- Skinner, M.M., Stephens, N.B., Tsegai, Z.J., Foote, A.C., Nguyen, N.H., Gross, T., Pahr, D.H., Hublin, J., Kivell, T.L. (2015) Human-like hand use in *Australopithecus africanus*. *Science*, 347, pp. 395-399.
- Skuban, T.P., Vogel, T., Baur-Mlelnyk, A., Jansson, V., Heimkes, B. (2009) Function-orientation structural analysis of the proximal human femur. *Cells Tissues Organs*, 190, pp. 247-255.
- Slemenda, C., Longcope, C., Peacock, M, Hui, S, Johnston, C.C. (1996) Sex steroids, bone mass, and bone loss. A prospective study of pre-, peri-, and postmenopausal women. *Journal of Clinical Investigation*, 97, pp. 14-21
- Slocum, D.B., James, S.L. (1968) Biomechanics of Running. *JAMA*, 205 (11), pp. 721-728.
- Smith, D.M., Nance, W.E., Kang, K.W., Christain, J.C., Johnston, C.C. Jr. (1973) Genetic factors in determining bone mass. *Journal of Clinical Investigation*, 52, pp. 2800-2808.
- Sonntag, C.F. (1923) On the anatomy physiology and pathology of the chimpanzee. *Proceedings of the Zoological Society of London*, 93 (2), pp. 323-429.
- Sonntag, C.F. (1924) On the anatomy physiology and pathology of the orang-outan. *Proceedings of the Zoological Society of London*, 94 (2), pp. 349-450.
- Sponheimer, M., Lee-Thorp, J., De Ruiter, D., Codron, D., Condrón, J., Baugh, A.T., Thackeray, F. (2005a) Hominins, sedges, and termites: new carbon isotope data from

the Sterkfontein valley and Kruger National Park. *Journal of Human Evolution*, 48, pp. 301-312.

Sponheimer, M., De Ruiter, D., Lee-Thorp, J., Späth, A. (2005b) Sr/Ca and early hominin diets revisited: new data from modern and fossil enamel. *Journal of Human Evolution*, 48, pp. 147-156.

Sprecher, C.M., Schmidutz, F., Helfen, T., Richards, R.G., Blauth, M., Milz, S. (2015) Histomorphometric assessment of cancellous and cortical bone material distribution in the proximal humerus of normal and osteoporotic individuals: significantly reduced bone stock in the metaphyseal and subcapital regions of osteoporotic individuals. *Medicine*, 94 (51), e2043.

Sran, M.M., Boyd, S.K., Cooper, D.M.L., Khan, K.M., Zernicke, R.F., Oxland, T.R. (2007) Regional trabecular morphology assessed by micro-CT is correlated with failure of aged thoracic vertebrae under a posteroanterior load and may determine the site of fracture. *Bone*, 40, pp. 751-757.

Stauber, M., Rapillard, L., van Lenthe, G.H., Zysset, P., Müller, R. (2006) Importance of individual rods and plates in the assessment of bone quality and their contribution to bone stiffness. *Journal of Bone and Mineral Research*, 21, pp. 586-595.

Stephens, N.B., Kivell, T.L., Gross, T., Pahr, D.H., Lazenby, R.A., Hublin, J.-J., Hershkovitz, I., Skinner, M.M. (2016) Trabecular architecture in the thumb of *Pan* and *Homo*: implications for investigating hand use, loading, and hand preference in the fossil record. *American Journal of Physical Anthropology*, 161, pp. 603-619.

Stern, J.T. Jr, Susman, R.L. (1983) The locomotor anatomy of *Australopithecus afarensis*. *American Journal of Physical Anthropology* 60, pp. 279-317.

Stock, J.T., Macintosh, A.A. (2016) Lower limb biomechanics and habitual mobility among mid-Holocene populations of the Cis-Baikal. *Quaternary International*, 405, 200-209.

Stock, J.T., Pfeiffer, S. (2001) Linking structural variability in long bone diaphyses to habitual behaviors: Foragers from the southern African Later Stone Age and the Andaman Islands. *American Journal of Physical Anthropology*, 115, pp. 337-348.

Sugardjito, J., van Hooff, J. (1986) Age-sex class differences in the positional behavior of the Sumatran orang utan (*Pongo pygmaeus abelii*) in the Gunung Leuser National Park, Indonesia. *Folia Primatol (Basel)*, 47, pp. 14-25.

Susman, R.L., Stern, J.T. (1982) Functional Morphology of *Homo habilis*. *Science*, 217, pp. 931-934.

Susman, R.L., Stern, J.T. Jr, Jungers, W. L. (1984) Arboreality and bipedality in the Hadar hominids. *Folia primatologica*, 43, pp. 113-156.

Sutherland, D.H., Olshen, R., Cooper, L., Woo, S.L. (1980) The development of mature gait. *The Journal of Bone and Joint Surgery. American Volume*, 62, pp. 336-353.

Suuriniemi, M., Mahonen, A., Kovanen, V., Alen, M., Lyytikäinen, A., Wang, Q., Kroger, H., Cheng, S. (2004) Association between exercise and pubertal BMD is modulated by estrogen receptor alpha genotype. *Journal of Bone and Mineral Research*, 19, pp. 1758-1765.

- Sylvester, A.D. (2006) Locomotor decoupling and the origin of hominin bipedalism. *Journal of Theoretical Biology*, 242, pp. 581-590.
- Sylvester, A.D., Terhune, C.E. (2017) Trabecular mapping: Leveraging geometric morphometrics for analyses of trabecular structure. *American Journal of Physical Anthropology*, 163, pp. 553-569.
- Tardieu, C. (1981) 'Morpho-functional analysis of the articular surface of the knee joint in primates', in Chiarelli A., Corruccini R. (eds). *Primate evolutionary biology*. New York: Springer-Verlag, pp. 68-80.
- Tardieu, C. (2000) 'Ontogenèse de la marche et croissance du squelette locomoteur', in Viel E. (Ed.). *La Marche Humaine. Kinésiologie Dynamique, Biomécanique et Pathomécanique*. Paris:Masson, pp. 163-182.
- Tardieu, C., Bonneau, N., Hecquet, J., Boulay, C., Marty, C., Legaye, J., Duval-Beaupère, G. (2013) How is sagittal balance acquired during bipedal gait acquisition? Comparison of neonatal and adult pelves in three dimensions. Evolutionary implications. *Journal of Human Evolution*, 65, pp. 209-222.
- Tardieu, C., Preuschoft, H. (1996) Ontogeny of the knee joint in humans, great apes and fossil hominids: pelvi-femoral relationships during postnatal growth in humans. *Folia Primatologica*, 66, pp. 68-81.
- Taussig, G., Delor, M.H., Masse, P. (1976) Les alterations de croissance de l'extrémité supérieure du fémur: leur apports à la connaissance de la croissance normale. *Revue de Chirurgie Orthopédique et Réparatrice de l'Appareil Moteur*, 62, pp. 191-210.
- Taylor, W.R., Heller, M.O., Bergmann, G., Duda, G.N. (2004) Tibio-femoral loading during human gait and stair climbing. *Journal of Orthopaedic Research*, 22, pp. 625-632.
- Thackeray, J.F., Mdaka, S., Navsa, N., Moshau, R., Singo, S. (2000) Morphometric analysis of conspecific males and females: an exploratory study of extant primate and extinct hominid taxa. *South African Journal of Science*, 96, pp. 534-536.
- Thomason, J.J. (1985a) Estimation of locomotory forces and stresses in the limb bones of Recent and extinct equids. *Paleobiology*, 11 (2), pp. 209-220.
- Thomason, J.J. (1985b) The relationship of structure to mechanical function in the third metacarpal bone of the horse, *Equus caballus*. *Canadian Journal of Zoology*, 63, pp.1420-1428.
- Thomason, J.J. (1985c) The relationship of trabecular architecture to inferred loading patterns in the third metacarpals of the extinct equids *Merychippus* and *Mesohippus*. *Paleobiology*, 11: 323-335.
- Thorpe, S.K.S, Holder, R.L., Crompton, R.H. (2007) Origin of human bipedalism as an adaptation for locomotion on flexible branches. *Science*, 316, pp. 1328-1331.
- Thorpe, S.K.S., Crompton, R.H. (2005) Locomotor ecology of wild orangutans (*Pongo pygmaeus abelii*) in the Gunung Leuser Ecosystem, Sumatra, Indonesia: A multivariate analysis using log-linear modelling. *American Journal of Physical Anthropology*, 127, pp. 58-78.

- Thorpe, S.K.S., Crompton, R.H. (2006) Orangutan positional behavior and the nature of arboreal locomotion in Hominoidea. *American Journal of Physical Anthropology*, 131, pp. 384-401.
- Thorpe, S.K.S., Holder, R.L., Crompton, R.H. (2009) Orangutans employ unique strategies to control branch flexibility. *Proceedings of the National Academy of Sciences*, 106, pp. 12646-12651.
- Tocheri, M.W., Solhan, C.R., Orr, C.M., Femiani, J., Frohlich, B., Groves, C.P., Harcourt-Smith, W.E., Richmond, B.G., Shoelson, B., Jungers, W.L. (2011) Ecological divergence and medial cuneiform morphology in gorillas. *Journal of Human Evolution*, 60, pp. 171-184.
- Treece, G.M., Gee, A.H. (2014) Independent measurement of femoral cortical thickness and cortical bone density using clinical CT. *Medical Image Analysis*, 20 (1), pp. 249-264.
- Trinkaus, E. (1976) The morphology of European and Southwest Asian Neandertal pubic bones. *American Journal of Physical Anthropology*, 44, pp. 95-103.
- Trinkaus, E. (1983) Functional aspects of Neanderthal pedal remains. *Foot Ankle*, 3, pp. 377-390.
- Trinkaus, E., Churchill, S.E., Ruff, C.B. (1994) Postcranial robusticity in *Homo*. II: Humeral bilateral asymmetry and bone plasticity. *American Journal of Physical Anthropology*, 93, pp. 1-34.
- Trinkaus, E., Jelínek, J. (1997) Human remains from the Moravian Gravettian: the Dolní Věstonice 3 postcrania. *Journal of Human Evolution*, 33, pp. 33-82.
- Tsegai, Z.J., Kivell, T.L., Gross, T., Nguyen, N.H., Pahr, D.H., Smaers, J.B., Skinner, M.M. (2013) Trabecular bone structure correlates with hand posture and use in hominoids. *PLoS ONE*, 8, e78781.
- Tsegai, Z.J., Skinner, M.M., Gee, A.H., Pahr, D.H., Treece, G.M., Hublin, J.-J., Kivell, T.L. (2017) Trabecular and cortical bone structure of the talus and distal tibia in *Pan* and *Homo*. *American Journal of Physical Anthropology*, 163, pp. 784-805.
- Tsegai, Z.J., Skinner, M.M., Pahr, D.H., Hublin, J.-J., Kivell, T.L. (2018a) Systemic patterns of trabecular bone across the human and chimpanzee skeleton. *Journal of anatomy*, 232 (4), pp. 641-656.
- Tsegai, Z.J., Skinner, M.M., Pahr, D.H., Hublin, J.-J., Kivell, T.L. (2018b) Ontogeny and variability of trabecular bone in the chimpanzee humerus, femur and tibia. *American Journal of Physical Anthropology*, 167 (4), pp. 713-736.
- Tutin, C. E., Fernandez, M. (1985). Foods consumed by sympatric populations of *Gorilla g. gorilla* and *Pan t. troglodytes* in Gabon: Some preliminary data. *International Journal of Primatology*, 6, pp. 27-43.
- Tuttle, R.H. (1969) Knuckle-walking and the problem of human origins. *Science*, 166, pp. 953-961.

- Tuttle, R.H., Cortright, W. (1988) 'Positional behavior adaptive complexes and evolution', in Schwartz J.H. (ed). *Orangutan biology*. Oxford: Oxford University Press, pp. 311-330.
- Ulrich, D., Hildebrand, T., Van Rietbergen, B., Muller, R., Ruegsegger, P. (1997) 'The quality of trabecular bone evaluated with micro- computed tomography, FEA and mechanical testing', in Lowet G., Ruegsegger P., Weinans H., Meunier A. (Eds.). *Bone Research in Biomechanics*. Amsterdam: IOS Press, pp. 97-112.
- Ulrich, D., van Rietbergen, B., Weinans, H., Rügsegger, P. (1998) Finite element analysis of trabecular bone structure: a comparison of image-based meshing techniques. *Journal of Biomechanics*, 31, pp. 1187-1192
- Van der Bogert, A.J., Read, L., Nigg, B.M. (1999) An analysis of hip joint loading during walking running and skiing. *Medicine, Science in Sports, Exercise*, 31 (1), pp. 131-142.
- Van der Meulen, M.C.H., Beaupré, G.S., Carter, D.R. (1993) Mechanobiologic influences in long bone cross-sectional growth. *Bone*, 14, pp. 63-642.
- Van Rietbergen, B., Odgaard, A., Kabel, J., Huiskes, R. (1996) Direct mechanics assessment of elastic symmetries and properties of trabecular bone architecture. *Journal of Biomechanics* 29, pp. 1653-1657.
- Van Rietbergen, B., Weinans, H., Huiskes, R., Odgaard, A. (1995) A new method to determine trabecular bone elastic properties and loading using micromechanical finite-element models. *Journal of Biomechanics* 28, pp. 69-81.
- Volpato, V., Viola, T.B., Nakatsukasa, M., Bondioli, M., Macchiarelli, R. (2008) Textural characteristics of the iliac-femoral trabecular pattern in a bipedally trained Japanese macaque. *Primates*, 49, pp. 16-25.
- Von Eisenhart-Rothe, R., Siebert, M., Bringmann, C., Vogl, T., Englmeier, K.H., Graichen, H. (2004) A new in vivo technique for determination of 3D kinematics and contact areas of the patello-femoral and tibio-femoral joint. *Journal of Biomechanics*, 37, pp. 927-934.
- Vrba, E.S. (1974) Chronological and ecological implications of the fossil Bovidae at the Sterkfontein Australopithecine site. *Nature*, 250, pp. 19-23.
- Vrba, E.S. (1975) Some evidence of chronology and palaeoecology of Sterkfontein, Swartkrans and Kromdraai from the fossil Bovidae. *Nature*, 254, pp. 301-304.
- Vrba, E.S. (1980) 'The significance of bovid remains as indicators of environment and predation patterns', in Behrensmeyer, A.K., Hill, A.P. (eds). *Fossil in the Making*. Chicago: University of Chicago Press, pp. 247-271.
- Wagner, F.V., Negrão, J.R., Campos, J., Ward, S.R., Haghighi, P., Trudell, D.J., Resnick, D. (2012) Capsular ligaments of the hip: anatomic histologic and positional study in cadaveric specimens with MR arthrography. *Radiology*, 263 (1), pp. 189-198.
- Walker, J.M. (1991) Musculoskeletal development: a review. *Physical Therapy*, 71, pp. 878-889.

- Wall-Scheffler, C.M., Geiger, K., Steudel-Numbers, K.L. (2007) Infant carrying: the role of increased locomotory costs in early tool development. *American Journal of Physical Anthropology*, 133, pp. 841-846.
- Wallace, I.J., Demes, B., Judex, S. (2017) 'Ontogenetic and genetic influences on bone's responsiveness to mechanical signals', in Percival C.J., Richtsmeier J.T. (eds). *Building Bones: Bone Formation and Development in Anthropology*. Cambridge: Cambridge University Press, pp. 233-253
- Wallace, I.J., Demes, B., Mongle, C., Pearson, O.M., Polk, J.D., Lieberman, D.E. (2014) Exercise-induced bone formation is poorly linked to local strain magnitude in the sheep tibia. *PLoS ONE*, 9, e99108.
- Wallace, I.J., Koch, E., Holowka, N.B., Lieberman, D.E. (2018) Heel impact forces during barefoot versus minimally shod walking among Tarahumara subsistence farmers and urban Americans. *Royal Society Open science*, 5, 180044.
- Wallace, I.J., Kwaczala, A.T., Judex, S., Demes, B., Carlson, K.J. (2013) Physical activity engendering loads from diverse directions augments the growing skeleton. *Journal of Musculoskeletal and Neuronal Interactions*, 13, pp. 245-250.
- Walsh, J.S. (2015) Normal bone physiology remodelling and its hormonal regulation. *Surgery (Oxford)*, 33 (1), pp. 1-6.
- Ward, C.V. (1991) Functional anatomy of the lower back and pelvis of the Miocene hominoid *Proconsul nyanzae* from Mfanga Island Kenya. PhD Dissertation, Johns Hopkins University.
- Ward, C.V. (2002) Interpreting the posture and locomotion of *Australopithecus afarensis*: where do we stand? *Yearbook of Physical Anthropology*, 45, pp. 185-215.
- Ward, C.V., Kimbel, W.H., Johanson, D.C. (2011) Complete Fourth Metatarsal and Arches in the Foot of *Australopithecus afarensis*. *Science*, 331 (6018), pp. 750-753.
- Ward, C.V., Leakey, M.G., Walker, A. (1999) The new hominid species *Australopithecus anamensis*. *Evolutionary Anthropology: Issues, News, and Reviews*, 7, pp. 197-205.
- Ward, C.V., Leakey, M.G., Walker, A. (2001) Morphology of *Australopithecus anamensis* from Kanapoi and Allia Bay, Kenya. *Journal of Human Evolution*, 41, pp. 255-368
- Ward, F.O. (1838) *Outlines of Human Osteology*. London: Henry Renshaw.
- Watson, J.C., Payne, R.C., Chamberlain, A.T., Jones, R.K., Sellers, W.I. (2008) The energetic costs of load-carrying and the evolution of bipedalism. *Journal of Human Evolution*, 54: 675-683.
- Weber, G.W., Bookstein, F.L. (2011) *Virtual Anthropology. A guide to a new interdisciplinary field*. Vienna, Austria: Springer-Verlag Wien.
- Weinstein, R.S., Hutson, M.S. (1987) Decreased trabecular width and increased trabecular spacing contribute to bone loss with aging. *Bone*, 8, pp. 127-142.
- Whalen, R.T., Carter, D.R., Steele, C.R. (1988) Influence of physical activity on the regulation of bone density. *Journal of Biomechanics*, 21, pp. 825-837.

- Wheeler, P.E. (1984) The evolution of bipedality and loss of functional body hair in hominids. *Journal of Human Evolution*, 13, pp. 91-98.
- Wheeler, P.E. (1992) The thermoregulatory advantages of large body size for hominids foraging in savannah environments. *Journal of Human Evolution*, 23, pp. 351-362.
- White, T.D., Asfaw, B., Beyene, Y., Haile-Selassie, Y., Lovejoy, C.O., Suwa, G., WoldeGabriel, G. (2009) *Ardipithecus ramidus* and the Paleobiology of Early Hominids. *Science*, 326, pp. 64-86.
- White, T.D., Suwa, G. (1987) Hominid footprints at Laetoli: facts and interpretations. *American Journal of Physical Anthropology*, 72, pp. 485-514.
- White, T.D., Suwa, G., Asfaw, B. (1994) *Australopithecus ramidus*, a new species of early hominid from Aramis, Ethiopia. *Nature*, 371, pp. 306-312.
- Whitehouse, W.J. (1974) The quantitative morphology of anisotropic trabecular bone. *Journal of microscopy*, 101 (2), pp. 153-168.
- WoldeGabriel, G., Haile-Selassie, Y., Renne, P.R., Hart, W.K., Ambrose, S.H., Asfaw, B., Heiken, G., White, T. (2001) Geology and paleontology of the Late Miocene Middle Awash valley, Afar rift, Ethiopia. *Nature*, 412, pp. 175-182.
- Wolff, J. (1892) *Das Gesetz der Transformation der Knochen*. Berlin: A Hirschwild.
- Wolff, J. (1986) *The law of bone remodeling*. Berlin: Springer-Verlag.
- Wolpoff, M.H., Senut, B., Pickford, M., Hawks, J. (2002) *Sahelanthropus* or 'Sahelpithecus'? *Nature*, (419), pp. 581-582.
- Wood, B., Collard, M. (1999) The Human Genus. *Science*, 284, pp. 65-71.
- Wright, D., Whyne, C., Hardisty, M., Kreder, H.J., Lubovsky, O. (2011) Functional and anatomic orientation of the femoral head. *Clinical orthopaedics and related research*, 469, pp. 2583-2589.
- Yeni, Y.N., Zinno, M.J., Yerramshetty, J.S., Zauel, R., Fyhrie, D.P. (2011) Variability of trabecular microstructure is age-, gender-, race- and anatomic site-dependent and affects stiffness and stress distribution properties of human vertebral cancellous bone. *Bone*, 49, pp. 886-894.
- Yoshida, H., Faust, A., Wilckens, J., Kitagawa, M., Fetto, J., Chao, E.Y. (2006) Three-dimensional dynamic hip contact area and pressure distribution during activities of daily living. *Journal of Biomechanics*, 39 (11), pp. 1996-2004.
- Zeininger, A. (2013) Ontogeny of bipedalism: pedal mechanics and trabecular bone morphology. PhD Dissertation, University of Texas at Austin.
- Zheng, N., Fleisig, G.S., Escamilla, R.F., Barrentine, S.W. (1998) An analytical model of the knee for estimation of internal forces during exercise. *Journal of Biomechanics*, 31, pp. 963-967.
- Zihlman, A.L., McFarland, R.K., Underwood, C.E. (2011) Functional Anatomy and Adaptation of Male Gorillas (*Gorilla gorilla gorilla*) With Comparison to Male Orangutans (*Pongo pygmaeus*). *The Anatomical Record: Advances in Integrative Anatomy and Evolutionary Biology*, 294, pp. 1842-1855.

Zipfel, B., DeSilva, J.M., Kidd, R.S., Carlson, K.J., Churchill, S.E., Berger, L.R. (2011) The Foot and Ankle of *Australopithecus sediba*. *Science*, 333, pp. 1417-1420.

Zollikofer, C.P.E., Ponce, d.L., Lieberman, D.E., Guy, F., Pilbeam, D., Likius, A., Mackaye, H.T., Vignaud, P., Brunet, M. (2005) Virtual cranial reconstruction of *Sahelanthropus tchadensis*. *Nature*, 434, pp. 755-759.

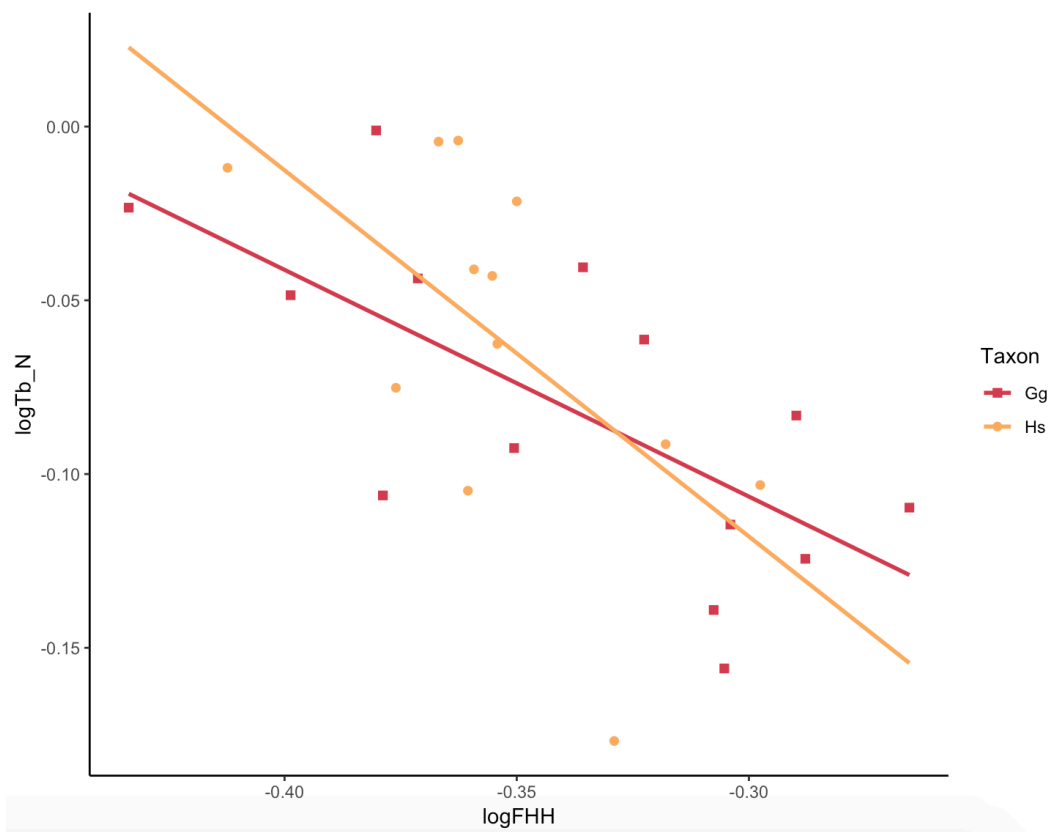
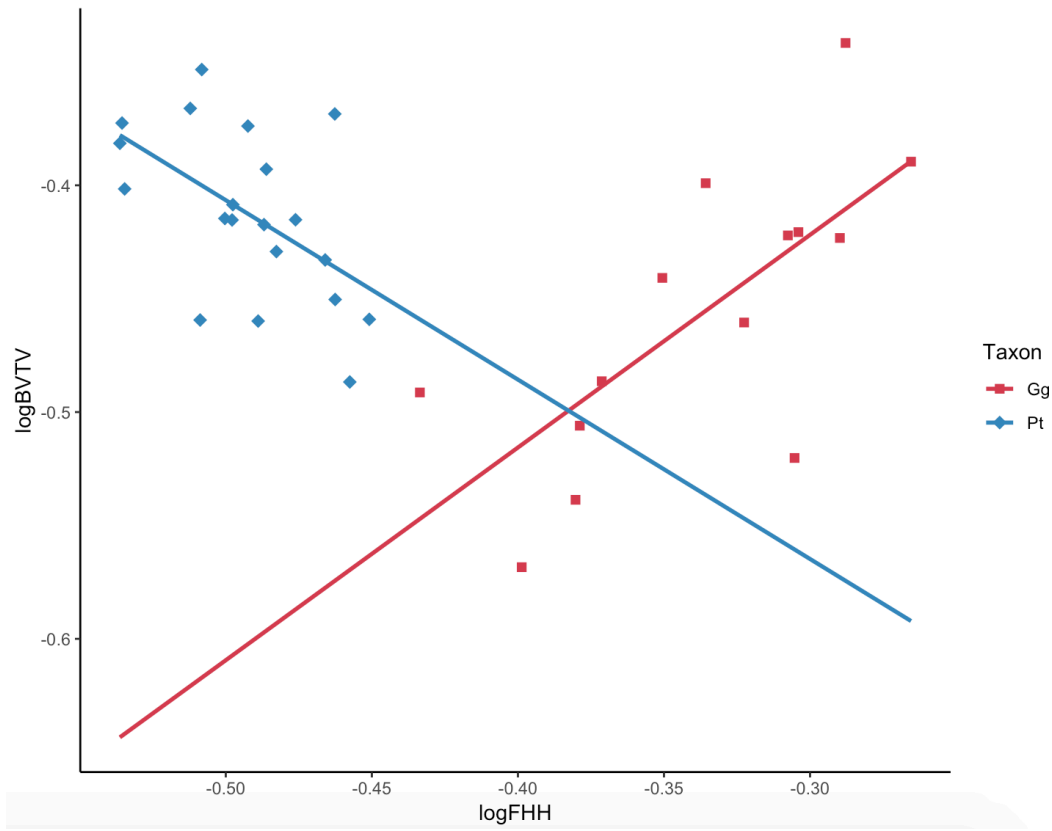
Appendix

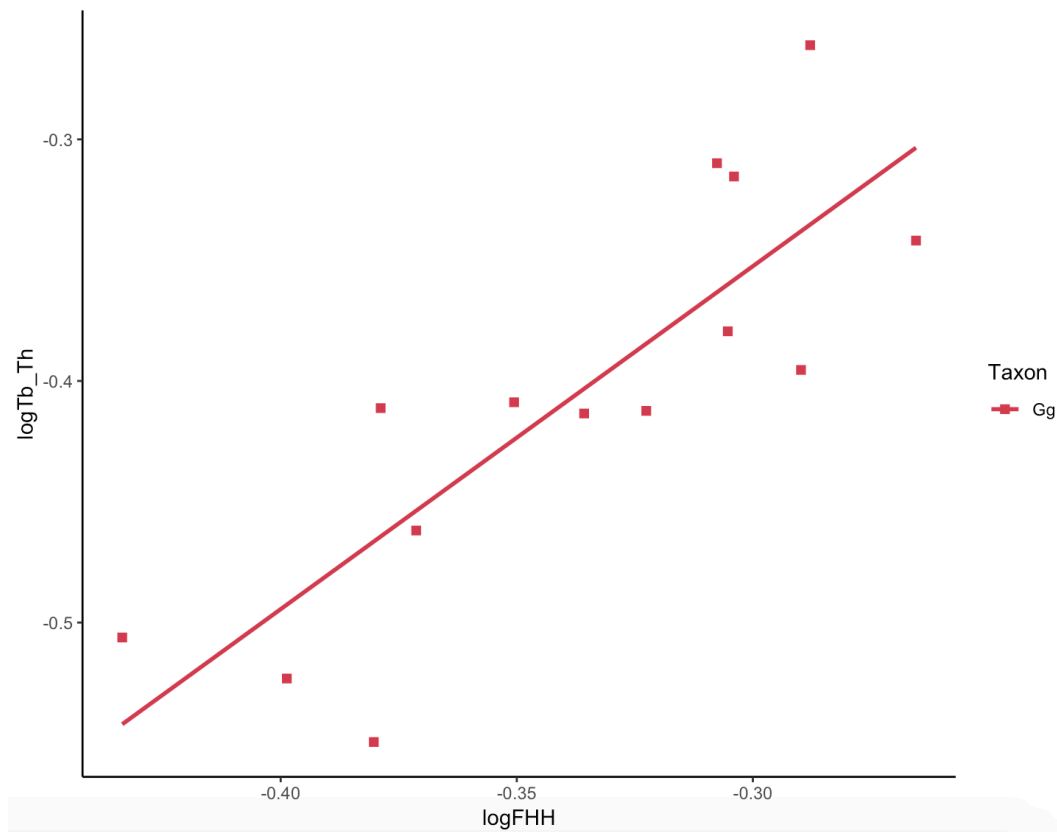
Allometry

Intraspecific allometric relationships

Table S1. P-values and R-squared values - in parentheses- for regressions of log-transformed trabecular parameters with femoral head height (FHH) within each taxon.

Taxon	Variable	Slope	Intercept	R²	p-value	Allometric relationship
<i>Pan</i>	BV/TV	-0.7912	-0.8022	0.2886	0.01459	-
	DA	0.1046	-0.7712	0.0007873	0.9065	NA
	Tb.N	-0.32789	-0.08886	0.04102	0.3918	NA
	Tb.Sp	0.57782	0.03091	0.1139	0.1456	NA
	Tb.Th	-0.1589	-0.6194	0.007024	0.7254	NA
<i>Gorilla</i>	BV/TV	0.938	-0.1404	0.5082	0.004214	+
	DA	0.2615	-0.6562	0.02062	0.6243	NA
	Tb.N	-0.65253	-0.30224	0.4759	0.006327	-
	Tb.Sp	0.276508	0.002378	0.1076	0.2522	NA
	Tb.Th	1.41944	0.07332	0.6871	0.0002476	+
<i>Homo</i>	BV/TV	-0.8879	-0.8425	0.1243	0.261	NA
	DA	-0.7229	-0.9011	0.07672	0.3835	NA
	Tb.N	-1.0539	-0.4342	0.3522	0.04194	-
	Tb.Sp	1.3275	0.3868	0.3285	0.05139	NA
	Tb.Th	0.2613	-0.3997	0.03298	0.5721	NA





Interspecific allometric relationships

Table S2. P-values and R-squared values for regressions of log-transformed trabecular parameters with femoral head height (FHH) including all taxa.

Variable	Slope	Intercept	R ²	p-value	Allometric relationship
BV/TV	-0.3711	-0.6084	0.171	0.004281	-
DA	0.66452	-0.48089	0.2293	0.0007614	+
Tb.N	-0.9274	-0.38878	0.7792	4.996e-16	-
Tb.Sp	1.017	0.2566	0.7325	3.503e-14	=
Tb.Th	0.70736	-0.198	0.4903	6.07e-08	-

